Università
degli Studi
di Padova

DIPARTIMENTO
DI INGEGNERIA
DELL'INFORMAZIONE

Synchronization algorithms for multi-agent systems: Analysis, Synthesis and Applications

Ph.D. candidate
Enrico Lovisari

Advisor
prof. Sandro Zampieri

Ph.D. School in
Information Engineering
2012

Summary

The main topic of this thesis is the study of the interaction of agents interconnected in a large-scale network. This type of systems received great attention in the last decade due to the disposal of actual networks composed of a large number of small devices.

In the thesis, three complementary problems have been afforded: Analysis of Consensus Networks, Synthesis of Higher Order Consensus Networks, and Application of Synchronization algorithms.

Analysis of Consensus Networks

One of the most studied problems in multi-agents networks is the so called *consensus problem*. Consider a number of agents, each having at disposal an initial guess of some quantity. Each agent is allowed to communicate with a possibly restricted subset of agents, its *neighborhood*. It is common to abstract this making use of the so called *communication graph*, in which the nodes are the agents of the network and there is an edge among a pair of agents if they can exchange information.

The problem is to design a rule to update the variable of the single node using information coming from its neighbors, in order to reach, possibly in finite time, an agreement, or *consensus*, on the quantity of interest. In case the agreement is on the average of the initial conditions we say that we achieve *average consensus*.

In the dissertation the simplest and most studied update rule is considered, which consists, iteratively, in a simple linear combination of the value at one agent and the values at its neighbors. Conditions on this linear iteration for consensus to be achieved are well-known. The goal is to measure the performance of a consensus algorithm through two metrics, namely the rate of convergence, which tells how fast consensus is achieved, and the ℓ_2 norm of the difference among state trajectory and asymptotic consensus value, related to the energy spent to achieve the agreement.

The first chapter of the thesis gives tools to estimate how these metrics are related to the geometry of the communication graph. In particular, a new result allows to estimate the ℓ_2 cost in terms of the average effective resistance of a suitable electrical network, which in many cases essentially depends on the communication graph only.

It is considered, due to its interest in sensor networks, the class of graphs known as *geometric graphs*, which can be seen as perturbed grids deployed in the Euclidean space $\mathbb{R}^d$. The above result and other techniques are used to prove that both the rate of convergence and the ℓ_2 cost essentially depend on the number of agents and the dimension d only in which the graph is embedded. This extends and unifies known results on Cayley k-regular graphs.

Synthesis of Higher Order Consensus Networks

It is well known that in the consensus algorithm each agent behaves as a simple integrator whose control is computed as a linear combination of the outputs of the neighbors. In the last years the researchers' attention moved to more complex cases, among which one of the most important is when we model the agents as generic dynamical operators. The second chapter of this thesis deals with *heterogeneous higher order consensus networks*, namely networks in which each agent is the perturbation of a common nominal linear time invariant operator.

A general framework is presented to study this type of systems when the goal is to achieve output-synchronization, namely reach, and maintain, an agreement on the outputs. This agreement can possibly be time-varying, differently from the classical consensus case. Various particular cases are considered, such as LTI perturbations, memoryless slope-restricted perturbations, and memoryless slope-restricted interconnection operators.

Making use of the input/output technique known as Integral Quadratic Constraints, a general theorem and several corollaries are proposed to design the control law, given certain bound on the perturbations of the single agents. When possible, simple and scalable graphical criteria are proposed, resembling the Nyquist and the Popov criteria.

Applications of Synchronization algorithms

The third and last chapter of this thesis is devoted to the application of the results in the first chapters to two important applicative problems, namely clock synchronization and cameras calibration.

We consider a well-known model for clocks, consisting in a double integrator with a zero dependent on the local skew of the clock, and we apply the previous results in order to achieve robust synchronization. Moreover, the case of quasi-saturation of the inputs is considered and solved using a Popov criterion. To conclude, some considerations in the case of randomized algorithms yield an existence result for a simple linear control to achieve mean-square synchronization.

Concerning cameras calibration, we consider the problem of computing a common reference frame making use only of relative orientations of pairs of cameras. The problem is recast into an optimization procedure on the manifold $\mathcal{S}_1$, which cannot be solved in the classical way due to the existence of local minima. In order to overcome this problem, we propose a general procedure, based on the cycles of the communication graph, which aims to rectify the manifold $\mathcal{S}_1$ into a suitable segment. Theoretical results give bound on the noises in order to achieve good performance.

Sommario

Questa tesi di dottorato è incentrata sullo studio dell'interazione di agenti interconnessi in rete. Sitemi di questo tipo sono stati oggetto di attenzione crescente negli ultimi dieci anni, data l'effettiva disponibilità di reti composte da un numero molto elevato di dispositivi. In questa tesi vengono affrontati tre problemi complementari l'un l'altro: Analisi di reti di consenso, Sintesi di reti di consenso di ordine superiore, e Applicazione di algoritmi di sincronizzazione.

Analisi di reti di consenso

Uno dei problemi più studiati nell'ambito delle reti multi-agente è il problema di *consenso*. Sia dato un certo numero di agenti, ciascuno in possesso di un valore stimato di una qualche quantità di interesse; il singolo agente può comunicare solo con un sottoinsieme di altri agenti, i suoi *vicini*. Ciò viene modellato attraverso un *grafo di comunicazione*, in cui i nodi rappresentano gli agenti: si ha un edge fra due nodi se i corrispondenti agenti sono in grado di comunicare tra loro.

Il problema è quello di progettare un algoritmo che aggiorni iterativamente il dato di ogni singolo nodo usando solo l'informazione proveniente dai nodi vicini, allo scopo di ottenere, possibilmente in tempo finito, lo stesso valore ad ogni agente, cioè il *consenso*. Nel caso tale valore sia la media delle condizioni iniziali, si parla di *consenso in media*.

In questa tesi ci concentreremo sul modo più semplice per risolvere il problema di consenso, che prevede l'iterazione di un algoritmo lineare da parte di ciascun agente. È noto sotto quali condizioni tale algoritmo permette il raggiungimento del consenso. Si è qui interessati a studiare le prestazioni di un dato algoritmo tramite due metriche, il rate di convergenza, relativo alla velocità con cui si raggiunge il consenso, e la norma ℓ_2 della differenza fra la traiettoria degli stati e il valore asintotico di consenso, che misura l'energia spesa.

Il primo capitolo della tesi offre metodi per stimare tali metriche in base alla geometria del grafo di comunicazione. In particolare, un primo risultato esprime il costo ℓ_2 in termini della resistenza effettiva media di una opportuna rete di resistori, che in molti casi di interesse dipende essenzialmente solo dalla geometria del grafo di comunicazione.

Sono stati presi in esame i grafi detti *geometrici*, che rapresentano griglie regolari perturbate disposte nello spazio euclideo $\mathbb{R}^d$ e sono dunque buoni modelli per reti di sensori. Utilizzando il risultato appena descritto e altre tecniche è stato possibile dimostrare che per grafi geometrici l'andamento sia del rate di convergenza, sia del costo ℓ_2, è dato essenzialmente solo dal numero di nodi e dalla dimensione d dello spazio in cui sono disposti. Ciò estende ed unifica noti risultati su grafi k-regolari di tipo Cayley.

Sintesi di reti di consenso di ordine superiore

È noto che una rete che implementi un algoritmo di consenso è una rete di integratori, il cui controllo è una combinazione lineare dell'uscita dei vicini. Una generalizzazione del consenso è quella in cui il singolo agente non si comporta come un semplice integratore, bensì è caratterizzato da dinamiche di ordine superiore.

Il secondo capitolo di questa tesi è incentrato sullo studio di *reti di consensus di ordine superiore eterogenee*, cioè reti in cui ciascun agente è rappresentato da un sistema che può essere visto come la perturbazione di un sistema nominale lineare tempo-invariante.

Viene proposto uno schema generale per lo studio di questi sistemi quando l'obiettivo è la sincronizzazione dell'uscita, cioè il controllo ad uno stato in cui le uscite di tutti gli agenti sono e rimangono coincidenti, eventualmente tempo-varianti. Numerosi casi particolari sono considerati, fra cui il caso di perturbazioni LTI, pertubazioni con vincoli di pendenza, operatori di interconnessione non lineari con vincoli di pendenza.

Viene dimostrato un criterio generale basato sulla teoria degli Integral Quadratic Constraints per lo studio della relazione ingresso/uscita, da cui derivano numerosi corollari che risolvono il problema nei casi succitati. Quando possibile, vengono proposti semplici criteri grafici equivalenti a tali corollari, ispirati ai criteri di Nyquist e di Popov.

Applicazione di algoritmi di sincronizzazione

Il terzo e ultimo capitolo della tesi è dedicato a due importanti problemi di natura applicativa, la sincronizzazione di orologi e la calibrazione di telecamere.

É stato considearato un noto modello per un orologio, che è visto come un doppio integratore con uno zero dipendente dai parametri dell'orologio. I risultati presentati in precedenza sono stati applicati in modo da ottenere un algoritmo per la sincronizzazione robusta di tali orologi. Inoltre, viene consideato il caso in cui il controllo quasi-satura. Per testare la robustezza viene usato in questo caso un criterio di Popov. In conclusione, viene considerato un protocollo randomizzato e viene dimostrata l'esistenza di un semplice controllo lineare per ottenere la sincronizzazione in media quadratica.

Per quanto riguarda la calibrazione di telecamere, viene considerato il problema di accordarsi su un sistema di riferimento comune usando solo le orientazioni relative di coppie di telecamere. Il problema può essere riscritto come un problema di ottimizzazione sulla varietà $\mathcal{S}_1$, il cerchio, ma non è risolvibile con tecniche standard, data la presenza di minimi locali. Per superare tale ostacolo, viene proposta una procedura basata su cicli del grafo, che permette di interpretare $\mathcal{S}_1$ come un opportuno segmento. L'analisi teorica dà vincoli sui rumori di misura in modo da garantire buone prestazioni.

Contents

1 Introduction

This thesis is concerned with the study of synchronization algorithm for Networked Controlled Systems. This topic, which dates back to the '80s with pioneering works on agreement [1], has seen in the last decade a huge interest by several scientific communities, motivated by the availability of networks of cheap sensors and/or robots, and a renewed interest in modeling biological systems such as swarms of animals or social networks [2, 3, 4].

Despite the fact that groups of robots, networks of sensors, networks of computers, swarms of animals etc. all have obvious distinctive features, it is often the case that four aspects characterize such complex systems

1. The networks has a *global goal*, which can be formation control, estimation of quantities, processing of a large amount of data, optimization of global functions, and so on. Often, this global goal can be though as minimization of a certain cost function which depends on the variables of the whole network;

2. The global goal *cannot be computed at one point*, namely it is impossible for a single unit, or a single super-agent, to acquire all the information from the network and then spread the answer, or the control, to the others. This can be due to several reasons, for example the fact that the network is physically too large to carry all the information at one point (due to communication capabilities), or the fact that

the network is dynamically changing and the process of centralized decision making would be too slow;

3. Each single agent possesses limited memory and computation capability, so even if it could receive all the information required to achieve the global goal, the computation load would be too high;

4. Each single agent can communicate only *locally*, namely with a possibly very restricted subset of the network, called its *neighborhood*.

Despite the fact that such characteristics and constraints pose clear limits on the control of these systems, fundamental motivation for scientific community comes from the fact that simple laws applied by simple agents in a large network let arise global behaviors which are sometimes unpredictable when looking at the single agent. Famous examples of this behavior can be found in biology, where swarms of animals behave in such a way that the entire group assumes a formation which discourages predators to attack. Another celebrated example comes from physics, and is related to ferromagnetic materials, which behave in different ways according to the "temperature" of the environment. This behavior has been studied making use of variations of the well-known spin glass model, in which interesting phase transitions arise from interaction of a very large number of simply behaving agents [5].

In this thesis we particularize our analysis to one of the simplest global goals possible, namely *synchronization*. Intuitively, a network is synchronized if all the agents "behave in the same manner", this meaning that each agent is characterized by some type of output, and the actual values of these outputs are the same for all the agents. To give a concrete example, we say that a network of clocks is synchronized if they all beat the same time.

The simplest and most studied synchronization problem is the *consensus problem*. In this case, each agent stores in memory a real number, and the grand goal of the network is to steer the agents to an agreement (or consensus) on such initial values. In particular, if the required agreement concerns the average value, then we talk about *average consensus*. In this thesis we will concentrate on one of the most studied algorithms to achieve consensus, namely the *linear consensus algorithm*, in which each agent updates its value as a linear combination of the values received by its neighbors. Despite the simplicity of this procedure, there are many important applications in the fields of formation control, load balancing, modeling and filtering.

It is known that linear consensus algorithm corresponds to a network of simple integrators. In a more general scenario, each agent is modeled as a system of higher order

with single input and single output. In this case, the synchronization problem is often called *higher order consensus problem*. This topic is relatively younger than classical consensus algorithm, but it has already found several interesting applications, for example in clock synchronization, in which the agents are modeled as double integrators, and in synchronization of oscillators, in which agents are second order systems with complex conjugate poles. In general, synchronization of higher order systems is more difficult to be achieved than consensus due to the more complex interaction of the internal dynamics of the agents with the information exchange along the network.

Notice that we will always assume that the network adopts *cooperative strategies* in order to compute the global task, this meaning that all the nodes in the network behave in such a way that the global goal is achieved, that they actively and positively use the information coming from the neighbors, and that they send faithfully their information to the neighbors. This optimistic scenario does not necessarily hold, since in the network there could be malicious nodes that, voluntarily or not, deviate from the designed update law and avoid the global task to be computed or, worse, indirectly control the network. This problem is the topic of the growing part of literature dealing with security in sensor network, in which tools are given to check whether malicious nodes exist in the network and how to let the other sensors ignore them [6, 7, 8].

Overview and Contributions

The dissertation is divided in three parts, which treat topics complementary one to each other: Analysis of graph topologies to estimate the performance of a consensus protocol, Synthesis of the interaction protocol to synchronize a network of dynamic agents, and Application of these results to two important problems of real networks of agents, namely clock synchronization of sensor networks and calibration of cameras networks.

In Chapter 3, Analysis of Consensus Networks, we study two performance costs for the linear consensus algorithm, namely the rate of convergence to agreement and the ℓ^2 norm of the difference among the trajectory of the states and the asymptotic consensus value. These metrics are classical in System Theory, with the only difference being that the asymptotic value to be reached is not zero but rather the consensus value.

Our interest is on the relation among these performance metrics and the geometric characteristics of the communication graph, namely the graph formed by agents and the allowed communication links. It is in fact known that given a certain structure of the graph (for example, it being a ring, or a regular grid, and so on), the performance of a consensus algorithm degrades as the number of nodes in the network increases. This is due to the fact that while the network becomes larger, it takes longer and longer for

information to be spread along the network.

One may however expect that since the structure of the network remains similar, it is possible to study analytically such a degradation trend. In fact, in case of the highly structured graphs known as k-regular Cayley graphs it is known how the performance metrics are related to the number of agents in the network.

Our goal is to extend these results by means of the analysis of the class of graphs known as *geometric graphs*. We give a formal definition of them in Chapter 3, but intuitively they are graphs in which the nodes are deployed in an Euclidean space, for example on the plane $\mathbb{R}^2$, and whose structure resembles a perturbed grid.

The main contributions of Chapter 3 can be summarized as follows:

- to show that in a geometric graph convergence to consensus happens with the same rate as in a regular grid of similar dimension;
- to rewrite the ℓ^2 cost in terms of a purely geometric parameter, the average effective resistance of a suitable electrical network. This yields important consequences due to the useful monotonicity properties of the effective resistances;
- to show that in a geometric graph the ℓ^2 performance cost is essentially the same as in a regular grid of similar dimension.

To give a tool to estimate the ℓ^2 cost in terms of the an average effective resistance is important since it allows to analyze the performance of the communication graph, instead of the particular consensus algorithm built on such a graph. Moreover, to prove that geometric graphs and regular grids "behave" in the same manner, with respect to the two metrics considered, is important since it shows that what really matters is not the highly symmetric structure of the former, but rather the dimension of the space in which the nodes are deployed. In particular, any fixed network of agents deployed in a "reasonable way" in an Euclidean space will perform qualitatively in the same manner, thus providing an important tool, for example to design a network of sensors.

Chapter 4 of this thesis deals with synchronization of networks of heterogeneous agents. In particular, each agent is modeled as a nominal SISO linear time invariant (LTI) system perturbed by a possibly nonlinear operator. The goal is to design an interconnection law to let each agent compute its input in such a way that the outputs asymptotically agree and remain synchronized. This is the already mentioned *higher order consensus problem*, and consensus is a particular case in which the common linear part is a simple integrator. Input/output techniques based on Integral Quadratic Constraints are used to propose a general theorem which ensures synchronization of the network. This result also ensures robustness, since it does not analyze a single perturbation case, but instead

offers a characterization for the perturbation operators to be satisfied in order for the synchronization to happen.

This basic result is particularized to many different cases of interest, such as

- interaction via a normal matrix: in this scenario the input at each agent is computed as a linear combination of the outputs of the neighbors, as in the linear consensus algorithm. If the matrix realizing such a combination is normal, it is shown that the general result can be reduced to a criterion involving its eigenvalues only;

- interaction via a normal matrix and linear perturbations: in many cases of interest, uncertainties in the internal dynamics of the agents can be modeled as LTI perturbations of the nominal system. If the interconnection matrix is normal, the system can be fully represented using frequency response, and we are able to propose a powerful Nyquist-like graphical criterion to check whether the network can synchronize or not.

- interaction via a normal matrix and quasi-saturation of the input: in case of formation control, the ideal input computed by an agent as a linear combination of the outputs of the neighbors might be too large to be directly applied, so it is quasi–saturated, namely underestimated, to a certain value. We show that this non–ideality can be modeled in our framework, and we prove that synchronization can be checked making use of a Popov graphical criterion;

- leader-following networks: this scenario arises in cases in which the nodes interact according to the aforementioned algorithm, but communication is not bidirectional. In particular, it can be that agents are divided in two groups, and that the agents of the first group, the leaders, are allowed to send information to those of the second group, the followers, while the reverse cannot happen. Under some conditions, the followers progressively forget their initial conditions and just align along the output synchronization trajectory of the leaders. This is well known in the consensus framework, and we analyze the more involving problem for higher order networks.

The consensus-like algorithms studied in the first two chapters are not only mathematical curiosities. In chapter 5 we concentrate on two important applications, clock synchronization and cameras calibration.

Clock synchronization is a fundamental goal in multi-agent networks since most algorithms require a common time reference in order to properly work. This is particularly important for energy consumption reasons in sensor networks, since they could be required to wake up and perform their operations in narrow temporal windows in order to save

energy and last longer. De–synchronization of such devices would be clearly fatal for the network since connection among the agents would be lost and impossible to be recovered.

We study a simplified version of a known model for clocks [9], in which each agent is modeled as a double integrator. If autonomous, the output of such a "clock" is a ramp shaped function whose initial value is the initial guess of the time, while the slope is related to a parameter of which is known only a nominal value. As we show, this is a typical case in which this uncertainty can be modeled as a LTI perturbation of a nominal system. We assume that clocks which are neighbors in the communication graph can exchange their time readings and make use of this information to produce an input which modifies both their time readings and an internal variable of them. In particular, the input to the k-th clock is produced as a linear combination of the time readings received, as in consensus.

We apply to this network of clocks the results of Chapter 4, and we provide a bound on how different the slopes of the clocks can be in order to still achieve synchronization. We also consider a network of equal clocks and we study how to ensure synchronization in case of quasi–saturation of the input.

As a last case for clock synchronization, we analyze what happens when the interconnection protocol is not deterministic but randomized, and we provide a criterion for synchronization in mean square.

The second important application we consider is cameras calibration. Pretty much similarly to clock synchronization, in a network of cameras a main problem is to ensure that all the cameras are aware of their pose, namely orientation and position, with respect to an external common reference frame. The information used by the agents in order to calibrate their orientation is the relative distance and the relative orientation among couples of cameras, which can be recovered offline by known algorithms. Of particular interest is calibration of the orientations, which very interestingly can be seen as an optimization problem in the manifold $SO(3)$ [10, 11, 12, 13]. In particular, such an optimization problem consists in minimizing a cost function defined on $SO(3)$ which shows multiple local minima, so that the gradient descent procedure usually proposed in literature must be initialized correctly in order to avoid to get stuck.

We study this problem in the simplified case of calibration on a plane, so that the manifold is the simpler $SO(2)$. Moreover, we consider a less ideal scenario in which the measurements of the relative orientations are corrupted by additive noise. We propose a novel two-step algorithm based on the cycles of the communication graph which aims to "cut" the manifold $SO(2)$ and transform it into a suitable segment. As we will see, this allows to rewrite the cost as a quadratic cost on the Euclidean space, which has a

unique minimum that is always reached by a gradient descent procedure. In case the measurements are noiseless, such a minimum is attained at the point which correctly calibrates the network. To handle the noisy case, we provide theoretical bounds on the noise in order to achieve the best possible performance.

2

Mathematical Tools

Throughout the dissertation we make use of several known notions on Graph Theory and Operators on Hilbert Spaces. We group in this Chapter the needed definitions and results without any claim of exhaustiveness, and we refer for a comprehensive treatment to the specialized books [14, 15, 16] for Graph Theory and [17, 18] for Operators.

2.1 Graph Theory

A graph is a quadruple $\mathcal{G} = (\mathcal{V}, \mathcal{E}, s, t)$ where $\mathcal{V}$ is called the set of nodes, $\mathcal{E}$ is called the set of edges, and t and h are two functions $t : \mathcal{E} \to V$ and $h : \mathcal{E} \to V$. If $t(e) = u$ we say that the edge e starts in u, or that u is the tail of e. If $h(e) = v$ we say that the edge e ends in v, or that v is the head of e. In this thesis we will always consider graphs in which there exist no *parallel edges*, namely edges e' and e'' such that $t(e') = t(e'')$ and $h(e') = h(e'')$, or in words which start and end at the same nodes. For this reason, we often denote a graph simply as the pair $\mathcal{G} = (\mathcal{V}, \mathcal{E})$, where $\mathcal{E} \subseteq \mathcal{V} \times \mathcal{V}$, and where an edge $e \in \mathcal{E}$ is simply denoted as $e = (u, v)$, where u is the tail and v is the head of e.

Given a graph $\mathcal{G} = (\mathcal{V}, \mathcal{E})$, a subset of nodes $\mathcal{V}' \subseteq \mathcal{V}$ and the subset of edges $\mathcal{E}' \subseteq \mathcal{E}$ such that for any edge $e = (u, v) \in \mathcal{E}'$, both $u \in \mathcal{V}'$ and $v \in \mathcal{V}'$, namely $\mathcal{E}' \subseteq (\mathcal{V}' \times \mathcal{V}') \cap \mathcal{E}$, we say that $\mathcal{G}' = (\mathcal{V}', \mathcal{E}')$ is a subgraph of $\mathcal{G}$. In particular, we say that $\mathcal{G}'$ is the subgraph induced by $\mathcal{V}'$ if $\mathcal{E}' = (\mathcal{V}' \times \mathcal{V}') \cap \mathcal{E}$.

We say that a graph is *undirected* if $(u,v) \in \mathcal{E} \iff (v,u) \in \mathcal{E}$, and in this case we use the simplified notation $\{u,v\}$. If a graph is not undirected, then it is called a *directed* graph, or *digraph*.

Given a node $u \in \mathcal{V}$, we denote by $\mathcal{N}_u^{in} = \{v \neq u : e = (v,\, u),\, \exists\, e \in \mathcal{E}\}$ the in-neighbor set of u, namely the set of nodes such that there exists an edge starting in such nodes and ending in u, apart from u itself in case of existence of self-loop. Analogously, we denote by $\mathcal{N}_u^{out} = \{v \neq u : e = (u,\, v),\, \exists\, e \in \mathcal{E}\}$ the out-neighbor set of u, namely the set of node such that there exists an edge ending in such nodes and starting from u, again excluding u. Clearly, for an undirected graph the two notions coincide, so we generically talk about the neighbor set, or neighborhood, $\mathcal{N}_u$ of u. For undirected graphs, the symbol $\delta_u = |\mathcal{N}_u|$ will denote the cardinality of the neighborhood of u.

A *path* $\gamma = \{(u_i, v_i)\}_{i=1,\dots,l}$ in the graph $\mathcal{G}$ from a node u to a node v is a set of edges $(u_i, v_i) \in \mathcal{E}$, $i = 1, \dots, l$, such that $u_1 = u$, $v_l = v$ and $v_i = u_{i+1}$ for all $i = 1, \dots, l-1$. The integer[1] $l := |\gamma|$ is called the length of the path. A path in which $u_1 = v_l$ is said to be a cycle.

A digraph is said to be *strongly connected* if there exists such a path from u to v for any pair $(u,v) \in \mathcal{V} \times \mathcal{V}$. A digraph is said to be *weakly connected* if, instead, there exists a path in the induced undirected graph in which any directed edge is replaced by an undirected one. Clearly, in undirected graphs, as it will often be the case in this dissertation, the notion of strongly and weakly connected coincide, so we generically say that an undirected graph is *connected*, or *disconnected*, which is, not connected.

Given a graph $\mathcal{G} = (\mathcal{V}, \mathcal{E})$, the *graphical distance* between u and v, denoted by the symbol $d_{\mathcal{G}}(u,v)$ is defined as follows

$$d_{\mathcal{G}}(u,v) = \begin{cases} 0, & u = v \\ \min\{|\gamma_{uv}| : \gamma_{uv} \text{ is a path from } u \text{ to } v\}, & \text{if a path exists from } u \text{ to } v \\ +\infty, & \text{otherwise} \end{cases} \tag{2.1}$$

namely $d_{\mathcal{G}}(u,v)$ is the minimum length of the paths from u to v or, if no path exists among them, then $d_{\mathcal{G}}(u,v) = +\infty$. This can happen in disconnected undirected graphs or in digraphs which are only weakly connected. Notice, instead, that in strongly connected digraphs the graphical distance of any pair of nodes is always a finite integer.

Given a graph $\mathcal{G} = (\mathcal{V},\, \mathcal{E})$, we denote by $N := |\mathcal{V}|$ and $M := |\mathcal{E}|$ respectively the number of nodes and edges, and often we label the set of nodes as $\mathcal{V} = \{1, 2, \dots, N\}$, and the same for the edges.

[1] The symbol $|X|$ denotes the cardinality of the set X.

It is often useful and elegant to describe a graph making use of its *incidence* matrix and of its *adjacency* matrix. Both fully describe graphs with no parallel edges, as in our case.

Definition 2.1.1 (Incidence matrix for directed graphs)**.** Let be given the digraph $\mathcal{G} = (\mathcal{V}, \mathcal{E})$, and label the nodes as $\mathcal{V} = \{1, \dots, N\}$ and the edges as $\mathcal{E} = \{1, \dots, M\}$. We define the incidence matrix $B \in \{0, \pm 1\}^{M \times N}$ as follows

$$B_{eu} = \begin{cases} -1 & \text{if } u = h(e) \\ 1 & \text{if } u = t(e) \\ 0 & \text{otherwise} \end{cases}, \tag{2.2}$$

so the e-th row, related to directed edge e, has a -1 in correspondence with its head, and a 1 in correspondence with its tail.

Remark 2.1.2. We will often assume that nodes and edges are labeled as in the previous definition in order to use the incidence matrix and the forecoming adjacency matrix. This labeling is arbitrary, and is only instrumental to write in matrix form the algorithms we propose.

The previous definition holds for digraphs. However, we often need to use incidence matrices in case of undirected graphs. In this case, the standard way to define the incidence matrix is by choosing, for each (undirected) edge $e = \{u, v\}$, an *orientation*, namely to decide which, among u and v, is the tail and which is the head. In other terms, given the undirected graph $\mathcal{G}_u$, we define a directed *oriented* graph $\mathcal{G}_o$ as follows: for each edge $e = \{u, v\}$ of $\mathcal{G}_u$, we choose either (u, v) or (v, u) and we form a set of oriented edges $\mathcal{E}_d$. Then $\mathcal{G}_o = (\mathcal{V}, \mathcal{E}_d)$. We define the incidence matrix of $\mathcal{G}_u$ as follows.

Definition 2.1.3 (Incidence matrix for undirected graphs)**.** Let be given the undirected graph $\mathcal{G} = (\mathcal{V}, \mathcal{E})$. Choose arbitrarily an orientation for it, namely choose $\mathcal{G}_o$. The incidence matrix of $\mathcal{G}$ is the incidence matrix of $\mathcal{G}_o$.

Clearly, this procedure leaves several degrees of freedom, since orientations (and labeling) are arbitrary. However, notice that the structure of the corresponding incidence matrices is essentially the same. A different definition of incidence matrix is sometimes given for undirected graphs [14]. However, the one given here is particularly useful for our scopes since incidence matrices give a naturally tool to describe flows of current in electrical networks, whose orientation is analogously arbitrary. We will see this in Chapter 3, Section 3.6.

Denote by $\mathbf{1}$ a vector of suitable dimension whose entries are all equal to 1. By definition, it is clear that $B\mathbf{1} = 0$ if B is the incidence matrix of a graph. The following lemma, which descends from the more general statement Theorem 8.3.1, [16], will be used, often implicitly, throughout the dissertation.

Lemma 2.1.4. *Let $\mathcal{G} = (\mathcal{V}, \mathcal{E})$ be a connected undirected graph. Then if B is an incidence matrix of $\mathcal{G}$*

$$\ker B = \operatorname{span}\{\mathbf{1}\}.$$

The second important matrix related to a graph is its adjacency matrix, defined as follows.

Definition 2.1.5. Let be given the graph $\mathcal{G} = (\mathcal{V}, \mathcal{E})$. The adjacency matrix of $\mathcal{G}$ is the matrix $A \in \{0, 1\}^{N \times N}$ in which

$$A_{uv} = \begin{cases} 1 & (v,u) \in \mathcal{E}, u \neq v \\ 0 & \text{otherwise} \end{cases}. \tag{2.3}$$

Notice that a graph is undirected if and only if its adjacency matrix is symmetric.

The following lemma gives the relation among adjacency and incidence matrix for undirected graphs. Notice that it holds for *any* incidence matrix of the undirected graph.

Lemma 2.1.6. *Let $\mathcal{G} = (\mathcal{V}, \mathcal{E})$ be an undirected graph, and let A and B be respectively its adjacency matrix and its incidence matrix, given an arbitrary orientation. Let $\Delta \in \mathbb{R}^{|\mathcal{V}| \times |\mathcal{V}|}$ a diagonal matrix whose (u,u)-th entry is the degree of u. Then*

$$B^T B = \Delta - A \tag{2.4}$$

Proof. On the diagonal $[B^T B]_{uu} = \sum_e B_{eu}^2 = \sum_{e:u=h(e)} 1 + \sum_{e:u=t(e)} 1 = \delta_u$ since an edge in the incidence matrix is either entering or exiting from u. Off diagonal $[B^T B]_{uv} = \sum_e B_{eu} B_{ev} = 0$ if $\{u,v\} \notin \mathcal{E}$, while $[B^T B]_{uv} = B_{(u,v)u} B_{(u,v),v} = -1$ if (u,v) is the chosen orientation of $\{u,v\} \in \mathcal{E}$, and analogously if the orientation is (v,u). □

Remark 2.1.7. Due to its importance in spectral graph theory, the matrix $\Delta - A$ is often called the *Laplacian* of the graph. In this dissertation the name Laplacian will be however used for a slightly different object, so we will usually avoid to talk about Laplacians of graphs. The unique exception is Section 4.4.

We often consider weighted graphs, namely couples $(\mathcal{G}, w)$ in which $\mathcal{G}$ is a graph and $w : \mathcal{E} \to \mathcal{R}$ is a function which associates to each (directed) edge its weight, a positive

real number. Given a matrix $P \in \mathbb{R}^{N\times N}$, we define the graph *associated with* P, and we denote it by $\mathcal{G}_P$, to be a graph with set of nodes $\mathcal{V} = \{1, 2, \ldots, N\}$ and edge set $\mathcal{E}_P := \{(u, v) \in V \times V \ : \ P_{vu} \neq 0\}$. We say, on the converse, that a graph $\mathcal{G}$ is *consistent with* P if $\mathcal{G}_P$ is a subgraph of $\mathcal{G}$. Notice that this means that $P_{uv} \neq 0 \Rightarrow (v, u) \in \mathcal{E}$.

2.2 Operator Theory

An Hilbert space $\mathcal{H}$ is a complete normed vector space over a field $\mathbb{F}$ with norm induced by an inner product. In this dissertation we are mainly interested in the cases in which $\mathcal{H}$ is either the continuous time signal space $\mathbf{L}_2[0, \infty)$ or the discrete time signal space $l_2(0, \infty)$. Vector valued versions are denoted $\mathcal{H}^n$, where n denotes the spatial dimension of the signals.

The truncation operator $P_T : \mathcal{H}^n \to \mathcal{H}^n$ is defined as

$$(P_T v)(t) = \begin{cases} v(t), & t \leq T \\ 0, & t > T \end{cases}$$

It is easy to see that P_T is linear, so we write for simplicity $P_T(v) = P_T v$.

Given $\mathcal{H}^n$, the corresponding extended space consists of signals for which $P_T v \in \mathcal{H}^n$, $\forall T \geq 0$.

An operator H on $\mathcal{H}_e^n$ is causal, or non-anticipative, if $P_T H(v) = P_T H(P_T v)$ for all $T \geq 0$ and all $v \in \mathcal{H}_e^n$.

We define the gain of the operator $H : \mathcal{H}_e^n \to H_e^n$ to be

$$\gamma(H) = \sup_{\substack{v\in\mathcal{H}^n \\ v\neq 0}} \left\{ \frac{\|H(v)\|}{\|v\|} \right\},$$

where $\|\cdot\|$ is a norm on $\mathcal{H}^n$. An operator is said to be *bounded* if its gain is bounded.

An operator is said to be *linear* if it holds

$$H(\alpha_1 v_1 + \alpha_2 v_2) = \alpha_1 H(v_1) + \alpha_2 H(v_2), \forall v_1, v_2 \in \mathcal{H}, \alpha_1, \alpha_2 \in \mathbb{F}$$

A causal linear–time invariant operator has a convolution representation in the sense

that it acts as

$$(Hv)(t) = \int_0^t h_c(t-\tau)v(\tau)d\tau + h_0 v(t) \tag{2.5}$$

$$(Hv)(t) = \sum_{k=0}^{n} h(t-k)v(k) \tag{2.6}$$

in continuous and discrete time, respectively. The signal h is called impulse response function.

If the operator is bounded then we have the equivalent frequency domain representation

$$\widehat{Hv}(j\omega) = \widehat{H}(j\omega)\widehat{v}(j\omega)$$

in continuous time, and

$$\widehat{Hv}(e^{j\omega}) = \widehat{H}(e^{j\omega})\hat{v}(e^{j\omega})$$

in discrete time, where $\widehat{H}$ and $\hat{v}$ are the frequency response and Fourier transform of $v \in \mathcal{H}^n$, respectively. $\widehat{H}(s)$ and $\widehat{H}(z^{-1})$ will denote respectively the Laplace transform and the Z transform of h in continuous and discrete time.

We denote by Ω the instability domain and $\partial\Omega$ its boundary. In the case of continuous time systems we have $\Omega = \{s : \mathrm{Re}s \geq 0\}$ and $\partial\Omega = j\mathbb{R}$. In the case of discrete time systems we have $\Omega = \{z : |z| \geq 1\}$ and $\partial\Omega = e^{j[0,\,2\pi]}$.

We denote by $\mathcal{H}_d^n$ the space of signals on the doubly infinite time–axis $\mathbf{L}_2^n(-\infty,\infty)$, or $l_2^n(-\infty,\infty)$, with corresponding frequency domain space $\widehat{\mathcal{H}}_d$ being either $\mathbf{L}_2(j\mathbb{R})$ or $\mathbf{L}_2[0,2\pi]$.

Given a bounded operator $\Psi : \mathcal{H}_d^n \to \mathcal{H}_d^n$, its adjoint Ψ^* is defined by the relation

$$\langle w, \Psi v\rangle = \langle \Psi^* w, v\rangle, \forall w, v \in \mathcal{H}_d^n$$

where $\langle\cdot,\cdot\rangle$ denotes the inner product. We say that Ψ is *self-adjoint* if $\Psi = \Psi^*$.

A self–adjoint bounded linear time–invariant operator $\Psi : \mathcal{H}_d^n \to \mathcal{H}_d^n$ defines in a natural way a quadratic form defined as

$$\sigma_\Psi(v) = \langle v, \Psi v\rangle$$

We say that Ψ is positive definite, and we denote this by $\Psi > 0$, if there exists a real $\epsilon > 0$ such that

$$\langle v, \Psi v\rangle \geq \epsilon\|v\|^2, \forall v \in \mathcal{H}_d^n$$

A necessary and sufficient condition for Ψ to be positive definite is that

$$\widehat{\Psi}(j\omega) = \widehat{\Psi}(j\omega)^* > 0, \forall \omega \in \mathbb{R} \cup \{\infty\}$$

in continuous time, and

$$\widehat{\Psi}(e^{j\omega}) = \widehat{\Psi}(e^{j\omega})^* > 0, \forall \omega \in [0, 2\pi]$$

in discrete time.

In this dissertation we use the algebra $\mathcal{A}_c$ consisting of LTI operators with impulse responses functions of type

$$h(t) = h_c(t)\theta(t) + h_0\delta(t)$$

where $h_c \in \mathbf{L}_1^{m\times m}[0,\infty)$, $h_0 \in \mathbb{R}^{m\times m}$, $\theta(\cdot)$ and $\delta(\cdot)$ denote the unit step function and the dirac delta function, respectively. Under these assumptions, h can be seen as the impulse response of a bounded LTI operator via the convolution in Eq. 2.5.

We let $S_{\mathcal{A}_c}^{n\times n}$ be the set of bounded LTI operators on $\mathbf{L}_2^n(-\infty,\infty)$ defined by impulse response functions of the form

$$h(t) = h_c(t) + h_0\delta(t)$$

where $h_c(t) = h_c(-t)^T \in \mathbf{L}_1^{m\times m}(-\infty,\infty)$ and $h_0 = h_0^T \in \mathbf{R}^{m\times m}$. The transfer function $\widehat{\Psi}(s)$ of $\Psi \in S_{\mathcal{A}}^{m\times m}$ satisfies $\widehat{\Psi}(s) = \widehat{\Psi}(-s)^T$ in its domain of definition, which includes the imaginary axis. It is thus self-adjoint and will be used to define quadratic forms under the framework of the Integral Quadratic Constraints theory.

Similarly, $\mathcal{A}_d$ denotes the bounded LTI operators on $l_2(0,\infty)$ defined by the convolution in Eq. 2.6 with an impulse response function satisfying $\sum_{k=0}^{\infty}|h_k| < \infty$. Similarly, $S_{\mathcal{A}_d}^{n\times n}$ denotes the LTI bounded operators on $l_2^n(-\infty,\infty)$ defined by impulse response functions with $h_k = h_{-k}^T$ and $\sum_{k=-\infty}^{\infty}|h_k| < \infty$. Any transfer function $\widehat{\Psi}(z)$ of $\Psi \in S_{\mathcal{A}_d}^{m\times m}$ satisfies $\widehat{\Psi}(z) = \widehat{\Psi}(-z)^T$ and is thus self-adjoint.

We often use the short–hand notation $\mathcal{A}$ and $S_{\mathcal{A}}^{n\times n}$ to denote an LTI operator that could be either continuous or discrete time.

3

Analysis of Consensus Networks

3.1 Introduction

As mentioned in the Introduction, one of the most important, interesting and challenging research topics of the last two decades is Network Control Theory. This topic arose from the disposal of large scale networks of sensors and robots, and from the necessity to unify the different approaches to control, estimation, data fusion.

Among the possible distributed tasks a multi-agent network is required to carry on, one of the most important is *agreement*, and in particular *averaging*. By agreement, we mean a procedure, or algorithm, such that a group of agents having different initial guesses of some quantity of interest share them and update them. The update rule must be designed to ensure that all the agents finally share the same estimate of the quantity of interest, possibly in finite time. This problem is commonly called *consensus problem*. In the particular case in which a notion of "average" exists, and if the agreement on the quantity of interest is required to be the average of the initial guesses, we speak of *average consensus problem*.

Due to its appealing simplicity, one of the most important and studied consensus algorithms is the *linear consensus algorithm*, which we introduce in Section 3.2. Intuitively, it is a linear iteration rule in which the local variable of each node u is updated as a convex combination the variables of the neighbors of u.

Among the applications proposed in the literature for the linear consensus algorithm there are

- formation control [19, 20, 21, 22]: given a network of robots moving in a plane, one of the most basic control formation problems is rendez-vous, namely the ability for the robots to gather at one point. This can be done using consensus, being the "quantity of interest" the position of the robot in the plane.

- distributed estimation [23, 24, 25, 26, 27, 28, 29]: in this scenario each agent possesses an initial measurement of some quantity of interest, for example the temperature in a room. The averaging procedure is then used in order to average out the measurement noise and refine the measurements when a way to collect all of them must be avoided. Moreover, with some refinement consensus algorithm is also used in estimation and filtering of dynamical systems as a tool to design an effective distributed Kalman-like filters;

- load balancing [30, 31]: consider a network of parallel computers. In this case the quantity of interest is the computational load each agent has to process, and the averaging procedure consists in exchanging duties in order the computational load to be more or less the same for all the agents;

- sensor calibration for sensor networks [32, 33, 34, 35, 36]: when a sensor network is deployed in a space, is is often of major interest that each agent knows its position in an external, common reference frame. It is known that sometimes the problem of estimating the distance among the sensors can be recast into a consensus problem with noise. In Chapter X5 we consider a variation of this problem in which each agent wants to estimate its *orientation* with respect to an external reference frame;

- distributed optimization [37, 38, 39, 40, 41, 42, 43]: it is often the case that a global function to be computed can be decomposed as the sum of local contributions, which are local minimization problems. In this framework, consensus is often used as an effective tool for data fusion and information merging;

- distributed demodulation [44, 45]: as in the previous cases, consensus can be effectively used as a tool in order to average out noise and provide data fusion when a group or sensors receive a low SNR signal from multi-antennas and what to improve their ability to demodulate the message.

In this dissertation we consider the simplest case of linear consensus, in which the update law is deterministic and time-invariant, and we always assume that the

minimal assumptions for agreement are satisfied. Our main interest is in measuring the performance of consensus algorithm. Given in fact the weights of the convex combination which represents the update law, we study two well-known metrics that give a measure of how "good" the linear consensus algorithm is. More precisely, we study the rate of convergence to consensus, which is related on how fast consensus is reached, and a linear quadratic (LQ) cost, also called ℓ_2 cost, which has an interpretation as the norm of the difference among the trajectory of the states and the asymptotic consensus value. In particular, two aspects are of great interest

- how the metric is influenced by geometric characteristics of the communication graph: this is of great importance when it is possible to choose among different graph topologies for the communication graphs, so it is necessary to give tools to compare them;
- how the metric scales with the dimension of the network, namely with the number of agents: it is known that in many cases the performance of a consensus algorithm degrades if the number of agents increases. Understanding how fast this degradation happens for a certain graph gives a qualitative threshold on the maximum number of agents in order to maintain prescribed performance.

Notice that, concerning the first point, one can wonder whether the metrics are coherent in comparing different graph structures or not, namely if the fact that a certain graph $\mathcal{G}_1$ is better than another graph $\mathcal{G}_2$ if compared through a certain performance metric implies that the same happens for any other metric. Recent papers gave some partial answers to this question, suggesting that the geometric structure of a graph does play a fundamental role, which should be a primal guidance in the design process.

The contributions of this Chapter to the literature can be summarized as follows:

- we consider a large class of undirected graphs, called *geometric graphs*, which well model actual fixed sensor networks deployed in the Euclidean space $\mathbb{R}^d$. We prove that for symmetric consensus protocols built on such graphs, the rate of convergence to consensus essentially depends on the dimension d and on the number of agents in the network only. This extends and unifies known results for highly symmetric graphs. These results are published in the papers [46, 47]
- for the ℓ_2 cost, we present an estimate which only depends on a geometric parameter of the communication graph, its *average effective resistance*. Despite the fact that this result does not hold for *any* linear consensus protocol, we provide important applicative examples in which this happens. These results are published in the papers [48, 49, 50]

- for geometric graphs, we show that the ℓ_2 cost again essentially depends on the dimension d and on the number of agents in the network only. This result extends and unifies known results in literature. These results are published in the papers [48, 49, 50]

We want to remark that the notion of geometric graph is not new, since it dates back at least to the outstanding book [51], in which the authors draw a deep and useful parallel among Markov Chains and electrical resistive networks, and use this parallel to prove the well known Polya's theorem in an elegant and simple way. This parallel is also the starting point for our theorem, since Markov Chains and consensus algorithms are essentially the same objects, as we will point out. We also underline that the notion we give of geometric graph can be seen as a deterministic counterpart of the well-known *random geometric graph* (see [52, 53]).

3.2 The linear consensus algorithm

Consider a network of interconnected agents, and assume that the agents are labeled as $\mathcal{V} = \{1, \dots, N\}$. Let $\mathcal{G} = (\mathcal{V}, \mathcal{E})$ be the communication graph, in which $\mathcal{E} \subseteq \mathcal{V} \times \mathcal{V}$ describes which communication links between the agents are allowed. In other terms, as already mentioned, we say that $(u, v) \in \mathcal{E}$ if and only if the agent u can send information to v. In the linear consensus algorithm, at each iteration the agents send their current state to their neighbors, and then update it as a suitable convex combination of the received messages. More precisely, if $x_u(t)$ denotes the state of the agent $u \in \mathcal{V}$ at time $t \in \mathbb{N}$, then

$$x_u(t+1) = \sum_{v \in \mathcal{V}} P_{uv} x_v(t)\,, \tag{3.1}$$

where P_{uv} are the entries of a matrix P. It is common to say that P_{uv} is the weight the agent u gives to the information coming from its neighbor v.

In order for Eq. 3.1 to describe a convex update, the matrix P must be stochastic, namely fulfill the following definition.

Definition 3.2.1. A matrix $P \in \mathbb{R}^{N \times N}$ is said to be stochastic if $P_{uv} \geq 0$ for all $u, v \in \mathcal{V} = \{1, \dots, N\}$ and $\sum_{v \in \mathcal{V}} P_{uv} = 1$ for all $u \in \mathcal{V}$.

In a compact matrix form, we can rewrite the update law in Eq. 3.1 as

$$\boldsymbol{x}(t+1) = P\boldsymbol{x}(t) \tag{3.2}$$

where $\boldsymbol{x}(t) \in \mathbb{R}^N$ denotes the vector collecting all agents' states. The constraint imposed

by the communication graph $\mathcal{G}$ is enforced by requiring that $\mathcal{G}_P$ is a subgraph of $\mathcal{G}$, where $\mathcal{G}_P = (\mathcal{V}, \mathcal{E}_P)$ is the graph associated with the matrix P defined assuming that $(v, u) \in \mathcal{E}_P$ if and only if $P_{uv} \neq 0$ (see Section 2.1). In other terms, given a directed edge (v, u) in the communication graph, node u can decide whether to use information coming from v, and in this case $P_{uv} > 0$, or not, and in this case $P_{uv} = 0$. There are cases in which it is more convenient to design the consensus algorithm avoiding to use some of the edges — even if they're at disposal — due to particular geometries of the communication graph, as in De Bruijn's graphs proposed in Section 3.4 and in relation to the rate of convergence to consensus.

In this framework, the theory of positive matrices can be profitably used in order to study consensus algorithms.

A stochastic matrix P is said to be *irreducible* if the associated graph is strongly connected, namely, for all $u, v \in \mathcal{V}$, there exists a path in $\mathcal{G}_P$ connecting u to v, and it is said to be *aperiodic* if the greatest common divisor of the lengths of all cycles in $\mathcal{G}_P$ is one. Notice that the presence of a self-loop, namely a $P_{uu} > 0$ for some $u \in \mathcal{V}$, ensures aperiodicity.

Remark 3.2.2. Irreducibility and aperiodicity are independent properties. For example the matrix

$$P = \begin{bmatrix} 0 & 1 \\ 1 & 0 \end{bmatrix}$$

corresponds to a ring with two agents exchanging each time their value. Such matrix is irreducible but not aperiodic.

On the converse, the matrix

$$P = \begin{bmatrix} 1 & 0 \\ 1 & 0 \end{bmatrix}$$

which corresponds to a tree with two nodes, is aperiodic, but not irreducible.

An irreducible aperiodic matrix is called primitive. As it is well known from Frobenius-Perron theory [54], if P is primitive, then P has the eigenvalue 1 with algebraic multiplicity 1, and all other eigenvalues have absolute value strictly smaller than 1 and so we have that

$$P^t \overset{t\to\infty}{\longrightarrow} \mathbf{1}\boldsymbol{\pi}^T$$

where the vector $\boldsymbol{\pi}$ is the *invariant measure* of the matrix P, namely the left eigenvector of P corresponding to the eigenvalue 1, properly scaled so as to have $\sum_u \pi_u = 1$. The same theorem also ensures that all the entries $\boldsymbol{\pi}$ are strictly positive, namely that $\pi_i > 0$, $\forall i$.

Remark 3.2.3. Aperiodicity is needed in order to ensure that the eigenvalue 1 has multiplicity 1, and thus the states align to the vector $\mathbf{1}$, thus reaching consensus. Irreducibility is also needed to ensure that $\pi_i > 0$, $\forall i$, which means that the agreement value makes some use of all the initial conditions. In fact, dropping irreducibility property we obtain a network in which the agents of a first subset (the strongly connected component, in which there is a path from any node to any other node) act as leaders, while a second subset of agents (which is only able to receive information from the leaders) act as followers, progressively forgetting their initial conditions and aligning to the consensus value decided by the leaders. After all, analysis can be reduced to analysis of the subgraph of the leaders. This fact becomes more interesting in Higher Order Consensus Networks, which we treat in Chapter 4, Section 4.4.

Under the assumption P to be primitive, the states of the consensus algorithm (namely, the states that evolve according to Eq. 3.1) converge to the same value $x_u(t) \overset{t\to\infty}{\longrightarrow} \alpha$, where $\alpha = \boldsymbol{\pi}^T \boldsymbol{x}(0)$. Thus, the agents reach consensus on the value of their states $x_u(t)$, since they all converge to the same number α, called the consensus value. Notice that, if P is doubly stochastic, namely if both P and P^T are stochastic, then $\boldsymbol{\pi} = \frac{1}{N}\mathbf{1}$ and so the consensus value α is equal to the average of the initial states. In this case we achieve average consensus.

Clearly, one wonders under which conditions the matrix P is primitive and thus is allows to achieve consensus. The following Proposition, adapted from [55], proposes an example of mild sufficient conditions on the communication graph. Basically, the strongly connectivity condition imposes that "information coming from one node is received from any other", while the self–loop conditions ensures aperidicity of the graph.

Proposition 3.2.4 ([55])**.** *Consider a stochastic matrix P associated to a directed graph $\mathcal{G}_P$. Assume that $P_{uu} > 0$, $\forall\, u \in \mathcal{V}$, and that $\mathcal{G}$ is strongly connected. Then the matrix P is primitive.*

Popular consensus strategies

We briefly present in this Section three popular and simple strategies to design a consensus protocol.

Let $\mathcal{G} = (\mathcal{V}, \mathcal{E})$ be a connected undirected communication graph. A first very popular and simple way to achieve consensus is to let the state $\boldsymbol{x}(t)$ evolve according to the rule

$$x_u(t+1) = x_u(t) + \varepsilon \sum_{v \in \mathcal{N}_u} (x_v(t) - x_u(t))$$

where ε is a suitable positive real scalar. In fact, if B is the incidence matrix of the graph, it is easy to see that this evolution can be expressed in matrix form as

$$\boldsymbol{x}(t+1) = (I - \varepsilon B^T B)\boldsymbol{x}(t) = P\boldsymbol{x}(t)$$

thus ε must be sufficiently small so that all the entries of $P = I - \varepsilon B^T B$ are positive. In particular, it must hold $\varepsilon \in \left(0, \frac{1}{\max_u\{\delta_u\}+1}\right)$, where δ_u is, recall, the degree of node u.

The choice of ε is therefore a *global* task, and can be sometimes difficult to be done. Another possibility is to choose the Metropolis-Hastings weights, for which

$$P_{uv} = \begin{cases} \frac{1}{\max\{\delta_u,\delta_v\}+1}, & (v,u) \in \mathcal{E}, u \neq v \\ 1 - \sum_{t\in\mathcal{N}_u} P_{ut}, & u = v \\ 0, & \text{otherwise} \end{cases}$$

As it is easy to see, the resulting matrix P is still symmetric and allows to achieve consensus. The good point is that it can be built using only very local properties, namely the number of the neighbors of the neighbors.

A third very popular way is to use uniform weights, namely to set

$$P_{uv} = \frac{1}{\delta_u + 1}$$

if $(u,v) \in \mathcal{E}$ or $u = v$, and $P_{uv} = 0$ otherwise. It is trivial to see that if A is the adjacency matrix of the graph, then

$$P = \operatorname{diag}\left((A+I)\mathbf{1}\right)^{-1}(A+I)$$

This strategy is the easiest to implement, since it requires only to know how from how many neighbors an agent receives information, however it does not allow, in general, average consensus, not even in case of undirected graphs.

Brief review of the literature

While the pioneering work [1] proposed and studied the linear consensus algorithm for applications to distributed estimation and load balancing, much work has been done in the last decade motivated by the formation control problem [19, 20]. Moving on with respect to the case in which the weights are fixed and the evolution is purely deterministic, many papers included in the model more realistic scenarios, such as packet-drop communication and delays [56, 57, 58, 59, 60, 61], and some others have been devoted to the study of

randomized consensus algorithms, namely consensus algorithms in which $P(t)$ is itself a matrix valued stochastic process [62, 63, 53, 64, 65].

As the classical theory suggests, the typical trajectory which the states draw while approaching the consensus value is exponential in time, and many papers have been devoted to the study of the exponential rate of convergence, both for structured graphs [66, 67, 68, 69, 70, 71, 72, 73], and in terms of optimization problems [74, 75, 76, 77, 78, 79]. We will consider this issue in Section 3.5. To conclude, since consensus is often considered an algorithm which has a direct application to many sensor network problems, much effort has been spent trying to understand how consensus behaves under some typical constraints in communications, such as quantization of information and noisy channels [80, 81, 82, 83, 84, 85, 60, 61].

Linear Consensus in Continuous Time, Laplacians, and Consensus as an Optimization Problem

In the previous Section we have recalled what is meant by linear consensus algorithm in discrete time. The analogous state update in continuous time takes the form

$$\dot{\boldsymbol{x}}(t) = -\nu L \boldsymbol{x}(t) \tag{3.3}$$

where $L \in \mathbb{R}^{N\times N}$ has a 1-dimension kernel spanned by the vector $\mathbf{1}$, namely $L\mathbf{1} = 0$, its off-diagonal entries are non-positive, and is consistent with the communication graph $\mathcal{G} = (\mathcal{V}, \mathcal{E})$, in the sense that $L_{uv} < 0 \Rightarrow (v, u) \in \mathcal{E}$. The value $\nu \in \mathbb{R}$ is a parameter which can be tuned, even if in real applications is cannot be raised above a certain threshold.

The most typical choice is to set L to be the Laplacian of a primitive stochastic matrix P consistent with the communication graph, namely

$$L := I - P \tag{3.4}$$

where I is the $N \times N$ identity. Notice that the properties of L are trivially satisfied due to the properties of P.

Is is also worth to notice that discrete-time consensus can be rewritten as

$$\boldsymbol{x}(t+1) = (I - L)\boldsymbol{x}(t)$$

thus Laplacian can be directly used in order to design a consensus algorithm. For example, the first protocol proposed above has $L = \varepsilon B^T B$.

Remark 3.2.5. An alternative way to introduce consensus is to consider the problem of

studying the evolution of the simple system

$$\boldsymbol{x}(t+1) = \boldsymbol{x}(t) + \boldsymbol{u}(t)$$

and to give a rule to compute $\boldsymbol{u}(t)$ in order for the system to reach consensus. This type of system was studied for the formation control case, in which the quantity $x_u(t)$ is not directly at disposal of node u, since it is an absolute position. Nonetheless, each robot is able to compute its control $u_u(t)$ according to the *relative distance* of u and its neighbors. The simplest way to produce the control is thus taking

$$u_u(t) = \nu \sum_{v \in \mathcal{N}_u} L_{uv}(x_v(t) - x_u(t))$$

where L_{uv} are positive weights which penalize the distance among u and its neighbor v. As is clear, the matrix $L = [L_{uv}]$ is the Laplacian of a stochastic matrix P.

This way of interpreting consensus as agreement by penalization of the distance among neighbors turns out to be very interesting in many cases in which only relative information is at disposal of the single agents, see for example [86].

To conclude this section, we briefly recall that given the Laplacian L and the "cost function"

$$J_L(\boldsymbol{x}) = \frac{1}{2}\boldsymbol{x}^T L \boldsymbol{x}$$

then consensus algorithm for example in continuous-time is simply a gradient descend optimization procedure for the cost, namely

$$\dot{\boldsymbol{x}}(t) = -\varepsilon \mathrm{grad} J_L(\boldsymbol{x}(t)) = -\varepsilon L \boldsymbol{x}(t)$$

This way to interpret a consensus algorithm will be used in Chapter 5, where we consider the natural generalization of this type of cost in the case of consensus in the manifold $\mathcal{S}_1$.

Linear Consensus and Markov Chains

As mentioned in the previous Section, a linear consensus protocol consists in a linear update of the type

$$\boldsymbol{x}(t+1) = P\boldsymbol{x}(t)$$

where P is a stochastic matrix. Called $\boldsymbol{\pi}$ the invariant measure of P, namely the (positive by Frobenius-Perron theorem) vector such as $\boldsymbol{\pi}^T\mathbf{1} = 1$ and $\boldsymbol{\pi}^T P = \boldsymbol{\pi}^T$, we have that

$$\boldsymbol{x}(t) \overset{t\to\infty}{\longrightarrow} \boldsymbol{\pi}^T\boldsymbol{x}(0)\mathbf{1}$$

thus achieving consensus.

Markov Chains are stochastic finite-state systems in which a probabilistic law is given to jump from the generic state u to the generic state v. In other terms, if $\mathcal{V} = \{1, \dots, N\}$ are the states of the chain, for every u there are N non-negative values, $p_{u1}, p_{u2}, \dots, p_{uN}$, which represent the probability to jump from u to the state $1, \dots, N$. Clearly, in order to avoid meaningless scenarios, it must hold true

$$\sum_{v=1}^{N} p_{uv} = 1, \forall\, i.$$

Once we gather these values in a matrix P such that $[P]_{uv} = p_{uv}$, it is manifest that we obtain a stochastic matrix, exactly of the same type as those used in consensus. The matrix P is called the matrix of transition probabilities of the chain. In case the matrix is primitive, the left invariant measure $\boldsymbol{\pi}$ has a straightforward interpretation as the asymptotic probability of the states in the chain. In other terms, starting from any state and waiting for "enough" time, the value π_u gives the probability that the chain is in the state u.

3.3 Reversible consensus matrices

Among all the stochastic matrices, a particularly important subclass is that of reversible consensus matrices, a name coming from the definition of reversible Markov Chains (see for example [87]).

Definition 3.3.1. Let $P \in \mathbb{R}^{N\times N}$ be the transition probability matrix of a Markov Chain, and assume that $\boldsymbol{\pi}$ is the invariant measure of P. The chain is said to be reversible if

$$\pi_u P_{uv} = \pi_v P_{vu}, \forall u, v \in \mathcal{V} \tag{3.5}$$

Somehow conversely, if Eq. 3.5 holds true for a set of nonnegative scalars $\pi_1, \dots, \pi_N$, then $\boldsymbol{\pi}^T = \begin{bmatrix}\pi_1 & \dots & \pi_N\end{bmatrix}$ is the invariant measure of the chain, which of course is reversible.

It can be easily shown that if the chain is reversible and we are at steady state, namely we wait for enough time so that the probability of the chain to be in state u is given by

π_u, then if we observe a sequence of states

$$x_1 x_2 \dots x_n$$

we cannot recognize whether it was walked forward or backward in time. Hence the name reversible.

On the basis of this definition, we clarify what we mean by reversible matrix.

Definition 3.3.2. Given a stochastic matrix P, we say that it is reversible if there exists a diagonal semi-positive definite matrix Π such that

$$\Pi P = P^T \Pi \tag{3.6}$$

One can easily see that this is the matrix form of Definition 3.3.1 once we normalize Π in such a way that $\sum_{u=1}^{N} \Pi_{uu} = 1$. Clearly, this implies that $\Pi = \operatorname{diag}(\boldsymbol{\pi})$ where $\boldsymbol{\pi}$ is the invariant measure of P.

Remark 3.3.3. The graph associated with a stochastic matrix P in general is a directed graph. However, if it happens that $\pi_u > 0$, $\forall u$, then reversibility of the matrix implies that the graph is undirected. This is clear by definition, since $\pi_u P_{uv} = \pi_v P_{vu}$ and $\pi_u > 0$, $\pi_v > 0$ imply that $P_{uv} > 0 \iff P_{vu} > 0$, and thus in the associated graph $(v, u) \in \mathcal{E} \iff (u, v) \in \mathcal{E}$.

Example 3.3.4. The most important case of reversible matrices is the symmetric case. In fact, in case P stochastic primitive is symmetric, we have $\boldsymbol{\pi} = \frac{1}{N}\mathbf{1}$, thus $\pi_i = \frac{1}{N}$, $\forall i$, and Eq. 3.6 is trivially satisfied.

Since we are interested in primitive matrices, we also have that $\pi_u > 0$, $\forall u \in \mathcal{V}$. For this case, some important properties of reversible stochastic matrices are summarized in the following lemma, of which we give the simple proof for completeness.

Lemma 3.3.5. *Let $P \in \mathbb{R}^{N \times N}$ be a primitive reversible stochastic matrix with invariant measure $\boldsymbol{\pi}$, and let $\Pi = \operatorname{diag}(\boldsymbol{\pi})$. Then*

- *P is self-adjoint with respect to the inner product $\langle \cdot, P\cdot \rangle_\Pi$*
- *$\tilde{P} = \Pi^{1/2} P \Pi^{-1/2}$ is symmetric.*
- *all the eigenvalues of P are real;*
- *P has N independent eigenvectors, which are orthogonal w.r.t. the inner product $\langle \cdot, \cdot \rangle_\Pi$.*

Proof. From Eq. 3.6 we have

$$\langle \boldsymbol{x}, P\boldsymbol{y} \rangle_\Pi = \boldsymbol{x}^T \Pi P \boldsymbol{y} = \boldsymbol{x}^T P^T \Pi \boldsymbol{y} = \langle P\boldsymbol{x}, \boldsymbol{y} \rangle_\Pi$$

Notice that this holds true also in the general case $\pi_u \geq 0$, $\forall u$.

The second property is immediate from Eq. 3.6 multiplying on the left and on the right by $\Pi^{-1/2}$, which exists, and obtaining $\tilde{P} = \tilde{P}^T$. By definition, $\tilde{P}$ and P are similar, thus share the same set of eigenvalue, which are real since $\tilde{P}$ is symmetric.

Putting $\tilde{P}$ in Jordan form, we get $\tilde{P} = UJU^T$, where the columns of U are N orthogonal eigenvectors of $\tilde{P}$. This implies $P = \Pi^{-1/2} U J U^T \Pi^{1/2} = V J V^{-1}$, where the columns of V form a set of independent eigevectors of P. The fourth propery now follows since

$$\langle V, V \rangle_\Pi = V^T \Pi V = U^T \Pi^{-1/2} \Pi \Pi^{-1/2} U = I$$

where I is the $N \times N$ identity. □

3.4 Graph architectures

Multi-agents systems of the type we are interested in usually consist in swarms of robots, networks of sensors, and so on. In this section we propose some graphs structures, or graph topologies, which are commonly found in literature as skeleton architectures for networks of such intelligent devices.

Cayley graphs

Cayley matrices and tori are highly structured matrices and graphs which present a number of symmetries, and that are defined through groups. They can be seen as idealized architectures, so that in actual communication graphs which are similar to tori we can expect similar behaviors in terms of algorithm performance.

Definition 3.4.1. Let G be an finite Abelian group of order $N = |G|$. A matrix $P \in \mathbb{R}^{G \times G}$ is said to be a Cayley matrix over the group G if

$$P_{i,\,j} = P_{i+h,\,j+h},\ \forall\, i,\ j,\ h \in G. \tag{3.7}$$

Notice that in the previous definition the elements of P are indexed not with the usual integer numbers, but rather with the elements of the group, so that the $+$ symbol in Eq. 3.7 denotes the operation of the group. Clearly, in order to consider P as a matrix we need, as usual, to label these elements with integers $\{1, \ldots, N\}$.

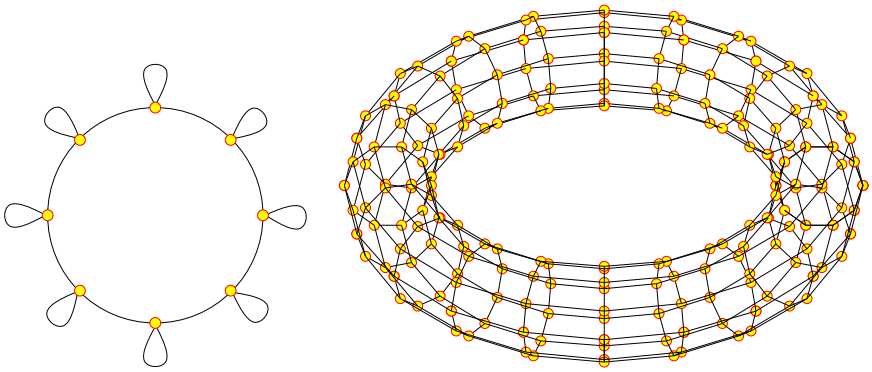

Figure 3.1: Two examples of d-dimensional tori.

It is easy to see [88] that there exists a function $\boldsymbol{g} : G \to \mathbb{R}$, called generator, such that $P_{ij} = \boldsymbol{g}(i-j)$. Note that $\boldsymbol{g}$ can be read from any row of P. A graph $\mathcal{G}$ is a d-dimensional torus if its adjacency matrix is a Cayley matrix. With this definition it is obvious that the graph associated with a Cayley matrix is automatically a torus, or more precisely a d_g-regular lattice on a d-dimensional torus, where d_g is the number of neighbors of each node. A d-dimensional torus is completely determined by giving the group G and a set $S \subseteq G$. Indeed, the set of edges $\mathcal{E}$ of a torus is such that $(i,\, j) \in \mathcal{E}$ if and only if $j - i \in S$.

In Fig. 3.1 two tori are presented. On the left, $G = \mathbb{Z}_8$ and $S = \{\pm 1,\, 0\}$ generate the circle with $N = 8$ nodes, in which each agent communicates with the node on the left and on the right. On the right, $G = \mathbb{Z}_{20} \times \mathbb{Z}_{10}$ and $S = \{(-1, 0),\, (1, 0),\, (0, 1),\, (0, -1)\}$ generates the torus with $N_1 = 20$ circles of $N_2 = 10$ nodes each, where each agent communicates with the nodes on the left, on the right, above and below.

Notice that any finite Abelian group G is isomorphic to the group $\mathbb{Z}_{n_1} \times \cdots \times \mathbb{Z}_{n_d}$, for some $n_1, \ldots, n_d \in \mathbb{N}$. In order to simplify the notation, in this paper we will restrict to d-dimensional tori with respect to groups of the type $\mathbb{Z}_n^d$. Moreover we will always assume that there is a positive constant η (small enough compared with n) such that[1] $(u,\, v) \in \mathcal{E}$ only if $||v - u|| \leq \eta$. This constraint describes the assumption that a node can not communicate with nodes that are too "far" away from it. Another parameter will play an important role in the sequel. If we assume that the d-dimensional torus is connected, its connectivity implies that there exists a path from the node $\mathbf{0} = (0, \ldots, 0) \in \mathbb{Z}_n^d$ to the node $\boldsymbol{e}_i \in \mathbb{Z}_n^d$, which is the vector with all entries equal to zero except the entry in

[1]Here we are assuming that the entries of i, j in $\mathbb{Z}_n$ are represented by the integers $-n/2 + 1, \ldots, -1, 0, 1, \ldots, n/2$ in case n is even or by the integers $-(n-1)/2, \ldots, -1, 0, 1, \ldots, (n-1)/2$ in case n is odd

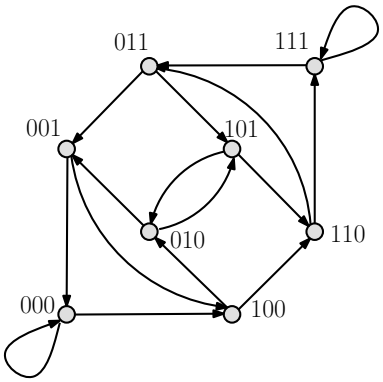

Figure 3.2: A de Bruijn graph with $N = 8$ nodes.

position i which is equal to 1. Let l_i be the graphical distance between $\mathbf{0}$ and $\boldsymbol{e}_i$ and let $l := \max_i\{l_i\}$. In many practical cases we have that $l = 1$. This parameter will play an important role when we will need to bound the graphical distance between nodes in tori.

De Bruijn's graphs

De Bruijn's graphs constitute a very particular family of graphs which allow convergence to consensus in finite time. Thanks to this nice behavior, which implies fast information spreading properties, de Bruijn's graphs have been proposed as the optimal architecture for multi-processor networks, inspiring scientific papers [89] as well as patents [90]. As a matter of fact, instead, in ad-hoc networks the De Bruijn is hardly implemented due to the long-range communication and high connectivity it requires. We choose it as an example to illustrate extreme behaviors of the performance costs we want to analyze. The paper [67] uses de Bruijn's graphs to solve linear consensus, gives detailed and general results on these graphs and provides several useful properties and characterizations. We will restrict here to a particular case. Let k and n be two positive integers, and consider the graph $\mathcal{G} = (\mathcal{V}, \mathcal{E})$ whose adjacency matrix is the following

$$A = \mathbf{1} \otimes I \otimes \mathbf{1}^T \tag{3.8}$$

where the column vector $\mathbf{1}$ is k dimensional, the identity I is k^{n-1} dimensional and the symbol $\otimes$ denotes Kronecker product. The graph $\mathcal{G}$ is called de Bruijn's graph [91], and it is displayed in Figure 3.2 in the case $k = 2$, $n = 3$.

Remark 3.4.2. De Bruijn's graphs fall under the large class of *expander graphs*, which constitute an interesting research topic in graph theory. Intuitively, the main characteristic of an expander graph is the fact that it is sparse, namely, its number of edges is "small"

in the number of nodes, but yet has high connectivity, namely, the number of paths from any node to any other node is "high" in the number of nodes. We refer to the inspiring survey [92] for a formal treatment of the topic and many examples of Expanders.

Geometric graphs

Cayley graphs and d-dimensional tori are often a good model for sensor networks, but their structure is too ideal to be actually implemented in reality. We need a model which requires less symmetry, or, even better, a model which consists in a *family* of graphs that share some common characteristics. In this Section we introduce geometric graphs as a solution to this problem.

Roughly speaking, a geometric graph is a perturbation of a regular grid or torus in d dimension, for instance by removing or adding edges, or moving nodes. There exist several different mathematical models for networks deployed in a real environment. One of the most important model is the random geometric graph, which consists in taking an hypercube $Q \subset \mathbb{R}^d$, deploying N nodes uniformly in it, and putting an edge among two nodes if their Euclidean distance is less then some threshold r. Other models instead just give rules to choose the edges connecting nodes deployed in an environment [93, 94, 95]. All these models fall in the general class of the so called ad-hoc networks, or proximity–induced graphs. Here we have chosen the one proposed in [51, 96], which we describe in a while, because it is, in our opinion, simpler, rather general and, compared to the definition of random geometric graph model, it requires no probabilistic rule.

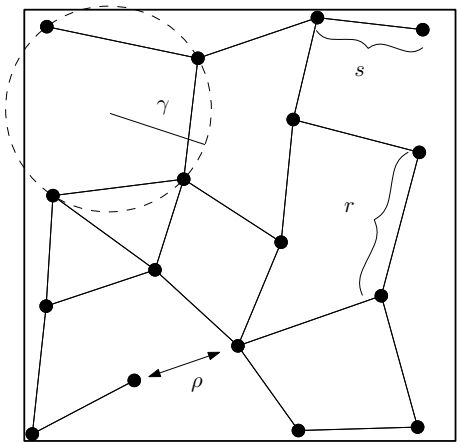

Figure 3.3: An example of geometric graph deployed in $\mathbb{R}^2$. In the figure it the parameters s, γ and r are shown. Concerning the parameter ρ, the two nodes for which the minimum in Eq. 3.13 is attained are shown.

Consider an hypercube $Q \subset \mathbb{R}^d$ with edge of length ℓ, namely $Q = [0, \ell]^d \subseteq \mathbb{R}^d$. We consider an undirected graph $\mathcal{G} = (\mathcal{V}, \mathcal{E})$, $|\mathcal{V}| = N$, in which each node u possesses a geometric coordinate and $u \in Q$, namely all the nodes of the graph are deployed inside the hypercube Q. We will often abuse the notation denoting by the same symbol $\mathcal{V} = \{1, \dots, N\}$, the set of labels, and $\mathcal{V} \subseteq Q$, the set of coordinates of the nodes. We denote by $d_E(u,\, v)$ the Euclidean distance among any couple of nodes $(u,\, v) \in \mathcal{V} \times \mathcal{V}$, which is defined to be

$$d_E(u,\, v) = \sqrt{\sum_{k=1}^{d} (u_k - v_k)^2}. \tag{3.9}$$

Following [96, 97, 98], the following parameters can be defined:

- the minimum Euclidean distance between any two nodes

$$s = \min_{u,\, v \in \mathcal{V},\, u \neq v} \{d_{\mathrm{E}}(u,\, v)\}\,; \tag{3.10}$$

- the maximum Euclidean distance between any two connected nodes

$$r = \max_{(u,\, v) \in \mathcal{E}} \{d_{\mathrm{E}}(u,\, v)\}\,; \tag{3.11}$$

- the radius γ of the largest ball centered in Q containing no nodes of the graph

$$\gamma = \sup \{r |\, B(x,\, r) \cap \mathcal{V} = \emptyset,\, \exists\, x \in Q\}\,; \tag{3.12}$$

- the minimum ratio between the Euclidean distance of two nodes and their graphical distance

$$\rho = \min \left\{ \frac{d_{\mathrm{E}}(u,\, v)}{d_{\mathcal{G}}(u,\, v)} |\, (u,\, v) \in \mathcal{V} \times \mathcal{V} \right\}. \tag{3.13}$$

Notice that, if $\mathcal{G}$ is connected, then ρ is well defined and positive. By convention, if the graph is not connected then one sets $\rho = 0$. Such a graph is called a geometric graph with parameters $(N, d, \ell, s, r, \gamma, \rho)$.

To give some conclusive intuitions, a geometric graph is a graph deployed in $\mathbb{R}^d$ in which the density of the nodes is approximatively uniform, in the sense that there are no regions where the nodes are "too close" (parameter s) and no large regions without nodes (parameter γ). Moreover, communication range is limited (parameter r) and two nodes which are geometrically close cannot be graphically far (parameter ρ).

3.5 Rate of convergence

The most classical performance index for the evaluation of the convergence of an iterative algorithm is the speed of convergence of the algorithm output towards its asymptotic value. It is well known from classical system theory that the rate of convergence of the state $\boldsymbol{x}(t)$ to its asymptotic value is exponential. The exponential rate of convergence is then defined as

$$R := \lim_{t\to\infty} (||\boldsymbol{x}(t) - \boldsymbol{x}(\infty)||)^{1/t}$$

where $||\cdot||$ denotes the 2-norm of a vector. Assume we are given a primitive stochastic matrix P. By standard linear algebra it can be seen that $R = \rho(P)$ where $\rho(P)$ is the essential spectral radius of P

$$\rho(P) := \max\{|\lambda| : \lambda \in \Lambda(P) \setminus \{1\}\}, \tag{3.14}$$

where $\Lambda(P)$ is the set of all the eigenvalues of P.

Notice that we can say that the vector $\mathbf{1}$ give the "consensus direction" in the sense that the state $\boldsymbol{x}$ tends to align with $\mathbf{1}$. Thus, the rate of convergence gives basically a worst-case performance cost on the velocity at which consensus is reached. In fact, if $\boldsymbol{v}$ is the eigenvector of P associated with the eigenvalue λ such that $\rho(P) = |\lambda|$, it is clear that $\boldsymbol{v}$ gives the direction, not parallel to $\mathbf{1}$, along which the decaying to zero is slower. For this reason, the more $\rho(P)$ is distant from 1, the faster the network achieves consensus.

The relation between the essential spectral radius of P and the topology of the graph $\mathcal{G}_P$ associated with P is a problem which has been widely studied both in the Markov chains community and in the community studying the theory of graphs. In Markov chain theory $\rho(P)$ is related to the so called mixing time of the Markov chain having P as the transition matrix [54]. Spectral graph theory instead studies the geometric properties of graphs using the Laplacian L of the matrix, which, recall, is defined to be $L = I - P$, so that $\Lambda(P) = 1 - \Lambda(L)$ and the spectral properties of the two matrices essentially coincide. Once we sort in increasing order the eigenvalues of L

$$0 = \mu_1 < \mu_2 \leq \mu_3 \leq \cdots \leq \mu_{N-1}$$

the value μ_2 is known as the Fiedler eigenvalue [99], or second smallest eigenvalue of L, or algebraic connectivity of L. Its characteristics are closely related to those of $\rho(P)$. For example, the more the smallest eigenvalue μ_2 is distant from 0, the more $\rho(P)$ is distant from 1, and thus the faster consensus is achieved. An extensive treatment of these and many other graph–theoretic topics can be found in the book [15].

Bounds on the convergence rate for general graphs

One of the major issues in research on consensus algorithms and Markov chains is to understand how to bound the essential spectral radius of P in terms of geometric parameters of the network.

In the sequel we will briefly recall some classical results (see [87, 100, 101, 102, 103]). For simplicity we will restrict our attention to symmetric stochastic matrices. Similar results hold for reversible matrices, with some slight modifications.

If P is symmetric, then its eigenvalues are real, and in the sequel we will assume that they are ordered in such a way that $1 = \lambda_0 > \lambda_1 \geq \lambda_2 \geq \cdots \geq \lambda_{N-1}$. Notice that in this case we have that

$$\rho(P) = \max\{\lambda_1, -\lambda_{N-1}\}$$

Therefore the second largest eigenvalue λ_1 will play an important role in determining bounds on $\rho(P)$. Indeed, if we find bounds on λ_1 and on $-\lambda_{N-1}$ we can get an upper bound on $\rho(P)$ too. Applying Gershgorin circle theorem we can argue that

$$-\lambda_{N-1} \leq 1 - 2\max_i\{P_{ii}\}.$$

Therefore, the difficulty in finding bounds on $\rho(P)$ essentially stands in finding bounds on λ_1. This eigenvalue will be denoted with the symbol $\lambda_1(P)$.

The well-known Rayleigh-Ritz theorem (see [104]) proves to be a helpful tool in bounding $\lambda_1(P)$. Rayleigh-Ritz theorem, in our case of P symmetric, coincides with the following variational characterization

$$1 - \lambda_1(P) = \min\left\{\frac{\boldsymbol{x}^T(I-P)\boldsymbol{x}}{\boldsymbol{x}^T\Omega\boldsymbol{x}}, \boldsymbol{x} \neq \alpha\mathbf{1}\right\}, \tag{3.15}$$

where $\Omega = I - \frac{1}{N}\mathbf{1}\mathbf{1}^T$ is the projector over span $\{\mathbf{1}\}^\perp$.

This characterization is the basis of several results relating geometric parameters of the graph associated with the stochastic matrix P to its second largest eigenvalue. We will briefly review two among the most important ones, namely the Poincaré and the Cheeger inequalities. For the general statements and the proofs of both of them, we refer to [87].

Poicaré inequality

Let P be a symmetric stochastic matrix and let $\mathcal{G}_P = (\mathcal{V}, \mathcal{E})$ be the undirected graph associated with P. For any couple $(u, v) \in \mathcal{V} \times \mathcal{V}$, $u \neq v$, let γ_{uv} be a path from u to v.

Namely, γ_{uv} is a set of edges $\gamma_{uv} = \{e_0, \ldots, e_l\}$ such that $e_0 = (u, u_1)$, $e_i = (u_i, u_{i+1})$ $\forall\, i = 1, \ldots, l-1$ and $e_l = (u_l, v)$. We will assume that in a path a vertex can be touched many times, while an edge may appear at most once. We define the following weighted length of the path γ_{uv}

$$|\gamma_{uv}|_P = \sum_{e \in \gamma_{uv}} P(e)^{-1}$$

where e are the edges forming γ_{uv} and $P(e) = p_{zw}$ if $e = (w, z)$.

Let Γ be a collection of such paths, one for each pair (u, v). We associate to Γ the following quantity

$$\kappa = \kappa(\Gamma) = \max_{e \in \mathcal{E}} \{ \sum_{\gamma_{uv} \ni e} |\gamma_{uv}|_P \} \tag{3.16}$$

namely κ is the maximum, as e varies over $\mathcal{E}$, of the sum of $|\gamma_{uv}|_P$ for all the paths γ_{uv} in which e appears as an edge.

This value has an immediate, intuitive, interpretation. We take, for any path, the measure of the resistance to the flow of information through that path. Then, we maximize it over the edges of the graph, obtaining thus a measure of the bottleneck in the network. This bottleneck influences the rate of convergence to the asymptotic distribution of the states as stated in the following theorem.

Theorem 3.5.1 ([87])**.** *The second largest eigenvalue of P satisfies*

$$\lambda_1(P) \leq 1 - \frac{N}{\kappa}, \tag{3.17}$$

with κ defined in (3.16).

This inequality is fundamentally an edge-perspective bound. It links geometric properties of paths along the network with the rate of convergence. Intuitively, less information can flow along the paths considered, the slowest is the convergence.

Cheeger inequality

In this section the interest is switched from paths to "surfaces", giving the definition of Cheeger ratio, as well as the relation between such quantity and the second largest eigenvalue. Unfortunately, even if the computation of the bound is someway simpler, this approach has been proved to offer less effective results over large families of graphs if compared with the Poincaré inequality [102].

Let P be a symmetric stochastic matrix and let $\mathcal{G}_P = (\mathcal{V}, \mathcal{E})$ be the undirected graph associated with P. Take a proper subset $S \subseteq \mathcal{V}$ of the nodes. It is rather intuitive that the flow of information from the set S to its complement $S^C = \mathcal{V} \setminus S$ is linked to the

transition probability from S to S^C. We can thus consider the conditional expectation of crossing the boundary of S given that we started from S, and minimize it over any possible set S. We obtain in this way the so called Cheeger ratio

$$h(P) = \min_{S:|S|\leq \frac{N}{2}} \left\{ \frac{P(S \times S^C)}{|S|} \right\}, \tag{3.18}$$

where $S \subseteq \mathcal{V}$ and $P(S \times S^C) = \sum_{(x,\, y)\in S\times S^C} P_{xy}$.

This quantity can be used in order to derive both an upper and a lower bound on the second largest eigenvalue, as stated in the following result.

Theorem 3.5.2 ([87])**.** *The second largest eigenvalue of P satisfies the following inequalities*

$$1 - 2h(P) \leq \lambda_1(P) \leq 1 - h(P)^2, \tag{3.19}$$

with $h(P)$ defined in (3.18).

Rate of convergence in Cayley graphs

In this section we will present the results about the rate of convergence for the class of Cayley matrices and d-dimensional tori. Details and proofs can be found for example in [66, 101, 53]. Consider the class of Cayley matrices and d-dimensional tori with respect to the group $\mathbb{Z}_n^d$ with given d and n. Notice that $N = n^d$. Assume that the graphs belonging to this class have the self loops and that they are connected. Recall from section Sect. 3.4 the definition of l and η.

The following theorem provides an upper bound on $\lambda_1(P)$. We don't give the proof of this result because it follows the same lines of the proof of Theorem 3.5.9 which treats a more general case.

Theorem 3.5.3. *Let P be a symmetric stochastic Cayley matrix with respect to the group $\mathbb{Z}_n^d$ whose associate graph $\mathcal{G}_P$ is in the previous class of d-dimensional tori characterized by the parameter h as described above. Assume that all the nonzero entries of P lie in an interval $[p_{\min}, p_{\max}]$. Then*

$$\lambda_1(P) \leq 1 - C\frac{1}{n^2}$$

where C is a strictly positive constant depending on d, l and $p_{\min}$.

The following theorem instead provides a lower bound on $\lambda_1(P)$. We give the proof of this result because this theorem will be instrumental in the proof of the more general result given in Theorem 3.5.8.

Theorem 3.5.4. *Let P be a symmetric stochastic Cayley matrix with respect to the group $\mathbb{Z}_n^d$ whose associate graph $\mathcal{G}_P$ is in the previous class of d-dimensional tori characterized by the parameter η as described above. Then*

$$1 - C\frac{1}{n^2} \leq \rho(P)$$

where C is a strictly positive constant depending on d and η.

Proof. First observe that, since $\rho(P) = \max\{\lambda_1, -\lambda_{N-1}\}$, it is enough to prove that

$$\lambda_1 \geq 1 - C'\frac{1}{n^2}$$

From the properties of the Cayley matrices [105] we can argue that the eigenvalues of P are given, for any $h = (h_1, \ldots, h_d) \in \mathbb{Z}_n^d$ by the formula

$$\lambda_h = \sum_{k \in \mathbb{Z}_n^d} P_{k,0} \cos\left(\frac{2\pi}{n} k^T h\right)$$

Take $h = \boldsymbol{e}_i$, where $\boldsymbol{e}_i$ is the canonical vector defined in Section 3.4. Then, using the fact that $\cos x \geq 1 - x^2/2$ and the definition of the generator $\boldsymbol{g}$ of the matrix, we have

$$\lambda_{\boldsymbol{e}_i} = \sum_{k \in \mathbb{Z}_n^d} \boldsymbol{g}(k) \cos\left(\frac{2\pi}{n} k_i\right) \geq \sum_{k \in \mathbb{Z}_n^d} \boldsymbol{g}(k) \left(1 - \frac{2\pi^2}{n^2} k_i^2\right) = 1 - \left(\sum_{k \in \mathbb{Z}_n^d} \boldsymbol{g}(k) k_i^2\right) \frac{2\pi^2}{n^2}$$

This in turn implies the thesis as follows

$$\begin{aligned}
\rho(P) &\geq 1 - \min_{i=1,\ldots,d} \left(\sum_{k \in \mathbb{Z}_n^d} \boldsymbol{g}(k) k_i^2\right) \frac{2\pi^2}{n^2} \\
&\geq 1 - \frac{1}{d} \sum_{i=1}^{d} \left(\sum_{k \in \mathbb{Z}_n^d} \boldsymbol{g}(k) k_i^2\right) \frac{2\pi^2}{n^2} \\
&= 1 - \frac{1}{d} \left(\sum_{k \in \mathbb{Z}_n^d} \boldsymbol{g}(k) ||k||^2\right) \frac{2\pi^2}{n^2} \\
&\geq 1 - \frac{2\pi^2 \eta^2}{d} \frac{1}{n^2}
\end{aligned}$$

□

It is possible to obtain a similar result if we consider instead of Cayley matrices,

more general matrices which are consistent with d-dimensional tori. We start from the following theorem providing an upper bound on $\lambda_1(P)$. We don't give the proof of this result because it follows the same lines of the proof of Theorem 3.5.9 which treats a more general case.

Theorem 3.5.5. *Let P be a symmetric stochastic matrix whose associate graph $\mathcal{G}_P$ is in the previous class of d-dimensional tori characterized by the parameter η as described above. Assume that all the nonzero entries of P lie in an interval $[p_{\min}, p_{\max}]$. Then*

$$\lambda_1(P) \leq 1 - C\frac{1}{n^2}$$

where C is a strictly positive constant depending on d, l and $p_{\min}$.

We give finally a lower bound on $\rho(P)$. For this result we consider the case in which the stochastic matrices are not restricted, as in the rest of the paper, to be symmetric, but we give the result for the more general class of reversible matrices, since it will turn out to be instrumental in proving Theorem 3.5.8. Recall that we order the (real) eigenvalues of P in such a way that

$$1 = \lambda_0 > \lambda_1 \geq \lambda_2 \geq \cdots \geq \lambda_{N-1}$$

Theorem 3.5.6. *Let P be a stochastic matrix which is consistent with a graph $\mathcal{G}$ which belongs to the previous class of d-dimensional tori characterized by the parameter η as described above. Assume moreover that P is reversible with respect to a diagonal matrix $\Pi = \mathrm{diag}\,(\pi_1, \ldots, \pi_N)$. Then*

$$1 - C\frac{1}{n^2} \leq \rho(P)$$

where C is a strictly positive constant depending on d, δ and $\pi_{\min}/\pi_{\max}$, where $\pi_{\min} := \min_u\{\pi_u\}$ and $\pi_{\max} := \max_u\{\pi_u\}$.

Proof. First observe that, since $\rho(P) = \max\{\lambda_1, -\lambda_{N-1}\}$, it is enough to prove that

$$\lambda_1(P) \geq 1 - C'\frac{1}{n^2}$$

Observe moreover that (3.15) can be adapted to reversible stochastic matrices as follows

$$\mu_1 = \min\left\{\frac{\boldsymbol{x}^T\Pi L\boldsymbol{x}}{\boldsymbol{x}^T(\Pi - \boldsymbol{\pi}\boldsymbol{\pi}^T)\boldsymbol{x}},\ \boldsymbol{x} \neq \alpha\mathbf{1}\right\}$$

where $L := I - P$ and μ_1 is its second largest eigenvalue. Consider now for any $h \in G := \mathbb{Z}_n^d$ the operator σ_h over the matrices in $\mathbb{R}^{G\times G}$ defined by letting $\sigma_h(P)_{i,j} := P_{i+h,j+h}$. Notice

that

$$\bar{P} := \sum_{h \in G} \sigma_h(\Pi P)$$

is still compatible with the graph $\mathcal{G}$ and moreover it is a symmetric Cayley matrix with respect to the group G. Let $1 = \bar{\lambda}_0 > \bar{\lambda}_1 \geq \bar{\lambda}_2 \geq \cdots \geq \bar{\lambda}_{N-1}$ be the eigenvalues of $\bar{P}$. Let moreover $\bar{L} := I - \bar{P}$ and $\bar{\mu}_1$ be its second largest eigenvalue. Then we have that

$$\begin{aligned}
\bar{\mu}_1 &= \min\left\{\frac{\boldsymbol{x}^T \bar{L}\boldsymbol{x}}{\boldsymbol{x}^T\Omega\boldsymbol{x}},\ \boldsymbol{x} \neq \alpha\mathbf{1}\right\} = \min\left\{\frac{1}{\boldsymbol{x}^T\Omega\boldsymbol{x}}\boldsymbol{x}^T\left(\sum_{h\in G}\sigma_h(\Pi L)\right)\boldsymbol{x},\ \boldsymbol{x} \neq \alpha\mathbf{1}\right\} \\
&\geq \sum_{h\in G}\min\left\{\frac{1}{\boldsymbol{x}^T\Omega\boldsymbol{x}}\boldsymbol{x}^T\sigma_h(\Pi L)\boldsymbol{x},\ \boldsymbol{x} \neq \alpha\mathbf{1}\right\} = \sum_{h\in G}\min\left\{\frac{\boldsymbol{x}^T\Pi L\boldsymbol{x}}{\boldsymbol{x}^T\Omega\boldsymbol{x}},\ \boldsymbol{x} \neq \alpha\mathbf{1}\right\} \\
&= N\min\left\{\frac{\boldsymbol{x}^T\Pi L\boldsymbol{x}}{\boldsymbol{x}^T\Omega\boldsymbol{x}},\ \boldsymbol{x} \neq \alpha\mathbf{1}\right\} \geq N^2\pi_{\min}^2\min\left\{\frac{\boldsymbol{x}^T\Pi L\boldsymbol{x}}{\boldsymbol{x}^T(\Pi - \boldsymbol{\pi}\boldsymbol{\pi}^T)\boldsymbol{x}},\ \boldsymbol{x} \neq \alpha\mathbf{1}\right\} \\
&\geq \left(\frac{\pi_{\min}}{\pi_{\max}}\right)^2\mu_1
\end{aligned}$$

The last inequalities are motivated by the fact that

$$\begin{aligned}
\boldsymbol{x}^T(\Pi - \boldsymbol{\pi}\boldsymbol{\pi}^T)\boldsymbol{x} &= \frac{1}{2}\sum_{uv}(x_u - x_v)^2\pi_u\pi_v \geq \pi_{\min}^2\frac{1}{2}\sum_{uv}(x_u - x_v)^2 \\
&= N\pi_{\min}^2\boldsymbol{x}^T\Omega\boldsymbol{x}
\end{aligned}$$

and that $\pi_{\max} \geq \frac{1}{N}$.

Considering that, by Theorem 3.5.4 we have that $\bar{\mu} \leq C/n^2$ for some constant C, we get that the previous inequality implies that

$$\lambda_1 = 1 - \mu_1 \geq 1 - \left(\frac{\pi_{\max}}{\pi_{\min}}\right)^2\bar{\mu}_1 \geq 1 - \left(\frac{\pi_{\max}}{\pi_{\min}}\right)^2\frac{C}{n^2}$$

□

Rate of convergence in De Bruijn's graphs

In this short Section it is shown why the de Bruijn's graphs are so appealing to be used to build a consensus network. Consider the de Bruijn's graph with $N = k^n$ we defined previously, and assume that each node uniformly weights all its neighbors, namely consider the stochastic matrix

$$P = \frac{1}{k}\mathbf{1} \otimes I \otimes \mathbf{1}^T \tag{3.20}$$

where the column vector $\mathbf{1}$ is k dimensional and the identity I is k^{n-1} dimensional. Notice that P defined in this way is not symmetric but it is doubly stochastic and that the number of neighbors of each agent is exactly k.

A simple computation [67] shows that

$$P^h = \frac{1}{N}\mathbf{1}\mathbf{1}^T, \forall\, h \geq k$$

where here the column vector $\mathbf{1}$ is N dimensional. This means that with this matrix the state converges to consensus in at most $n = \log_k N$ steps. It is possible to show [67] that there exists no $k^n \times k^n$ stochastic matrix for which we have faster, namely in less steps, convergence. Notice finally that P has the minimum possible essential spectral radius since $\rho(P) = 0$.

Remark 3.5.7. De Bruijn's graphs provide a simple example of the fact that it is not always true that given a communication graph $\mathcal{G} = (\mathcal{V}, \mathcal{E})$ we attain best performance making use of all the edges at disposal. In fact, if one takes a de Bruijn's graph and adds a small number of other edges, the best rate of convergence is still obtained with the construction in Eq. 3.20. On the contrary, forcing to use the added edges yields to a critical degradation of the performance, since the second eigenvalue would become strictly positive.

Rate of convergence in Geometric graphs

In this section we will analyze the rate of convergence of a generic symmetric stochastic matrix whose associated graph is a geometric graph. Our aim is to obtain a lower and an upper bound for such a quantity, and the tools used will be a Poincaré inequality-type for the upper bound, and the state–aggregation approach for Markov Chains for the lower bound. The procedure is similar to the one proposed in [53], where the authors study the random geometric graphs [52] in dimension d and show that the rate of convergence in such graphs is with high probability the same as the rate of convergence of a d-dimensional grid. Here we obtain a similar result for our deterministic model of geometric graphs. We start from the lower bound. The proof is postponed to Section 3.5.

Theorem 3.5.8. *Let P be a symmetric stochastic matrix whose associate graph $\mathcal{G}_P$ is a geometric graph with parameters $(N, d, \ell, s, r, \gamma, \rho)$, where we assume that $\ell \geq 4\gamma$. Then*

$$1 - \frac{C}{N^{2/d}} \leq \rho(P) \tag{3.21}$$

where C is a strictly positive constant depending on the parameters d, s, r, γ and ρ but

not on ℓ, N.

We will give now an upper bound on the second largest eigenvalue of a symmetric stochastic P whose associated graph is a geometric graph and whose entries lie in an interval $[p_{\min}, p_{\max}]$. The proof of this theorem, given in the Section 3.5, makes use of the Poincaré inequality given in Eq. 3.17.

Theorem 3.5.9. *Let P be a symmetric stochastic matrix whose associate graph $\mathcal{G}_P$ is a geometric graph with parameters $(N, d, \ell, s, r, \gamma, \rho)$, where we assume that $\ell \geq 4\gamma$. We assume moreover that all the nonzero entries of P belongs to $[p_{\min}, p_{\max}]$. Then*

$$\lambda_1(P) \leq 1 - \frac{C}{N^{2/d}} \tag{3.22}$$

where C is a strictly positive constant depending on the parameters $p_{\min}$, d, s, r, γ and ρ but not on ℓ, N.

Applications

As a first example of application of the previous theorem we can consider the regular grid of $N = n^2$ nodes on the plane. In this case the nodes are deployed in a square of edge length equal to $\ell = n - 1$ and have coordinates i, j with $i, j \in \{0, \ldots, n-1\}$. In this scenario, it is clear that the distance among any pair of nodes is 1 and so we have that $s = 1$. Moreover the communication range is $r = 1$ and the disks which do not contain any node have radius which is at most $\gamma = \sqrt{2}/2$. Moreover, given a pair of nodes, it can be seen that the minimum of the ratio between the nodes Euclidean distance and graphical distance is $\rho = \sqrt{2}/2$. The regular grid it thus a geometric graph with these parameters, and so, if P is a symmetric stochastic matrix having the regular grid as its associated graph, then we can apply Theorem 3.5.9 which yields the well known result

$$\lambda_1 \leq 1 - C_r \frac{1}{N},$$

where C_r is a strictly positive constant depending only on the minimum value of the entries of P associated with the edges of the grid.

Consider now a perturbation of such a grid. We take the same set of nodes, in the same positions, and we modify the communication topology as illustrated in Fig. 3.4. It is clear that in this case r, s and γ remain the same as in the previous example. Only the parameter ρ changes. It can be seen that ρ is determined by any two nodes at Euclidean distance 1 which are not neighbours in the perturbed grid. The application of Theorem

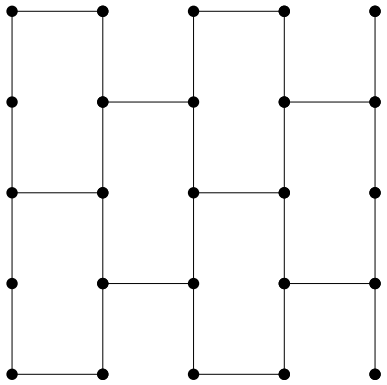

Figure 3.4: Perturbation of the regular grid.

3.5.9 yields

$$\rho(P) \leq 1 - C_p \frac{1}{N}.$$

where C_p is a strictly positive constant depending only on the minimum value of the entries of P associated with the edges of the grid. Notice that in both the grid and in the perturbed grid the number of node is $N = n^2$. On the other hand in the regular grid we have $2n(n-1)$ edges, while in the perturbed grid we have $\frac{3}{2}n(n-1)$ edges. As shown in the proof of Theorem 3.5.9, the constants C_r and C_p are proportional to ρ and so $C_p = \frac{1}{\sqrt{2}} C_r$. This means that, in this case, even dropping one fourth of the edges we still obtain a rate of convergence which shows the same behavior in N.

Proofs of Theorem 3.5.8

In order to prove the theorem we need to introduce some notation and some lemmas. Given a connected graph $\mathcal{G}$ let

$$\rho(\mathcal{G}) := \min\{\rho(P) : \ P \text{ primitive symmetric stochastic matrix consistent with } \mathcal{G}\}$$

namely $\rho(\mathcal{G})$ denotes the minimum $\rho(P)$ when P varies in the set of symmetric, stochastic, primitive matrices consistent with $\mathcal{G}$. Notice that the matrix attaining such minimum might be not unique. It is clear that lower bound in the thesis of the theorem is proved if we prove that

$$\rho(\mathcal{G}) \geq 1 - \frac{C}{N^{2/d}}. \tag{3.23}$$

First of all we give a lemma which will be useful in the proof of the theorem.

Lemma 3.5.10. *Let $P, M \in \mathbb{R}^{N \times N}$ be symmetric stochastic matrices and assume that*

P is primitive. Then

$$\rho(MPM) \leq \rho(P)$$

Proof. Notice first that

$$\rho(MPM) = \max\left\{\frac{|y^T MPMy|}{y^T y},\, y \perp \mathbf{1},\, y \neq 0\right\}$$

$$\rho(P) = \max\left\{\frac{|x^T Px|}{x^T x},\, x \perp \mathbf{1},\, x \neq 0\right\}$$

To prove that $\rho(MPM) \leq \rho(P)$ it is sufficient to prove that for any $y \neq 0$ such that $\mathbf{1}^T y = 0$, there exists $x \neq 0$ such that $\mathbf{1}^T x = 0$ such that

$$\frac{|y^T MPMy|}{y^T y} \leq \frac{|x^T Px|}{x^T x}.$$

In finding x we distinguish two cases:

1. In case $My \neq 0$, we let $x := My$. Notice that in this case we have that $x \neq 0$ and that $\mathbf{1}^T x = \mathbf{1}^T My = \mathbf{1}^T y = 0$. Notice finally that, since all the eigenvalues of M are in $[-1, 1]$, then $y^T MMy \leq y^T y$ and so

$$\frac{|y^T MPMy|}{y^T y} \leq \frac{|y^T MPMy|}{y^T M^2 y} = \frac{|x^T Px|}{x^T x}.$$

2. In case $My = 0$, we let x to be any nonzero vector such that $\mathbf{1}^T x = 0$.

□

Proof of Theorem 3.5.8

Let $h := \lfloor \ell/2\gamma \rfloor$ and tessellate the hypercube Q into $H := h^d$ identical hypercubes with edge of length $\bar{\ell} := \ell/h$. Notice that, since $\ell/h \geq 2\gamma$ then each of such hypercubes contains at least one node of $\mathcal{G}$. This implies that $h^d \leq N$. Notice moreover that, from the assumption that $\ell \geq 4\gamma$, we can argue that

$$\bar{\ell} = \frac{\ell}{\lfloor \ell/2\gamma \rfloor} \leq \frac{\ell}{\ell/2\gamma - 1} \leq 4\gamma$$

We can define now a graph $\mathcal{G}_{\mathcal{L}} = (\mathcal{Q}, \mathcal{L})$ having all hypercubes as nodes and having as edges all the pairs (q', q'') of hypercubes such that, either $q' = q''$ (self-loops), or there exists $(u, v) \in \mathcal{E}$ with $u \in q'$ and $v \in q''$. Notice that $\mathcal{G}_{\mathcal{L}}$ is a subgraph of a d-dimensional torus over the group $\mathbb{Z}_n^d$. Notice moreover that if two nodes x, $y \in \mathbb{Z}_n^d$

are connected, then there exists $(u, v) \in \mathcal{E}$ with $u \in q_x$ and $v \in q_y$, with q_x and q_y the hypercubes correspondent to x and y respectively. Identify now $x \in \mathbb{Z}_n^d$ with the center of its hypercube q_x, and the same for y. We can argue that

$$||x - y||\bar{\ell} = d_E(x, y) \leq d_E(x, u) + d_E(u, v) + d_E(v, y) \leq r + \bar{\ell}\sqrt{d}$$

From this we can argue that $x, y \in \mathbb{Z}_n^d$ are connected only if $||x - y|| \leq \eta$ where $\eta = r/2\gamma + \sqrt{d}$.

Build now a new graph, $\tilde{\mathcal{G}} = (V, \tilde{\mathcal{E}})$, which has the same set of nodes as $\mathcal{G}$, and has an edge connecting any couple of nodes u, v if and only if one of the following two conditions hold:

1. u, v lie in the same hypercube,
2. $u \in q'$ and $v \in q''$ and $(q', q'') \in \mathcal{L}$.

Notice that, by construction, we have that $\mathcal{E} \subseteq \tilde{\mathcal{E}}$, namely $\mathcal{G}$ is embedded in $\tilde{\mathcal{G}}$ so that

$$\rho(\tilde{\mathcal{G}}) \leq \rho(\mathcal{G})$$

since minimization in $\tilde{\mathcal{G}}$ is subjected to a smaller set of constraints. Our aim is now to lower bound $\rho(\tilde{\mathcal{G}})$, since this will yield in turn a lower bound for $\rho(\mathcal{G})$ as well.

Let $n_i \geq 1$, $i = 1, 2, \ldots, H$, be the number of nodes inside the i-th hypercube so that $\sum_{i=1}^{H} n_i = N$. Assume that the nodes of $\tilde{\mathcal{G}}$ are ordered in such a way that the nodes $n_{i-1} + 1, n_{i-1} + 2, \ldots, n_i$ end in the i-th hypercube. Introduce the following matrices, $D := \text{diag}\,(n_1, \ldots, n_H)$ and

$$S := \begin{bmatrix} \mathbf{1}_{n_1} & 0 & \ldots & 0 & 0 \\ 0 & \mathbf{1}_{n_2} & \ldots & 0 & 0 \\ \vdots & & & & \vdots \\ 0 & 0 & \ldots & 0 & \mathbf{1}_{n_H} \end{bmatrix} \in \{0, 1\}^{N \times H}$$

Notice that $M := SD^{-1}S^T$ is stochastic. Assume now that $P^{\tilde{\mathcal{G}}}$ be a symmetric, stochastic, primitive matrix consistent with $\tilde{\mathcal{G}}$ such that $\rho(P^{\tilde{\mathcal{G}}}) = \rho(\tilde{\mathcal{G}})$. By the definition of M it is easy to see that

$$MP^{\tilde{\mathcal{G}}}M = \begin{bmatrix} p_{11}\mathbf{1}_{n_1}\mathbf{1}_{n_1}^T & p_{12}\mathbf{1}_{n_1}\mathbf{1}_{n_2}^T & \ldots & p_{1H}\mathbf{1}_{n_1}\mathbf{1}_{n_H}^T \\ p_{12}\mathbf{1}_{n_2}\mathbf{1}_{n_1}^T & p_{22}\mathbf{1}_{n_2}\mathbf{1}_{n_2}^T & \ldots & p_{2H}\mathbf{1}_{n_2}\mathbf{1}_{n_H}^T \\ \vdots & & & \vdots \\ p_{1H}\mathbf{1}_{n_H}\mathbf{1}_{n_1}^T & p_{2H}\mathbf{1}_{n_H}\mathbf{1}_{n_2}^T & \ldots & p_{HH}\mathbf{1}_{n_H}\mathbf{1}_{n_H}^T \end{bmatrix}.$$

where p_{ij} are the elements of the matrix $\tilde{P} = D^{-1}S^T P^{\tilde{\mathcal{G}}} S D^{-1}$. By definition of $\tilde{\mathcal{G}}$ we have that $MP^{\tilde{\mathcal{G}}}M$ is compatible with $\tilde{\mathcal{G}}$ and so $\rho(MP^{\tilde{\mathcal{G}}}M) \geq \rho(\tilde{\mathcal{G}}) = \rho(P^{\tilde{\mathcal{G}}})$. On the other hand, by lemma 3.5.10 we have that $\rho(MP^{\tilde{\mathcal{G}}}M) \leq \rho(P^{\tilde{\mathcal{G}}})$, proving in this way that $\rho(MP^{\tilde{\mathcal{G}}}M) = \rho(\tilde{\mathcal{G}})$.

Let $\bar{P} := D^{-1}S^T P^{\tilde{\mathcal{G}}} S = \tilde{P}D$. This is a stochastic matrix. It can be shown that

$$\Lambda(MP^{\tilde{\mathcal{G}}}M) \setminus \{0\} \subseteq \Lambda(\bar{P}) \subseteq \Lambda(MP^{\tilde{\mathcal{G}}}M) \tag{3.24}$$

To prove (3.24) first observe that, if $\mu \in \Lambda(\bar{P})$ then there exists a nonzero vector v such that $\bar{P}v = \mu v$. If we let $\tilde{v} := Sv \neq 0$, then

$$MP^{\tilde{\mathcal{G}}}M\tilde{v} = SD^{-1}S^T P^{\tilde{\mathcal{G}}} S D^{-1} S^T S v = S\bar{P}v = S\mu v = \mu\tilde{v},$$

and so $\mu \in \Lambda(MP^{\tilde{\mathcal{G}}}M)$. Assume conversely that $\mu \in \Lambda(MP^{\tilde{\mathcal{G}}}M) \setminus \{0\}$. Then $MP^{\tilde{\mathcal{G}}}M\tilde{v} = \mu\tilde{v}$ for some nonzero vector $\tilde{v}$. Let $v := S^T\tilde{v}$. Observe that v is nonzero because otherwise we would have that $\mu = 0$. Observe finally that

$$\mu v = \mu S^T\tilde{v} = S^T MP^{\tilde{\mathcal{G}}}M\tilde{v} = S^T S D^{-1} S^T P^{\tilde{\mathcal{G}}} S D^{-1} S^T\tilde{v} = \bar{P}v$$

This implies that $\mu \in \Lambda(\bar{P})$.

Notice that (3.24) implies that $\rho(\bar{P}) \leq \rho(\tilde{\mathcal{G}}) \leq \rho(\mathcal{G}) \leq \rho(P)$. It remains to find a lower bound of $\rho(\bar{P})$. Notice first that, if we define $\Pi := N^{-1}D$, then we have that

$$\bar{P}^T\Pi = \Pi\bar{P}$$

This means that $\bar{P}$ is a reversible stochastic matrix with respect to Π. Notice moreover that $\bar{P}$ is compatible with the graph $\mathcal{G}_{\mathcal{L}}$ which is a subgraph of a d-dimensional torus with respect to the group $\mathbb{Z}_h^d$ in which two nodes $x, y \in \mathbb{Z}_n^d$ are connected only if $||x - y|| \leq \eta$, where $\eta = r/2\gamma + \sqrt{d}$. Therefore we can apply Theorem 3.5.6 to obtain

$$\rho(\bar{P}) \geq 1 - \left(\frac{\pi_{\max}}{\pi_{\min}}\right)^2 \frac{C}{h^2}.$$

where C depends on d, γ and r.

Recall finally that, since each hypercube contains at least a node, then $h^d \geq N$. Notice moreover that $\pi_{\max}/\pi_{\min} \leq \max_i\{n_i\}$. Observe that the volume of the d-dimensional sphere of radius $s/2$ is $A_d\left(\frac{s}{2}\right)^d$, where $A_d = \frac{\pi^{d/2}}{\Gamma(d/2+1)}$. Then, by definition of s, we have that

$$n_i A_d \left(\frac{s}{2}\right)^d \leq \bar{\ell}^d$$

and so

$$n_i \leq \frac{1}{A_d}\left(\frac{2\bar{\ell}}{s}\right)^d \leq \frac{1}{A_d}\left(\frac{8\gamma}{s}\right)^d$$

where we used the fact that $\bar{\ell} \leq 4\gamma$. We can conclude that

$$\rho(\mathcal{G}) = \rho(\tilde{\mathcal{G}}) = \rho(\bar{P}) \geq 1 - \frac{1}{A_d}\left(\frac{8\gamma}{s}\right)^d \frac{C}{N^{2/d}}.$$

Proofs of Theorem 3.5.9

For simplicity we will develop the proof only for $d = 2$, showing at the end how it is possible to generalize the result to any dimension.

For any pair of nodes x, y we build a path γ_{xy} connecting x and y as follows (see Fig. 3.5). We first tessellate the square Q as we did in the previous proof, namely by letting $h := \lfloor \ell/2\gamma \rfloor$ and by tessellating Q into h^2 identical squares with edge of length $\bar{\ell} := \ell/h$. Notice that, since $\ell/h \geq 2\gamma$ then each of such squares contains at least one node of $\mathcal{G}_P$. As in the previous proof, we have that $h^2 \leq N$ and that $\bar{\ell} \leq 4\gamma$.

Assume that, for any square q, we choose one of its nodes, denoted by u_q, as its representative node in such a square. Moreover, for any node v let u_v be the representative of the square x belongs to.

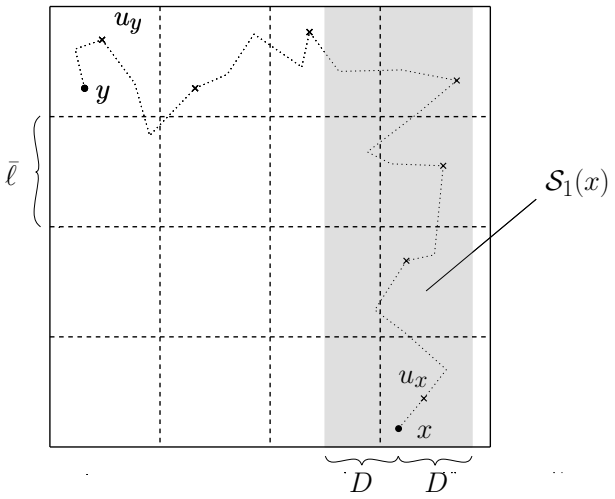

Figure 3.5: Building γ_{xy}. For each square, we choose a representative, which is marked by a cross. We proceed from representative to representative upwards and then leftwards (or rightwards). We can exit from the squares, but not from stripes of width $2D$.

Take the two nodes x, y we want to connect. Assume that x is below with respect to y. Link, via the shortest path, x to u_x, the representative of the square q_x. Then,

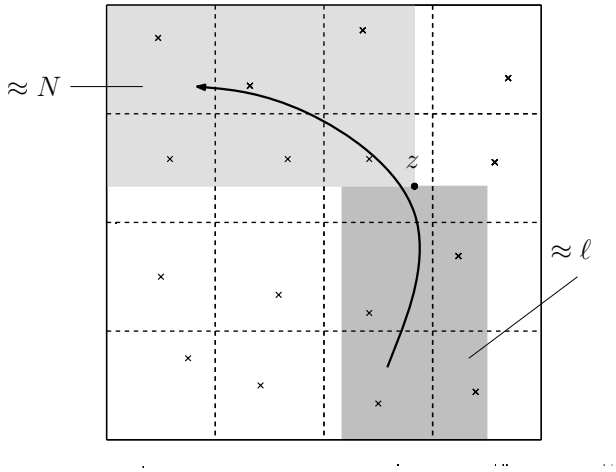

Figure 3.6: Maximum usage of a node. Given z, we can use it if we start from a node in the dark grey below it, which is a subset of $\mathcal{S}_1(z)$. The number of nodes in this region is proportional to $\ell \approx N^{1/d}$. Once we used z, we can possibly reach any node in the soft grey region. The number of nodes in this region is, in the worst case, proportional to the number of nodes in the network, N.

start proceeding upward, linking via the shortest path the representatives of each of the neighbor squares till we reach a square which is at the same height of the square q_y containing y. Then, proceed left or right with in a similar way. At a certain point, we will reach the representative u_y of q_y, and then we will link u_y with y via the shortest path.

Let Γ be the collection of these paths, one for each pair x, y. We want to give an estimate of $\kappa(\Gamma)$, where $\kappa(\Gamma)$ is defined (3.16). By definition of $|\gamma_{xy}|_P$, given (3.12), we have that

$$|\gamma_{xy}|_P = \sum_{e \in \gamma_{xy}} \frac{1}{P_e} \leq \frac{1}{p_{\min}} |\gamma_{xy}|,$$

where $|\gamma_{xy}|$ is the length of the path γ_{xy}. We want to upper bound $|\gamma_{xy}|$. We will start by bounding the graphical distance between two representatives u and v of neighbor squares. Observe that $d_E(u, v) \leq \sqrt{5}\bar{\ell} \leq 4\sqrt{5}\gamma$, and so

$$d_G(u, v) \leq \frac{d_E(u, v)}{\rho} \leq 4\sqrt{5}\frac{\gamma}{\rho}$$

Through similar arguments it can be proved that

$$d_G(x, u_x) \leq \frac{d_E(x, u_x)}{\rho} \leq 4\sqrt{2}\frac{\gamma}{\rho}, \qquad d_G(y, u_y) \leq \frac{d_E(y, u_y)}{\rho} \leq 4\sqrt{2}\frac{\gamma}{\rho}$$

Now, observe that a path in Γ touches at most $2h$ squares, so including the starting and the ending points, we have that

$$|\gamma_{xy}| \leq 8\sqrt{5}\frac{\gamma}{\rho}h + 8\sqrt{2}\frac{\gamma}{\rho} \leq 8(\sqrt{5}+\sqrt{2})\frac{\gamma}{\rho}h \tag{3.25}$$

Now, given an edge e, we have that

$$\sum_{\gamma_{xy}\ni e} |\gamma_{xy}|_P \leq 8(\sqrt{5}+\sqrt{2})\frac{\gamma}{p_{\min}\rho}h|\{\gamma_{xy}|\gamma_{xy}\ni e\}|. \tag{3.26}$$

Hence, it remains to bound the maximum number of paths which cross a certain edge. To do this we will bound the number of paths which cross a certain node (see Fig. 3.6). Assume that a node z belongs to γ_{xy}. We want to understand where z has to be with respect to x, y. Let

$$D := 4\sqrt{5}\frac{r\gamma}{\rho} + 4\gamma \geq \sqrt{5}\frac{r\bar{\ell}}{\rho} + \bar{\ell}$$

which is a constant depending only on γ, ρ and r. We show now that

$$z \in \mathcal{S}_1(x) \cup \mathcal{S}_2(y) \tag{3.27}$$

where for any point $w \in Q$ we define

$$\mathcal{S}_1(w) := \{w' \in Q \ : \ |w_1 - w'_1| \leq D\}, \qquad \mathcal{S}_2(w) := \{w' \in Q \ : \ |w_2 - w'_2| \leq D\}$$

and where w_1 and w_2 denote the two coordinates of the point $w \in Q$. Namely, $S_1(w)$ is a "vertical stripe" centered in w and of width $2D$, $S_2(w)$ is the horizontal analogous.

We distinguish various cases:

1. If z belongs to the shortest path between x and the representative u_x of the square x belongs to, then since the path from x to u_x is the shortest possible, $d_G(x,z) \leq d_G(x,u_x) \leq \sqrt{2}\bar{\ell}/\rho$. This implies

   $$d_E(x,z) \leq r d_G(x,z) \leq \sqrt{2}\frac{r\bar{\ell}}{\rho} \leq D$$

   and hence $|x_1 - z_1| \leq d_E(x,z) \leq D$.

2. In an analogous way it can be shown that, in case z belongs to the shortest path between y and u_y, then $|y_2 - z_2| \leq D$.

3. If z belongs to the shortest path between u and v, which are representatives of

neighbor squares in the vertical portion of the path from x, then $|x_1 - u_1| \leq \bar{\ell}$ and moreover, since $d_G(u,z) \leq d_G(u,v) \leq \sqrt{5}\bar{\ell}/\rho$, we can argue that

$$d_E(u,z) \leq r d_G(u,z) \leq \sqrt{5}\frac{r\bar{\ell}}{\rho}$$

and so $|x_1 - z_1| \leq |x_1 - u_1| + |u_1 - z_1| \leq \bar{\ell} + d_E(u,z) \leq D$.

4. In an analogous way it can be shown that, in case z belongs to the shortest path between u and v, which are representatives of neighbor squares in the horizontal portion of the path to y, we have that $|y_2 - z_2| \leq D$.

Now we are able to bound the number of paths γ_{xy} which cross z. Indeed, if γ_{xy} crosses z then (3.27) holds and so we can distinguish to cases:

(i) Assume that $z \in \mathcal{S}_1(x)$. This holds if and only if $x \in \mathcal{S}_1(z)$. Then the number of γ_{xy} such that $x \in \mathcal{S}_1(z)$ is upper bounded by

$$\frac{8}{\pi}\frac{D\ell}{s^2}N.$$

In fact, such value is less than or equal to the number of nodes in the stripe $\mathcal{S}_1(z)$ multiplied by the total number of nodes N. The first quantity can be upper bounded as before by the area of the stripe, $2D\ell$, over the area of a sphere of radius $\frac{s}{2}$.

(ii) Assume in this case that $z \notin \mathcal{S}_1(x)$. Then the number of γ_{xy} such that $x \notin \mathcal{S}_1(z)$ can be bounded as follows. Indeed observe from (3.27) that, if $x \notin \mathcal{S}_1(z)$, then $y \in \mathcal{S}_2(z)$, and so the number of γ_{xy} such that $x \notin \mathcal{S}_1(z)$ is less than or equal to the number of nodes in $\mathcal{S}_2(z)$ multiplied by the total number of nodes N. This value is upper bounded by the same number above.

Putting together the two cases, the number of paths γ_{xy} which cross z is upper bounded by

$$\frac{8}{\pi}\frac{D\ell}{s^2}N$$

Finally, by considering this last bound, with the bounds (3.26) and (3.25) we obtain that

$$\kappa(\Gamma) \leq 8(\sqrt{5}+\sqrt{2})\frac{\gamma}{p_{\min}\rho}h\frac{8}{\pi}\frac{D\ell}{s^2}N \leq \frac{64(\sqrt{5}+\sqrt{2})\gamma D}{\pi p_{\min}\rho s^2}4\gamma N^2.$$

where we used the fact that $\ell = \bar{\ell}h \leq 4\gamma h$ and the fact that $h^2 \leq N$.

To conclude, by exploiting the Poicaré inequality, we have

$$\lambda_1 \leq 1 - \frac{N}{\kappa(\Gamma)} \leq 1 - C\frac{1}{N},$$

where C is a constant depending on the geometric parameters s, γ, r and ρ and on $p_{\min}$.

In the general case, the whole reasoning still holds. What differs is the value of many numerical constants, since for example the Euclidean distance among the representatives of two neighbor hypercubes is in general $d_E(u, v) \leq \sqrt{3+d}$. The most important difference lies however in the fact that now $h^d \leq N$, whence $\ell \leq 4\gamma N^{1/d}$. This yields

$$\kappa(\Gamma) \leq C' h\ell N \leq C N^{1+2/d},$$

and thus Poincaré inequality implies

$$\lambda_1 \leq 1 - C\frac{N}{N^{1+2/d}} = 1 - C\frac{1}{N^{2/d}}.$$

3.6 The linear quadratic cost

As presented in the previous Section, the convergence to the consensus value is exponential with exponent equal to the second largest eigenvalue of the matrix P

$$\rho(P) = \sup\{|\lambda| : \lambda \in \sigma(P), \lambda \neq 1\}$$

where $\sigma(P)$ is the spectrum of P. For this reason, the value $\rho(P)$ is a classical performance cost for the algorithm. However, as recent papers have pointed out [106, 107], this performance index on P is not the only possible choice for evaluating the performance of the algorithm. Different costs arise from different specific problems where the consensus algorithm is used. Moreover, it can be shown [108, 109] that, by considering different performance indices, it is possible to obtain different optimal graph topologies.

In this Section we propose thus a second way to measure the performance of a consensus algorithm, namely a Linear Quadratic (LQ) cost which is an index widely used in the control community. To evaluate the convergence of P^t towards its limit value $\mathbf{1}\boldsymbol{\pi}^T$ we propose the index

$$J(P) := \frac{1}{N}\sum_{t\geq 0} ||P^t - \mathbf{1}\boldsymbol{\pi}^T||_F^2 = \frac{1}{N}\,\mathrm{Tr}\left[\sum_{t\geq 0}(I - \boldsymbol{\pi}\mathbf{1}^T)(P^T)^t P^t (I - \mathbf{1}\boldsymbol{\pi}^T)\right] \tag{3.28}$$

where $\|M\|_{\mathrm{F}} := \sqrt{\mathrm{Tr}(MM^T)}$ is the Frobenius norm of a matrix and where we added the normalizing factor $1/N$ for reasons which will be clarified in the following.

This cost appears in at leas two different contexts. Assume first that we want to evaluate the speed of convergence of the consensus algorithm by the ℓ^2 norm of the transient, namely

$$\frac{1}{N}\sum_{t\geq 0}\left[\|\boldsymbol{x}(t)-\boldsymbol{x}(\infty)\|^2\right] .$$

Notice that this ℓ^2 norm will depend on the initial condition $\boldsymbol{x}(0)$. For this reason, we assume that the initial condition is a random variable with zero-mean and covariance matrix $\mathbb{E}\left[\boldsymbol{x}(0)\boldsymbol{x}(0)^T\right] = I$. We can now consider the expected value of the ℓ^2 norm of the transient which is now a function only of the matrix P. Indeed, by some simple computations [108] it can be shown that

$$\mathbb{E}\left[\frac{1}{N}\sum_{t\geq 0}\|\boldsymbol{x}(t)-\boldsymbol{x}(\infty)\|^2\right] = J(P)\,.$$

so $J(P)$ can be interpreted as the ℓ_2 norm of the difference among the trajectory of the states and the asymptotic consensus value.

The cost $J(P)$ appears also in the context of noisy consensus [106, 108, 76]. Consider a network of agents implementing the consensus algorithm, in which update is affected by additive noise, so that the actual update of the state is the following

$$\boldsymbol{x}(t+1) = P\boldsymbol{x}(t) + \boldsymbol{n}(t)\,,$$

where $\boldsymbol{n}(t)$ is a random white process. Assume that $\mathbb{E}[\boldsymbol{n}(t)] = 0$ and $\mathbb{E}[\boldsymbol{n}(t)\boldsymbol{n}(t)^T] = I$ for all $t \in \mathbb{N}$. Assume that the initial condition is random and that it is uncorrelated from the noise process. We are interested in the dispersion of $\boldsymbol{x}(t)$. If we measure it by evaluating the displacement of $\boldsymbol{x}(t)$ from the weighted average $\sum_i \pi_i x_i(t)$, namely by introducing the vector

$$\boldsymbol{e}(t) = (I - \mathbf{1}\boldsymbol{\pi}^T)\boldsymbol{x}(t),$$

then it can be shown that

$$\lim_{t\to\infty}\mathbb{E}\left[\|\boldsymbol{e}(t)\|^2\right] = J(P),$$

Thus, the proposed LQ cost also characterizes the spreading of the asymptotic value of the state vector around its weighted average in a noisy network.

It is possible to consider the problem of determining the matrix P satisfying a constraint and minimizing the index $J(P)$. On the same spirit of the previous Section

on rate of convergence, we try instead to provide estimates of $J(P)$ which allow to understand how this index depends on the structure of P and more precisely on the topological properties of the graph $\mathcal{G}_P$. In fact we are able to prove that $J(P)$ is related to the effective resistance of a suitable electrical network. This geometric parameter depends on the topology only, and not on the particular entries of P. Since the electrical analogy holds only if P is reversible [51], we restrict our attention to this class of matrices also in this Section.

Using these results we show that, analogously to what happens for convergence rate, under some assumptions, geometric graphs exhibit a particular behavior of the cost $J(P)$ as a function of the number of nodes which depends on the geometric dimension of the graph, and on the number of agents, only. In particular, if the graph has geometric dimension one, namely it is a geometric graph on a segment, then $J(P)$ grows linearly in the number of nodes, while, if the graph has geometric dimension two, namely it is a geometric graph on a square, then $J(P)$ grows logarithmically in the number of nodes. Finally, if the graph has geometric dimension three (or more), namely it is a geometric graph on a cube, then $J(P)$ is bounded from above by a constant independent on the number of nodes. This result is based on (and extends) an analogous result [106] which holds for d-dimensional tori. In this way we show that the spatial invariance of tori is not a necessary requirement for having this kind of behavior of $J(P)$.

LQ norm: preliminaries

In this section we analyze the cost function $J(P)$ when P is a primitive stochastic matrix, so that $J(P)$ is finite. This is an immediate consequence of the fact that convergence of P^t toward its limit $\mathbf{1}\boldsymbol{\pi}^T$, where $\boldsymbol{\pi}$ denotes as usual the invariant measure of P, is exponential.

In fact, aperiodicity is consequence of a stronger technical assumption on P which we impose in this Section only. In particular, we impose that the diagonal elements of P are all positive. Observe that this condition is not restrictive for the consensus algorithm as it assumes only that in the state-update (see 3.1) each agent gives to its own current state a positive weight and this does not requires additional communication. For this reason, throughout this Section we use the following short-hand definition.

Definition 3.6.1. We say that a matrix P is a *consensus matrix* if it stochastic and irreducible, and it satisfies $P_{uu} > 0$ for all u.

Remark 3.6.2. A self-loop is a cycle of length 1, so the definition of aperiodicity is trivially satisfied.

Recall that a reversible matrix is such that $\Pi P = P^T \Pi$ where $\Pi = \text{diag}(\boldsymbol{\pi})$ and $\boldsymbol{\pi}$ is the invariant measure of P. Recall moreover that the graph associated with primitive reversible matrices is necessarily undirected. For this reason, in the following we will always assume that the communication graph $\mathcal{G}$ is undirected.

Also, despite the fact that each node has its self-loop, recall that the neighborhood of a node $u \in \mathcal{V}$ is the set of its neighbors, except u itself

$$\mathcal{N}_u := \{v \in \mathcal{V} : v \neq u, (u, v) \in \mathcal{E}\} \tag{3.29}$$

Now we briefly recall the notion of Green matrix of a consensus matrix P, which is also known as fundamental matrix in the Markov chains literature. Here we concentrate only on the results that we need. A more complete list of the properties and treatment of the fundamental matrix can be found in [110], Chapter 2.

Definition 3.6.3. Let P be a consensus matrix, with invariant measure $\boldsymbol{\pi}$. The Green matrix G of P is defined as

$$G := \sum_{t \geq 0} (P^t - \mathbf{1}\boldsymbol{\pi}^T). \tag{3.30}$$

The Green matrix plays a fundamental role in this Section due to its property of being almost an inverse of the Laplacian $L = I - P$, as the following lemma states. The proof follows from direct computation using the fact that if all the eigenvalues of a square matrix M are inside the unitary circle then

$$(I - M)^{-1} = \sum_{j=0}^{\infty} M^j.$$

Lemma 3.6.4. *Let P be a consensus matrix, with invariant measure $\boldsymbol{\pi}$, and let G be its Green matrix. Then G is the unique solution to the system*

$$\begin{cases} GL = I - \mathbf{1}\boldsymbol{\pi}^T \\ G\mathbf{1} = 0 \end{cases}$$

and satisfies

$$G + \mathbf{1}\boldsymbol{\pi}^T = (L + \mathbf{1}\boldsymbol{\pi}^T)^{-1}.$$

Moreover, the matrix $\tilde{L} = \begin{bmatrix} L & \mathbf{1} \\ \boldsymbol{\pi}^T & 0 \end{bmatrix}$ *is invertible and its inverse is the matrix*

$$\tilde{L} = \begin{bmatrix} G & \mathbf{1} \\ \boldsymbol{\pi}^T & 0 \end{bmatrix}. \tag{3.31}$$

The expression in Eq. 3.31 implies in particular the following equation, which will be useful later on

$$\begin{bmatrix} G & \mathbf{1} \end{bmatrix} \begin{bmatrix} L \\ \boldsymbol{\pi}^T \end{bmatrix} = I, \tag{3.32}$$

where I is the $N \times N$ identity matrix.

The electrical analogy

In this Section we present electrical networks, their relation with consensus matrices, and the well-known notion of effective resistance. Making use of these notions, we state our main results, Theorem 3.6.5 and Theorem 3.6.7, which give useful bounds of the cost $J(P)$ of a reversible consensus matrix P.

The analogy between consensus matrices, or Markov chains, and resistive electrical networks dates back to the work of Doyle and Snell [51]. It is a powerful tool which gives strong intuitions on the behavior of the chain on the basis of the physics of electrical networks, as well as permitting simple and clear proofs for many results. Our interest, as already mentioned, is mainly related to the possibility to rewrite the LQ cost we are interested in in terms of a geometric parameter, the average effective resistance. To this respect we are strongly indebted in terms of inspiration to the papers by Barooah and Hespanha [97, 96, 98], from which we took many results we state here without a proof. Effective resistances also arise as a performance metric for clock synchronization algorithms in [111, 112], and methods for its minimization are proposed in [113].

Electrical networks

A resistive electrical network is a weighted graph in which pairs of nodes are connected by resistors. A resistive electrical network is therefore determined by a symmetric matrix C with non-negative entries which tells for each pair of nodes u, v which is the conductance of the resistor connecting those two nodes. A resistive electrical network is said to be connected if the graph $\mathcal{G}_C$ associated with C is connected.

In order to describe the current flowing in the electrical network and to write Kirchoff's and Ohm's laws, we choose (arbitrarily) a conventional orientation for each edge of the

undirected graph $\mathcal{G}$, so that current will be denoted as positive when flowing consistently with the direction of the edge and negative otherwise. To this aim, for any pair of nodes u, v, such that $u \neq v$ and $C_{uv} = C_{vu} \neq 0$, we choose either (u, v) or (v, u) in $\mathcal{V} \times \mathcal{V}$. Let $\mathcal{E} \subseteq \mathcal{V} \times \mathcal{V}$ be the set of directed edges built in this way and let M be the number of edges. Let moreover B be the incidence matrix of the graph making use of this orientation.

We define the diagonal matrix $\mathcal{C} \in \mathbb{R}^{M \times M}$ having the conductance of the edge e as the entry in position (e, e). The relation between $\mathcal{C}$ and C is easily obtained as

$$B^T \mathcal{C} B = \operatorname{diag}(C\mathbf{1}) - C\,, \tag{3.33}$$

namely

$$[B^T \mathcal{C} B]_{uv} = \begin{cases} C_u & \text{if } u = v, \\ -C_{uv} & \text{if } (u, v) \in \mathcal{E}, \\ 0 & \text{if } (u, v) \notin \mathcal{E}, \end{cases}$$

where $C_u := \sum_{v \in V} C_{uv}$. Notice that this relation is the generalization of Lemma 2.1.6 to weighted graph with positive weights. The lemma is a particular case in which all the conductances are set to 1.

Let $\boldsymbol{i} \in \mathbb{R}^N$ be given such that $\boldsymbol{i}^T \mathbf{1} = 0$, and interpret the k-th entry of $\boldsymbol{i}$ as the current which is injected (or extracted if negative in sign) into the k-th node of the network from an external source. We denote by $\boldsymbol{j} \in \mathbb{R}^M$ and $\boldsymbol{v} \in \mathbb{R}^N$, respectively, the current flows on the edges and the potentials at the nodes which are produced in the network by injecting the current $\boldsymbol{i}$, with the convention that j_e, $e \in \mathcal{E}$, is positive when the current flows in the direction of e. The previously defined matrices B and $\mathcal{C}$ allow us to compactly write Kirchhoff's node law and Ohm's law as the system as follows

$$\begin{cases} B^T \boldsymbol{j} = \boldsymbol{i}\,, \\ \mathcal{C} B \boldsymbol{v} = \boldsymbol{j}\,, \end{cases} \tag{3.34}$$

where the first equation states that the total current flow entering into each node equals the total flow exiting from it (Kirchhoff's current law), while the second equation represents Ohm's law, $C_{uu'}(v_u - v_{u'}) = j_e$ for all $e = (u, u') \in \mathcal{E}$.

Solving the electrical network means finding the solutions $\boldsymbol{j}$ and $\boldsymbol{v}$ of Eq. (3.34), in particular finding the solution $\boldsymbol{v}$ of the following electrical equation

$$B^T \mathcal{C} B \boldsymbol{v} = \boldsymbol{i}\,. \tag{3.35}$$

It is well known (see, e.g., [51]) that a solution exists and, for a connected network, is

unique up to a constant additive term for $\boldsymbol{v}$, i.e., the differences $v_u - v_{u'}$ are uniquely defined. In the next subsection, we will give an explicit expression for the solutions $\boldsymbol{v}$, involving the Green matrix of the associated reversible consensus matrix.

Given a connected electrical network with conductance matrix C, the *effective resistance* between two nodes u, u' is defined to be

$$\mathcal{R}_{uu'}(C) := v_u - v_{u'}$$

where we impose $\boldsymbol{i} = \boldsymbol{e}_u - \boldsymbol{e}_{u'}$ and $\boldsymbol{v}$ is any solution of the corresponding electrical equation (3.35)namely, $\boldsymbol{v}$ is the potential at each node of the network in the case when a unit current is injected at node u and extracted ad node u'. Finally the *average effective resistance* of the electrical network is defined as

$$\bar{\mathcal{R}}(C) := \frac{1}{2N^2} \sum_{u,\, u' \in V} \mathcal{R}_{uu'}(C). \tag{3.36}$$

Given a connected undirected graph $\mathcal{G}$, in the following we will use the notations $\mathcal{R}_{uu'}(\mathcal{G})$ and $\bar{\mathcal{R}}(\mathcal{G})$ to mean respectively $\mathcal{R}_{uu'}(A)$ and $\bar{\mathcal{R}}(A)$, where A is the adjacency matrix of the graph $\mathcal{G}$. These are the effective resistance and the average effective resistance associated with the electrical network having conductance equal to 1 for all the edges of $\mathcal{G}$ and conductance equal to 0 otherwise. We prefer to use the symbols $\mathcal{R}_{uu'}(\mathcal{G})$ and $\bar{\mathcal{R}}(\mathcal{G})$ in order to stress the role of the graph.

Electrical network associated with a consensus matrix

There is a way to obtain a one to one relation between reversible consensus matrices and connected resistive electrical networks with some fixed total conductance (i.e., sum of the conductances of all edges). Let P be a reversible consensus matrix and let

$$\Phi(P) := N\Pi P$$

where $\Pi = \operatorname{diag}(\boldsymbol{\pi})$ and $\boldsymbol{\pi}$ is the invariant measure of P. It is clear that $\Phi(P)$ is the conductance matrix of a connected resistive network. It can be shown that the map Φ is injective. Indeed, if P_1, P_2 are reversible consensus matrices and if $\Phi(P_1) = \Phi(P_2)$, then $\operatorname{diag}(\boldsymbol{\pi}_1) P_1 = \operatorname{diag}(\boldsymbol{\pi}_2) P_2$. Multiplying on the right both members by $\mathbf{1}$ we obtain that $\boldsymbol{\pi}_1 = \boldsymbol{\pi}_2$ and consequently $P_1 = P_2$. We show now that $\operatorname{Range}(\Phi) = \mathcal{S}$, where

$$\mathcal{S} := \{C \in R_+^{N\times N} : C = C^T,\, C_{uu} > 0 \;\forall\; u \in V,\, \mathcal{G}_C \text{ is connected, and } \mathbf{1}^T C \mathbf{1} = N\}$$

Clearly Range $(\Phi) \subseteq \mathcal{S}$. To prove the equality, for any given $C \in \mathcal{S}$ we consider

$$P = (\text{diag}\,(C\mathbf{1}))^{-1} C \tag{3.37}$$

and we show that P is a reversible consensus matrix such that $\Phi(P) = C$. It is straightforward to see that $P\mathbf{1} = \mathbf{1}$, $P_{uu} > 0$, $\forall\ u \in V$, and that $\mathcal{G}_P$ is connected.

To prove that P is reversible and that $\Phi(P) = P$, the key remark is that

$$\boldsymbol{\pi} = \frac{1}{N} C\mathbf{1}$$

is the invariant measure of P, and thus $\Pi = \frac{1}{N}\text{diag}\,(C\mathbf{1})$. This immediately implies that $\Phi(P) = C$. The reversibility of P is then proved by using the symmetry of C: $\Pi P = \frac{1}{N}C = \frac{1}{N}C^T = P^T\Pi$. In this way, we have proved not only that Φ is bijective on $\mathcal{S}$, but also that (3.37) provides the inverse of Φ over $\mathcal{S}$.

Consider now a reversible consensus matrix P and its associated conductance matrix $C := \Phi(P)$. Let moreover B and $\mathcal{C}$ be the matrices associated with the resistive electrical network with conductance C, as defined above. Notice that the Laplacian matrix $L := I - P = \frac{1}{N}\Pi^{-1}B^T\mathcal{C}B$ and so the electrical equation 3.35 is equivalent to

$$L\boldsymbol{v} = \tfrac{1}{N}\Pi^{-1}\boldsymbol{i}. \tag{3.38}$$

The network being connected, $\ker L = \{\alpha\mathbf{1} : \alpha \in \mathbb{R}\}$, and thus, for any $\boldsymbol{i}$ such that $\boldsymbol{i}^T\mathbf{1} = 0$, Eq. (3.38) has infinitely many solutions, of the form $\boldsymbol{v} + \alpha\mathbf{1}$ for some real constant α, where $\boldsymbol{v}$ is a particular solution. In our setting it is convenient to find $\boldsymbol{v}$ which satisfies the following constraint

$$\boldsymbol{\pi}^T\boldsymbol{v} = 0,$$

which means that we need to solve the equation

$$\begin{bmatrix} L \\ \boldsymbol{\pi}^T \end{bmatrix} \boldsymbol{v} = \begin{bmatrix} \frac{1}{N}\Pi^{-1}\boldsymbol{i} \\ 0 \end{bmatrix}.$$

Thanks to Eq. (3.32), the solution can be explicitly written by using the Green matrix G associated with P, as follows

$$\boldsymbol{v} = \begin{bmatrix} G & \mathbf{1} \end{bmatrix} \begin{bmatrix} \frac{1}{N}\Pi^{-1}\boldsymbol{i} \\ 0 \end{bmatrix} = \tfrac{1}{N}G\Pi^{-1}\boldsymbol{i}\,. \tag{3.39}$$

Consequently, we can obtain the effective resistance as follows

$$\mathcal{R}_{uu'}(C) = \tfrac{1}{N}(\boldsymbol{e}_u - \boldsymbol{e}_{u'})^T G\Pi^{-1}(\boldsymbol{e}_u - \boldsymbol{e}_{u'})\,. \tag{3.40}$$

LQ cost and effective resistance

This section is devoted to our main results on the relation between the LQ cost $J(P)$ for a reversible consensus matrix P and the average effective resistance of a suitable electrical network. The results are then formulated in the special case of symmetric consensus matrices, since for this case they turn out to be clearer and more readable. The proofs are postponed to Section 3.6.

Consider a reversible consensus matrix P and let $\boldsymbol{\pi}$ be its invariant measure. Build the electrical network associated with the matrix P^2 as suggested in Sec. 3.6, namely build the matrix of conductances

$$C := \Phi(P^2) = N\Pi P^2. \tag{3.41}$$

In the particular case in which P is symmetric we have that $C = P^2$. The following theorem allows us to estimate the cost in terms of the average effective resistance of this electrical network, and of quantities depending on the elements of the invariant measure of P.

Theorem 3.6.5. *Let $P \in \mathbb{R}^{N\times N}$ be a reversible consensus matrix and $\boldsymbol{\pi}$ its invariant measure, and C the matrix of conductances defined in Eq. (3.41). Then it holds*

$$\frac{\pi_{\min}^3 N^2}{\pi_{\max}}\bar{\mathcal{R}}(C) \le J(P) \le \frac{\pi_{\max}^3 N^2}{\pi_{\min}}\bar{\mathcal{R}}(C)\,, \tag{3.42}$$

where $\pi_{\min}$ and $\pi_{\max}$ are respectively the minimum and maximum entries of $\boldsymbol{\pi}$.

In the particular case of symmetric matrix we have the following corollary which is a straightforward consequence of the previous theorem.

Corollary 3.6.6. *Let $P \in \mathbb{R}^{N\times N}$ be a symmetric consensus matrix, and C the matrix of conductances defined in Eq. (3.41). Then it holds*

$$J(P) = \bar{\mathcal{R}}(C).$$

The previous results catch the dependance of the cost on the electrical network built from P^2. The following theorem allows us to write the cost $J(P)$ in terms of the effective

resistance of the graph associated with P only, regardless of the particular entries of the matrix.

Theorem 3.6.7. *Let P be a reversible consensus matrix with invariant measure $\boldsymbol{\pi}$ and let $\mathcal{G}$ be the graph associated with P. Assume that all the non-zero entries of P belong to the interval $[p_{\min}, p_{\max}]$, and that the degree of any node is bounded from above by an integer δ. Then,*

$$\frac{\pi_{\min}^3 N}{8p_{\max}^2\delta^2\pi_{\max}^2}\bar{\mathcal{R}}(\mathcal{G}) \leq J(P) \leq \frac{\pi_{\max}^3 N}{p_{\min}^2\pi_{\min}^2}\bar{\mathcal{R}}(\mathcal{G})\,. \tag{3.43}$$

A simpler result can be obtained for symmetric matrices as a straightforward consequence of the previous theorem.

Corollary 3.6.8. *Let P be a symmetric consensus matrix associated with a graph $\mathcal{G}$. Assume that all the non-zero entries of P belong to the interval $[p_{\min}, p_{\max}]$, and that the degree of any node is bounded from above by an integer δ. Then,*

$$\frac{1}{8p_{\max}^2\delta^2}\bar{\mathcal{R}}(\mathcal{G}) \leq J(P) \leq \frac{1}{p_{\min}^2}\bar{\mathcal{R}}(\mathcal{G})\,.$$

These last two results can be used to estimate the proposed LQ cost in terms of the effective resistance of graphs only, as we will show in Section 3.6.

LQ cost and network dimension

One of the most important problems in the design of a sensor network is to dimension it, namely to decide how many sensors we need to deploy for obtaining a given performance. From this point of view, it is very important to understand how our cost function scales in terms of the number N of nodes in a sequence of graphs of growing size, belonging to a given family. The results in the previous sections can be used to achieve this goal.

Consider in fact a sequence of graphs $\{\mathcal{G}_N\}_{N\geq 2}$, and assume that $f(N) = \bar{\mathcal{R}}(\mathcal{G}_N)$ is a known function of N. Assume that the degree of any node of each $\mathcal{G}_N$ is uniformly bounded from above by a positive integer δ. At first, assume to build a sequence of symmetric matrices P_N, each one consistent with the corresponding $\mathcal{G}_N$, and such that if $[P_N]_{ij} \neq 0$, then $p_{\min} \leq [P_N]_{ij} \leq p_{\max}$, for all N. Then we immediately obtain by Corollary 3.6.8 that the asymptotic scaling of $J(P_N)$ for $N \to \infty$ is given by $f(N)$, up to some multiplicative constant.

Notice that the above-mentioned assumptions on the family P_N are satisfied, for example, by both the consensus protocols proposed in Section 3.2 which lead to symmetric

matrices. For example, if the update law for $\mathcal{G}_N$ is[2]

$$x_u^N(t+1) = x_u^N(t) + \varepsilon \sum_{v \in \mathcal{N}_u} (x_v^N(t) - x_u^N(t))$$

where ε is small enough, then clearly $[P_N]_{uv} \in [\varepsilon, \varepsilon\delta]$, for any $\mathcal{G}_N$.

If we relax the assumption that all P_N's are symmetric, and we consider a family of reversible matrices P_N, each one consistent with the corresponding $\mathcal{G}_N$, the uniform bound from above and from below on the non-zero entries $[P_N]_{ij}$ is not enough to ensure that the asymptotic behavior of $J(P_N)$ is given by $f(N)$. In fact, once we denote by $\boldsymbol{\pi}_N$ the invariant measure of P_N, and by $\pi_{N,\min}$ and $\pi_{N,\max}$ respectively the minimum and maximum value of the entries of $\boldsymbol{\pi}_N$, we need the further assumption that the sequences $N\pi_{N,\min}$ and $N\pi_{N,\max}$ are uniformly bounded from above and below by constants independent of N. Under this assumption, Theorem 3.6.7 clearly ensures that the asymptotic behavior of $J(P_N)$ is given by $f(N)$. Although the assumption requiring that $N\pi_{N,\min}$ and $N\pi_{N,\max}$ are uniformly bounded can be rather difficult to check for the general reversible consensus matrices, we can easily see that it holds true in case we choose uniform weights, or simple random walk, for which

$$P_N = \operatorname{diag}\left((A_N + I)\mathbf{1}\right)^{-1}(A_N + I)$$

where A_N is the adjacency matrix of the graph $\mathcal{G}_N$. If we set

$$\pi_N = \frac{1}{\mathbf{1}(A_N + I)\mathbf{1}}(A_N + I)\mathbf{1}$$

it is trivial to see that π_N is a stochastic vector, and moreover since (notice that $A_N = A_N^T$ since the graph is undirected)

$$\begin{aligned}
\pi_N^T P_N &= \frac{1}{\mathbf{1}(A_N + I)\mathbf{1}}\mathbf{1}^T(A_N + I)\operatorname{diag}\left((A_N + I)\mathbf{1}\right)^{-1}(A_N + I) \\
&= \frac{1}{\mathbf{1}(A_N + I)\mathbf{1}}\mathbf{1}^T(A_N + I) \\
&= \pi_N^T
\end{aligned}$$

we conclude that π_N is the left invariant measure of P_N. Under the assumption that for any graph of the family $\mathcal{G}_N$ and for any node u of it, its degree, δ_u^N, is bounded from above by a value δ, it is clear that the entries of the consensus matrix belong to the interval $[\frac{1}{\delta+1}, \frac{1}{2}]$. One can also check that each entry of the invariant measure lies in the

[2]Here $x_u^N(t)$ mean the state of node u at time t in case we consider the graph $\mathcal{G}_N$.

interval $[\frac{2}{(\delta+1)N}, \frac{\delta+1}{2N}]$, and hence the assumptions are satisfied.

We conclude this remark noticing that the assumption requiring that $N\pi_{N,\min}$ and $N\pi_{N,\max}$ are uniformly bounded is not implied by the other assumptions that P_N are reversible consensus matrices whose entries belong to a fixed interval $[p_{\min}, p_{\max}]$ and are consistent with graphs with degrees uniformly bounded by δ. This is proved in the example showed in figure 3.7. One can check that the corresponding consensus matrix is reversible and that the invariant measure $\boldsymbol{\pi}$ is such that $\pi_k = \alpha(a/b)^{k-1}$, where α is a suitable normalizing factor. If we assume that $a > b$, then $\pi_{N,\min} = \pi_1 = \alpha$ and $\pi_{N,\max} = \pi_N = \alpha(a/b)^{N-1}$. In this case $N\pi_{N,\min}$ and $N\pi_{N,\max}$ cannot be uniformly bounded from below and above, because if this were the case, then also the ratio $N\pi_{N,\max}/N\pi_{N,\min}$ would be uniformly bounded from below and above, but this is not possible, as $N\pi_{N,\max}/N\pi_{N,\min} = \pi_{N,\max}/\pi_{N,\min} = (a/b)^{N-1}$.

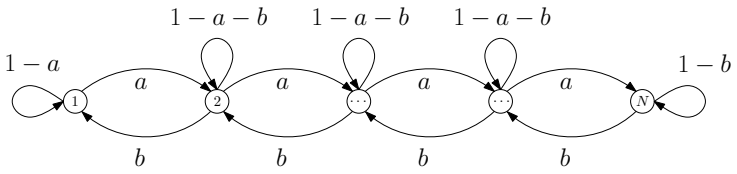

Figure 3.7: Example: a family of growing lines. We assume that $a > 0$, $b > 0$ and $a + b < 1$.

The relation between the LQ cost and effective resistance: proofs of Theorem 3.6.5 and Theorem 3.6.7

This section is devoted to the proof of the theorems relating the LQ cost with the average effective resistance. We recall some useful facts from the literature, and then use these notions to prove the results.

Electrical networks: properties of the effective resistances

This section is devoted to briefly recall without proofs some well-known results on the behavior of the effective resistances in case of perturbation of the electrical network. These are of fundamental importance, since effective resistances show monotonicity properties which are not trivial to prove for consensus matrices without the electrical analogy.

A first important property is the fact if we consider the map $d_R : \mathcal{V} \times \mathcal{V} \to \mathbb{R}^+$ in which we set $d_R(u, v) = \mathcal{R}_{uv}$, then d_R is a distance, as stated in the following Lemma (see e.g. [114, Thm. B] for a proof).

Lemma 3.6.9. *If the electrical network is connected, then the effective resistance is a distance, namely it satisfies the following properties*

- $\mathcal{R}_{uv} \geq 0$ *for all* $u, v \in \mathcal{V}$, *and* $\mathcal{R}_{uv} = 0$ *if and only if* $u = v$;
- $\mathcal{R}_{uv} = \mathcal{R}_{vu}$, *for all* $u, v \in \mathcal{V}$;
- $\mathcal{R}_{uw} \leq \mathcal{R}_{uv} + \mathcal{R}_{vw}$ *for all* $u, v, w \in \mathcal{V}$.

A second result, known as Rayleigh's monotonicity law, says that increasing (resp., decreasing) the conductance in any edge of the network implies that the effective resistance between any other couple of nodes respectively cannot increase (resp., decrease). The statement is essentially taken from [96, 115], where the authors were considering a more general case.

Lemma 3.6.10 (**Rayleigh's monotonicity law**). *Let* C *and* C' *be the conductance matrices of two electrical networks such that*

$$C_{uu'} \leq C'_{uu'}, \forall\, (u,\, u') \in \mathcal{V} \times \mathcal{V}\,.$$

Then, the effective resistances between any two nodes v, v' *in the network are such that*

$$\mathcal{R}_{vv'}(C) \geq \mathcal{R}_{vv'}(C').$$

The following lemma [115, Lemma 4.6.1] says that, if we take two resistive networks with the conductance matrices scaled by a constant α, then the effective resistances will be scaled by the constant $1/\alpha$.

Lemma 3.6.11.

$$\mathcal{R}_{uu'}(\alpha C) = \frac{1}{\alpha}\mathcal{R}_{uu'}(C), \forall\, (u,\, u') \in V \times V.$$

Remark 3.6.12. Lemma 3.6.11 and Rayleigh's monotonicity law imply that the effective resistance in an electrical network is essentially due to the graph topology. In fact, if we have an electrical network with conductance matrix C whose non-zero entries belong to the interval $[c_{\min},\, c_{\max}]$ and if C' is a conductance matrix having entries equal to 1 in the positions in which C has non-zero entries and to 0 elsewhere, then

$$\frac{1}{c_{\max}}\mathcal{R}_{uu'}(C') \leq \mathcal{R}_{uu'}(C) \leq \frac{1}{c_{\min}}\mathcal{R}_{uu'}(C'), \forall\, (u,\, u') \in \mathcal{V} \times \mathcal{V}.$$

The last technical lemma deals with h-fuzzing in electrical networks with unitary conductances. Given an integer $h \geq 1$ and a graph $\mathcal{G}$, we call h-fuzz of $\mathcal{G}$, denoted by the symbol $\mathcal{G}^{(h)} = (\mathcal{V}^{(h)}, \mathcal{E}^{(h)})$, a graph with the same set of nodes, $\mathcal{V}^{(h)} = \mathcal{V}$, and with an edge connecting two nodes u and v if and only if the graphical distance $d_{\mathcal{G}}(u,\, v)$ between

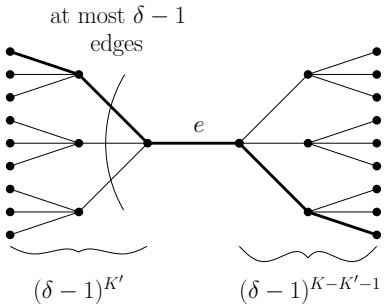

Figure 3.8: Illustration of the proof of Lemma 3.6.14: upper bound on the number of paths of length K in which e is the $(K' + 1)$-th edge, in a graph with node degree at most $\delta = 4$.

u and v in $\mathcal{G}$ is at most h, namely

$$\mathcal{E}^{(h)} = \{(u, v) \in \mathcal{V} \times \mathcal{V} : d_{\mathcal{G}}(u, v) \leq h\}.$$

Notice that, if $h = 1$, then $\mathcal{G}^{(1)} = \mathcal{G}$. If D is the diameter of the graph, namely the maximum graphical distance between a couple of nodes, then $\mathcal{G}^{(D)}$ is the complete graph. It is easy to see that, if P is a stochastic matrix with positive diagonal entries, then the graph $\mathcal{G}_{P^h}$ associated with a P^h is the h-fuzz of the graph $\mathcal{G}_P$ associated with P.

The lemma, which is stated with proof in [115, Lemma 5.5.1], suggests that the effective resistance of $\mathcal{G}$ and of its h-fuzz $\mathcal{G}^{(h)}$ have effective resistances with a similar asymptotic behavior.

Lemma 3.6.13. *Let $h \in \mathbb{Z}$, $h \geq 1$, and let $\mathcal{G} = (\mathcal{V}, \mathcal{E})$ be a graph and $\mathcal{G}^{(h)} = (\mathcal{V}, \mathcal{E}^{(h)})$ be its h-fuzz. For any edge $e \in \mathcal{E}$, define $\mu_h(e)$ to be the number of paths of length at most h passing through e in $\mathcal{G}$ (without any self-loop in the path), and define $\mu_h = \max_{e \in \mathcal{E}} \mu_h(e)$. The following bounds hold true*

$$\frac{1}{h\mu_h} \mathcal{R}_{uv}(\mathcal{G}) \leq \mathcal{R}_{uv}(\mathcal{G}^{(h)}) \leq \mathcal{R}_{uv}(\mathcal{G}).$$

The value of μ_h in the previous result clearly depends on the particular graph under consideration. The following lemma gives a conservative bound for μ_h which depends only on the maximum degree of the nodes in the graph.

We will use this bound later, in the particular case of $h = 2$.

Lemma 3.6.14. *Let μ_h be defined as in Lemma 3.6.13. If in $\mathcal{G}$ all nodes have degree at most δ, then*

$$\mu_h \leq h^2(\delta - 1)^{h-1}. \tag{3.44}$$

Proof. For any $K = 1, \dots, h$, we want to find an upper bound on the number of paths of length K passing through the edge e. We let K' be an integer $0 \leq K' \leq K-1$, and we consider the number of paths in which edge e is the $(K'+1)$-th edge in the path, namely there are K' edges before e and $K - K' - 1$ edges after e. As it can be easily seen in Figure 3.8, there are at most $(\delta-1)^{K'}$ choices for portion of path preceding e, and at most $(\delta-1)^{K-K'-1}$ choices for the portion following e, so that there are at most $(\delta-1)^{K-1}$ paths having e in $(K'+1)$-th position. Summing upon all $K' = 0, \dots, K-1$, and then summing also upon all path lengths $K = 1, \dots, h$, we obtain that, for any $e \in \mathcal{E}$,

$$\mu_h(e) \leq \sum_{K=1}^{h} \sum_{K'=0}^{K-1} (\delta-1)^{K-1} = \sum_{K=1}^{h} K(\delta-1)^{K-1} \leq \sum_{K=1}^{h} h(\delta-1)^{h-1} = h^2(\delta-1)^{h-1}\,.$$

Finally notice that this upper bound for $\mu_h(e)$ is the same for all edges $e \in \mathcal{E}$, and thus it is also an upper bound for the maximum, μ_e. □

Proof of Theorem 3.6.5 and Theorem 3.6.7

The previous definitions and properties are used in this section to prove the main results Theorem 3.6.5 and Theorem 3.6.7 for reversible consensus matrices. Then Corollary 3.6.6 and Corollary 3.6.8 are immediate for symmetric matrices, since in for them $\pi_u = \frac{1}{N}$ for all $u = 1, \dots, N$. In order to prove the results, we need to introduce two more technical objects which will help us to develop the theory.

Consider a reversible consensus matrix P with invariant measure $\boldsymbol{\pi}$. We call *weighted cost* the following function of P

$$J_{\mathrm{w}}(P) \;:=\; \mathrm{Tr}\left[\sum_{t\geq 0} (I - \boldsymbol{\pi}\mathbf{1}^T)(P^T)^t \Pi P^t (I - \mathbf{1}\boldsymbol{\pi}^T)\right] \tag{3.45}$$

where $\Pi = \mathrm{diag}\,(\boldsymbol{\pi})$. Notice that in the case of symmetric matrices $J(P) = J_{\mathrm{w}}(P)$. Now, let $C := \Phi(P^2) = N\Pi P^2$. The second object we need is the *weighted average effective resistance*, which is defined as

$$\bar{\mathcal{R}}_{\mathrm{w}}(C) \;:=\; \frac{1}{2}\boldsymbol{\pi}^T \mathcal{R}(C)\boldsymbol{\pi} = \frac{1}{2} \sum_{(u,v)\in V\times V} \mathcal{R}_{uv}(C)\pi_u\pi_v\,. \tag{3.46}$$

Again, notice that in the symmetric case the weighted definition coincides with the un-weighted one, namely $\bar{\mathcal{R}}(C) = \bar{\mathcal{R}}_{\mathrm{w}}(C)$. We present now a lemma which clarifie the relation between the costs $J(P)$ and $J_{\mathrm{w}}(P)$, and between the weighted and the un-weighted average effective resistances, respectively. The proof is immediate from the

fact that $\pi_u > 0$ for all u.

Lemma 3.6.15. *Let P be a consensus matrix with invariant measure $\boldsymbol{\pi}$ and let $C := \Phi(P^2) = N\Pi P^2$. Then*

$$\frac{1}{N\pi_{\min}} J_{\mathrm{w}}(P) \leq J(P) \leq \frac{1}{N\pi_{\max}} J_{\mathrm{w}}(P)\pi_{\min}^2 N^2 \bar{\mathcal{R}}(C) \leq \bar{\mathcal{R}}_{\mathrm{w}}(C) \leq \pi_{\max}^2 N^2 \bar{\mathcal{R}}(C) \ .$$

After the inequalities of the above lemma, which concern separately the LQ cost and the average effective resistance, our goal is to find the relation between the cost of the consensus matrix P and the average effective resistance of the connected electrical network associated with P^2. Before doing so, we need the following technical lemma.

Lemma 3.6.16. *If P is a consensus matrix, then the diagonal entries of its Green matrix G are positive.*

Proof. For ease of notation, we prove that $G_{11} > 0$; the proof for the other diagonal entries of G can be obtained by the same arguments.

We fix the following notation: we let $\boldsymbol{g}^T = [G_{11}, \tilde{\boldsymbol{g}}^T]$ be the first row of G, and we define the following partitions

$$L = \begin{bmatrix} l_{11} & \boldsymbol{r}_1^T \\ \boldsymbol{c}_1 & \tilde{L} \end{bmatrix}, \ P = \begin{bmatrix} p_{11} & \boldsymbol{r}_1'^T \\ \boldsymbol{c}_1' & \tilde{P} \end{bmatrix}, \ \boldsymbol{g}^T = \begin{bmatrix} G_{11}, \tilde{\boldsymbol{g}}^T \end{bmatrix}, \ \boldsymbol{\pi}^T = \begin{bmatrix} \pi_1, \tilde{\boldsymbol{\pi}}^T \end{bmatrix}.$$

Because $GL = I - P$, we have $\boldsymbol{g}^T L = \boldsymbol{e}_1^T - \boldsymbol{\pi}^T$, where $\boldsymbol{e}_1$ denotes the first vector of the canonical basis of $\mathcal{R}^N$. Notice that $G\mathbf{1} = \mathbf{0}$ implies that $\boldsymbol{g}^T\mathbf{1} = 0$ and thus, in particular, $G_{11} = -\tilde{\boldsymbol{g}}^T\mathbf{1}_{N-1}$. Similarly, $\boldsymbol{\pi}^T L = \mathbf{0}^T$ gives $l_{11} = -\frac{1}{\pi_1}\tilde{\boldsymbol{\pi}}^T\boldsymbol{c}_1$. Hence, we can write the equality $\boldsymbol{g}^T L = \boldsymbol{e}_1^T - \boldsymbol{\pi}^T$ in the following equivalent way

$$\tilde{\boldsymbol{g}}_1^T \begin{bmatrix} -\mathbf{1}_{N-1} & I_{N-1} \end{bmatrix} \begin{bmatrix} -\frac{1}{\pi_1}\tilde{\boldsymbol{\pi}}^T \\ I_{N-1} \end{bmatrix} \tilde{L} \begin{bmatrix} -\mathbf{1}_{N-1} & I_{N-1} \end{bmatrix} = \boldsymbol{e}_1^T - \boldsymbol{\pi}^T.$$

By right-multiplying both sides of the above equality with a factor $\begin{bmatrix} \mathbf{0}_{N-1}^T \\ \tilde{L}^{-1} \end{bmatrix} \mathbf{1}_{N-1}$, we obtain that $\tilde{\boldsymbol{g}}_1^T\mathbf{1}_{N-1} = -\tilde{\boldsymbol{\pi}}^T\tilde{L}^{-1}\mathbf{1}_{N-1}$, and thus

$$G_{11} = \tilde{\boldsymbol{\pi}}^T\tilde{L}^{-1}\mathbf{1}_{N-1}\,.$$

Now notice that since by definition of Laplacian $L = I - P$, it follows $\tilde{L} = I - \tilde{P}$. Moreover, our definition of consensus matrix implies that P is primitive, and thus it is well-known that $\tilde{P}$ has all eigenvalues inside the unit circle (see e.g. [6, Lemma III.1] for

a proof). This implies that $\tilde{L}$ is invertible, and that the series $\sum_{t\geq 0}\tilde{P}^t$ is convergent and is equal to $(I-\tilde{P})^{-1}=\tilde{L}^{-1}$. This allows to obtain

$$G_{11}=\tilde{\boldsymbol{\pi}}^T\sum_{t\geq 0}\tilde{P}^t\mathbf{1}_{N-1}\,.$$

Recalling that the entries of $\tilde{\boldsymbol{\pi}}$ are all positive, and that $\tilde{P}$ has non-negative entries with at least some positive element, this proves that $G_{11}>0$. □

Now we have the tools to prove the following lemma, which shows the relation between the weighted cost and the weighted average effective resistance.

Lemma 3.6.17. *Let P be a reversible consensus matrix with invariant measure $\boldsymbol{\pi}$ and let $C:=\Phi(P^2)=N\Pi P^2$. Then*

$$\pi_{\min}N\bar{\mathcal{R}}_{\mathrm{w}}(C)\leq J_{\mathrm{w}}(P)\leq\pi_{\max}N\bar{\mathcal{R}}_{\mathrm{w}}(C).$$

Proof. To prove this lemma, we will prove the following two equalities involving the Green matrix associated with P^2, which we will denote by $G(P^2)$

1. $J_{\mathrm{w}}(P)=\operatorname{Tr}\Pi G(P^2)$;
2. $\bar{\mathcal{R}}_{\mathrm{w}}(C)=\frac{1}{N}\operatorname{Tr}G(P^2)$.

From such equalities, the statement follows, because Π is diagonal and positive definite, and $G(P^2)$ has positive diagonal entries (see Lemma 3.6.16).

As far as the first equality is concerned, observe that

$$\begin{aligned}J_{\mathrm{w}}(P)&=\operatorname{Tr}\left(\sum_{t\geq 0}(P^t-\mathbf{1}\boldsymbol{\pi}^T)^T\Pi(P^t-\mathbf{1}\boldsymbol{\pi}^T)\right)\\&=\operatorname{Tr}\left(\sum_{t\geq 0}\left((P^t)^T\Pi P^t-\boldsymbol{\pi}\boldsymbol{\pi}^T\right)\right)\\&=\operatorname{Tr}\left(\sum_{t\geq 0}\Pi\left(P^{2t}-\mathbf{1}\boldsymbol{\pi}^T\right)\right)=\operatorname{Tr}\left(\Pi G(P^2)\right).\end{aligned}$$

As far as the second equality is concerned, observe that, by substituting the expression for $\mathcal{R}_{uv}(C)$ given in Eq. (3.40) inside the definition of $\bar{\mathcal{R}}_{\mathrm{w}}(C)$, we get

$$\bar{\mathcal{R}}_{\mathrm{w}}(C)=\frac{1}{2}\sum_{u,v}\tfrac{1}{N}(\boldsymbol{e}_u-\boldsymbol{e}_v)^TG(P^2)\Pi^{-1}(\boldsymbol{e}_u-\boldsymbol{e}_v)\pi_u\pi_v,$$

from which we can compute

$$\begin{aligned}
\bar{\mathcal{R}}_{\mathrm{w}}(C) &= \frac{1}{2}\sum_{u,v} \tfrac{1}{N}(\boldsymbol{e}_u - \boldsymbol{e}_v)^T G(P^2)\Pi^{-1}(\boldsymbol{e}_u - \boldsymbol{e}_v)\pi_u\pi_v \\
&= \frac{1}{N}\frac{1}{2}\sum_{u,v}(\boldsymbol{e}_u^T - \boldsymbol{e}_v^T)G(P^2)(\pi_v\boldsymbol{e}_u - \pi_u\boldsymbol{e}_v) \\
&= \frac{1}{N}\Big(\frac{1}{2}\sum_{u,v}(\pi_v\boldsymbol{e}_u^T G(P^2)\boldsymbol{e}_u + \pi_u\boldsymbol{e}_v^T G(P^2)\boldsymbol{e}_v) \\
&\qquad\qquad - \frac{1}{2}\sum_{u,v}(\pi_v\boldsymbol{e}_v^T G(P^2)\boldsymbol{e}_u + \pi_u\boldsymbol{e}_u^T G(P^2)\boldsymbol{e}_v)\Big) \\
&= \frac{1}{N}\left(\mathrm{Tr}(G(P^2)) - \boldsymbol{\pi}^T G(P^2)\mathbf{1}\right) ,
\end{aligned}$$

which yields the proof of the equality since $\boldsymbol{\pi}^T G(P^2)\mathbf{1} = 0$. □

These lemmas can be easily used to infer the first main result, since Theorem 3.6.5's proof follows immediately from the inequalities in Lemma 3.6.15 together with those in Lemma 3.6.17.

In order to prove the second main result, we need a last technical lemma, which allows us to reduce the computation of the average effective resistances on the 2-fuzz of $\mathcal{G}$ to those on $\mathcal{G}$ only.

Lemma 3.6.18. *Let P be a reversible consensus matrix with invariant measure $\boldsymbol{\pi}$ and with associated graph $\mathcal{G}$. Let $C := \Phi(P^2)$. Then*

$$\frac{1}{8N\pi_{\max}\delta^2 p_{\max}^2}\bar{\mathcal{R}}(\mathcal{G}) \le \bar{\mathcal{R}}(C) \le \frac{1}{N\pi_{\min}p_{\min}^2}\bar{\mathcal{R}}(\mathcal{G}) ,$$

where δ denotes the largest degree of the graph nodes in $\mathcal{G}$ and $p_{\min}$ and $p_{\max}$ are, respectively, the minimum and the maximum of the non-zero elements of P.

Proof. First of all notice that, for all u, v such that $C_{uv} \neq 0$ we have that

$$C_{uv} = N\pi_u[P^2]_{uv} = N\pi_u \textstyle\sum_w P_{uw}P_{wv}.$$

By definition of $p_{\min}$ and $p_{\max}$, and because there are at most $\delta + 1$ non-zero terms P_{uw} for any fixed u, this yields

$$\forall C_{uv} \neq 0,\ N\pi_{\min}p_{\min}^2 \le C_{uv} \le N\pi_{\max}(\delta+1)p_{\max}^2. \tag{3.47}$$

By Remark 3.6.12, $\frac{1}{c_{\max}}\bar{\mathcal{R}}(\mathcal{G}^{(2)}) \le \bar{\mathcal{R}}(C) \le \frac{1}{c_{\min}}\bar{\mathcal{R}}(\mathcal{G}^{(2)})$, where $c_{\min}$ and $c_{\max}$ are the

minimum and maximum non-zero entries of C, respectively. This, together with Eq. 3.47, gives

$$\frac{1}{N\pi_{\max}(\delta+1)p_{\max}^2}\bar{\mathcal{R}}(\mathcal{G}^{(2)}) \leq \bar{\mathcal{R}}(C) \leq \frac{1}{N\pi_{\min}p_{\min}^2}\bar{\mathcal{R}}(\mathcal{G}^{(2)})\,.$$

Then we apply Lemmas 3.6.13 and 3.6.14, both with $h = 2$, and we obtain

$$\frac{1}{8(\delta-1)N\pi_{\max}(\delta+1)p_{\max}^2}\bar{\mathcal{R}}(\mathcal{G}) \leq \bar{\mathcal{R}}(C) \leq \frac{1}{N\pi_{\min}p_{\min}^2}\bar{\mathcal{R}}(\mathcal{G})\,,$$

which yields the claim, because $(\delta+1)(\delta-1) < \delta^2$. □

Now we can prove the second main result: Theorem 3.6.7 immediately follows from Theorem 3.6.5 and Lemma 3.6.18.

LQ cost in Geometric graphs

In this Section we apply the previous results to the class of geometric graphs, which we have already studied in relation to the rate of convergence. This is important since, as already mentioned, geometric graphs can be used to model actual sensor networks deployed in an Euclidean space.

The following theorem provides an estimate of the LQ cost for a generic geometric graph.

Theorem 3.6.19. *Let $P \in \mathbb{R}^{N\times N}$ be a reversible consensus matrix with invariant measure $\boldsymbol{\pi}$, associated with a graph $\mathcal{G} = (V, \mathcal{E})$. Assume that all the non-zero entries of P belong to the interval $[p_{\min}, p_{\max}]$ and that $\mathcal{G}$ is a geometric graph with parameters (s, r, γ, ρ) and nodes lying in $Q = [0, \ell]^d$ in which $\gamma < \ell/4$. Then*

$$k_1 + q_1 f_d(N) \leq J(P) \leq k_2 + q_2 f_d(N)\,, \tag{3.48}$$

where

$$f_d(N) = \begin{cases} N & \text{if } d = 1, \\ \log N & \text{if } d = 2, \\ 1 & \text{if } d \geq 3, \end{cases} \tag{3.49}$$

and where k_1, k_2, q_1 and q_2 depend on $p_{\max}$, $p_{\min}$, δ, d, on $\pi_{\min}N$ and $\pi_{\max}N$ and on the parameters s, r, γ, ρ of the geometric graph.

One of the most important consequences of this result is the fact that a d-dimensional regular grid has the same behavior of the LQ cost as a function of N of a irregular geometric graph. This implies that the behavior of the LQ cost as a function of N is

essentially captured by the dimensionality, rather than by the symmetry, exactly as it happens for the rate of convergence towards consensus.

In order to prove Theorem 3.6.19, we need two preliminary results. The first one is an immediate corollary of a theorem taken from [106], which states that the claimed asymptotic behavior of geometric graphs holds true at least in the case of regular grids. Recall that, by regular grid, we mean a d-dimensional geometric graph with $N = n^d$ nodes lying on the points $(i_1, \dots, i_d)$, where $i_1, \dots, i_d \in \{0, \dots, n-1\}$ and in which there is an edge connecting two nodes u, v if and only if their distance is $d_{\mathrm{E}}(u, v) \leq 1$.

Lemma 3.6.20. *Let $B_{\mathcal{L}}$ be the incidence matrix of a regular grid in dimension d with $N = n^d$ nodes. Let $P \in \mathbb{R}^{N \times N}$ be the consensus matrix defined as follows*

$$P = I - \frac{1}{2d+1} B_{\mathcal{L}}^T B_{\mathcal{L}}$$

whose associated graph is the regular grid. Then

$$c_l f_d(N) \leq \bar{\mathcal{R}}(\mathcal{L}) \leq c_u f_d(N)$$

where c_l and c_u depend on d only, and where $f_d(N)$ is defined in Eq. (3.49).

Proof. With the same assumptions, from [106], Proposition 1, we known that

$$c_l' f_d(N) \leq J(P) \leq c_u' f_d(N)\,,$$

where c_l' and c_u' depend on δ only. The result immediately follows from Corollary 3.6.8. □

The second result allows us to reduce the problem of computing the average effective resistance in the geometric graph to the simpler case of two suitable grids. First of all, we state the following three technical results.

Lemma 3.6.21. *In an hypercube $H \subseteq Q$ with side length less than $\frac{s}{\sqrt{d}}$, there is at most one node $u \in \mathcal{V}$. In an hypercube $H' \subseteq Q$ with side length greater than 2γ, there is at least one node $u' \in \mathcal{V}$.*

Proof. If the side length of an hypercube is $\frac{s}{\sqrt{d}}$, then its diagonal has length s. If we had two nodes in the hypercube, their distance would be less than s, in contradiction with the definition of s. The second claim is proved noticing that an hypercube of side length 2γ includes a sphere of radius γ. If it did not contain any node, then we could find a sphere of radius larger than γ not containing any node, in contradiction with the definition of γ. □

As a corollary of the previous lemma we have the following result.

Lemma 3.6.22. *Let H be a hypercube in Q with edge length ℓ_H and let N_H be the number of nodes in it. Then*

$$\left\lfloor \frac{\ell_H}{2\gamma} \right\rfloor < \sqrt[d]{N_H} < \left\lceil \frac{\sqrt{d}\ell_H}{s} \right\rceil.$$

Proof. The result follows from Lemma 3.6.21 simply counting how many disjoint hypercubes of side length $\frac{s}{\sqrt{d}}$ and 2γ we can find in an hypercube of side length ℓ_H. □

In particular for the whole graph we have the following corollary.

Corollary 3.6.23. *The number of nodes N of the graph is such that*

$$\ell \frac{1 - \frac{2\gamma}{\ell}}{2\gamma} < \sqrt[d]{N} < \ell \frac{\sqrt{d} - \frac{s}{\ell}}{s}.$$

Notice that, in the case where ℓ is big with respect to γ and s, the previous corollary essentially implies that N is proportional to ℓ^d. The following lemma concerns geometric graphs and their embeddings in lattices.

Lemma 3.6.24. *Let $\mathcal{G} = (\mathcal{V}, \mathcal{E})$ be a geometric graph with parameters (s, r, γ, ρ) and with nodes in an hypercube $Q = [0, \ell]^d$ in which $\gamma < \frac{\ell}{4}$. Then there exist two lattices, $\mathcal{L}_1$ and $\mathcal{L}_2$ such that*

$$k_1 + q_1 \bar{\mathcal{R}}(\mathcal{L}_1) \leq \bar{\mathcal{R}}(\mathcal{G}) \leq k_2 + q_2 \bar{\mathcal{R}}(\mathcal{L}_2), \tag{3.50}$$

where q_1, q_2, k_1 and k_2 depend on s, r, γ, ρ, and on d. Moreover, there exist four constants, c_1', c_1'', c_2', and c_2'', depending on the same set of parameters, such that, if N_1 and N_2 are respectively the number of nodes of $\mathcal{L}_1$ and $\mathcal{L}_2$, then

$$c_1' N_1 \leq N \leq c_1'' N_1 \qquad c_2' N_2 \leq N \leq c_2'' N_2. \tag{3.51}$$

Proof. The idea is to tessellate the hypercube Q in order to obtain a rough approximation of $\mathcal{G}$, and then compute the bound for the effective resistance. Let us consider the upper bound first. Define $n_1 := \left\lceil \frac{\ell}{2\gamma} \right\rceil - 1$ and $\lambda := \frac{\ell}{n_1}$ and (exactly) tessellate the hypercube Q with $N_1 := n_1^d$ hypercubes of side length λ as in Fig. 3.9. Notice that the technical assumption $\gamma < \frac{\ell}{4}$ also implies $\gamma < \frac{\ell}{2}$, which in turn avoids the pathological case in which $n_1 = 0$. Using the properties of $\lceil \cdot \rceil$, it can be seen that

$$2\gamma < \lambda < 4\gamma.$$

Notice that the assumption $\ell > 4\gamma$ ensures that $N_1 \geq 2^d$.

Notice that, by Lemma 3.6.21, in each of these hypercubes there is at least one node of the graph $\mathcal{G}$. On the other hand, by Lemma 3.6.22, we can argue that in each hypercube there are at most $\left\lceil \frac{\sqrt{d}\lambda}{s} \right\rceil^d$ nodes. Since $2\gamma < \lambda$, then

$$\frac{1}{\left\lceil \frac{2\sqrt{d}\gamma}{s} \right\rceil^d} N \leq N_1 \leq N.$$

This proves the first of the two bounds in Eq. 3.51. Another consequence of the fact that in each of these hypercubes there is at least one node of $\mathcal{G}$ is that for each hypercube we can select one "representative" node in V belonging to it. Let $\mathcal{V}_{\mathcal{L}_1} \subseteq \mathcal{V}$ be the set of these representatives. Consider now the regular lattice $\mathcal{L}_1 = (\mathcal{V}_{\mathcal{L}_1}, \mathcal{E}_{\mathcal{L}_1})$ having as the set of nodes the set of representatives $\mathcal{V}_{\mathcal{L}_1}$ and in which there exists an edge connecting two nodes in $\mathcal{V}_{\mathcal{L}_1}$ if the two corresponding hypercubes touch each other (not diagonally). Define the function $\eta : \mathcal{V} \to \mathcal{V}_{\mathcal{L}_1}$ such that $\eta(u) = u'$ if u belongs to the hypercube associated with u'.

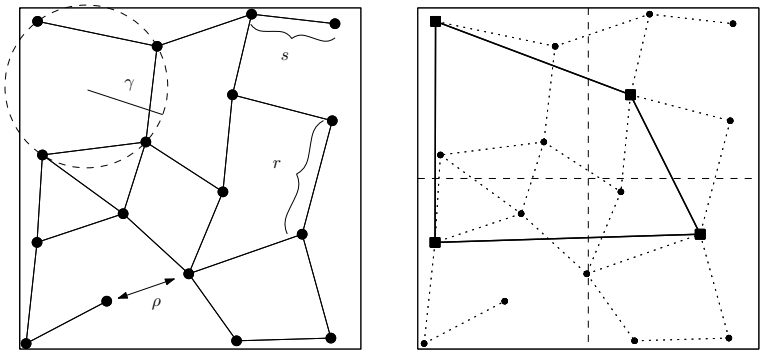

Figure 3.9: On the left, an example of geometric graph in $\mathbb{R}^2$ with parameters s, r, γ and ρ (for ρ, the two nodes for which the minimum in the definition is attained). On the right, the lattice $\mathcal{L}_1$ built for the upper bound. The box-marked nodes are the representatives of the hypercubes, in thick solid line the edges of the lattice $\mathcal{L}_1$. Small nodes and dotted lines are the other nodes and edge of the original graph $\mathcal{G}$.

The next step is to prove that there exists an integer $h \geq 1$ such that the h-fuzz $\mathcal{G}^{(h)}$ of $\mathcal{G}$ embeds $\mathcal{L}_1$, namely that all the nodes and edges of $\mathcal{L}_1$ are also nodes and edges of $\mathcal{G}^{(h)}$. Take thus $u', v' \in \mathcal{V}_{\mathcal{L}_1}$ such that $(u', v') \in \mathcal{E}_{\mathcal{L}_1}$. Their Euclidean distance is bounded as follows

$$d_{\mathrm{E}}(u', v') \leq \lambda\sqrt{d+3}$$

as a simple geometric argument shows. By definition of ρ, we obtain

$$d_{\mathcal{G}}(u',\, v') \leq \frac{\lambda\sqrt{d+3}}{\rho} \leq \frac{4\gamma\sqrt{d+3}}{\rho}.$$

Take thus $h = \lfloor \frac{4\gamma\sqrt{d+3}}{\rho} \rfloor$ and build $\mathcal{G}^{(h)}$. By the previous discussion, it is manifest that $\mathcal{G}^{(h)}$ embeds $\mathcal{L}_1$.

Now, we claim that in $\mathcal{G}^{(h)}$ all the nodes lying in the same hypercube have graphical distance 1, namely they are all connected each other. In fact, if u and v lie in one hypercube, and thus $d_{\mathrm{E}}(u,\, v) \leq \lambda\sqrt{d}$, then we have

$$d_{\mathcal{G}}(v,\, u) \leq \frac{1}{\rho} d_{\mathrm{E}}(v,\, u) \leq \frac{\lambda\sqrt{d}}{\rho} \leq \frac{4\gamma\sqrt{d}}{\rho} \leq \frac{4\gamma\sqrt{d+3}}{\rho},$$

and thus $d_{\mathcal{G}}(v,\, u) \leq h$. This clearly yields

$$d_{\mathcal{G}^{(h)}}(u,\, \eta(u)) \leq 1. \tag{3.52}$$

We can now prove the claim. Since $\mathcal{G}^{(h)}$ embeds $\mathcal{L}_1$, by the properties of the effective resistances, for each $u', v' \in \mathcal{V}_{\mathcal{L}_1}$ we have that

$$\mathcal{R}_{u'v'}(\mathcal{G}^{(h)}) \leq \mathcal{R}_{u'v'}(\mathcal{L}_1).$$

This is still limited to the set of representatives $\mathcal{V}_{\mathcal{L}_1}$. If u and v are two generic nodes of $\mathcal{G}^{(h)}$, using Eq. (3.52) and the fact that the effective resistance is a distance (Lemma 3.6.9), we can obtain that

$$\begin{aligned}\mathcal{R}_{u,\, v}(\mathcal{G}^{(h)}) &\leq \mathcal{R}_{u,\, \eta(u)}(\mathcal{G}^{(h)}) + \mathcal{R}_{\eta(u),\, \eta(v)}(\mathcal{G}^{(h)}) + \mathcal{R}_{\eta(v),\, v}(\mathcal{G}^{(h)}) \\ &\leq 2 + \mathcal{R}_{\eta(u),\, \eta(v)}(\mathcal{G}^{(h)}).\end{aligned}$$

Thus, we have

$$\begin{aligned}\bar{\mathcal{R}}(\mathcal{G}^{(h)}) &= \frac{1}{2N^2} \sum_{u,v \in V} \mathcal{R}_{u,\, v}(\mathcal{G}^{(h)}) \leq 1 + \frac{1}{2N^2} \sum_{u,v \in V} \mathcal{R}_{\eta(u),\, \eta(v)}(\mathcal{G}^{(h)}) \\ &\leq 1 + \frac{1}{2N^2} \sum_{u,v \in V} \mathcal{R}_{\eta(u),\, \eta(v)}(\mathcal{L}_1) = 1 + \frac{1}{2N^2} \sum_{u',v' \in V_{\mathcal{L}_1}} \sum_{\substack{u \in \eta^{-1}(u') \\ v \in \eta^{-1}(v')}} \mathcal{R}_{u',v'}(\mathcal{L}_1) \\ &\leq 1 + \frac{M^2}{2N^2} \sum_{u',v' \in V_{\mathcal{L}_1}} \mathcal{R}_{u',v'}(\mathcal{L}_1) = 1 + M^2 \frac{N_1^2}{N^2} \bar{\mathcal{R}}(\mathcal{L}_1)\end{aligned}$$

where, as already pointed out, M, the maximum number of nodes of $\mathcal{G}$ in each hypercube of length λ, can be bounded as $M \leq \left\lceil \frac{\sqrt{d}\lambda}{s} \right\rceil^d$. By previous arguments, $M\frac{N_1}{N}$ can be bounded from above by a constant dependent on the geometric parameters of the geometric graph and on d. Thus, the claim of the Lemma immediately descends from Lemma 3.6.13.

The proof for the lower bound follows basically the same steps once a good regular lattice candidate is selected. We tessellate again Q by means of hypercubes of side length

$$\lambda := \frac{\ell}{\lfloor \frac{\ell\sqrt{d}}{s} \rfloor + 1}$$

as in Fig. 3.10. Observe that $\lambda < s/\sqrt{d}$ so that by Lemma 3.6.21 in each of them there can be at most one node. The candidate lattice is $\mathcal{L}_2 = (\mathcal{V}_{\mathcal{L}_2}, \mathcal{E}_{\mathcal{L}_2})$, where $\mathcal{V}_{\mathcal{L}_2}$ is the set of hypercubes and the edges connect again two nodes in $\mathcal{V}_{\mathcal{L}_2}$ if the two corresponding hypercubes touch each other (not diagonally).

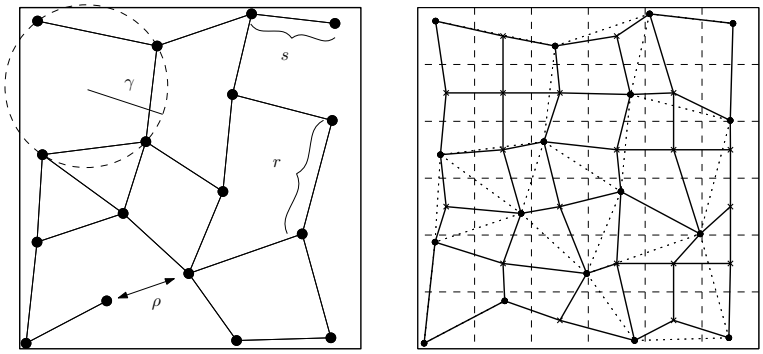

Figure 3.10: On the left, the geometric graph already used for the upper bound. On the right, the lattice $\mathcal{L}_2$ built for the lower bound. The centers of the hypercubes in which there are no nodes of $\mathcal{G}$ are marked by a cross, while the bullet nodes are the nodes of $\mathcal{G}$. In solid lines are all the edges of $\mathcal{L}_2$, in dotted lines the other edges of the original graph $\mathcal{G}$.

It can be proved that, if we take $u, v \in \mathcal{V}$ such that $(u, v) \in \mathcal{E}$, then $d_{\mathcal{L}_2}(u, v) \leq d\lceil r/\lambda \rceil$. We define now the map $\eta : \mathcal{V}_{\mathcal{L}_2} \to \mathcal{V}$ so that $\eta(u')$ is the node in $\mathcal{V}$ which is closest to u' in the Euclidean distance. It can be proved that, for all $u' \in \mathcal{V}_{\mathcal{L}_2}$ we have that $d_{\mathrm{E}}(u', \eta(u')) \leq \gamma$ and so for any pair of nodes u' and v' such that $\eta(u') = \eta(v')$ we have that $d_{\mathrm{E}}(u', v') \leq 2\gamma$ and consequently $d_{\mathcal{L}_2}(u', v') \leq d\lceil 2\gamma/\lambda \rceil$.

Analogously to the upper bound case, we write $\mathcal{V} \subseteq \mathcal{V}_{\mathcal{L}_2}$ identifying a node of the graph with the hypercube it belongs to. Once this is done, and taking $h := \max\{d\lceil r/\lambda \rceil, d\lceil 2\gamma/\lambda \rceil\}$ we can argue that $\mathcal{L}_2^{(h')}$ embeds $\mathcal{G}$ and that, given $u \in \mathcal{V}$, for

any pair of nodes u' and v' in $\eta^{-1}(u)$ we have

$$d_{\mathcal{L}_2^{(h)}}(u', v') \leq 1.$$

The last part of the proof, including the second bound in Eq. 3.51, is totally analogous to the upper bound case. □

We can now prove our theorem on geometric graphs.

of Theorem 3.6.19. We know by Theorem 3.6.7 that

$$c_l \bar{\mathcal{R}}(\mathcal{G}) \leq J(P) \leq c_u \bar{\mathcal{R}}(\mathcal{G})$$

with c_l and c_u dependent on $p_{\min}$, $p_{\max}$, δ and the products $\pi_{\min}N$ and $\pi_{\max}N$. By Lemma 3.6.24, we can argue that

$$k_1' + q_1' \bar{\mathcal{R}}(\mathcal{L}_1) \leq J(P) \leq k_2' + q_1' \bar{\mathcal{R}}(\mathcal{L}_2) \tag{3.53}$$

where $\mathcal{L}_1$ and $\mathcal{L}_2$ are two lattices such that $c_1' N_1 \leq N \leq c_1'' N_1$, $c_2' N_2 \leq N \leq c_2'' N_2$ and where k_1', q_1', k_2' and q_2' is a set of constants dependent on $p_{\min}$, $p_{\max}$, δ, the products $\pi_{\min}N$ and $\pi_{\max}N$, d and the parameters of the geometric graph.

Take now the grid $\mathcal{L}_1$, let $B_{\mathcal{L}_1}$ be its adjacency matrix, and build the consensus matrix

$$P_1 = I - \frac{1}{2d+1} B_{\mathcal{L}_1}^T B_{\mathcal{L}_1}.$$

By Lemma 3.6.20, we know that

$$\alpha_1 f_d(N_1) \leq \bar{\mathcal{R}}(\mathcal{L}_1) \leq \alpha_2' f_d(N_1),$$

where α_1 and α_2 depend on the parameter δ only.

Notice now that Lemma 3.6.24 also states that $c_1' N_1 \leq N \leq c_1'' N_1$, where c_1' and c_1'' depend on the parameters of the geometric graph only. Simple computations using the definition of $f_d(\cdot)$ in Eq. (3.49) yield to

$$k_1' + q_1' f_d(N) \leq \bar{\mathcal{R}}(\mathcal{L}_1) \leq k_1'' + q_1'' f_d(N),$$

where k_1', q_1', k_1'' and q_1'' depend on the geometric parameters and on d.

Analogously, there exists a symmetric consensus matrix P_2 associated with $\mathcal{L}_2$ for which

$$k_2' + q_2' f_d(N) \leq \bar{\mathcal{R}}(\mathcal{L}_1) \leq k_2'' + q_2'' f_d(N),$$

where k_2', q_2', k_2'' and q_2'' depend on the geometric parameters and on d.

By substituting in Eq. (3.53), it is now clear that

$$k_1 + q_1 f_d(N) \leq J(P) \leq k_2 + q_2 f_d(N)$$

with k_1, q_1, k_2 and q_2 as in the statement of the theorem. □

Growing families of geometric graphs

Theorems 3.5.8 and 3.5.8 for rate of convergence and Theorem 3.6.19 for the ℓ_2 cost hold for each given geometric graph with parameters s, r, γ and ρ. However, very much similarly to what is done in Section 3.6, we want to use these result in order to capture the asymptotic behavior in term of the dimension of the network.

Consider a growing family of geometric graphs $\mathcal{G}_N$ with $\mathcal{G}_N = (\mathcal{V}_N, \mathcal{E}_N)$ and $|\mathcal{V}_N| = N$. Let each $\mathcal{G}_N$ be a geometric graph with parameters s_N, r_N, γ_N and ρ_N. Assume that there exist parameters s, r, γ and ρ, which we call *the geometric parameters of the family*, such that

$$s_N \geq s,\, r_N \leq r,\, \gamma_N \leq \gamma,\, \rho_N \geq \rho, \qquad \forall\, N\ . \tag{3.54}$$

Let P_N be the reversible consensus matrix associated with $\mathcal{G}_N$ and with invariant measure $\boldsymbol{\pi}_N$. First of all, we need that all the non-zero entries of P_N belong to the interval $[p_{\min}, p_{\max}]$, for all N. Moreover, called $\pi_{N,\min}$ an $\pi_{N,\max}$ respectively the minimum and maximum entries of π_N, we need to assume that there exist two constants c_l and c_u such that $N\pi_{N,\min} \geq c_l$ and $N\pi_{N,\max} \leq c_u$. Notice now that

- by definition of s_N and r_N,

$$s_N = \min_{u,\, v \in V,\, u \neq v} \{d_{\mathrm{E}}(u,\, v)\} \leq \min_{(u,\, v) \in \mathcal{E}} \{d_{\mathrm{E}}(u,\, v)\} \leq r_N$$

  and thus

$$s \leq s_N \leq r_N \leq r;$$

- given a graph $\mathcal{G}_N$, if $\bar{u}$ and $\bar{v}$ are two nodes connected by an edge, we have

$$\rho_N = \min \left\{ \frac{d_{\mathrm{E}}(u,\, v)}{d_{\mathcal{G}}(u,\, v)} |\, (u,\, v) \in V \times V \right\} \leq d_{\mathrm{E}}(\bar{u},\, \bar{v}) \leq r_N$$

  and thus

$$\rho \leq \rho_N \leq r;$$

- by definition of γ_N, it is immediate to see that we must have $2\gamma_N \geq s_N$, and thus

$$\frac{s}{2} \leq \gamma_N \leq \gamma.$$

Hence, given the geometric parameters of the family, we have a lower and an upper bound for the actual parameters in any graph. Notice moreover that the degree of each node is bounded by the ratio of the volume of the sphere of radius r_N and the volume of the sphere of radius s_N. Therefore the maximum degree δ_N of the nodes of $\mathcal{G}_N$ is uniformly bounded as follows

$$\delta_N \leq \frac{r_N^d}{s_N^d} \leq \frac{r^d}{s^d}\,.$$

On the other side, clearly for all N we have $\delta_N \geq 1$, because $\mathcal{G}_N$ is connected.

Therefore, similarly to Section 3.6, this discussion allows us to conclude that for the family of symmetric consensus matrices P_N constructed as above, it holds for rate of convergence

$$1 - \frac{C}{N^{2/d}} \leq \rho(P_N) \leq 1 - \frac{C'}{N^{2/d}}$$

where C and C' are strictly positive constant depending on d, and on the parameters of the family s, r, γ, ρ. Instead, for the family of reversible consensus matrices P_N constructed as above, it holds for the ℓ_2 cost

$$k_1 + q_1 f_d(N) \leq J(P_N) \leq k_2 + q_2 f_d(N)$$

where k_1, q_1, k_2 and q_2 depend on d, $p_{\max}$, $p_{\min}$, c_l and c_u and the geometric parameters of the family.

4

Synchronization in Higher Order Consensus Network

4.1 Introduction

The previous Chapter was devoted to the study of consensus algorithms. We have shown that despite the fact that the decision laws are local, namely, each agent makes use of the information coming from its neighbors only, the network is able to accomplish a global goal, which is agreement on the consensus value.

Another typical example of global task is the decentralized stabilization of large–scale systems, which finds applications for example in the case of Internet congestion controls [116]. In the simplest scenario for this problem, we model each agent as the same input/output operator N_0, so that at the k-th agent the output y_k is produced according to

$$y_k = N_0(u_k)$$

where u_k is the k-th input. In this case the network is *homogeneous*, namely all the agents are equal. In the more involving case in which the agents are different one each other, we talk instead about *heterogeneous* networks.

The agents are interconnected via the communication graph $\mathcal{G} = (\mathcal{V}, \mathcal{E})$, where the

existence of the edge $e = (j, k)$ means that agent k is allowed to sense the output of agent j. The information received allows agent k to compute its input according to an interconnection operator $\Gamma_k(\cdot)$, namely

$$u_k(t) = \Gamma_k(\boldsymbol{y}(t))$$

where $\Gamma_k(\boldsymbol{y}(t))$ explicitly depends on the outputs $y_j(t)$ of the neighbors of j only. The goal is to design $\Gamma_k(\cdot)$, for all the agents, such that the network is stable, namely

$$|y_k(t)| \overset{t\to\infty}{\longrightarrow} 0, \forall k \in \mathcal{V}$$

In other terms, the goal is to provide tools to check the stability of the interconnected system

$$\begin{cases} \boldsymbol{y} = N_0 \boldsymbol{u} \\ \boldsymbol{u} = \Gamma(\boldsymbol{y}) \end{cases}$$

where $\Gamma(\cdot)$ is just the stacked version of the $\Gamma_k(\cdot)$'s.

For this problem, the direct application of the classical methods is inefficient, due to the extremely high computational load caused by the large number of agents usually involved in the system. The typical issue which is addressed is how to exploit any type of structure in the problem (be it physical, logical, spatial, etc.) in order to provide *scalable* criteria, namely criteria which can be checked locally, by the single agent, possibly given some information on the network. A second issue is to provide *robust* results, namely conditions which, rather than depending on a particular structure, are satisfied by entire families of networks which respect some characteristics. The typical example is when the operator $\Gamma(\boldsymbol{y}) = -\nu L \boldsymbol{y}$ just consists in a matrix multiplication, analogously to consensus algorithm, so that often the check is reduced to a constraint on the spectral properties of L.

In this dissertation the main goal is not stabilization, but (output –)synchronization. In the next Sections we give a more formal definition of synchronization, but the most important case can be simply defined as follows: we say that the network (asymptotically) synchronize if

$$|y_k(t) - y_j(t)| \overset{t\to\infty}{\longrightarrow} 0, \forall k, j \in \mathcal{V}$$

namely $\boldsymbol{y} \overset{t\to\infty}{\longrightarrow} \text{span}\,\{\mathbf{1}\}$.

As already mentioned in the Introduction, notice that this definition of synchronization just requires all the outputs to converge to the same value, which is not required to be zero or a fixed value like in consensus. In fact, in many cases of interest, the synchronization

value is naturally time–varying, for example in the interesting applications of clock synchronization [32, 9] and power network control [117].

The goal of this Chapter is to provide an first step for an unified framework to study synchronization problems in large–scale networks of the type

$$\begin{cases} \boldsymbol{y} = N_0(I + \Delta)\boldsymbol{u} \\ \boldsymbol{u}(t) = \Gamma(\boldsymbol{y}) \end{cases}$$

in which N_0 is a linear time–invariant operator called the nominal system, Δ is a diagonal operator which represents a perturbation of the nominal system, and Γ is called the interconnection operator. As for decentralized stabilization, if $\Delta = 0$ we say that the network is homogeneous, since all the agents behave in the same manner. On the contrary, if $\Delta \neq 0$ we say that the network is heterogeneous. In both cases, we will refer to this type of system as Higher Order Consensus Network, since if $N_0(z^{-1}) = \frac{z^{-1}}{1-z^{-1}}$, a retarded integrator, $\Delta = 0$ and $\Gamma(\boldsymbol{y}) = -\nu L\boldsymbol{y}$, the system becomes

$$\begin{cases} \boldsymbol{y} = \frac{z^{-1}}{1-z^{-1}}\boldsymbol{u} \\ \boldsymbol{u}(t) = -L\boldsymbol{y} \end{cases}$$

which is another way to rewrite the consensus algorithm (see also Section 3.2)

$$\boldsymbol{x}(t+1) = P\boldsymbol{x}(t)$$

if $P = I - L$. The name Higher Order Consensus thus clearly expresses the fact that while in the classical consensus the agreement among the agents is on a constant scalar value, because the agents are simple integrators, in general the agreement can be on a time–varying value because the agents are systems of order greater than one.

The contributions of this Chapter to the literature are manifold

- we propose a rather general framework which is rich enough to catch many synchronization scenarios proposed in the literature;

- we present a synchronization result based on input/output techniques which is robust in the sense that it gives conditions which must by satisfied be the perturbation operator Δ and the interconnection operator Γ, instead of studying particular instances of them;

- we particularize this general result to many cases of interest, such that

  - the case in which Δ is a diagonal matrix of transfer functions, which models uncertainties in the parameters of the nominal system;
  - the case in which Δ is a slope–restricted memoryless nonideality;
  - the case in which Γ is non–linear and slope restricted.

- we study the conditions for which leader following can take place in a Higher Order Consensus Netowork.

As for decentralized stabilization, it is important to provide also tools to check in a simple and scalable way the proposed theorems. We answer this problem proposing, when possible, graphical criteria equivalent to our results. In particular, in the case of linear time invariant Δ we propose a Nyquist–like graphical criterion, while in case of slope–restricted Δ synchronization can be checked making use of a Popov criterion. The research yielding to these results partially appeared in [118, 119].

Review of literature

The problem of network stabilizing, despite not being the topic of this dissertation, is interesting as a fundamental step toward synchronization. For example, in [120] the authors analyze the stability of the systems in the case of homogeneous networks and suggest how to ensure given specifics in terms of damping ratio, convergence rate and overshoot degree. Moreover, they provide a small–gain analysis of the system for heterogeneous networks for some families of LTI perturbations. The papers [121, 122] provide a basic step for the research leading to this thesis since IQC techniques are used in order to provide graphical criteria for the stability of heterogeneous networks. Moreover, in[122], such results are used in order to provide a *perturbed* consensus result. We make use and generalize the tools proposed there in Section 4.5.

Concerning synchronization, the paper [22] can be considered a milestone since its topic is synchronization for formation control purposes of homogeneous systems of the type

$$\begin{cases} \boldsymbol{y} = N_0 \boldsymbol{u} \\ \boldsymbol{u} = -L\boldsymbol{y} \end{cases}$$

where $\boldsymbol{y}$ and $\boldsymbol{u}$ are, as already said, the stacked versions of the outputs and of the inputs of the agents. The main idea is to assume L to be diagonalizable and study the system along the directions different from $\mathbf{1}$, as stated in Lemma 4.4.2, which is a particular case of a result in [22].

In [123] the authors consider an homogeneous network in which each agent is described by a state space realization (A, B, C) so that

$$\begin{cases} \dot{x}_k(t) = Ax_k(t) + Bu_k(t) \\ y_k(t) = Cx_k(t) \end{cases}$$

and again $\boldsymbol{u}(t) = L\boldsymbol{y}(t)$. The authors prove that if L is chosen in a clever way, then not only output synchronization is possible, but, more, the states of the agents synchronize, entry–wise.

It is important, as recalled before, to be able to check the proposed criteria for synchronization in an easy way, for example using graphic criteria. In [122] the authors address the perturbed consensus case, in which each agent is modeled as an integrator multiplied by a stable transfer function (the network is thus heterogeneous), providing a graphical criterion for asymptotic consensus. The papers [124, 125, 126] address a more general case in which the nominal system has a zero in the origin, and the feedback operator is a generic dynamical LTI system, not just a matrix multiplication. Also in this case, a graphical criterion which is based on the notion of S–hull is proposed.

More specifically related to consensus in finite–time, the paper [127] offers an exhaustive theorem to check whether a network is able to achieve agreement in case the nominal system is an integrator (classic consensus) but the interconnection operator also models delays, in the sense that

$$u_i(t) = -\sum_{j \in \mathcal{N}_i} P_{ij}(y_i(t - T_{ji}) - y_j(t - \tau_{ji})$$

thus considering all the possible cases of self-delay and delay in information transmission from the neighbors.

In [128] the authors propose a general model of interacting network inspired by biology. Such a network can be thought to be made of compartments, namely equal subsystems, each composed of the same type of species, namely agents. Interaction can take place among the species of the same compartments (equal for all the compartments) and among species of different compartments. Here synchronization means that the outputs of the species in different compartments try to reach the same value, for each type of species. Making use of input/output tools the authors provide conditions such that the "discrepancy" to the synchronization is bounded.

Finally, the paper [129] presents an LMI-based tool for the synchronization of systems around a given autonomous trajectory of the nominal, possibly nonlinear, system.

4.2 A general framework for synchronization of heterogeneous multi-agent systems

The purpose of this Section is to present a framework for the study of heterogeneous networks of agents. Our model aims to include enough generality to be used for a variety of different applications that recover many cases already present in the literature. In this Chapter an agent will be modeled by a linear time–invariant operator characterized by an output, call it y_k for k-th agent, an interconnection input u_k, an internal input w_k and an external input r_k

$$y_k = h_{uy}u_k + h_{ry}r_k + h_{wy}w_k,$$

where h_{uy}, h_{ry}, h_{wy} are linear time–invariant convolutional operators on $\mathcal{H}_e$. If we stack all the outputs and the three inputs respectively in the signals $\boldsymbol{y} \in \mathcal{H}^N$, $\boldsymbol{u} \in \mathcal{H}_e^N$, $\boldsymbol{r} \in \mathcal{H}_e^N$ and $\boldsymbol{w} \in \mathcal{H}_e^N$, so that at each time instant we have vectors in $\mathbb{R}^N$, we have the compact matrix form

$$\boldsymbol{y} = H_{uy}\boldsymbol{u} + H_{ry}\boldsymbol{r} + H_{wy}\boldsymbol{w}$$

where $H_{uy} = h_{uy}I_N$, $H_{ry} = h_{ry}I_N$, $H_{wy} = h_{wy}I_N$ are diagonal LTI operators. We need to impose some assumptions on the characteristics of such LTI operators. They are satisfied in many cases of interest. Notice that the last condition is a technical assumption which is immediately satisfied, for example, in the case $h_{ry} = h_{wy}$.

Assumption 4.2.1. The transfer functions representing the operators h_{uy}, h_{ry} and h_{wy} are such that

$$\hat{h}_{*y} = \frac{b_{*y}}{a}\hat{f}_{*y}, \quad * \in \{u, r, w\},$$

where $\hat{f}_{*y}$ is the transfer function corresponding to $f_{*y} \in \mathcal{A}$, b_{*y} is a stable polynomial and

$$a(s) = \prod_{k=1}^{m}(s - s_k)^{\rho_k}$$

where $s_k \in \Omega$ such that $\deg(b_{*y}) < \deg(a)$. We finally assume that $\hat{f}_{*y}$ has no zeros in Ω. This means that the systems are strictly proper, has no unstable zeros, and share the same unstable poles.

What has been described so far is the so called *nominal part* of the agents. The

heterogeneity of the network is modeled by making use of the internal input w_k and another signal we call *internal output*, v_k. We assume that the couple (v_k, w_k) evolves according to

$$\begin{cases} v_k &= h_{uv}u_k + h_{wv}w_k, \\ w_k &= \Delta_k(v_k), \end{cases}$$

where $h_{uv}, h_{wv} \in \mathcal{A}$ and Δ_k is a bounded causal operator on the Hilbert space $\mathcal{H}_e$. Such Δ_k represents the *perturbation* of k-th agent. It models differences in dynamics among the agents, non–linearities and uncertainties in the system. If we stack all the internal outputs in the signal $\boldsymbol{v} \in \mathcal{H}^N$, the previous relations can be expressed according to

$$\begin{cases} \boldsymbol{v} &= H_{uv}\boldsymbol{u} + H_{wv}\boldsymbol{w}, \\ \boldsymbol{w} &= \Delta(\boldsymbol{v}), \end{cases}$$

where $H_{uv} = h_{uv}I$ and $H_{wv} = h_{wv}I$ and $\Delta = \operatorname{diag}(\Delta_1, \ldots, \Delta_N)$.

So far we have given details on the agents, and it remains to explain how such (by now) isolated elements interact. The interaction is modeled by the interconnection input u_k, which, for agent k and at time t, is produced according to

$$u_k(t) = \Gamma_k(t, \boldsymbol{y}(t))$$

where Γ_k is a bounded memoryless operator $\mathcal{H}_e^N \to \mathcal{H}_e$. Notice that Γ is not "diagonal". Its structure, as in the consensus algorithm, is in fact determined according to the communication graph $\mathcal{G} = (V, \mathcal{E})$ in which as usual the set of nodes coincides with the set of agents, and in which the edge $(j, k) \in \mathcal{E}$ if j is allowed to send its information to agent k, or, equivalently, if $\Gamma_k(\boldsymbol{y})$ depends explicitly on y_j. In vector form, interconnection inputs and outputs are related according to

$$\boldsymbol{u}(t) = \Gamma(t, \boldsymbol{y}(t)).$$

We have thus obtained the complete set of equations describing our model of an

heterogeneous network of interconnected agents

$$\begin{cases} \begin{bmatrix} \boldsymbol{y} \\ \boldsymbol{v} \end{bmatrix} = \begin{bmatrix} H_{uy} & H_{ry} & H_{wy} \\ H_{uv} & 0 & H_{wv} \end{bmatrix} \begin{bmatrix} \boldsymbol{u} \\ \boldsymbol{r} \\ \boldsymbol{w} \end{bmatrix} = H \begin{bmatrix} \boldsymbol{u} \\ \boldsymbol{r} \\ \boldsymbol{w} \end{bmatrix}, \\ \boldsymbol{w} = \Delta(\boldsymbol{v}), \\ \boldsymbol{u} = \Gamma(\boldsymbol{y}), \end{cases} \tag{4.1}$$

which is illustrated in Fig. 4.1. Notice that due to the diagonal structure, the block–entries of H can be rewritten using the Kronecker product

$$H = \begin{bmatrix} h_{uv} & h_{ry} & h_{wy} \\ h_{uv} & 0 & h_{wv} \end{bmatrix} \otimes I_N.$$

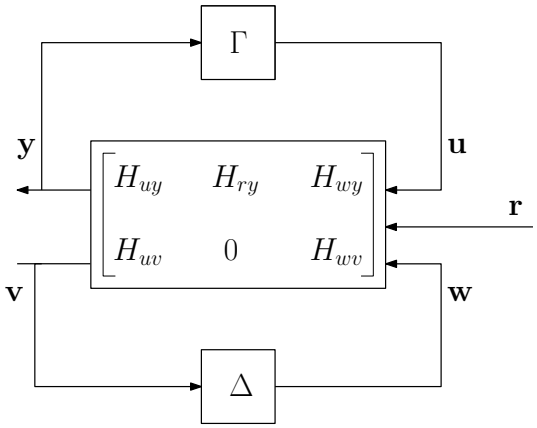

Figure 4.1: The system under consideration.

Example 4.2.2. The most important case of an heterogeneous network is what we call an Higher Order Consensus Network. In this particular case, $h_{uv} = h_{ry} = h_{wy} = N_0 \in \mathcal{A}$, $h_{uv} = 1$ and $h_{wv} = 0$, so that the model can be rewritten as

$$\begin{cases} \begin{bmatrix} \boldsymbol{y} \\ \boldsymbol{v} \end{bmatrix} = \begin{bmatrix} N_0 & N_0 & N_0 \\ I & 0 & 0 \end{bmatrix} \begin{bmatrix} \boldsymbol{u} \\ \boldsymbol{r} \\ \boldsymbol{w} \end{bmatrix}, \\ \boldsymbol{w} = \Delta(\boldsymbol{v}), \\ \boldsymbol{u} = \Gamma(\boldsymbol{y}). \end{cases} \tag{4.2}$$

and a slight manipulation allows us to rewrite this system as

$$\begin{cases} \boldsymbol{y} = N_0(I+\Delta)(\boldsymbol{u}) + N_0\boldsymbol{r} \\ \boldsymbol{u} = \Gamma(\boldsymbol{y}) \end{cases}$$

which is depicted in Fig. 4.2. Notice that here, and below, $(I+\Delta)(\boldsymbol{u})$ means $\boldsymbol{u} + \Delta(\boldsymbol{u})$.

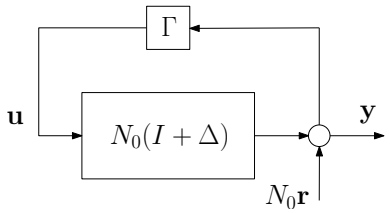

Figure 4.2: A particular and important case of heterogeneous network.

In the particular case $\Delta = 0$ and $\Gamma(\boldsymbol{y}) = \Gamma_0\boldsymbol{y}$ with $\Gamma_0\mathbf{1} = 0$, we have

$$\begin{cases} \boldsymbol{y} = N_0\boldsymbol{u} + N_0\boldsymbol{r} \\ \boldsymbol{u} = \Gamma_0\boldsymbol{y} \end{cases}$$

which, apart from the signal $\boldsymbol{r}$, is our model for an homogeneous network with linear interconnection, and if, for example in discrete–time, $N_0(z^{-1}) = \frac{z^{-1}}{1-z^{-1}}$, we have a network implementing a consensus algorithm.

As for the operator Δ, it is allowed to represent any possible perturbation of the nominal system. One of the most important case is when it represents uncertainties on the non-nominal dynamics of the agents, as we will show for the case of clock synchronization (see Chapter 5).

We notice that our model is written in such a way that Δ represents a multiplicative perturbation. The somehow more usual additive perturbation can be recovered as

$$N0 + N_k = N_0(1 + \Delta_k)$$

where $\Delta_k = N_k/N_0$.

4.3 Synchronization over heterogeneous networks

In the previous section we have described the system we want to study. In this section we will provide the basic tool to prove the *synchronization* of the network in the sense of

the following definition.

Definition 4.3.1. Consider the system in Eq. 4.1 and a subspace $\mathcal{Z} \subset \mathbb{R}^N$. Let $\boldsymbol{y}^\perp = \mathcal{P}_{\mathcal{Z}^\perp}\boldsymbol{y}$ be the pointwise projection of $\boldsymbol{y}$ onto the orthogonal complement of $\mathcal{Z}$, in the sense that $\boldsymbol{y}^\perp(t) = \mathcal{P}_{\mathcal{Z}^\perp}\boldsymbol{y}(t)$, $\forall t$. Let $\mathcal{M} : \mathcal{H}_e^N \to \mathcal{H}_e^N$ denote the causal map representing the closed loop system $\boldsymbol{y}^\perp = \mathcal{M}(\boldsymbol{r})$. We say that the system synchronizes to $\mathcal{Z}$ if $||\mathcal{M}||_{\mathcal{H}_e^N \to \mathcal{H}_e^N} < \infty$.

Synchronization will under weak assumptions on the nominal dynamics imply for $\boldsymbol{r} \in \mathcal{H}$, that $\boldsymbol{y}$ asymptotically converges to $\mathcal{Z}$, which is why we call it *synchronization subspace*. The typical case is $\mathcal{Z} = \operatorname{span}\{\mathbf{1}\}$ in which the term synchronization recovers its usual meaning that the differences among the components of $\boldsymbol{y}$ to converge to zero, as mentioned in the Introduction to this Chapter.

We will take the following steps toward our main synchronization result. First we reduce the dimension of the system by projecting down to the orthogonal complement of $\mathcal{Z}$. Then we perform a loop transformation to stabilize the linear part of the system. The main result will then follow by an application of the IQC theorem in [130].

Projection onto $\mathcal{Z}^\perp$

In order to perform the first step of our argument we impose the following assumptions on the operator Γ.

Assumption 4.3.2. The synchronization subspace $\mathcal{Z}$ is the right and left kernel of the static operator Γ in the following sense: if $\boldsymbol{z} \in \mathcal{Z}$ and $\boldsymbol{v} \in \mathbb{R}^N$ is generic, then $\Gamma(t, \boldsymbol{z} + \boldsymbol{v}) = \Gamma(t, \boldsymbol{v})$ and $\boldsymbol{z}^*\Gamma(t, \boldsymbol{v}) = 0$, $\forall\, t \geq 0$. Moreover, $\Gamma(t, 0) = 0$.

The conditions stated in Assumption 4.3.2 can be written in the following manner. Let Z be a matrix whose columns form an orthonormal basis for $\mathcal{Z}$, and V be any orthonormal complement to it, i.e.

$$Z^*Z = I_p,\ V^*V = I_{N-p},\ V^*Z = 0,\ VV^* + ZZ^* = I_N$$

where $p = \dim \mathcal{Z}$, and where VV^* and ZZ^* are two projectors respectively onto $\mathcal{Z}^\perp$ and $\mathcal{Z}$. The two conditions can be thus expressed by the constraint

$$\Gamma(t, \boldsymbol{y}) = \Gamma(t, VV^*\boldsymbol{y})$$

for the right kernel, and

$$\Gamma(t, \boldsymbol{y}) = VV^*\Gamma(t, \boldsymbol{y})$$

for the left kernel.

These two assumptions imply that

$$\boldsymbol{u} = \Gamma(t, \boldsymbol{y}) = VV^*\Gamma(t, VV^*\boldsymbol{y}) = V\Gamma_\perp(\boldsymbol{y}_\perp)$$

where we defined $\boldsymbol{y}_\perp := V^*\boldsymbol{y}$ and $\Gamma_\perp(t, \boldsymbol{y}_\perp) := V^*\Gamma(t, V\boldsymbol{y}_\perp)$. We let $\boldsymbol{r}_\perp = V^*\boldsymbol{r}$ in order to rewrite the system as follows

$$\begin{cases} \begin{bmatrix} \boldsymbol{y}_\perp \\ \boldsymbol{v} \end{bmatrix} = \begin{bmatrix} H_{uy} & H_{ry} & H_{wy}V^* \\ H_{uv}V & 0 & H_{wv} \end{bmatrix} \begin{bmatrix} \boldsymbol{u}_\perp \\ \boldsymbol{r}_\perp \\ \boldsymbol{w} \end{bmatrix}, \\ \boldsymbol{w} = \Delta(\boldsymbol{v}), \\ \boldsymbol{u}_\perp = \Gamma_\perp(t, \boldsymbol{y}_\perp), \end{cases}$$

Remark 4.3.3. For sake of simplicity, we assume from now on that $H_{wv} = 0$, namely we suppress the dependence of the internal output from the internal input. This can be done defining the feedback of Δ and H_{wv} as the operator

$$\tilde{\Delta} := \Delta \circ (I - H_{wv} \circ \Delta)^{-1}$$

and making the assumption that $\tilde{\Delta}$ is well–defined and bounded. Both these properties are satisfied under some mild conditions, and in particular boundedness can be checked using the small–gain theorem applied to the gains of Δ (which is diagonal) and of h_{wv}, since $H_{wv} = h_{wv}I$.

Then the system can be easily rewritten as

$$\begin{cases} \begin{bmatrix} \boldsymbol{y}_\perp \\ \boldsymbol{v} \end{bmatrix} = \begin{bmatrix} H_{uy} & H_{ry} & H_{wy}V^* \\ H_{uv}V & 0 & 0 \end{bmatrix} \begin{bmatrix} \boldsymbol{u}_\perp \\ \boldsymbol{r}_\perp \\ \tilde{\boldsymbol{w}} \end{bmatrix}, \\ \tilde{\boldsymbol{w}} = \tilde{\Delta}(\boldsymbol{v}), \\ \boldsymbol{u}_\perp = \Gamma_\perp(t, \boldsymbol{y}_\perp), \end{cases}$$

which is in the form we want.

If $H_{wv} = 0$ and defining $\boldsymbol{v}_\perp = V^*\boldsymbol{v}$, $\boldsymbol{w}_\perp = V^*\boldsymbol{w}$ and $\Delta_\perp(\boldsymbol{v}_\perp) = V^*\Delta(V\boldsymbol{v}_\perp)$, easy

manipulations of the previous equations yield to the following reduced–dimension model

$$\begin{cases} \begin{bmatrix} \boldsymbol{y}_\perp \\ \boldsymbol{v}_\perp \end{bmatrix} = H \begin{bmatrix} \boldsymbol{u}_\perp \\ \boldsymbol{r}_\perp \\ \boldsymbol{w}_\perp \end{bmatrix} \\ \boldsymbol{w}_\perp = \Delta_\perp(\boldsymbol{v}_\perp) \\ \boldsymbol{u}_\perp = \Gamma_\perp(\boldsymbol{y}_\perp) \end{cases} \tag{4.3}$$

It is worth to notice that the diagonal structure of the linear part H has been maintained after the dimension reduction at the price that the diagonal structure of the perturbation is lost. As we will see, this loss of structure is negligible since the input/output characteristics of Δ are the same as those of $\Delta_\perp$.

Loop transformation

The system H still contains the original possibly unstable or marginally stable poles, and is not in a good shape for input/output techniques to be applied. The second step of our approach is thus to perform a loop transformation in order to stabilize it. This can be done by means of a suitable matrix

$$Q = \begin{bmatrix} 0 & Q_{12} \\ Q_{21} & Q_{22} \end{bmatrix}$$

and by defining the operator Γ_Q[1] via the upper linear fractional transformation of $\Gamma_\perp$, $\Gamma_\perp = \mathcal{F}_u(Q, \Gamma_Q)$. Namely, we transform the equation

$$\boldsymbol{u}_\perp = \Gamma_\perp(\boldsymbol{y}_\perp)$$

into the system

$$\begin{cases} \boldsymbol{u}_Q = \Gamma_Q \boldsymbol{y}_Q \\ \begin{bmatrix} \boldsymbol{y}_Q \\ \boldsymbol{u}_\perp \end{bmatrix} = Q \begin{bmatrix} \boldsymbol{u}_Q \\ \boldsymbol{y}_\perp \end{bmatrix} \end{cases} .$$

This operation is depicted in Fig. 4.3, in which $\mathcal{F}_u(Q, \Gamma_Q)$ is substituted for $\Gamma_\perp$. Once this is done, we consider the interconnection of the linear part H and the matrix Q,

[1] We will often suppress the arguments of $\Gamma(t, \boldsymbol{y})$ for sake of notation.

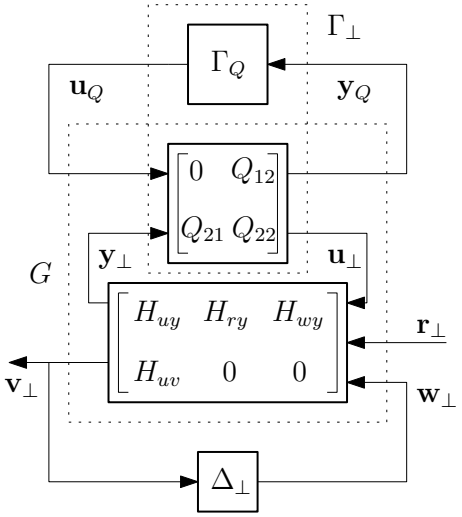

Figure 4.3: Loop transformation of the system. The upper linear fractional system $\mathcal{F}_u(Q, \Gamma_Q)$ has been substituted for $\Gamma_\perp$. The Redheffer star product of Q and the linear and unstable part, H, is employed in order to obtain a matrix of stable transfer functions G.

obtaining the matrix of transfer functions

$$G = Q \star H = \begin{bmatrix} G_{uy} & G_{ry} & G_{wy} \\ G_{uv} & G_{rv} & G_{wv} \end{bmatrix} \tag{4.4}$$

where the star product defines

$$\begin{aligned} G_{uy} &= h_{uy} Q_{12} (I - Q_{22} h_{uy})^{-1} Q_{21} \\ \begin{bmatrix} G_{ry} & G_{wy} \end{bmatrix} &= Q_{12} (I - Q_{22} h_{uy})^{-1} \begin{bmatrix} h_{ry} & h_{wy} \end{bmatrix} \\ G_{uv} &= h_{uv} (I - Q_{22} h_{uy})^{-1} Q_{21} \\ \begin{bmatrix} G_{rv} & G_{wv} \end{bmatrix} &= h_{uv} Q_{22} (I - Q_{22} h_{uy})^{-1} \begin{bmatrix} h_{ry} & h_{wy} \end{bmatrix} \end{aligned}$$

This operation is depicted in Fig. 4.4. If G is stable, we have thus achieved the goal of this section, and this will be an assumption from now on.

Assumption 4.3.4. The matrix $Q \in \mathbb{R}^{2N \times 2N}$ is chosen in such a way that all the entries of the matrix of transfer functions G in Eq. 4.4 are stable.

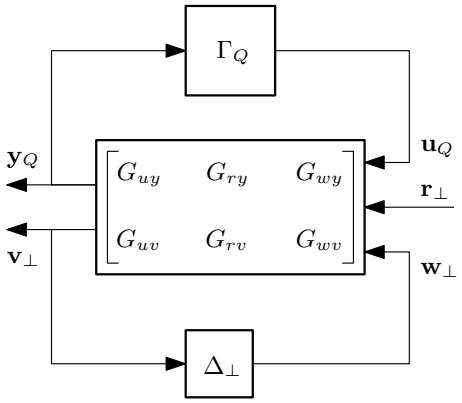

Figure 4.4: System obtained after the loop transformation. All the elements of the matrix G are stable transfer functions, and in place of $\Gamma_\perp$ it remains the operator Γ_Q.

On the interpretation of Q and a simple example

As it will be further clarified by the applications, the blocks of the matrix Q have a simple and intuitive meaning.

As it easy to see, after projecting via the matrix V and performing the loop transformation via the matrix Q, we obtain

$$\Gamma(t,\, \boldsymbol{y}) = VQ_{22}V^*\boldsymbol{y} + VQ_{21}\Gamma_Q(t,\, Q_{12}V^*\boldsymbol{y})$$

so that

$$\Gamma_\perp(t, \boldsymbol{y}_\perp) = Q_{22}\boldsymbol{y}_\perp + Q_{21}\Gamma_Q(t,\, Q_{12}\boldsymbol{y}_\perp)$$

This relation implies that the more we know about the structure of $\Gamma_\perp$, the better we can approximate it using the matrix Q_{22}. The better this approximation, the less conservative will turn out to be the synchronization criterion, as we will see.

As extreme cases, if $\Gamma_\perp(t, \boldsymbol{y}_\perp) = Q_{22}\boldsymbol{y}_\perp$ we have $\Gamma_Q(t,\, Q_{12}\boldsymbol{y}_\perp) = 0$, namely no approximation is needed. In this case that the projection step and the loop transformation step are enough to obtain a stable system, represented by G, in feedback with the perturbation $\Delta_\perp$. A more detailed analysis of this case is given in Section 4.4.

On the other extreme case, sometimes only a very rough knowledge of $\Gamma_\perp(t, \cdot)$ is available, apart from Assumption 4.3.2. In this case, a reasonable choice (see Section 4.5) is

$$Q = \begin{bmatrix} 0 & 1 \\ 1 & -\eta \end{bmatrix} \otimes I_{N-1}, \tag{4.5}$$

for which it is easy to see that

$$\Gamma_Q = \Gamma_\perp + \eta I_{N-1}.$$

In other terms, this choice approximates the interconnection operator Γ with the matrix $-\eta VV^*$ and $\Gamma_\perp$ with $-\eta I_{N-1}$. Clearly, this is often a too rough approximation. However, this choice is simple and yields

$$G = \begin{bmatrix} \frac{h_{uy}}{1+\eta h_{uy}} & \frac{1}{1+\eta h_{uy}}[h_{ry},\, h_{wy}] \\ \frac{h_{uw}}{1+\eta h_{uy}} & -\frac{h_{uw}\eta}{1+\eta h_{uy}}[h_{ry},\, h_{wy}] \end{bmatrix} \otimes I_{N-1},$$

namely we aim to stabilize the system using a simple proportional controller η, so the resulting matrix of transfer functions G has a simple repeated structure.

Example 4.3.5. Let us return to Example 4.2.2 and consider the consensus problem in discrete–time case, in which $N_0(z^{-1}) = \frac{z^{-1}}{1-z^{-1}}$. Using the simple Q presented in Eq. 4.5 we obtain the system

$$G = \frac{1}{1 - z^{-1}(1-\eta)} \begin{bmatrix} z^{-1} & z^{-1} & z^{-1} \\ 1 - z^{-1} & -\eta z^{-1} & -\eta z^{-1} \end{bmatrix} \otimes I_{N-1},$$

and in this case Assumption 4.3.4 is satisfied for any $\eta \in (0,\, 2)$.

A synchronization criterion

In this section we will derive our basic synchronization criterion that will serve as a foundation for the subsequent analysis. In the previous subsections we have simplified the original system in Eq. 4.1 by first projecting the dynamics onto the orthogonal complement of the synchronization subspace and then stabilizing the linear dynamics using a loop transformation. We employ the IQC theorem from [130] on the transformed system to obtain our first result below. We use following definitions of stability and Integral Quadratic Constraint.

Definition 4.3.6. The interconnection $[G, \operatorname{diag}(\Gamma_Q, \Delta_\perp)]$ in Fig. 4.5 is called stable if there exists $c > 0$ such that

$$\|y_Q\|^2 + \|v_\perp\|^2 \leq c\|r_\perp\|^2$$

for all $r_\perp \in \mathcal{H}^{n-1}$.

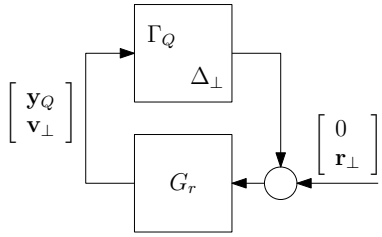

Figure 4.5: Feedback system on which we apply the IQC theorem. In this system G_r is a matrix of stable transfer functions and in order to prove stability we have to provide IQC characterizations for both the operators Γ_Q and Δ.

Definition 4.3.7 (IQC)**.** Let $\Pi \in S_{\mathcal{A}}^{2m\times 2m}$. Then a bounded causal operator $\Delta : \mathcal{H}_e^m \to \mathcal{H}_e^m$ is said to satisfy the IQC defined by Π ($\Delta \in IQC(\Pi)$) if

$$\left\langle \begin{bmatrix} \Delta(w) \\ w \end{bmatrix}, \Pi \begin{bmatrix} \Delta(w) \\ w \end{bmatrix} \right\rangle \leq 0, \, \forall \, w \in \mathcal{H}.$$

We say that Δ satisfies the strict IQC ($\Delta \in SIQC(\Pi)$) if the inequality is strict, namely if there exists $\epsilon > 0$ such that

$$\left\langle \begin{bmatrix} \Delta(w) \\ w \end{bmatrix}, \Pi \begin{bmatrix} \Delta(w) \\ w \end{bmatrix} \right\rangle \leq -\epsilon ||w||^2, \, \forall \, w \in \mathcal{H}.$$

The IQC theorem can be formulated as follows.

Theorem 4.3.8 ([130])**.** *Consider the continuous–time system*

$$\begin{cases} \boldsymbol{y} = G\boldsymbol{u} \\ \boldsymbol{u} = \Delta(\boldsymbol{y}) + \boldsymbol{r} \end{cases} \tag{4.6}$$

where $G : \mathcal{H} \to \mathcal{H}$ is a linear causal bounded LTI operator and $\Delta : \mathcal{H} \to \mathcal{H}$ is a generic bounded causal operator. The feedback system is stable in the sense of Definition 4.3.6 if

i) there exists a continuous (in the norm topology) parametrization $\Delta(\tau)$ such that for every $\tau \in [0, 1]$, the feedback of G and $\Delta(\tau)$ is well posed;

ii) for every $\tau \in [0, 1]$, $\Delta(\tau) \in IQC(\Pi)$, where $\Pi \in S_{\mathcal{A}_c}^{2m\times 2m}$;

iii) it holds true

$$\begin{bmatrix} I \\ G(j\omega) \end{bmatrix}^* \Pi \begin{bmatrix} I \\ G(j\omega) \end{bmatrix} > \varepsilon I, \forall \omega \in \mathbb{R}$$

Note that our definition of IQC in Definition 4.3.7 has the opposite sign compared to [130]. The parametrization of the perturbation $\mathrm{diag}\,(\Gamma_Q,\, \Delta_\perp)$ is also slightly different but the proof and its consequences are anyway completely analogous. Notice moreover that the theorem holds for the discrete–time case with the obvious modifications.

Now we are ready to state and prove our result.

Theorem 4.3.9. *Assume that the operator Γ respects Assumption 4.3.2 and that there exists a matrix $Q \in \mathbb{R}^{2N\times 2N}$ which respects Assumption 4.3.4. Assume moreover that*

i) there exists continuous (in the norm topology) parametrizations $\Gamma_Q(\tau)$ and $\Delta_\perp(\tau)$ such that $\Gamma_Q(1) = \Gamma_Q$, $\Delta_\perp(1) = \Delta_\perp$ and such that the nominal interconnection *$[G, \mathrm{diag}\,(\Gamma_Q(0), \Delta_\perp(0))]$ is stable,*

ii) there exists bounded self–adjoint linear operators Π_{Γ_Q} and $\Pi_{\Delta_\perp}$ such that

(a) $\Gamma_Q(\tau) \in IQC(\Pi_{\Gamma_Q})$, $\tau \in [0,1]$,

(b) $\Delta_\perp(\tau) \in IQC(\Pi_{\Delta_\perp})$, $\tau \in [0,1]$,

iii)

$$\begin{bmatrix} I \\ G_r \end{bmatrix}^* \mathrm{daug}\left(\Pi_{\Gamma_Q}, \Pi_{\Delta_\perp}\right) \begin{bmatrix} I \\ G_r \end{bmatrix} > 0 \tag{4.7}$$

where

$$G_r = \begin{bmatrix} G_{uy} & G_{wy} \\ G_{uv} & G_{wv} \end{bmatrix}, \tag{4.8}$$

iv) h_{uv}, $h_{uv}^{-1} \in \mathcal{A}$, Q_{12}, $Q_{12}^{-1} \in \mathbb{R}^{N\times N}$.

Then the network in Eq. 4.1 synchronizes to the subspace $\mathcal{Z}$ in the sense of Definition 4.3.1

Remark 4.3.10. In order to prove that the vector $\boldsymbol{y}$ converges to $\mathcal{Z}$ it is sufficient to prove that $\boldsymbol{y}_\perp$ converges to zero. Under the assumptions of the theorem we have shown that $\boldsymbol{y}_\perp$ belongs to $\mathcal{H}^{N-p}$, where we recall that p is the dimension of the synchronizing subspace $\mathcal{Z}$. In the two cases of interest, namely if the system is continuous time or discrete time, we then have

- $\mathcal{H}_e = \mathbf{L}_{2e}[0;\infty)$: if the elements G_{uy}, G_{ry} and G_{wy} are strictly proper, then $\boldsymbol{y}_\perp \overset{t\to\infty}{\longrightarrow} 0$.
- $\mathcal{H}_e = \ell_{2e}[0;\infty)$: what has been shown is sufficient to conclude $\boldsymbol{y}_\perp \overset{t\to\infty}{\longrightarrow} 0$.

Proof. The first step is to prove stability of the feedback system $[G_r, \text{diag}\,(\Gamma_Q[\tau], \Delta_\perp[\tau])$, which is depicted in Fig. 4.5. This is a direct consequence of the IQC theorem in this particular case, since G_r is a matrix of stable transfer functions and the conditions $i)$, $ii)$ and $iii)$ imply that all hypotheses of Theorem 4.3.8 are satisfied.

Stability of the system in Fig. 4.5 implies that for any $\boldsymbol{r} \in \mathcal{H}^N$ we have $\|\boldsymbol{y}_Q\|^2 + \|\boldsymbol{v}_\perp\|^2 \leq c\|r_\perp\|^2$. In turn, recalling the projection step and the loop transformation step, we have the following relations

$$\begin{aligned} \boldsymbol{y}_Q &= Q_{12}\boldsymbol{y}_\perp \\ \boldsymbol{v}_\perp &= H_{uv}\boldsymbol{u}_\perp \end{aligned}$$

so that assumption $iv)$ implies that

$$\|y_\perp\|^2 + \|u_\perp|^2 \leq c\max(\|Q_{12}^{-1}\|, \|H_{uv}^{-1}\|)\|r_\perp\|^2,$$

which implies that the condition in Definition 4.3.1 holds. □

We will next state and prove a technical lemma which will prove to be useful several times in what follows. It shows that if the perturbation operators are sufficiently structured then the same multiplier can be used for the modified operator $\Delta_\perp$ as for the individual Δ_k.

Lemma 4.3.11. *Let*

$$\Delta_\perp(\cdot) = V^*\Delta(V\cdot) = V^*\text{diag}\,(\Delta_1(V_1\cdot), \ldots, \Delta_N(V_n\cdot))$$

where V_k denotes the k^{th} row of V and V is as above. Suppose that π_Δ is a multiplier such that $\Delta_k \in IQC(\pi_\Delta)$, for any k. Let moreover $\pi_{\Delta,11} \geq 0$. Then $\Delta_\perp \in IQC(\pi_\Delta \otimes I_{N-1})$.

Proof. We want to show that, for any $v_\perp \in \mathcal{H}^{N-1}$, we have

$$\left\langle \begin{bmatrix} \Delta_\perp(v_\perp) \\ v_\perp \end{bmatrix}, \pi_\Delta \otimes I_{N-1} \begin{bmatrix} \Delta_\perp(v_\perp) \\ v_\perp \end{bmatrix} \right\rangle \leq 0.$$

And in fact, recalling that $V^*V = I_{N-1}$ and that $\langle v, Aw\rangle = \langle A^*v, w\rangle$, we obtain

$$\begin{aligned}
&\left\langle \begin{bmatrix} \Delta_\perp(v_\perp) \\ v_\perp \end{bmatrix}, \pi_\Delta \otimes I_{N-1} \begin{bmatrix} \Delta_\perp(v_\perp) \\ v_\perp \end{bmatrix} \right\rangle \\
&= \left\langle \begin{bmatrix} V^*\Delta(Vv_\perp) \\ v_\perp \end{bmatrix}, \pi_\Delta \otimes I_{N-1} \begin{bmatrix} V^*\Delta(Vv_\perp) \\ v_\perp \end{bmatrix} \right\rangle \\
&= \left\langle \begin{bmatrix} \Delta(\tilde{v}) \\ \tilde{v} \end{bmatrix}, \pi_\Delta \otimes I_N \begin{bmatrix} \Delta(\tilde{v}) \\ \tilde{v} \end{bmatrix} \right\rangle \\
&\qquad + \langle \Delta(\tilde{v}), \pi_{\Delta,11}(VV^* - I_N)\Delta(\tilde{v})\rangle
\end{aligned}$$

where we defined $\tilde{v} := Vv_\perp$. The result now follows since the second term is non positive because $VV^* - I_N \leq 0$ and $\pi_{\Delta,11} \geq 0$, and the first term is non positive because

$$\begin{aligned}
&\left\langle \begin{bmatrix} \Delta(\tilde{v}) \\ \tilde{v} \end{bmatrix}, \pi_\Delta \otimes I_N \begin{bmatrix} \Delta(\tilde{v}) \\ \tilde{v} \end{bmatrix} \right\rangle \\
&\qquad = \sum_{k=1}^{N} \left\langle \begin{bmatrix} \Delta_k(\tilde{v}_k) \\ \tilde{v}_k \end{bmatrix}, \pi_\Delta \begin{bmatrix} \Delta_k(\tilde{v}_k) \\ \tilde{v}_k \end{bmatrix} \right\rangle \leq 0.
\end{aligned}$$

□

Interpretation of the condition in the original variables

It is of interest to rewrite Theorem 4.3.9 in terms of the original interconnection operators. We start by observing that the relation $\Gamma_\perp = \mathcal{F}_u(Q, \Gamma_Q)$ is easily rewritten as

$$\begin{bmatrix} \Gamma_Q(\boldsymbol{y}_Q) \\ \boldsymbol{y}_Q \end{bmatrix} = \underbrace{\begin{bmatrix} Q_{21}^{-1} & -Q_{21}^{-1}Q_{22} \\ 0 & Q_{12} \end{bmatrix}}_{F_Q} \begin{bmatrix} \Gamma_\perp(\boldsymbol{y}_\perp) \\ \boldsymbol{y}_\perp \end{bmatrix} \tag{4.9}$$

provided that Q_{21} is invertible. The condition $\Gamma_Q \in IQC(\Pi_{\Gamma_Q})$ can be rewritten, in terms of the original operator, as $\Gamma_\perp \in IQC(\Pi_{\Gamma_\perp})$, where $\Pi_{\Gamma_\perp} = F_Q^*\Pi_{\Gamma_Q}F_Q$.

We may use this to formulate Theorem 4.3.9 in the original variables.

Theorem 4.3.12. *Assume that*

i) there exists continuous (in the norm topology) parametrizations $\Gamma_\perp[\tau]$ and $\Delta_k[\tau]$ such that $\Gamma_\perp[1] = \Gamma_\perp$, $\Delta_k[1] = \Delta_k$,

ii) there exists bounded self–adjoint linear operators $\Pi_{\Gamma_\perp}$ and π_Δ such that

(*a*) $\Gamma_\perp[\tau] \in IQC(\Pi_{\Gamma_\perp})$, $\tau \in [0,1]$,

(*b*) $\Delta_k[\tau] \in IQC(\pi_\Delta)$, $\tau \in [0,1]$,

iiia) *for all* $s \in \partial\Omega \setminus \{s_k\}$ *where* $\{s_k\}$ *denotes the set of singular points at the imaginary axis*

$$\begin{bmatrix} I \\ \widehat{H}_r \end{bmatrix} \operatorname{daug}\left(\widehat{\Pi}_{\Gamma_\perp}, \widehat{\pi}_\Delta \otimes I_{N-1}\right) \begin{bmatrix} I \\ \widehat{H}_r \end{bmatrix}(s) > 0 \tag{4.10}$$

where

$$H_r = \begin{bmatrix} h_{uy}I & h_{wy}I \\ h_{uv}I & 0 \end{bmatrix},$$

iiib) *there exists a matrix* $Q \in \mathbb{R}^{2N\times 2N}$ *with* $Q_{21} = q_{21}I_{N-1}$ *which respects Assumption 4.3.4, i.e.* $G_r = Q \star H_r$ *is stable.*

iiic) *for each pole* $s_k \in \partial\Omega$ *and for the matrix* Q

$$T_k^* \operatorname{daug}\left(\widehat{\Pi}_{\Gamma_\perp}(s_k), \widehat{\pi}_\Delta(s_k) \otimes I_{N-1}\right) T_k > 0$$

where

$$T_k = \begin{bmatrix} 0 & Q_{22}\widehat{h}'_{wy} \\ 0 & Q_{22}\widehat{h}'_{uy} \\ q_{21}\widehat{h}'_{uy}I_{N-1} & \widehat{h}'_{wy}I_{N-1} \\ 0 & Q_{22}\widehat{h}_{uv}\widehat{h}'_{wy} \end{bmatrix}(s_k)$$

and

$$h'_{uy}(s_k) = \lim_{s\to s_k}(s-s_k)^{\rho_k}h_{uy}(s)$$
$$h'_{wy}(s_k) = \lim_{s\to s_k}(s-s_k)^{\rho_k}h_{wy}(s)$$

ρ_k *being the order of the pole.*

iv) h_{uv}, $h_{uv}^{-1} \in \mathcal{A}$,

v) Q_{12}, $Q_{12}^{-1} \in \mathbb{R}^{N\times N}$, q_{21}, $q_{21}^{-1} \in \mathbb{R}$,

then the network in Eq. 4.1 synchronizes to the subspace $\mathcal{Z}$.

Proof. The proof follows by transforming the system using the Redheffer star product so that Theorem 4.3.9 applies. It follows from Eq. 4.9 above that we may use the multipliers

$\Pi_{\Gamma_Q} = (F_Q^*)^{-1}\Pi_{\Gamma_\perp}F_Q^{-1}$. Hence, by Lemma 4.3.11 we have

$$\operatorname{diag}\left(\Gamma_Q[\tau], \Delta[\tau]\right)] \in IQC(\operatorname{daug}\left(\Pi_{\Gamma_Q}, \pi_\Delta \otimes I\right))$$

for $\tau \in [0, 1]$.

By defining

$$T_Q := \operatorname{daug}\left(F_Q, I_{N-1}\right) = \begin{bmatrix} Q_{21}^{-1} & 0 & -Q_{21}^{-1}Q_{22} & 0 \\ 0 & I & 0 & 0 \\ 0 & 0 & Q_{12} & 0 \\ 0 & 0 & 0 & I \end{bmatrix}.$$

we have the relation

$$\operatorname{daug}\left(\Pi_{\Gamma_Q}, \pi_\Delta \otimes I_{N-1}\right) = (T_Q^*)^{-1}\operatorname{daug}\left(\Pi_{\Gamma_\perp}, \pi_\Delta \otimes I_{N-1}\right) T_Q^{-1}.$$

One can moreover show that

$$T_Q \begin{bmatrix} I \\ H_r \end{bmatrix} = \begin{bmatrix} I \\ G_r \end{bmatrix} M$$

where G_r is defined in Eq. 4.8 and

$$M := \begin{bmatrix} Q_{21}^{-1}(I - Q_{22}h_{uy}) & -Q_{21}^{-1}Q_{22}h_{wy} \\ 0 & I \end{bmatrix},$$

so that

$$M^{-1} = \begin{bmatrix} (I - Q_{22}h_{uy})^{-1}Q_{21} & (I - Q_{22}h_{uy})^{-1}Q_{22}h_{wy} \\ 0 & I \end{bmatrix}.$$

Hence, using these relationships, *iiia*) implies that on any compact subset of $\partial\Omega \cup \{\infty\} \setminus \{s_k\}$, there exists $\epsilon > 0$ such that

$$\begin{aligned} &\left(\begin{bmatrix} I \\ \widehat{G}_r \end{bmatrix}^* \operatorname{daug}\left(\widehat{\Pi}_{\Gamma_Q}, \widehat{\pi}_\Delta \otimes I\right) \begin{bmatrix} I \\ \widehat{G}_r \end{bmatrix}\right)(s) \\ &\quad = \left((\widehat{M}^{-1})^* \begin{bmatrix} I \\ \widehat{H}_r \end{bmatrix}^* \operatorname{daug}\left(\widehat{\Pi}_{\Gamma_\perp}, \widehat{\pi}_\Delta \otimes I\right) \begin{bmatrix} I \\ \widehat{H}_r \end{bmatrix} \widehat{M}^{-1}\right)(s) \\ &\quad \geq \epsilon I. \end{aligned}$$

Here we have used that that the multipliers and the transfer functions are continuous on

$\partial\Omega \cup \{\infty\} \setminus \{s_k\}$.

We have now to explore what happens in a neighborhood of the singular points. It is a matter of computation to show that, since $Q_{21} = q_{21} I_{N-1}$, we have

$$\begin{bmatrix} I \\ \widehat{H}_r \end{bmatrix} \widehat{M}^{-1}$$

$$= \begin{bmatrix} q_{21}(s-s_k)^{\rho_k} I_{N-1} & Q_{22}(s-s_k)^{\rho_k}\widehat{h}_{wy} \\ 0 & (I - Q_{22}\widehat{h}_{uy})(s-s_k)^{\rho_k} \\ q_{21}(s-s_k)^{\rho_k}\widehat{h}_{uy} I_{N-1} & (s-s_k)^{\rho_k}\widehat{h}_{wy} I_{N-1} \\ q_{21}(s-s_k)^{\rho_k}\widehat{h}_{uv} I_{N-1} & Q_{22}(s-s_k)^{\rho_k}\widehat{h}_{uy}\widehat{h}_{uv} \end{bmatrix} \times$$

$$(I - Q_{22}\widehat{h}_{uy})^{-1}(s-s_k)^{-\rho_k}$$

$$\to -T_k Q_{22}^{-1} \frac{1}{\widehat{h}'_{uy}(s_k)} \quad \text{as } s \to s_k.$$

Assumption *iiic*) implies thus that in any sufficiently small compact neighborhood of the singular point s_k, $N_k \subset \partial\Omega$, there exists $\nu > 0$ such that

$$\begin{bmatrix} I \\ \widehat{G}_r \end{bmatrix}^* \mathrm{daug}\left(\widehat{\Pi}_{\Gamma_Q}, \widehat{\pi}_\Delta \otimes I\right) \begin{bmatrix} I \\ \widehat{G}_r \end{bmatrix}(s)$$

$$\geq T_k^* \mathrm{daug}\left(\widehat{\Pi}_{\Gamma_\perp}(s_k), \widehat{\pi}_\Delta(s_k) \otimes I\right) T_k - \nu I \geq \epsilon I$$

for all $s \in N_k$ and all k. It follows that *iii*) in Theorem 4.3.9 holds. □

4.4 Synchronization in case of static interconnection

The results given in the previous sections provide general tools to study the synchronization properties of a network of heterogeneous agents. One however wonders whether it is possible to particularize the result in cases in which the structure of the operators Γ and Δ_k are such that a natural choice for the matrices V and Q of the projection and loop transformation steps, as well as IQC characterizations, arise. In this and the following Sections we will analyze in some detail several special cases.

We start by considering the simplest and usual choice for the interconnection operator $\Gamma(t, \boldsymbol{y})$, namely the multiplication by a constant matrix

$$\Gamma(t, \boldsymbol{t}) = \Gamma_0 \boldsymbol{y}.$$

We will restrict attention to the class of matrices Γ_0 which respect the following Assumption.

Assumption 4.4.1. The matrix Γ_0

i) respects Assumption 4.3.2

iia) is normal, namely such that $\Gamma_0\Gamma_0^* = \Gamma_0^*\Gamma_0$

iib) is able to synchronize the nominal system to the subspace $\mathcal{Z} = \ker \Gamma_0$. In other words, the *nominal interconnection* (with $\Delta = 0$)

$$\begin{cases} \boldsymbol{y} = h_{uy}\boldsymbol{u} + h_{ry}\boldsymbol{r} \\ \boldsymbol{u} = \Gamma_0 \boldsymbol{y} \end{cases} \tag{4.11}$$

synchronizes to $\mathcal{Z}$.

For the most usual situation, namely synchronization to $\mathbf{1}$, a natural choice is, as we already known for consensus, $\Gamma_0 = -\nu L$ where L is the Laplacian of a primitive stochastic matrix P associated with the communication graph.

Normal matrices are orthogonally diagonalizable, and this allows us to characterize the synchronization properties by making use only of its spectral properties. Indeed, let $U \in \mathbb{R}^{N\times N}$ be an unitary matrix such that

$$\Gamma_0 = U \begin{bmatrix} 0_p & 0 \\ 0 & \Gamma_{0\perp} \end{bmatrix} U^*$$

where the upper–left block 0_p is a $p \times p$ block of zeros, while $\Gamma_{0\perp} \in \mathbb{R}^{N-p\times N-p}$ is a diagonal matrix whose (i, i)-th entry is the i-th non-zero eigenvalue of Γ_0:

$$\Gamma_{0\perp} = \begin{bmatrix} \mu_{p+1} & & \\ & \ddots & \\ & & \mu_N \end{bmatrix}.$$

Correspondingly, the matrix U can be partitioned as $U = \begin{bmatrix} Z & V \end{bmatrix}$, where the columns of Z are an orthonormal basis for the kernel of Γ_0, namely for $\mathcal{Z}$, while the columns of V span its orthogonal complement $\mathcal{Z}^\perp$. Clearly $\Gamma_{0\perp} = V^*\Gamma_0 V$.

To perform the loop transformation we need a matrix Q respecting Assumption 4.3.4. A simple choice is

$$Q_{12} = I_{N-1},\ Q_{21} = I_{N-1},\ Q_{22} = \Gamma_{0\perp}.$$

To prove this, we need to show that all the matrices in G in Eq. 4.8 are stable, and this is a consequence of Assumption 4.4.1 *iib*). In fact if we consider the nominal interconnection in Eq. 4.11 and perform the projection using V, we obtain

$$\boldsymbol{y}_\perp = (I_{N-p} - \Gamma_{0\perp} h_{uy})^{-1} h_{ry} \boldsymbol{r}_\perp = G_{ry} \boldsymbol{r}_\perp.$$

Notice that G_{ry} is a diagonal matrix of transfer functions, so it is stable if and only if all its entries on the diagonal are stable transfer functions. This argument proves the following Lemma, which gives an equivalent condition for Assumption *iib*) (a slightly different version appeared in [22]).

Lemma 4.4.2 ([22])**.** *A sufficient and necessary condition for the synchronization of the* nominal interconnection *to* $\mathcal{Z} = \ker \Gamma_0$ *is that the transfer functions* $\frac{h_{ry}}{1-\mu_i h_{uy}}$ *are stable, for any nonzero eigenvalue* μ_i, $i = 1, \ldots, N-p$, *of* Γ_0.

On this discussion is based the proof of the following result.

Corollary 4.4.3. *Consider the system in Eq. 4.1 in which* $\Gamma(t, \boldsymbol{y}) = \Gamma_0 \boldsymbol{y}$, *where* Γ_0 *respects Assumption 4.4.1.*

Assume there exists a multiplier π_Δ *in*

$$\Pi_\Delta = \{\pi = \pi^* \in S^{2\times 2}_{\mathcal{A}_d} : \Delta_k \in IQC(\pi),\, \pi_{11} \geq 0,\, \pi_{22} \leq 0\} \tag{4.12}$$

such that

$$\begin{bmatrix} I \\ \frac{\mu_i h_{ry}}{1-\mu_i h_{uy}} \end{bmatrix}^* \pi_\Delta \begin{bmatrix} I \\ \frac{\mu_i h_{ry}}{1-\mu_i h_{uy}} \end{bmatrix} > 0,$$

for any nonzero eigenvalue $\mu_i, i = 1, \ldots, N-p$ *of* Γ_0. *Assume moreover that* h_{uv}, $h_{uv}^{-1} \in \mathcal{A}$. *Then the system synchronizes to the subspace* $\mathcal{Z}$.

Proof. The proof of this corollary consists in showing that it is possible to choose the matrix $V \in \mathbb{R}^{N\times N-p}$ for the projection and the matrix Q for the loop transformation in such a way that the conditions of Theorem 4.3.9 are satisfied.

First of all, since Γ_0 is normal we know that it is orthogonally diagonalizable. By arranging the eigenvalues in such a way that the first p are the zero eigenvalues, corresponding to the normalized matrix of eigenvectors Z, we obtain the eigenvalue decomposition

$$\Gamma_0 = \begin{bmatrix} Z & V \end{bmatrix}^* \left[\begin{array}{c|c} 0 & 0 \\ \hline 0 & \Gamma_{0\perp} \end{array}\right] \begin{bmatrix} Z & V \end{bmatrix}$$

Notice that $\Gamma_\perp(t,\, \boldsymbol{y}) = \Gamma_{0\perp}\boldsymbol{y}_\perp$ so V, whose columns are an orthonormal basis for $\mathcal{Z}^\perp$, is a natural choice to perform the projection.

The second step is to choose Q, and we can simply set

$$Q = \begin{bmatrix} 0 & I \\ I & \Gamma_{0\perp} \end{bmatrix},$$

which trivially yields $\Gamma_Q(t,\, gy) = 0$. The resulting system is thus

$$\begin{cases} \begin{bmatrix} \boldsymbol{y}_\perp \\ \boldsymbol{v}_\perp \end{bmatrix} = \begin{bmatrix} G_{ry} & G_{wy} \\ G_{rv} & G_{wv} \end{bmatrix} \begin{bmatrix} \boldsymbol{r}_\perp \\ \boldsymbol{w}_\perp \end{bmatrix} \\ \boldsymbol{w}_\perp = \Delta_\perp \boldsymbol{v}_\perp \end{cases}$$

since $\boldsymbol{y}_Q = \boldsymbol{y}_\perp$ and $\boldsymbol{u}_Q(t) = 0$, $\forall\, t$, so its contribution is dropped.

Set now $\Pi_{\Gamma_Q} = \begin{bmatrix} \nu I_{N-p} & 0 \\ 0 & 0 \end{bmatrix}$, where ν is a real value. Using the fictitious parametrization $\Gamma_Q(t,\, \boldsymbol{y}_Q)[\tau] = \tau\Gamma_Q(t,\, \boldsymbol{y}_Q) \equiv 0$, it is immediate to see that

$$\left\langle \begin{bmatrix} \Gamma_Q(t,\, \boldsymbol{y}_Q) \\ \boldsymbol{y}_Q \end{bmatrix}, \Pi_{\Gamma_Q} \begin{bmatrix} \Gamma_Q(t,\, \boldsymbol{y}_Q) \\ \boldsymbol{y}_Q \end{bmatrix} \right\rangle = 0$$

so that $\Gamma_Q \in IQC(\Pi_{\Gamma_Q})$. The parametrization $\Delta_k[\tau] = \tau\Delta_k$, together with $\pi_{\Delta,11} \geq 0$ and $\pi_{\Delta,22} \leq 0$, implies $\Delta_k[\tau] \in IQC(\pi_\Delta)$ and thus, by Lemma 4.3.11, also $\Delta_\perp \in IQC(\pi_\Delta \otimes I_{N-1})$. Moreover, the nominal interconnection, which is given by $\Gamma_Q[0] = 0$ and $\Delta_\perp[0] = 0$, is

$$[G, \operatorname{diag}(\Gamma_Q[0], \Delta_\perp[0])] = \begin{bmatrix} G_{ry} & G_{wy} \\ G_{rv} & G_{wv} \end{bmatrix}$$

since the signal $u_Q = 0$ so it has no influence. Assumption 4.4.1 implies now that $[G, \operatorname{diag}(\Gamma_Q[0], \Delta_\perp[0])]$ is stable. This holds since G_{ry} is stable by assumption and stability of G_{wy} follows from Assumption 4.2.1. This reasoning implies conditions *i*) and *ii*) in Theorem 4.3.9 are satisfied. Concerning *iii*), instead, notice that the multiplier for the linear part is

$$\operatorname{daug}\left(\Pi_{\Gamma_Q}, \pi_\Delta \otimes I_{N-p}\right) = \left[\begin{array}{c|ccc} \nu I & 0 & 0 & 0 \\ \hline 0 & \pi_{\Delta,\,11} I_{N-p} & 0 & \pi_{\Delta,\,12} I_{N-p} \\ 0 & 0 & 0 & 0 \\ 0 & \pi^*_{\Delta,\,12} I_{N-p} & 0 & \pi_{\Delta,\,22} I_{N-p} \end{array}\right] = \left[\begin{array}{c|c} \nu I & 0 \\ \hline 0 & \tilde{\Pi}_\Delta \end{array}\right].$$

Denote for simplicity

$$\left[\begin{array}{c|c} I & 0 \\ \hline 0 & I \\ G_{ry} & G_{wy} \\ G_{rv} & G_{wv} \end{array}\right] = \left[\begin{array}{c|c} I & 0 \\ \hline \Upsilon_1 & \Upsilon_2 \end{array}\right].$$

It turns out that

$$\begin{bmatrix} I & 0 \\ \Upsilon_1 & \Upsilon_2 \end{bmatrix}^* \begin{bmatrix} \nu I & 0 \\ 0 & \tilde{\Pi}_\Delta \end{bmatrix} \begin{bmatrix} I & 0 \\ \Upsilon_1 & \Upsilon_2 \end{bmatrix} = \begin{bmatrix} \nu I + \Upsilon_1^* \tilde{\Pi}_\Delta \Upsilon_1 & \Upsilon_1^* \tilde{\Pi}_\Delta \Upsilon_2 \\ \Upsilon_2^* \tilde{\Pi}_\Delta \Upsilon_1 & \Upsilon_2^* \tilde{\Pi}_\Delta \Upsilon_2 \end{bmatrix} \tag{4.13}$$

where an easy computation yields

$$\Upsilon_2^* \tilde{\Pi}_\Delta \Upsilon_2 = \begin{bmatrix} I \\ G_{wv} \end{bmatrix}^* \Pi_\Delta \begin{bmatrix} I \\ G_{wv} \end{bmatrix} > 0$$

by assumption. Regardless the actual values of the other components of the matrix in Eq. 4.13, by choosing now ν "big enough", we can be sure that it is positive definite, since it is well known that

$$\det \begin{bmatrix} \mu I - a & -b \\ -c & \mu I - D \end{bmatrix} = \qquad \det\{\mu I - D\} \det\{\mu I - a - b(\mu I - D)^{-1} c\}$$

and in this expression a can be raised to any positive value, while the roots of the first term are positive by assumption. These proves also condition *iii*) in Theorem 4.3.9, so we can apply our result and conclude for the synchronization of the given system. □

Quasi–saturation in the interconnection inputs

The aim of this section is to prove the synchronization of Higher Order Consensus Network in which the operators Δ_k are used to express an example of non–ideality affecting the system. Setting $h_{uy} = h_{ry} = h_{wy} = N_0$ and $h_{uv} = I$, the system under analysis can be reduced to

$$\begin{cases} \boldsymbol{y} = N_0(1 + \Delta)\boldsymbol{u} + N_0 \boldsymbol{r} \\ \boldsymbol{u} = \Gamma_0 \boldsymbol{u} \end{cases} \tag{4.14}$$

We assume that the agents can use directly the input they produce by sensing their neighbors only if such input is, in absolute value, less then a certain threshold u_{th}. If, instead, the input does not respect this inequality, then the value is modified. We model

this setting as

$$(1+\Delta_k)(u) = \begin{cases} u, & |u| \leq u_{th} \\ u - \phi(t,\, u - \mathrm{sgn}(u)u_{th}), & |u| \geq u_{th} \end{cases}$$

so that

$$\Delta_k(u) = \begin{cases} 0, & |u| \leq u_{th} \\ -\phi(t,\, u - \mathrm{sgn}(u)u_{th}), & |u| > u_{th} \end{cases}$$

where $\phi_k(t,\, v)$ is an odd memoryless nonlinearity such that $\phi_k(t,\, 0) = 0$, $\forall\, t \geq 0$. We assume that $\phi_k(t, v)$ is sufficiently regular so that the feedback system is well posed, and moreover that it satisfies a sector condition

$$(\phi_k(t,\, v) - \alpha_{\min} v)\phi_k(t,\, v) \leq 0$$

where $\alpha_{\min} > 0$. The assumption $\alpha_{\min} > 0$ does not allow to express the pure saturation of input, since, as it is easy to prove, it is always possible to find initial conditions (e.g. using the external input $\boldsymbol{r}$), such that if the input is saturated then synchronization (according to Definition 4.3.1) cannot take place. The sector condition implies moreover that the input is always "underestimated". An example of this is depicted in Fig. 4.6.

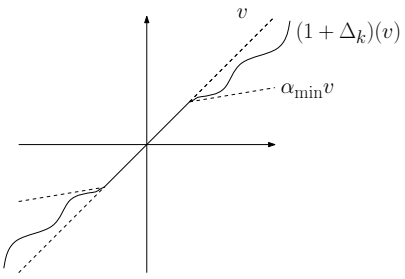

Figure 4.6: An example of quasi–saturation.

An immediate consequence of the sector condition for ϕ is that the following sector condition is satisfied by each Δ_k too

$$(\Delta_k(t,\, v) + \alpha_{\min} v)\Delta_k(t,\, v) \leq 0$$

and this inequality immediately implies that $\Delta_k \in IQC(\pi_{\Delta,\, C})$ where $\pi_{\Delta,\, C}$ is the constant

multiplier

$$\pi_{\Delta,C} = \begin{bmatrix} 2 & \alpha_{\min} \\ \alpha_{\min} & 0 \end{bmatrix}.$$

This multiplier can be useful, but often the derived criterion is too conservative. A major improvement can be obtained if the nonlinearity is time-invariant and such that the following slope condition is imposed on the Δ_k's

$$-\alpha_{\min} \leq \frac{\Delta_k(x_1) - \Delta_k(x_2)}{x_1 - x_2} \leq 0. \tag{4.15}$$

It can be proven, see e.g. [131], that this condition is enough to conclude that $\Delta_k \in IQC(\pi_{\Delta,ZF})$, which is called Zames-Falb multiplier and is defined as

$$\pi_{\Delta,ZF} = \begin{bmatrix} 2\mathrm{Re}(m_0 - M) & \alpha_{\min}(m_0 - M) \\ \alpha_{\min}(m_0 - M) & 0 \end{bmatrix}$$

where $M(s)$ is the Laplace transform of an L_1 function $m(t)$, namely

$$M(s) = \int_{-\infty}^{\infty} m(t)e^{-st}dt$$

and $\|m\|_1 = \int_{-\infty}^{\infty} |m(t)|dt < \infty$, while m_0 is a positive constant such that $\|m\|_1 \leq m_0$. Analogous results hold in the discrete time case.

Our choice is $M(s) = \frac{-\tau}{s-\tau}$ for which $m(t) = -\tau e^{t\tau}\theta(-t)$, θ being the Heaviside step. Since $\|m\|_1 = 1$, we set $m_0 = 1$, and it turns out that $1 - M(s) = \frac{-s/\tau}{1-s/\tau}$, so, premultipling by the positive value τ, the obtained multiplier is

$$\pi_{\Delta,ZF}(j\omega) = \begin{bmatrix} 2\mathrm{Re}(\frac{-j\omega}{1-j\omega/\tau}) & \alpha_{\min}\frac{-j\omega}{1-j\omega/\tau} \\ \alpha_{\min}\frac{j\omega}{1+j\omega/\tau} & 0 \end{bmatrix}.$$

If we choose τ large enough, this bounded multiplier approximate can be approximated, at sufficiently low frequency, as $\pi_{\Delta,ZF}(j\omega) \approx \alpha_{\min}\pi_{\Delta,P}$, where the latter is the Popov multiplier

$$\pi_{\Delta,P}(j\omega) = \begin{bmatrix} 0 & -j\omega \\ j\omega & 0 \end{bmatrix}.$$

Hence, at low frequencies the Zames–Falb multiplier recovers the Popov one.

Our choice for the multiplier to be used is a linear combination of the two

$$\pi_{\Delta,C} + \lambda\alpha_{\min}\pi_{\Delta,P} = \begin{bmatrix} 2 & \alpha_{\min}(1 - j\lambda\omega) \\ \alpha_{\min}(1 + j\lambda\omega) & 0 \end{bmatrix}. \tag{4.16}$$

We can invoke Corollary 4.4.3 to immediately prove the following result.

Corollary 4.4.4. *Consider the system in Eq. 4.14 where Δ_k satisfies Eq. 4.15 and Γ_0 satisfies Assumption 4.4.1. Then the system synchronizes if there exists $\lambda \in \mathbb{R}$ such that*

$$\begin{bmatrix} 1 \\ \frac{\mu_i N_0}{1-\mu_i N_0} \end{bmatrix}^* (\pi_{\Delta,C} + \lambda \pi_{\Delta,P}) \begin{bmatrix} 1 \\ \frac{\mu_i N_0}{1-\mu_i N_0} \end{bmatrix} > 0, \tag{4.17}$$

where $\pi_{\Delta,C}$ and $\pi_{\Delta,P}$ are defined above and $\mu_i, i = 1, \dots, N-p$ are the nonzero eigenvalues of Γ_0.

This inequality can be easily checked graphically using a Popov plot. Define $G_{r,i} = \frac{\mu_i N_0}{1-\mu_i N_0}$ and

$$\mathcal{P}_i := \{z : z = \mathrm{Re}G_{r,i}(j\omega) - j\omega \mathrm{Im}G_{r,i}(j\omega)\}.$$

The system synchronizes if each $\mathcal{P}_i$ entirely lies on the right to the line with slope $\frac{1}{\lambda}$ and crossing the x–axis in the point $-\frac{1}{\alpha_{\min}}$. Is is worth to notice that if $\alpha_{\min} \to 0$, namely if $\Delta_k \to 0$, then the Popov criterion is always satisfied, and this is clear since the nominal interconnection is stable.

Remark 4.4.5. Corollary 4.4.4 and the graphical criterion are stated and verified using the Popov multiplier instead of the Zames–Falb multiplier. As we have noticed above, the former is a good approximation of the latter at low frequencies, so in this range the two criteria essentially coincide. One has then to be sure that at high frequencies in which the correct multiplier is $\pi_{\Delta,ZF}$, the inequality in Eq. 4.17 is satisfied. This holds if τ is large enough since $N_0(s)$ is a strictly proper transfer function.

A non–normal Γ_0 example

In the previous section we have shown how it is possible to provide an IQC characterization to ensure the synchronization of a network of heterogeneous agents given that the constant matrix Γ_0 is normal. A step toward the direction of the full generality, but maintaining a certain degree of structure, can be made considering reversible Laplacians, which we introduced in the Analysis chapter (Section 3.3).

Recall that the matrices we are interested in are of the form $\Gamma_0 = -\nu L$, where $L = I - P$ is the Laplacian associated a primitive stochastic matrix P associated with the communication graph $\mathcal{G} = (\mathcal{V}, \mathcal{E})$, and $\nu > 0$ is a real, tuning, number.

With a slight abuse of language, we will call also Γ_0 to be reversible if the corresponding P is reversible, which, recall from Definition 3.3.2, means that if $\boldsymbol{\pi}$ is the invariant measure of P and if $\Pi = \mathrm{diag}\,(\boldsymbol{\pi})$, then

$$\Pi P = P^T \Pi.$$

It is immediate to see, writing $\Gamma_0 = -\nu(I - P)$, that Γ_0 is reversible as well since

$$\Pi\Gamma_0 = \Gamma_0^T\Pi. \tag{4.18}$$

In this case normality is in general lost. Assume however that the graph is strongly connected and P primitive, so that $\pi_k > 0, \forall k$. We can thus consider the matrix $R_0 = \Pi^{1/2}\Gamma_0\Pi^{-1/2}$, which is symmetric due to Eq. 4.18, hence its eigenvalues are real, and has as left kernel span $\left\{\Pi^{1/2}\mathbf{1}\right\}$.

Consider the Higher Order Consensus Network

$$\begin{cases} \boldsymbol{y} = N_0(I + \Delta)\boldsymbol{u} + N_0\boldsymbol{r} \\ \boldsymbol{u} = \Gamma_0\boldsymbol{y} \end{cases}, \tag{4.19}$$

and perform a multiplier transformation defining $\bar{\boldsymbol{y}} = \Pi^{1/2}\boldsymbol{y}$, $\bar{\boldsymbol{u}} = \Pi^{1/2}\boldsymbol{u}$, $\bar{\boldsymbol{r}} = \Pi^{1/2}\boldsymbol{r}$ and $\bar{\Delta}(\bar{\boldsymbol{u}}) = \Pi^{1/2}\Delta(\Pi^{-1/2}\bar{\boldsymbol{u}})$. In the new variables, the Higher Order Consensus Network obeys to

$$\begin{cases} \bar{\boldsymbol{y}} = N_0(I + \bar{\Delta})\bar{\boldsymbol{u}} + N_0\bar{\boldsymbol{r}} \\ \bar{\boldsymbol{u}} = R_0\bar{\boldsymbol{y}} \end{cases} \tag{4.20}$$

where now R_0 respects the normality assumptions, and we can apply the previous theorems. We can now state the following simple result.

Proposition 4.4.6. *Consider the system in Eq. 4.19 where $\Gamma_0 = -\nu(I - P)$ and P is a primitive, stochastic, reversible matrix with invariant measure $\boldsymbol{\pi}^T$. Assume moreover that the transfer functions $\frac{N_0}{1-\mu_i N_0}$ are stable for any nonzero eigenvalue μ_i of Γ_0. Assume there exists a multiplier π_Δ in*

$$\Pi_\Delta = \{\pi = \pi^* \in S_{\mathcal{A}}^{2\times 2} : \Delta_k \in IQC(\pi),\, \pi_{11} \geq 0,\, \pi_{22} \leq 0\}.$$

such that

$$\begin{bmatrix} I \\ \frac{\mu_i h_{ry}}{1-\mu_i h_{uy}} \end{bmatrix}^* \pi_\Delta \begin{bmatrix} I \\ \frac{\mu_i h_{ry}}{1-\mu_i h_{uy}} \end{bmatrix} > 0,$$

for any nonzero eigenvalue μ_i, $i = 1, \ldots, N - p$ of Γ_0. Then the system synchronizes to the subspace $\mathcal{Z} = \text{span}\,\{\mathbf{1}\}$.

Proof. From the above discussion it is clear that R_0 satisfies Assumption 4.4.1. Since the eigenvalues of Γ_0 are also eigenvalues of R_0, we can immediately apply Corollary 4.4.3 and conclude that the system in Eq. 4.20 synchronizes to span $\left\{\Pi^{-1/2}\mathbf{1}\right\}$. Since $\Pi^{-1/2}$ is an invertible constant matrix, and since $\bar{\boldsymbol{y}} = \Pi^{1/2}\boldsymbol{y}$ and $\bar{\boldsymbol{r}} = \Pi^{1/2}\boldsymbol{r}$, it is immediate to

conclude that the system in Eq. 4.19 synchronizes to span $\{\mathbf{1}\}$. □

Leader-following for Higher Order Consensus Networks

In the previous Section the assumption was that all the entries of $\boldsymbol{\pi}$ had to be strictly positive, as a consequence of the fact that the graph was strongly connected. In this Section we want to analyze what happens if, instead, some of them are zero.

For sake of simplicity, we will consider the homogeneous case, in which $\Delta_k = 0$, $k = 1, \ldots, N$. We can assume w.l.o.g. (possibly after relabeling the agents) that $V = S_1 \cup S_2$ where $S_1 = \{1, \ldots, q\}$ and $S_2 = \{q+1, \ldots, N\}$, and $\pi_i > 0$ if $i \in S_1$ and $\pi_j = 0$ if $j \in S_2$. By reversibility, from Eq. 4.18 we can conclude that Γ_0 has the structure

$$\Gamma_0 = \begin{bmatrix} \Gamma_{S_1} & 0 \\ \Gamma_{S_{12}} & \Gamma_{S2} \end{bmatrix}$$

so that, suitably partitioning the outputs, the interconnection inputs and the external inputs, we can rewrite the system Eq. 4.19 as

$$\begin{cases} \begin{bmatrix} \boldsymbol{y}_{S_1} \\ \boldsymbol{y}_{S_2} \end{bmatrix} = \begin{bmatrix} N_0 I_{S_1} & 0 \\ 0 & N_0 I_{S_2} \end{bmatrix} \begin{bmatrix} \boldsymbol{u}_{S_1} \\ \boldsymbol{u}_{S_2} \end{bmatrix} + N_0 \begin{bmatrix} \boldsymbol{r}_{S_1} \\ \boldsymbol{r}_{S_2} \end{bmatrix}, \\ \begin{bmatrix} \boldsymbol{u}_{S_1} \\ \boldsymbol{u}_{S_2} \end{bmatrix} = \begin{bmatrix} \Gamma_{S_1} & 0 \\ \Gamma_{S_{12}} & \Gamma_{S_2} \end{bmatrix}, \end{cases} \tag{4.21}$$

so that the dynamics for the set S_1 is described by the system

$$\begin{cases} \boldsymbol{y}_{S_1} = N_0 I_{S_1} \boldsymbol{u}_{S_1} + N_0 \boldsymbol{r}_{S_1}, \\ \boldsymbol{u}_{S_1} = \Gamma_{S_1} \boldsymbol{y}_{S_1}, \end{cases} \tag{4.22}$$

while the dynamics for the set S_2 is described by

$$\begin{cases} \boldsymbol{y}_{S_2} = N_0 I_{S_2} \boldsymbol{u}_{S_2} + N_0 \boldsymbol{r}_{S_2}, \\ \boldsymbol{u}_{S_2} = \Gamma_{S_{12}} \boldsymbol{y}_{S_1} + \Gamma_{S_2} \boldsymbol{y}_{S_2}, \end{cases} , \tag{4.23}$$

which yields, after some manipulation, the simplified expression

$$\boldsymbol{y}_{S_2} = (I - \Gamma_{S_2} N_0)^{-1} N_0 (\Gamma_{S_{12}} \boldsymbol{y}_{S_1} + r_{S_2}). \tag{4.24}$$

Notice now that because of the block–lower–triangular structure of Γ_0, its eigenvalues are distributed among Γ_{S_1} and Γ_{S_2}. As an immediate consequence, since it is clear that

$\Gamma_{S_1}\mathbf{1}_{S_1} = 0$, the matrix Γ_{S_2} is Hurwitz and, by previous arguments, $(I - \Gamma_{S_2}N_0)^{-1}N_0$ is a matrix of stable transfer functions. Since $\Gamma_{S_{12}}$ is a constant matrix and r_{S_2} is a bounded signal, we can conclude that, asymptotically, $\boldsymbol{y}_{S_2}$ will simply be driven by $\boldsymbol{y}_{S_1}$, or, more intuitively, that the set S_1 will be the leader of the network, and that the set S_2 will follow it, progressively forgetting initial conditions and external inputs.

A numerical example

In this section we are going to present a case of leader following for a homogeneous network of $N = 8$ interconnected oscillators. Each agent is represented by the nominal transfer function

$$N_0(s) = \frac{1+s}{s^2+\omega_0^2}$$

where $\omega_0 = 1$. The network is divided in two subsets, a first set S_1 in which the agents are interconnected in a circle and communicate using the matrix

$$\Gamma_{S_1} = -I_4 + +0.5\mathcal{C}_4 + 0.5\mathcal{C}_4^{-1},$$

and a second set S_2 in which the agents are interconnected in a circle via a matrix Γ_{S_2} and, moreover, can receive information from one of the agents of the set S_1 via a matrix $\Gamma_{S_{12}}$. The two Γ_{S_2} and $\Gamma_{S_{12}}$, apart from the structure, are chosen randomly with the only constraint that

$$\begin{bmatrix}\Gamma_{S_{12}} & \Gamma_{S_2}\end{bmatrix}\mathbf{1} = 0.$$

This is depicted in Fig. 4.7.

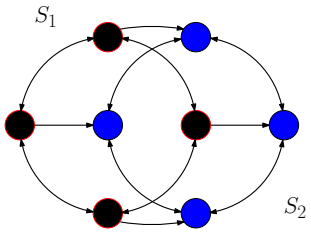

Figure 4.7: Leader following for a network of perturbed oscillators. The graph of communication, in which S_1 is the set of leaders, while S_2 is the set of followers. Notice that the agents in S_2 receive information from S_1 without replying.

Once we run the simulation, taking randomly the initial conditions, we obtain as typical trajectory what is depicted in Fig. 4.8. As it can be seen, the agents in S_1 agree on a sinusoid of angular frequency $\omega_0 = 1 rad/sec$, which corresponds to the "nominal behavior", followed by the agents in S_2 which forget their initial conditions and slowly

converge to the behavior of the leader agents.

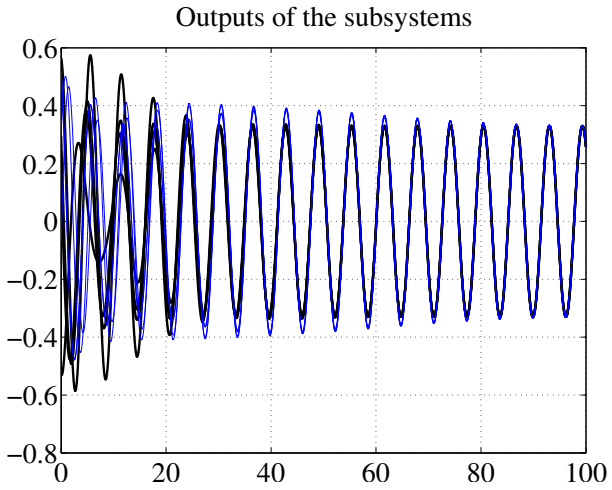

Figure 4.8: Leader following for a network of perturbed oscillators. In thick the trajectory of the leaders, which reach asymptotically the agreement on a sinusoid of angular frequency $\omega_0 = 1 rad/sec$. In thin the followers, which progressively forget their initial conditions and simply follow the leaders.

A nonlinear interconnection: An example

In this section we are going to analyze in some detail a particular type of non-linear interconnection operator Γ for which we can find a powerful IQC characterization.

Let $\mathcal{G} = (\mathcal{V}, \mathcal{E})$ be an undirected graph with vertices $\mathcal{V} = \{1, \ldots, N\}$ and edge set $\mathcal{E}$, a let $A = [a_{jk}]_{j,k=1}^{N}$ be its adjacency matrix, which, recall, is defined as

$$a_{kj} = \begin{cases} 1, & (j,\, k) \in \mathcal{E},\, j \neq k \\ 0, & \text{otherwise} \end{cases}$$

We use in this Section the notion of Laplacian of the graph $\mathcal{G}$, which is defined as

$$L_G = \Delta - A$$

where Δ is the diagonal matrix of the degrees of the nodes.

We assume that the graph is connected, which implies, analogously to Laplacians of primitive matrices, that the eigenvalues of L_G are distributed as $0 = \mu_1 < \mu_2 \leq \ldots \leq \mu_N$.

We use the Rayleigh-Ritz ratio (see Eq. 3.15) in the form

$$\mu_2 = \min_{\mathbf{1}^T \boldsymbol{y}=0,\, \boldsymbol{y}\neq 0} \frac{\boldsymbol{y}^T L_G \boldsymbol{y}}{|\boldsymbol{y}|^2}. \tag{4.25}$$

We consider the following algorithm in order to produce the control at k-th agent

$$\Gamma_k(\boldsymbol{y}) = \frac{1}{\delta_u} \sum_{j=k}^{N} a_{ij} \phi_{[\eta,\beta]}(\, y_j - y_i),$$

where $\phi_{[\eta,\beta]}$ is an odd, namely such that $\phi_{[\eta,\beta]}(-v) = -\phi_{[\eta,\beta]}(v)$, memoryless nonlinearity satisfying the slope restriction condition

$$\eta \leq \frac{\phi_{[\eta,\beta]}(y_1) - \phi_{[\eta,\beta]}(y_2)}{y_1 - y_2} \leq \beta, \ \forall y_1 \neq y_2$$

for some $0 < \eta < \beta < \infty$. Namely, agent k receives the outputs from its neighbors, computes the relative difference with its own output and maps each difference through a memoryless nonlinearity $\phi_{[\eta,\beta]}$. Then it just sums the results up and divides by the number of neighbors in the network. Notice that, if $\phi_{[\eta,\beta]}(v) = v$, this way to produce the control u corresponds to choosing uniform weights for a primitive consensus matrix P as described in Section 3.6.

A simpler formulation is obtained by using the incidence matrix B, which allows use to write $L_G = B^T B$. With this notation, network operator can be formulated as

$$\Gamma(\boldsymbol{y}) = B^T \Phi_{[\eta,\beta]}(B\boldsymbol{y}) \tag{4.26}$$

where

$$\Phi_{[\eta,\beta]}(\boldsymbol{y}) = \begin{bmatrix} \phi_{[\eta,\beta]}(B_1 \boldsymbol{y}) \\ \vdots \\ \phi_{[\eta,\beta]}(B_n \boldsymbol{y}) \end{bmatrix}, \tag{4.27}$$

and where B_k denotes the k^{th} row of B.

In order to apply our results we need to introduce the transformation and parametrization of Γ. With

$$Q = \begin{bmatrix} 0 & 1 \\ 1 & -\eta \end{bmatrix} \otimes I_{N-1}$$

we have

$$\Gamma_Q(\boldsymbol{y}_Q) = -V^* B^T \Phi_{[0,\alpha]}[\tau](BV\boldsymbol{y}_Q), \tag{4.28}$$

where $\Phi_{[0,\alpha]}[\tau]$ is defined as in Eq. 4.27 above but with the transformed nonlinearity

$$\phi[\tau](y) = (1-\tau)\beta y + \tau\phi_{[0,\beta-\eta]}(y) - \eta y,$$

which is odd and slope restricted in the sense that

$$0 \leq (y_1 - y_2)(\phi[\tau](y_1) - \phi[\tau](y_2)) \leq \alpha(y_1 - y_2)^2,$$

for all $y, \forall\tau \in [0,1]$, where $\alpha = \beta - \eta > 0$.

The following IQC characterization of Eq. 4.28, in which we consider the continuous time case for simplicity, offers a multiplier which can be used with Theorem 4.3.9.

Lemma 4.4.7. *We have $\Gamma_Q \in IQC(\pi \otimes I_{N-1})$ where*

$$\pi(j\omega) = \begin{bmatrix} -\frac{2}{\kappa}(1 + \operatorname{Re} M(j\omega)) & 1 + M(j\omega) \\ 1 + \overline{M(j\omega)} & 0 \end{bmatrix}$$

where $\kappa = \alpha/\mu_2$, μ_2 is defined in Eq. 4.25 and

$$M(j\omega) = \int_{-\infty}^{\infty} m(t)e^{j\omega t}dt \tag{4.29}$$

for some real valued function satisfying $\int_{-\infty}^{\infty} |m(t)|dt \leq 1$.

Proof. We have

$$\begin{aligned}\left\langle \boldsymbol{\Gamma}_Q(\boldsymbol{y}_Q), (1 + M(j\omega)(\boldsymbol{y}_Q - \frac{1}{\kappa}\Gamma_Q(\boldsymbol{y}_Q) \right\rangle \\ \leq -\left\langle \Phi_{[0,\alpha]}[\tau](\tilde{\boldsymbol{y}}), (1 + M(j\omega))(\tilde{\boldsymbol{y}} - \frac{1}{\alpha}\Phi_{[0,\alpha]}[\tau](\tilde{\boldsymbol{y}}) \right\rangle \\ = -\sum \left\langle \phi(\tilde{y}_k), (1 + M(j\omega))(\tilde{y}_k - \frac{1}{\alpha}\phi(\tilde{y}_k) \right\rangle \leq 0\end{aligned}$$

where $\tilde{\boldsymbol{y}} = BV\boldsymbol{y}_Q$ and $\tilde{y}_k = B_k V \boldsymbol{y}_Q$. In the second inequality we used that

$$-|BV\Phi_{[0,\alpha]}[\tau](\tilde{y})|^2 = -(\Phi(\tilde{\boldsymbol{y}})^T V^* L_G V \Phi(\tilde{\boldsymbol{y}}) \leq -\mu_2 |\Phi_{[0,\alpha]}[\tau](\tilde{\boldsymbol{y}})|^2,$$

where we used Eq. 4.25 and that $V \perp \mathbf{1}$. Finally, the last inequality follows since the

slope restricted nonlinearity satisfies the Zames-Falb IQC, see e.g. [131]. □

Time–invariant topology

So far we have consider an extreme case in which we had no information *a priori* information on the graph used at each time. Consider the much easier case in which, instead, the graph topology does not change over time, so that each a_{ij} is a constant value. In this case, the same argument still holds considering as Q_{22} the constant matrix $\Gamma_{0\perp} = -V^* L_G V$ instead of the simpler $Q_{22} = -I_{N-1}$. This, if the columns of V are the normalized eigenvectors of L_G, yields the bounds

$$(1-\beta)\mu_2|\boldsymbol{y}_\perp|^2 \leq \boldsymbol{y}_\perp^T \Gamma_Q(t, \boldsymbol{y}_\perp) \leq (1-\alpha)\mu_N|\boldsymbol{y}_\perp|^2.$$

This bound offers two advantages over the previous one

- The values μ_2 and μ_N are exactly the second and least eigenvalues of L_G;
- The other two terms, $1-\beta$ and $1-\alpha$, only depend on the map ϕ, thus the communication topology does not pose constraints on them.

Clearly, a similar argument to reduce conservativeness of the bound can be carried on again if the topology is a slight perturbation of a "nominal" topology, for example if the elements of the adjacency matrix are a perturbed version of the elements of the nominal one.

It should be noticed, to conclude, that the steady assumption in this Section is that each element on the diagonal of $\Gamma_{0\perp}$ is able to stabilize the nominal system N_0. Otherwise, the linear part $H \star Q$ is not stable, and we cannot apply our argument.

4.5 Synchronization in case of LTI perturbations

In this section we address the problem of guaranteeing synchronization in case the perturbation operators Δ_k's can be modeled as single input single output linear time-invariant operators, thus admitting a representation in terms of transfer function.

We particularize our attention to the Higher Order Consensus Network with N agents

$$\begin{cases} \boldsymbol{y} = H\boldsymbol{u} \\ \boldsymbol{u} = \Gamma_0 \boldsymbol{y} + \boldsymbol{r} \end{cases} \tag{4.30}$$

where the (k,k)-th entry of H, which models the k-th agent, is of the form (in continuous time for example)

$$H_k(s) = N_0(s)(I + \Delta_k(s))$$

The matrix Γ_0 is, as in the previous Sections, the rescaled Laplacian of a primitive stochastic matrix P (apart from the sign), and is normal by Assumption 4.3.2. It is thus diagonalizable via a unitary matrix

$$U = \begin{bmatrix} \mathbf{1} & V \end{bmatrix}$$

and $U^*\Gamma_0 U = \Gamma_{0\perp} = \mathrm{diag}\,(0,\, \mu_2, \ldots, \mu_N)$. The matrix V will serve, as before, in order to perform the projection out from $\mathrm{span}\,\{\mathbf{1}\}$.

Let us define two sets which will be used in the main result. We denote by $\mathcal{N}\,[H_1, \ldots, H_m]\,(\omega)$ the 3d-Nyquist polytope of the set of subsystems $H_1, \ldots, H_m$

$$\mathcal{N}\,[H_1, \ldots, H_m]\,(\omega) \;:=\; \mathrm{co}\{\big(\mathrm{Re}H_k(j\omega),\, \mathrm{Im}H_k(j\omega),\, |H_k(j\omega)|^2\big) \,:\, k = 1, \ldots, m\}, \quad (4.31)$$

and the *instability region* defined by the spectrum of Γ_0 as

$$\Omega_e \;:=\; (0,\, 0,\, \mathbb{R}^+) + \mathrm{co}\left\{\left(\mathrm{Re}\frac{1}{\mu_i},\, \mathrm{Im}\frac{1}{\mu_i},\, \frac{1}{|\mu_i|^2}\right) \,:\, i = 2, \ldots, N\right\}. \quad (4.32)$$

We are now ready to state and prove our main result.

Theorem 4.5.1. *Consider the continuous time system*

$$\begin{cases} \boldsymbol{y} = H\boldsymbol{u} \\ \boldsymbol{u} = \Gamma_0 \boldsymbol{y} + \boldsymbol{r} \end{cases} \quad (4.33)$$

where $H(s) = \oplus_{k=1}^N H_k(s) \;:=\; \mathrm{diag}\,(H_k(s) : k = 1, \ldots, N)$. *Assume moreover that* $H_k(s)$ *can be decomposed as*

$$H_k(s) = N_0(s)(1 + \Delta_k(s)).$$

Set for convenience $H_0(s) = N_0(s)$, *and call* $\mathcal{P} \subset \mathcal{R}$ *the set of poles of* $N_0(s)$ *on the imaginary axis.*

Assume that

i) for every nonzero eigenvalue μ_i *of* Γ_0 *we have that* $W_0(s) = \frac{N_0(s)}{1 - N_0(s)\mu_i}$ *is a stable system and such that* $1 - N_0(s)\mu_i$ *is nonsingular on the imaginary axis;*

ii) the transfer functions $\Delta_k(s)$*'s are stable;*

iii) for any $\omega_m \in \mathcal{P}$ pole of $N_0(s)$ with multiplicity ν_m, it holds

$$\sum_{k=1}^{N} \frac{1}{1+\tau\Delta_k(j\omega_m)} \neq 0, \forall \tau \in [0,1]$$

iii) it holds

$$\mathcal{N}\left[H_0, \ldots, H_N\right](\omega) \cap \Omega_e = \emptyset, \forall\, \omega \in \mathbf{R} \cup \{\infty\} \setminus \mathcal{P}.$$

Then $\boldsymbol{y}(t)$ synchronizes to $\operatorname{span}\{\mathbf{1}\}$ *as $t \to \infty$ for any input $\boldsymbol{r}$ which satisfies $\boldsymbol{r}(t), \dot{\boldsymbol{r}}(t) \in \mathbf{L}_2[0, \infty)$.*

Proof. See the Section 4.5. □

Note that the input $\boldsymbol{r}$ represents disturbances and the effect of initial conditions. If we assume that H has a state space realization $\Sigma = (A, B, C, D)$, namely

$$\boldsymbol{y} = \boldsymbol{H}u \Leftrightarrow \begin{cases} \dot{\boldsymbol{x}} = A\boldsymbol{x} + B\boldsymbol{u} \\ \boldsymbol{y} = C\boldsymbol{x} + D\boldsymbol{u} \end{cases}$$

then provided that the pair (A, B) is controllable we can generate arbitrary initial conditions using $\boldsymbol{r}$. Indeed, for any $\boldsymbol{x}_0$, there exists an input signal, $\boldsymbol{u}^0$, defined over $-T_0 \leq t \leq 0$ such that the solution to $\dot{\boldsymbol{x}} = A\boldsymbol{x} + B\boldsymbol{u}$, $\boldsymbol{x}(-T_0) = 0$ is $\boldsymbol{x}(0) = \boldsymbol{x}_0$. Then the choice $\boldsymbol{r}(t) = u^0(t) - \Gamma(C\boldsymbol{x}^0(t) + D\boldsymbol{u}^0(t))$, for $-T_0 \leq t \leq 0$ and $\boldsymbol{r}(t) = 0$ for $t > 0$ gives the desired initial condition, i.e. the system (4.33) could then be interpreted as the state space system

$$\dot{\boldsymbol{x}} = (A + B(I - \Gamma_0 D)^{-1}\Gamma C)\boldsymbol{x}, \quad \boldsymbol{x}(0) = x_0.$$

The result in Theorem 4.5.1 has a discrete time counterpart. For example, if we for the sake of simplicity use a unitary sample period, the discrete time formulation follows by using the Tustin transform (see e.g. [132]), so that the Nyquist plots of $H_k(s)$ and of $H_k(z^{-1})$ are the same and one system is stable if, and only if, the other one is stable.

We thus have the following corollary.

Corollary 4.5.2. *Consider the discrete time system*

$$\begin{cases} \boldsymbol{y} = H\boldsymbol{u} \\ \boldsymbol{u} = \Gamma\boldsymbol{y} + \boldsymbol{r} \end{cases} \tag{4.34}$$

where $H(z^{-1}) = \operatorname{diag}\left(H_k(z^{-1}) : k = 1, \dots, N\right)$. *Assume moreover that* $H_k(z^{-1})$ *can be decomposed as*

$$H_k(z^{-1}) = N_0(z^{-1})(1 + \Delta_k(z^{-1}))$$

where $N_0(z^{-1})$ *is a "nominal plant". Set for convenience* $H_0(z^{-1}) = N_0(z^{-1})$, *and call* $\mathcal{P} \subset [0, 2\pi]$ *the set of values* ω_m *for which* $e^{j\omega_m}$ *is a pole of* $N_0(z^{-1})$ *on the unitary circle.*

Assume that

i) for every nonzero eigenvalue μ_i *of* Γ_0 *we have that* $W_0(z^{-1}) = \frac{N_0(z^{-1})}{1-N_0(z^{-1})\mu_i}$ *is a stable system and such that* $1 - N_0(z^{-1})\mu_i$ *is nonsingular on the unit circle.*

ii) the transfer functions $\Delta_k(z^{-1})$ *are stable;*

iii) for any $\omega_m \in \mathcal{P}$ *such that* $e^{j\omega_m}$ *is a pole of* $N_0(z^{-1})$ *with multiplicity* ν_m, *it holds*

$$\sum_{k=1}^{N} \frac{1}{1 + \tau\Delta_k(e^{j\omega_m})} \neq 0, \forall \tau \in [0, 1]$$

iv) it holds

$$\mathcal{N}\left[H_0, \dots, H_N\right](e^{j\omega}) \cap \Omega_e = \emptyset, \forall\, \omega \in [0, 2\pi] \setminus \mathcal{P}.$$

Then the signals $\boldsymbol{y}(t)$ *synchronize to* $\operatorname{span}\{\mathbf{1}\}$ *as* $t \to \infty$ *for any input* $\boldsymbol{r}$ *which satisfies* $\boldsymbol{r}(t) \in l_2[0, \infty)$.

The interpretation of Corollary 4.5.2) in state space domain is analogous to the continuous time case.

Derived simplified criteria

The roles of the H_k's and of the spectrum of Γ_0 in condition *iv*) in Theorem 4.5.1 can be somehow switched. In fact, once we define the so called Inverse Nyquist polytope

$$\check{\mathcal{N}}\left[H_0, \dots, H_N\right](\omega) = \operatorname{co}\left\{\left(\operatorname{Re}\frac{1}{H_k(j\omega)}, \operatorname{Im}\frac{1}{H_k(j\omega)}, \frac{1}{|H_k(j\omega)|^2|}\right) : k = 0, 1, \dots, N\right\} \tag{4.35}$$

and the corresponding instability region

$$\check{\Omega}_e := \operatorname{co}\left\{\left(\operatorname{Re}\mu_i, \operatorname{Im}\mu_i, |\mu_i|^2\right) : i = 2, \dots, N\right\}. \tag{4.36}$$

it is possible to shown, as explained in [122] and making use of the fact that $\mu_1 = 0$, that *iii*) in Theorem 4.5.1 is equivalent to

iv') it holds

$$\check{\mathcal{N}}\left[H_0,\ldots,H_N\right](\omega)\cap\check{\Omega}_e=\emptyset,\forall\,\omega\in\mathbf{R}\cup\{\infty\}\setminus\mathcal{P}.$$

These criteria can sometimes be hard to visualize since they involve three dimensions. A way to simplify the drawing of the Nyquist polytope and of the instability region, it is possible to consider the projection of these sets to the complex plane. Clearly, the obtained "$2-D$" conditions are in general more conservative then conditions iv) or iv') above.

Concerning the first criterion, instead of condition iv) we have to impose that the sets

$$\mathcal{N}_{2d}\left[H_0,\ldots,H_N\right](\omega)\;:=\;\mathrm{co}\{H_0(j\omega),\ldots,H_N(j\omega)\} \tag{4.37}$$

and

$$\Omega_{2de}\;:=\;\mathrm{co}\left\{\frac{1}{\mu_2},\ldots,\frac{1}{\mu_N}\right\} \tag{4.38}$$

do not intersect.

For the Inverse criterion, the corresponding sets are

$$\check{\mathcal{N}}_{2d}\left[H_0,\ldots,H_N\right](\omega)\;:=\;\mathrm{co}\left\{\frac{1}{H_0(j\omega)},\ldots,\frac{1}{H_N(j\omega)}\right\} \tag{4.39}$$

and

$$\check{\Omega}_{2de}\;:=\;\mathrm{co}\{\mu_2,\ldots,\mu_N\}. \tag{4.40}$$

Examples

In this section we are going to apply Theorem 4.5.1 to the cases of unstable systems synchronization and synchronization of oscillators. A more detailed example is given in Chapter 5 and concerns clocks synchronization.

Synchronization of unstable subsystems

In this example we show that if the interconnection network is well designed, synchronization can take place even if the subsystems are not stable. Consider in fact the situation in which

$$H_k(s)=\frac{1+\Delta_k(s)}{s-\tau}$$

where $\tau>0$ and $\Delta_k(s)$ are stable filters. Assume $\mathrm{re}\,\mu_i<-\eta$ for every nonzero eigenvalue μ_i of Γ_0. It is easy to see that if $\tau<\eta$ then assumption i) is satisfied. If we consider stable and "small" $\Delta_k(s)$, such that ii), iii) and iv) in Theorem 4.5.1 are satisfied, then

we have the synchronization to the unstable mode $e^{\tau t}$.

To give a numerical example, assume we have $N = 11$ agents, $\tau = 0.3$, $N_0(s) = \frac{1}{s-\tau}$ and $N_k(s) = \frac{s+\varepsilon_k}{(s+2\nu_k)(s-\tau)}$, where ε_k, $\nu_k \in \mathcal{U}[0, 1]$, where $\mathcal{U}[l, u]$ means uniformly taken in $[l, u]$. The matrix Γ_0 is $\Gamma_0 = -I_N + 0.2 * (\mathcal{C}_N + \mathcal{C}_N^{-1}) + 0.35 * \mathcal{C}_N^5 + 0.25 * \mathcal{C}_N^6$, where $\mathcal{C}_N$ is the Cayley matrix generated by the row $\boldsymbol{g} = \begin{bmatrix} 0 & 1 & 0 & \dots & 0 \end{bmatrix}$. In Fig. 4.9, respectively on the left and on the right panel, are shown a possible trajectory of the subsystems (initial conditions are uniformly taken in $[0, 100]$) and the $2 - D$ Nyquist criterion (see Eq. 4.37 and Eq. 4.38).

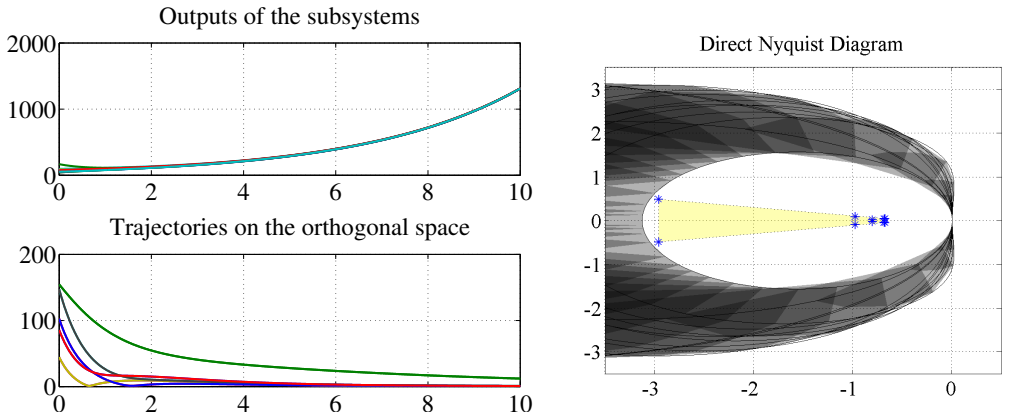

Figure 4.9: Unstable synchronization. Left panel: trajectories of the output of the systems for the given network. Right panel: Direct 2d Nyquist criterion for the system. The light shaded region is the convex hull of the inverse of the eigenvalues of Γ_0, the dark shaded region is the Nyquist polytope.

A counterexample: the synchronization of different linear oscillators

In this example we will show that assumption $ii)$ of the theorems is necessary. Assume our subsystems to be composed by a nominal plant of some type, $N_0(s)$, to which is added a perturbation with two complex conjugate purely imaginary poles:

$$H_k(s) = N_0(s) + \frac{P_k(s)}{s^2 + \omega_k^2}.$$

In this case, if $N_0(s)$ and the $H_k(s)$ are suitably chosen, it is not difficult to satisfy assumptions $i)$ and $iv)$. The problem here is that assumption $ii)$ surely cannot be satisfied, since

$$\Delta_k(s) = \frac{P_k(s)}{(s^2 + \omega_k^2)N_0(s)}$$

is never stable having the two neutrally stable poles $\pm j\omega_k^2$. Hence, the theorem cannot

be applied and in fact, in general we do not have synchronization.

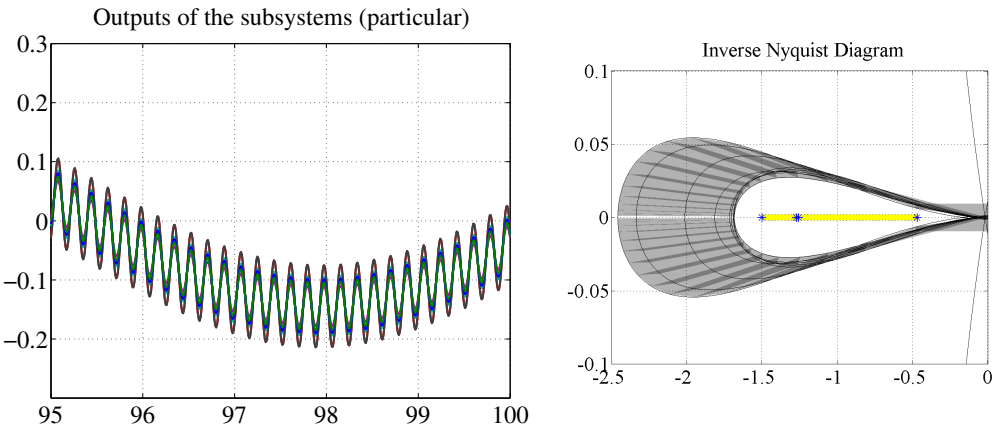

Figure 4.10: Synchronization of oscillators: bad case. Left panel: Zoom showing the "weak" synchronization. The low frequency carrier corresponds to the sinusoid at frequency 0.1 Hz. Right panel: Inverse 2d Nyquist criterion for the system. The light shaded region is the convex hull of the eigenvalues of Γ_0, the dark shaded region is the inverse Nyquist polytope. Zoom showing that the nonzero eigenvectors of Γ_0 respect the assumptions.

To give a numerical example, let us consider the case in which $N = 9$ and

$$N_0(s) = \frac{s+1}{s^2 + (2\pi 0.1)^2}$$

and

$$N_k(s) = -\frac{1}{5}\frac{(s-1)((2+\varepsilon_k)s + 1 + \nu_k)}{s^2 + \omega_k^2}$$

where ε_k, $\nu_k \in \mathcal{U}[0,\, 1]$ and $\omega_k \in 10\pi + 2\pi\mathcal{U}[0,\, 1]$. The interconnection matrix is $\Gamma_0 = -I_N + 0.2(\mathcal{C}_N + \mathcal{C}_N^{-1}) + 0.3(\mathcal{C}_N^4 + \mathcal{C}_N^5)$ ($\mathcal{C}_N$ as before).

Because the subsystems do not satisfy the assumptions, the system does not synchronize. Nonetheless, as we can see in the left panel of Fig. 4.10, some sort of "weak" synchronization is approached. This is related to the fact that the subsystems actually satisfy the Nyquist Criterion, as can be seen in the right panel of Fig. 4.10.

As a second example, consider the case in which

$$H_k(s) = -\frac{1}{5}\frac{(s-1)(2s+1)}{s^2 + \omega_0^2} - \frac{1}{5}\frac{(s-1)(\varepsilon_k s + \nu_k)}{s^2 + \omega_0^2}$$

where ε_k, $\nu_k \in \mathcal{U}[0,\, 1]$ and $\omega_0 = 2\pi$, thus the nominal plant is in this case $N_0(s) = \frac{1}{s^2+\omega_0^2}$. The interconnection matrix is the same as in the previous example. The assumptions are all satisfied, and in fact, as we can see in Fig. 4.11, the subsystems synchronize.

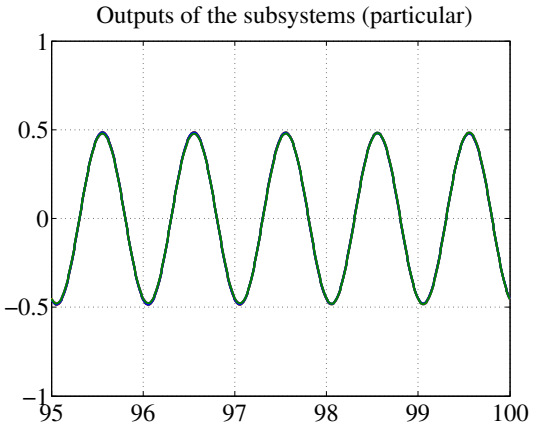

Figure 4.11: Synchronization of oscillators: good case. Zoom showing the synchronization.

Proof of Theorem 4.5.1

In order to prove the Theorem we need the following two results, taken from [122].

Assume $\Pi \in S_{\mathbf{C}}^{2\times 2}$, the set of 2×2 complex valued hermitian matrices: this set is a Hilbert space if we endow it with the scalar product $\langle \Pi_1, \Pi_2 \rangle = \mathrm{Tr}(\Pi_1 \Pi_2)$. Consider now a convex polytope $\Lambda \subset \mathbf{C}$, and define the convex cone Π_Λ as

$$\begin{aligned} \Pi_\Lambda := \{ & \Pi \in S_{\mathbf{C}}^{2\times 2} : \Pi_{22} \leq 0; \\ & |\lambda|^2 \Pi_{11} + 2\mathrm{Re}\lambda \Pi_{12}^* + \Pi_{22} \leq 0, \, \forall \, \lambda \in \Lambda \}. \end{aligned} \tag{4.41}$$

Finally, the polar cone of $\mathcal{C}$ in the Hilbert space $\mathcal{H}$ is defined as

$$\mathcal{C}^{\ominus} := \{ y \in \mathcal{H} : \, \langle y, x \rangle \leq 0, \, \forall \, x \in \mathcal{H} \} \tag{4.42}$$

we obtain the following characterization for the polar cone $\Pi_\Lambda^{\ominus}$ of Π_Λ.

Lemma 4.5.3. *Consider Π_Λ as defined in Eq. 4.41 and suppose $\Lambda = \mathrm{co}\,\{\mu_1, \ldots, \mu_n\}$. Then the polar cone of Π_Λ is characterized as follows*

$$\Pi_\Lambda^{\ominus} = \mathrm{cone}\,\{W_k : \, k = 1, \ldots, n+1\}$$

where $W_k = v_k v_k^*$ for $k = 1, \ldots, n+1$ and

$$v_k = \begin{bmatrix} \mu_k \\ 1 \end{bmatrix}, \, k = 1, \ldots, n, \, v_{n+1} = \begin{bmatrix} 0 \\ 1 \end{bmatrix}.$$

The next proposition deals with both these multipliers Π and the structure of our system. Let H_k be the transfer function of the k-th subsystem, and assume $H_k \in \mathcal{A}$ for $k = 1, \dots, n$, with $\mathcal{A}$ be the set of Laplace transforms of functions of the type $h(t) = h_c(t)\theta(t) + h_0\delta(t)$, $\theta(t)$ be the step function, $h_c(t) \in \mathbf{L}_1[0, \infty)$ and $h_0 \in \mathbf{R}$.

Proposition 4.5.4. *Let $H_k \in \mathcal{A}$ for $k = 1, \dots, n$, and $\Pi_\Lambda \subset S^{2\times 2}_{\mathbf{C}}$ be a closed (in the topology defined by the Frobenius norm) convex cone. The either of the following two statements holds*

a) for all $\omega \in \mathbf{R} \cup \{\infty\}$ there exists $\Pi \in \Pi_\Lambda$ such that

$$\Pi_{11} + 2\mathrm{Re}\,\Pi_{12}H_k(j\omega) + \Pi_{22}|H_k(j\omega)|^2 > 0,$$

for all $k = 1, \dots, n$,

b) There exists an $\omega \in \mathbf{R} \cup \{\infty\}$ and a nonzero tuple $Z = (z_1, \dots, z_n) \in \mathbf{C}^n$ with $z_k \leq 0$ such that

$$\sum_{k=1}^{n} z_k \begin{bmatrix} 1 \\ H_k(j\omega) \end{bmatrix} \begin{bmatrix} 1 \\ H_k(j\omega) \end{bmatrix}^* \in \Pi_\Lambda^{\ominus}.$$

We can now prove Theorem 4.5.1

Proof of Theorem 4.5.1. The idea of the proof is, as it is known, to project the trajectory to the space orthogonal to span $\{\mathbf{1}\}$, and to prove that the obtained system is $\mathbf{L}_2$-stable.

First of all, we define

$$\boldsymbol{y}_\perp(t) = V^*\boldsymbol{y}(t)$$

It can be checked that the system in the new variables obeys the following equation

$$\begin{aligned} \boldsymbol{y}_\perp &= V^*H(V\,\mathrm{diag}\,(\mu_2, \dots, \mu_N)\,\boldsymbol{y}_\perp + \boldsymbol{r}) \\ &= H_\perp\Gamma_{0\perp}\boldsymbol{y}_\perp + V^*H\boldsymbol{r} \end{aligned} \tag{4.43}$$

once we define

$$\begin{aligned} H_\perp(s) &= V^*H(s)V \\ \Gamma_{0\perp} &= \mathrm{diag}\,(\mu_2, \dots, \mu_N)\,. \end{aligned}$$

We will prove that the closed loop transfer function is stable. This in turn implies that $\boldsymbol{y}_\perp = (I - H_\perp\Gamma_{0\perp})^{-1}V^*H\boldsymbol{r} \in \mathbf{L}_2[0, \infty)$ and hence $\boldsymbol{y}_\perp$ converges continuously by the assumption on $\boldsymbol{r}$. This in turn implies that $\boldsymbol{y}(t) \to \ker V^* = \mathrm{span}\,\{\mathbf{1}\}$

Next we follow the proof in [122] to prove the claimed stability. The condition iv) implies that, for any $\omega \in \mathbf{R} \cup \infty$ and for any nonzero $(z_0, \ldots, z_n)$ with $z_k \geq 0$, we have

$$\sum_{k=0}^{n} z_k \begin{bmatrix} 1 \\ H_k \end{bmatrix} \begin{bmatrix} 1 \\ H_k \end{bmatrix}^* \notin \Pi^{\ominus}_{\Lambda,\, e} \tag{4.44}$$

where $\Pi^{\ominus}_{\Lambda,\, e} = \text{cone}\{v_i v_i^* : i = 2, \ldots, N\}$, where

$$v_i = \begin{bmatrix} \mu_i \\ 1 \end{bmatrix}, \; i = 2, \ldots, N, \text{ and } v_{N+1} = \begin{bmatrix} 0 \\ 1 \end{bmatrix}.$$

Let $\omega \in \mathbb{R} \cup \infty \setminus \mathcal{P}$ be arbitrary. It follows from lemma 4.5.3 and proposition 4.5.4 that Eq. 4.44 implies the existence of multipliers $\Pi \in \mathcal{S}^{2\times 2}_{\mathbf{C}}$ such that $\Pi_{22} \leq 0$ such that the following two conditions hold:

1: For $i = 2, \ldots, N$,

$$|\mu_i|^2 \Pi_{11} + \overline{\mu}_i \Pi_{12} + \mu_i \Pi_{12}^* + \Pi_{22} \leq 0 \tag{4.45}$$

which immediately yields the matrix form constraint

$$\Gamma_{0\perp}^* \Pi_{11} \Gamma_{0\perp} + \Gamma_{0\perp}^* \Pi_{12} + \Pi_{12}^* \Gamma_{0\perp} + \Pi_{22} I_{n-1} \leq 0. \tag{4.46}$$

2. For $k = 1, \ldots, N$, (from now we supress the dependence on ω, i.e. $H_k = H_k(j\omega)$)

$$H_k^* \Pi_{11} H_k + H_k^* \Pi_{12} + \Pi_{12}^* H_k + \Pi_{22} > 0. \tag{4.47}$$

We also want to find a matrix form for this second constraint. Define the parametrized dynamics, for $\tau \in [0,\, 1]$,

$$\tilde{H}_{[\tau]} = N_{\alpha 0} \left(I_{n-1} + \tau \oplus_{k=1}^{N} \Delta_k \right)$$

Notice that if $\tau = 0$ we have the nominal system, if $\tau = 1$ we obtain the perturbed ones. Since $\Pi_{22} \leq 0$, the left-hand side of Eq. 4.47 is a concave function of the H_k, $k = 1, \ldots, N$. This implies that, for $\tau \in [0,\, 1]$,

$$\Pi_{11} I_{N-1} + \Pi_{12} \tilde{H}_{[\tau]} + \tilde{H}_{[\tau]}^* \Pi_{12}^* + \tilde{H}_{[\tau]}^* \Pi_{22} \tilde{H}_{[\tau]} > 0 \tag{4.48}$$

Let us now define $H_{[\tau]\perp}(s) = V^* \tilde{H}_{[\tau]} V$: if $\tau = 1$, this is exactly the $H_\perp(s)$ which appears

in the system whose stability we want to prove. By definition, we have

$$\begin{aligned}&\Pi_{11}I_{N-1} + \Pi_{12}H_{[\tau]\perp} + H^*_{[\tau]\perp}\Pi^*_{12} + H^*_{[\tau]\perp}\Pi_{22}H_{[\tau]\perp}\\ &= V^*(\Pi_{11}I_{n-1} + \Pi_{12}\tilde{H}_{[\tau]} + \tilde{H}^*_{[\tau]}\Pi^*_{12} + \tilde{H}^*_{[\tau]}\Pi_{22}\tilde{H}_{[\tau]})V - V\tilde{H}^*_{[\tau]}\mathbf{1}\Pi_{22}\mathbf{1}^T\tilde{H}_{[\tau]}V\end{aligned}$$

where we used the fact that $VV^* = I_{N-1} - \frac{1}{N}\mathbf{1}\mathbf{1}^T$. Using Eq. 4.48 and $\Pi_{22} \leq 0$, we conclude that the previous expression is positive definite. So, we have

$$\Pi_{11}I_{N-1} + \Pi_{12}H_{[\tau]\perp} + H^*_{[\tau]\perp}\Pi^*_{12} + H^*_{[\tau]\perp}\Pi_{22}H_{[\tau]\perp} > 0 \tag{4.49}$$

The quadratic constraints Eq. 4.46 and Eq. 4.49 can then be used to show that there exists $\varepsilon > 0$ such that, for $\tau \in [0,\, 1]$,

$$\underline{\sigma}_{\min}(I - H_{[\tau]\perp}(j\omega)\Gamma_{0\perp}) \geq \varepsilon,\, \forall\, \omega \in \mathbf{R} \cup \infty \setminus \mathcal{P}. \tag{4.50}$$

Let us now define the following matrix transfer function:

$$\begin{aligned}G_V(s) &= (H_0(s)^{-1}I_{N-1} - \Gamma_{0\perp})^{-1}\\ &= H_0(s)(I_{N-1} - H_0(s)\Gamma_{0\perp})^{-1}\end{aligned} \tag{4.51}$$

which is a diagonal matrix whose $(i-1,\, i-1)$ element is $\frac{H_0(s)}{1-H_0(s)\mu_i}$ for $i = 2, \ldots, N$. By assumption i), $G_V(s)$ is stable.

Once we define $\Delta_\perp(s) = V^*\Delta(s)V$, we can perform the decomposition

$$\begin{aligned}I_{N-1} - H_{[\tau]\perp}\Gamma_{0\perp} &= I_{N-1} - N_0\Gamma_{0\perp} - \tau N_0(s)\Delta_\perp(s)\Gamma_{0\perp}\\ &= N_0\left[N_0^{-1}I_{N-1} - \Gamma_{0\perp} - \tau\Delta_\perp(s)\Gamma_{0\perp}\right]\\ &= N_0G_V^{-1}\left[I_{N-1} - \tau G_V\Delta_\perp(s)\Gamma_{0\perp}\right].\end{aligned}$$

Notice now that $N_0G_V^{-1} = I - N_0\Gamma_{0\perp}$, which by assumption i) satisfies $\sigma_{\min}(N_0G_V^{-1}(j\omega)) \geq \epsilon$, for all $\omega \in \mathbf{R} \cup \infty$ where $\epsilon > 0$ is some positive number. From Eq. 4.50 we can therefore conclude the existence of $\tilde{\varepsilon} > 0$ such that

$$\underline{\sigma}_{\min}(I_{N-1} - \tau G_V\check{\Delta}\Gamma_{0\perp})\ geq\tilde{\varepsilon},\, \forall\, \omega \in \mathbf{R} \cup \infty \setminus \mathcal{P}. \tag{4.52}$$

We can now introduce the following matrix transfer function:

$$G_{[\tau]}(s) = (I_{N-1} - \tau G_V\Delta_\perp(s)\Gamma_{0\perp})^{-1}\, G_VV^*(I_{N-1} + \tau\Delta(s), \tag{4.53}$$

where we see that $G_{[0]} = G_V V^*$ and $G_{[1]} = (I_{N-1} - H_\perp \Gamma_{0\perp})^{-1} V^* H$, which is the closed loop transfer function from $\boldsymbol{r}$ to $\boldsymbol{y}_\perp$.

We will finally show that this transfer function is stable, i.e. it is analytic in the right half plane. For this purpose, we introduce

$$\psi(s,\tau) = \det(I_{N-1} - \tau G_V(s)\Delta_\perp(s)\Gamma_{0\perp})$$

By assumption *i*) we know that $\psi(s,0)$ is analytic in the right half plane. Moreover, by Eq. 4.52 it follows that $\psi(j\omega,\tau) \neq 0$ for all $\omega \in \mathbf{R} \cup \infty \setminus \mathcal{P}$ and $\tau \in [0,1]$. Condition *iii*) implies that Eq. 4.52 holds by continuity for $\omega \in \setminus\mathcal{P}$ too. Assume in fact $N_0(s) = \frac{1}{d_m(s)}\tilde{N}_0(s)$ where $d_m(s) = (s - j\omega_m)^{\nu_m}$. It is easy to obtain

$$\lim_{\omega\to\omega_m} (I_{N-1} - \tau G_V \Delta_\perp \Gamma_\perp) = \Gamma_\perp^{-1} V^* (I_N + \tau\Delta(s)) V \Gamma_\perp.$$

Now Eq. 4.52 holds for $\omega_m \in \mathcal{P}$ and for any $\tau \in [0,\ 1]$ if

$$\Gamma_\perp^{-1} V^* (I_N + \tau\Delta(s)) V \Gamma_\perp \boldsymbol{x} = 0$$

implies $\boldsymbol{x} = 0$. In fact, since $\Gamma_\perp$ is invertible and V is full column rank, the only possibility is

$$(I_N + \tau\Delta(s)) V \tilde{\boldsymbol{x}} = \beta \mathbf{1}$$

where $\tilde{\boldsymbol{x}} = V\boldsymbol{x}$ and $\beta \in \mathbb{R}$. Hence

$$V\tilde{\boldsymbol{x}} = \beta (I_N + \tau\Delta(s))^{-1} \mathbf{1}$$

and multiplying on the left by $\mathbf{1}^T$

$$\beta \mathbf{1}^T (I_N + \tau\Delta(s))^{-1} \mathbf{1} = 0$$

Now by *iii*) $\mathbf{1}^T (I_N + \tau\Delta(s))^{-1} \mathbf{1} \neq 0, \forall\tau$, and thus it must be $\beta = 0$ implying $\tilde{\boldsymbol{x}} = 0$ and thus actually $\boldsymbol{x} = 0$.

It follows now by the zero exclusion principle that $\psi(j\omega, 1)$ is analytic in the right half plane, see e.g. Lemma A.1.18 in [17]. By assumption *ii*) it also holds that $G_{[1]}$ is analytic in the right half plane.

This concludes the proof. □

5

Applications of Synchronization Algorithms

5.1 Introduction

The fifth Chapter of this dissertation is devoted to Applications of synchronization algorithms. The first application is clock synchronization, which is among the most studied Higher Order Consensus problems in the literature. A clock will be basically modeled as a double integrator and the results in Chapter 4 will be applied in order to study robust synchronization with respect to uncertainties and non–idealities. The second application is cameras calibration, which is seen as an optimization problem on the manifold $\mathcal{S}_1$, and then recast as consensus on $\mathcal{S}_1$, a difficult problem due to the presence of multiple local minima. We address this problem exploiting cycles on the communication graph in order to rewrite consensus as if it was on the Euclidean space, where it is known how to solve it. This goes along lines somehow different from what has been done in the rest of the dissertation, and yet shows the difficulty of the simple consensus problem on non–Euclidean sets.

5.2 Synchronization of Networks of Clocks

The first application for our criteria is in the field of clock synchronization. This is a topic which has attracted much attention due to the fact that in many practical applications

agents need to perform their actions in a restricted time interval in order to reduce energy consumption, and thus the necessity of a common time. The problem has been addressed via hierarchical algorithms such as leader election in a spanning tree ([32, 133]), or clustering of the network ([134]). Despite the effectiveness of such algorithms, they suffer from bad scalability characteristics and especially from failure of nodes. In fact, if one node fails, the whole subtree which has that node as root gets disconnected from the rest of the network. Full distributed algorithms have been proposed ([135, 136]). Since all the agents in such algorithms act in exactly the same way, there is no need for a leader and since the network remains connected it does not suffer from node failures. We proceed along this direction. The model we consider has been originally proposed in [137], where clocks are modeled as integrators with constant and identical disturbances. This simple and ideal case has been modified in [9, 138], where each clock is modeled as a double integrator whose behavior is subject to uncertainty, and where there is no leader. This is the model we use in this Section.

A mathematical model for the clocks

In this paragraph we propose a simplified version of the clock model in [138]. A network of clocks is modeled, as usual, trough the communication graph $\mathcal{G} = (\mathcal{V}, \mathcal{E})$ in which $\mathcal{V} = \{1, \dots, N\}$ is the set of clocks. We imagine that each clock, say the k-th, possesses a counter and an oscillator which produces periodically some event, and for each event the counter is incremented by 1. The value $s_k(t)$ is the value of the counter at time t, and the reading of the k-th clock is produced according to the rule

$$y_k(t) = y_k(t_0) + z_k(t)(s_k(t) - s_k(t_0))$$

where $y_k(t_0)$ is called the initial offset. The role of $z_k(t)$ can be explained as follows. Assume that the oscillator of the k-th clock produces events with period δ_k, which is called its skew. If let alone, its time reading would be

$$y_k(t) = y_k(t_0) + z_k(t)\delta_k(t - t_0)$$

namely a ramp–shaped function whose initial condition is the initial offset $y_k(t_0)$ and whose slope is given by $z_k(t)\delta_k$. The variable $z_k(t)$ is thus an estimate of the inverse of the skew. Notice that if a clock does not receive any information from other agents, it has no incentive to modify $z_k(t)$. In particular, we can imagine that a nominal value δ_{nom} is given for the skews, so that a good initialization for $z_k(t)$ is $1/\delta_{\text{nom}}$.

Consider now a network of clocks with different initial offsets and skews which can

exchange the time readings $y_k(t)$'s along the edges of a communication graph $\mathcal{G} = (\mathcal{V}, \mathcal{E})$. In analogy with consensus, the goal is to design a way to progressively tune the initial offsets $y_k(t_0)$'s and the estimate of the skews $z_k(t)$'s on the basis of how different are the time readings, in order to synchronize the clocks.

In order to carry on our analysis, first of all we further simplify the model. In particular, we assume that the clock readings are exchanged periodically with period T, so that

$$s_k(t) - s_k(t-1) = T \tag{5.1}$$

for any k and t. This is clearly totally unrealistic since is requires synchronization of the clocks, which is the goal of the algorithm. The rationale is that if T is small, then the idealized model should behave in a similar way to the original system. A more detailed analysis is given in [9].

Making use of the assumption in Eq. 5.1, we model thus each clock as a 2–dimensional system which evolves according to the following rule

$$\begin{cases} x_k(t+1) = \begin{bmatrix} 1 & T\delta_k \\ 0 & 1 \end{bmatrix} x_k(t) + \begin{bmatrix} f_1 \\ f_2 \end{bmatrix} u_k(t) \\ y_k(t) = \begin{bmatrix} 1 & 0 \end{bmatrix} x_k(t) \end{cases} \tag{5.2}$$

A robust synchronization result

We choose the simplest way to produce the control, namely a simple linear combination of the clock readings

$$u_i(t) = \sum_{j \in \mathcal{V}} \gamma_{ij} y_j(t)$$

thus $\boldsymbol{u}(t) = \Gamma_0 \boldsymbol{y}(t)$. We assume that Γ_0 respects Assumption 4.3.2, namely it is normal and its kernel is given by span $\{\mathbf{1}\}$.

The whole system can be written in the form of Eq. 4.33 as

$$\begin{cases} \boldsymbol{y} = H\boldsymbol{u} \\ \boldsymbol{u} = \Gamma_0 \boldsymbol{y} + \boldsymbol{r} \end{cases} \tag{5.3}$$

where $\boldsymbol{r}$ is an ℓ_2 signal used to set the initial conditions. The matrix of transfer functions $H(z^{-1})$ is diagonal and its (k, k)-th entry is given by

$$H_k(z^{-1}) = \frac{z^{-2}(T\delta_k f_2 - f_1) + f_1 z^{-1}}{(1 - z^{-1})^2}$$

namely in this model the clocks are double integrators with one zero dependent on the skew.

We assume that a nominal value is given for the skews of the clocks, so that

$$\delta_k = \delta_{\text{nom}} + \tilde{\delta}_k, \forall k \in \mathcal{V}$$

With this notation, we have

$$\begin{aligned} H_k(z^{-1}) &= \frac{z^{-2}(\delta_{\text{nom}} T f_2 - f_1) + f_1 z^{-1}}{(1-z^{-1})^2} + \frac{\tilde{\delta}_k T f_2 z^{-2}}{(1-z^{-1})^2} \\ &= H_0(z^{-1})(1 + \Delta_k(z^{-1})) \end{aligned}$$

where

$$\begin{aligned} H_0(z^{-1}) &= \frac{z^{-2}(\delta_{\text{nom}} T f_2 - f_1) + f_1 z^{-1}}{(1-z^{-1})^2} = \frac{(\delta_{\text{nom}} T f_2 - f_1) + f_1 z}{(z-1)^2} \\ \Delta_k(z^{-1}) &= \frac{\tilde{\delta}_k T f_2 z^{-2}}{z^{-2}(\delta_{\text{nom}} T f_2 - f_1) + f_1 z^{-1}} \end{aligned}$$

Notice that $N_0(z^{-1})$ can be interpreted as the nominal system, whereas the perturbation operator $\Delta_k(z^{-1})$ constitutes a multiplicative perturbation which well fits within our framework.

The synchronization criterion is based on the following result, which is immediately implied by the derived simplified direct criterion presented in Section 4.5 for the case under analysis.

Lemma 5.2.1. *Consider the system in Eq. 5.3 where H and Γ_0 as above. Denote by $\mu_0, \lambda_1, \ldots, \mu_{N-1}$ the eigenvalues of Γ_0, with $\mu_0 = 0$. The system synchronizes to* $\text{span}\{\mathbf{1}\}$ *if*

1. *stability of nominal system: the feedback system $[H_0, \mu_i]$ is stable for any $\mu_i \neq 0$*
2. *conditions on the unstable poles: the transfer functions $\Delta_k(z^{-1})$ are stable for any $k \in \mathcal{V}$*
3. *condition at the pole: it holds*

$$\sum_{i=1}^{n} \frac{1}{\delta_{\text{nom}} + \tau \tilde{\delta}_k} > 0, \forall \tau \in [0, 1]$$

4. *Nyquist-criterion: it holds the direct projected Nyquist-like criterion, namely the*

convex hull of the inverse of the spectrum of Γ_0, $\operatorname{co}\left\{\frac{1}{\mu_2}, \ldots, \frac{1}{\mu_{N-1}}\right\}$, *and the projected Nyquist polytope,* $\operatorname{co}\{H_0, H_1, \ldots, H_N\}$ *are disjoint.*

Based on this, we can state and prove the follow synchronization criterion. We restrict for simplicity to the case in which the communication graph $\mathcal{G}$ is undirected and Γ_0 is the Laplacian of a symmetric primitive stochastic matrix P associated with $\mathcal{G}$.

Theorem 5.2.2. *Consider a clock network with* N *clocks modeled by the undirected communication graph* $\mathcal{G} = (\mathcal{V}, \mathcal{E})$. *Assume that each clock has a skew* $\delta_k = \delta_{\text{nom}} + \tilde{\delta}_k > 0$, *with* $\delta_{\text{nom}} > 0$. *Assume the* k*-th clock is modeled as*

$$\begin{cases} x_k(t+1) = \begin{bmatrix} 1 & T\delta_k \\ 0 & 1 \end{bmatrix} x_k(t) + \begin{bmatrix} f_1 \\ f_2 \end{bmatrix} u_k(t) \\ y_k(t) = \begin{bmatrix} 1 & 0 \end{bmatrix} x_k(t) \\ u_k(t) = \sum_{j \in \mathcal{N}_k} \gamma_{kj} y_j(t) \end{cases} \tag{5.4}$$

and that the matrix $\Gamma_0 = [\gamma_{kj}] \in \mathbb{R}^{N \times N}$ *is symmetric and such that* $\Gamma_0 = I - P$ *where* P *is a primitive stochastic matrix.*

Then the network synchronizes to $\mathbf{1}$ *if*

$$\begin{cases} f_1 > 0,\ f_2 > 0 \\ 0 < \frac{f_2}{f_1} < \frac{1}{\delta_{\text{nom}} T} \\ 0 < \delta_k < \frac{f_1}{T f_2},\ \forall\, k = 1, \ldots, N \\ \frac{4}{\delta_k T f_2 - 2 f_1} < -2,\ \forall\, i = 0, 1, \ldots, N \end{cases} \tag{5.5}$$

Proof. We want to show that the stated conditions are sufficient to satisfy all the constraints in Lemma 5.2.1. Notice that by assumption $\delta_k > 0$, $\forall\, k$.

- Condition on the unstable poles: in order it to be satisfied, each transfer function

$$\frac{\tilde{\delta}_k T f_2 z^{-2}}{z^{-2}(\delta_{\text{nom}} T f_2 - f_1) + f_1 z^{-1}} = \frac{\tilde{\delta}_k T f_2}{(\delta_{\text{nom}} T f_2 - f_1) + f_1 z}$$

must be stable, namely it must hold

$$\left|\frac{f_1 - \delta_{\text{nom}} T f_2}{f_1}\right| < 1 \Rightarrow \left|1 - \frac{\delta_{\text{nom}} T f_2}{f_1}\right| < 1$$

or equivalently

$$0 < \frac{f_2}{f_1} < \frac{2}{\delta_{\text{nom}} T} \tag{5.6}$$

which is implied by the second in Eq. 5.5.

- Condition on the nominal system: the transfer function of the feedback is

$$[H_0,\, \mu_i] = \frac{H_0}{1-\mu_i H_0} = \frac{(\delta_{\text{nom}} T f_2 - f_1) + f_1 z}{z^2 + z(-2-\mu_i f_1) + 1 - \mu_i(\delta_{\text{nom}} T f_2 - f_1)}.$$

  By applying the bilinear transformation $z = \frac{1+s}{1-s}$ to the denominator we obtain

$$\frac{s^2(4-\mu_i(\delta_{\text{nom}} T f_2 - 2f_1)) + 2\mu_i(\delta_{\text{nom}} T f_2 - f_1)s - \mu_i \delta_{\text{nom}} T f_2}{(1-s)^2}$$

  and in order the zeros to have negative real part we need all the signs of the coefficients to be positive. From the last one we obtain $f_2 > 0$, since $-\mu_i > 0$. This implies that $f_1 > 0$ as well[1].
  We also need $\delta_{\text{nom}} T f_2 - f_1 < 0$, which implies $\frac{f_2}{f_1} < \frac{1}{\delta_{\text{nom}} T}$, which is the third of Eq. 5.5. Finally, $4 - \mu_i(\delta_{\text{nom}} T f_2 - 2f_1) > 0$ implies, by $\delta_{\text{nom}} T f_2 - 2f_1 < 0$, $\frac{4}{\delta_{\text{nom}} T f_2 - 2f_1} < \mu_i$.

- Condition at the pole: by imposing $\delta_k > 0, \forall\, k$ the condition is immediately satisfied.

- Nyquist-like condition: take the generic $H_k(\omega) := H_k(e^{-j\omega})$, and call $x := x(\omega) = \text{Re}H_k(\omega)$ and $y := y(\omega) = \text{Im}H_k(\omega)$.

  It is not difficult to show that

$$\begin{cases} x &= \frac{f_1 + (\delta_k T f_2 - f_1)\cos\omega}{2(\cos\omega - 1)} \\ y &= \frac{(\delta_k T f_2 - f_1)\sin\omega}{2(1-\cos\omega)} \end{cases}.$$

  We consider the case $\omega \in [0,\, \pi]$, being $\omega \in [-\pi,\, 0]$ totally analogous. We obtain, since $\delta_k > 0$,

$$y = \frac{\delta_k T f_2 - f_1}{2} \frac{\sqrt{\delta_k T f_2}}{\delta_k T f_2} \text{sgn}(2x - \delta_k T f_2 + f_1) \sqrt{\delta_k T f_2 - 2f_1 - 4x}$$

  where $\text{sgn}(x)$ is the sign of x. Since $x < \frac{\delta_k T f_2 - 2f_1}{4}$, we have

$$2x - \delta_k T f_2 + f_1 < -\frac{\delta_k T f_2}{2} < 0.$$

[1] Otherwise, if all the eigenvalues of Γ_0 were positive, we could just switch the signs of f_1 and f_2.

Thus, again using $f_2 > 0$, we have

$$y = \frac{\delta_k T f_2 - f_1}{2\sqrt{\delta_k T f_2}} \sqrt{\delta_k T f_2 - 2f_1 - 4x}.$$

We need to ensure that the convex hull of the Nyquist curves does not touch, frequency-wise, the interval on the real line $[1/\mu_2, \ldots, 1/\mu_N]$. In order this to be true, we need to impose

$$\frac{1}{\mu_N} < \frac{4}{\delta_k T f_2 - 2f_1}, \forall\, k$$

and thus

$$\tilde{\delta}_k > \frac{4 + 2f_1\mu_N - \delta_{\text{nom}}\mu_N T f_2}{\mu_N T f_2}.$$

Moreover, we need the imaginary parts of the Nyquist plots to have the same sign for all the values of $\omega \in (0, \pi]$ and $\omega \in [-\pi, 0)$. This can be ensured requiring that

$$\delta_k T f_2 - f_1 < 0 \Rightarrow \tilde{\delta}_k < \frac{f_1}{T f_2} - \delta_{\text{nom}},$$

which is, again, satisfied by Eq. 5.5.

The proof is now concluded once we notice that since $\Gamma_0 = I - P$, and all the eigenvalues of P lie in the interval $(-1, 1]$, then $\mu_N > -2$. □

As an applicative and vivid example, we can state the following example-corollary. The proof is straightforward.

Corollary 5.2.3. *Assume for sake of simplicity $\delta_{\text{nom}} = 1$, and set $f_1 = \frac{1}{2}$ and $T f_2 = \frac{1}{2}$. Then the clocks network synchronizes if*

$$-1 < \tilde{\delta}_k < 1 \tag{5.7}$$

namely the possible relative variation w.r.t. the nominal value is 100%.

Numerical examples

In this section we are going to provide several examples and counterexamples to our result.

As a first case, consider a network of $N = 10$ clocks. For each state, the first component (the offset) is taken according to the gaussian density $\mathcal{N}(20, 1)$, while the second component is set to the value 1. Namely, each clock at the beginning assumes

that its skew is the "natural" one. We take $\delta_{\text{nom}} = 1$ and $\tilde{\delta}_k \in \mathcal{U}[-1, 1]$, $\forall\, k = 1, \ldots, N$. The interconnection matrix is

$$\Gamma_0 = -I_n + .5 * \mathcal{C}_N + 0.5 * \mathcal{C}_N^{-1}$$

where $\mathcal{C}_N$ is defined as in Section 4.5, as the Cayley matrix generated by the row vector $\boldsymbol{g} = \begin{bmatrix} 0 & 1 & 0 & \ldots & 0 \end{bmatrix}$. We set moreover $T = 1$, $f_1 = 1$ and $f_2 = \frac{1}{2T}$ as in Corollary 5.2.3. In Fig. 5.1 we show on the left panel a typical trajectory of the clocks. On the right panel we show the Nyquist plots of the N systems and the instability region, which is the thick horizontal segment on the real axis. In accordance with Corollary 5.2.3, the system synchronizes since the convex hull (done frequency–wise) of the Nyquist plots does not intersect the instability region.

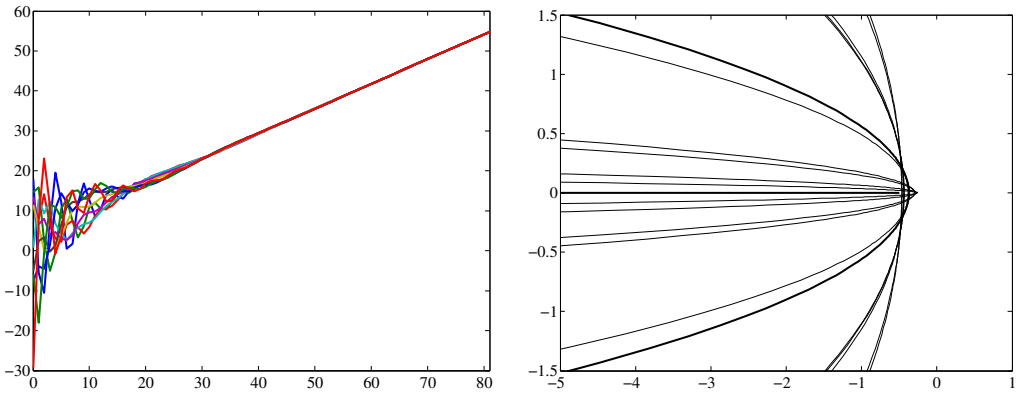

Figure 5.1: An example of the network synchronizing. Left panel: the trajectory of the states. Right panel: the Nyquist plots of the systems and the instability region (thick segment along the real axis).

We consider now the first counterexample. Take a network of $N = 5$ clocks with the same settings as before, apart from the fact that $\delta_k = 1$ for $k = 1, \ldots, 4$, and $\delta_5 = -\frac{1}{4}$. Since

$$\sum_{k=1}^{5} \frac{1}{\delta_{\text{nom}} + \tau\tilde{\delta}_k} = 0$$

for $\tau = 1$ the criterion is not satisfied. This is shown in Fig. 5.2. On the left panel, the trajectory of the clocks is shown, while on the right panel we show the projection of such trajectories on span $\{\mathbf{1}\}^{\perp}$. If the system synchronizes, this projection must decay asymptotically. Instead, because of the unsatisfied constraint, a constant steady state error appears in the projection. The Nyquist criterion is not shown but it is respected, as well as all the other assumptions of Theorem 5.2.2.

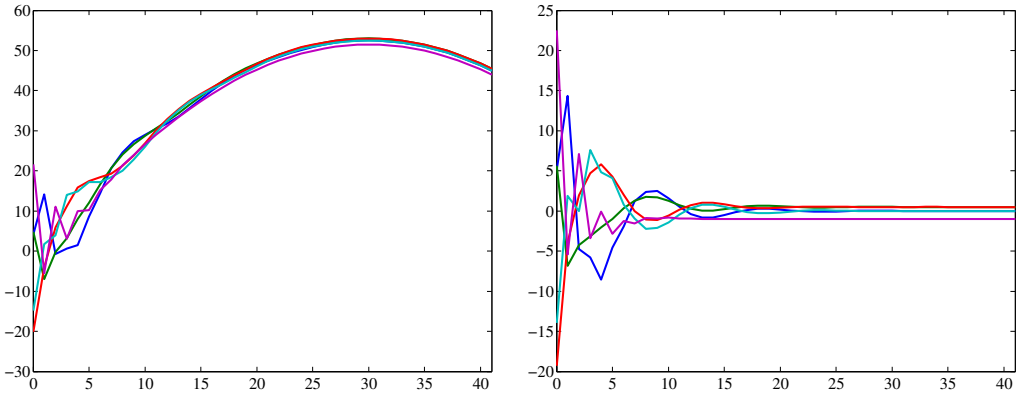

Figure 5.2: First counterexample: condition at the pole unsatisfied.

For the second counterexample, consider again the same network with the same settings as before where $\delta_k = 1 + \mathcal{U}[0, 0.2]$ for $k = 1, \ldots, 9$ and $\delta_{10} = 3$. Here the Nyquist criterion is not satisfied since, as depicted on the right panel of Fig. 5.3, the sign of the imaginary part of the Nyquist plots for $\omega \in [0, \pi]$ is not always negative. This means that their convex hull intersects the instability region (shown as thick segment on the real axis), and the criterion is not satisfied. In fact, on the left panel of Fig. 5.3 a typical trajectory of the outputs of the systems is depicted.

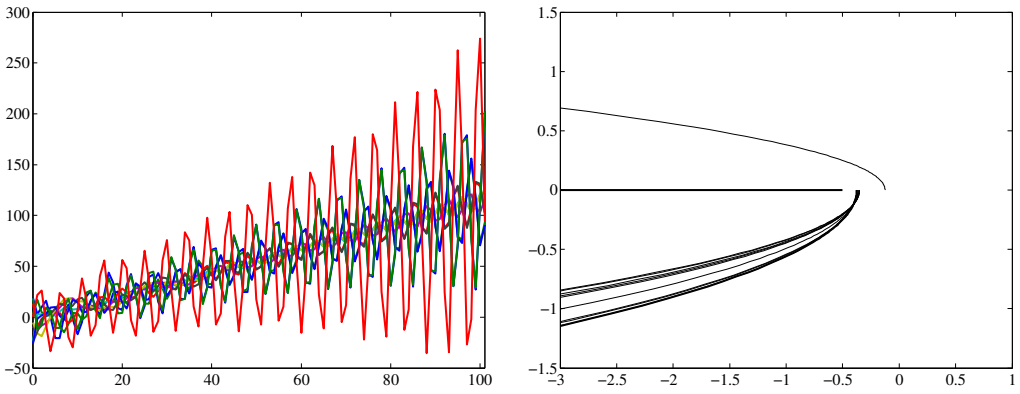

Figure 5.3: Second counterexample. Left panel: trajectory of the states. Right panel: the Nyquist plots, for $\omega \in [0, \pi]$, of the systems and the instability region (thick segment along the real axis). The Nyquist plots do not belong all to the half–plane of negative imaginary parts, so their convex hull will for sure intersect the instability region.

The third counterexample is a network with $N = 10$, the same Γ_0 as before, $f_1 = 1.24$, $T = 1$, $f_2 = 0.5$, an $\delta_k = \delta_{\text{nom}} + \mathcal{U}[-0.2, 0.2]$, with $\delta_{\text{nom}} = 1$. In this case some of the Nyquist plots intersect the instability region, so the criterion cannot be satisfied, as

depicted ont he right panel of Fig. 5.4. On the left panel, the corresponding trajectories of the clocks, clearly not synchronizing.

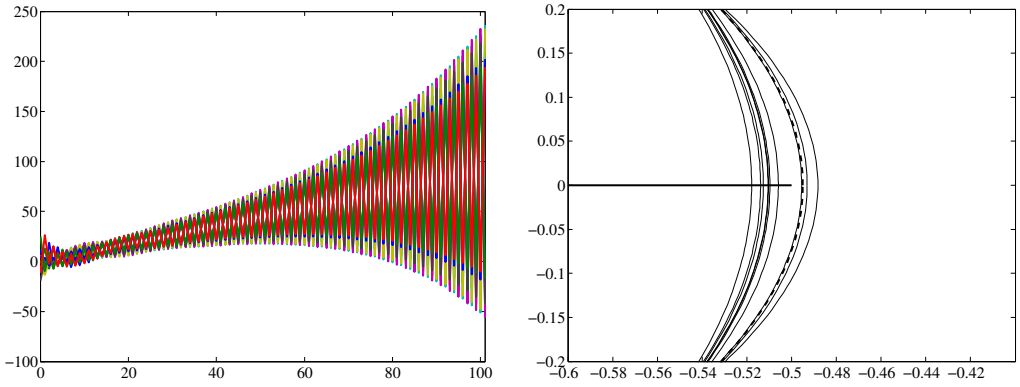

Figure 5.4: Third counterexample. Left panel: trajectory of the clocks. Right panel: Nyquist plots and instability region (in thick along the real axis). The criterion is not satisfied.

Synchronization of clocks with quasi-saturation of the input

In this paragraph we give an example of the application of the the results in Section 4.4 in order to analyze a network of clocks which for sake of simplicity is considered homogeneous, in the sense that all the skews are equal to the nominal value $\delta_{\text{nom}} = 1$.

In order to directly apply the Popov criterion proposed in Section 4.4, we consider the system in continuous–time, so that the update equations are changed to

$$\begin{cases} \dot{x}_k(t) = \begin{bmatrix} 0 & T \\ 0 & 0 \end{bmatrix} x_k(t) + \begin{bmatrix} f_1 \\ f_2 \end{bmatrix} u_k(t), \\ y_k(t) = \begin{bmatrix} 1 & 0 \end{bmatrix} x_k(t), \end{cases} \tag{5.8}$$

The input is quasi saturated in the sense that the ideal input is as usual

$$u_{k,id}(t) = \sum_{j \in \mathcal{N}_k} \gamma_{0,jk} y_j(t)$$

while the applied input is

$$u_k(t) = (1 + \Delta_k)(u_{k,id}(t)) = \begin{cases} u_{k,id}(t), & |u_{k,id}(t)| \leq u_{th} \\ u_{th} + \alpha_k(u_{k,id}(t) - \text{sgn}(u_{k,id}(t))u_{th}), & |u_{k,id}(t)| > u_{th} \end{cases}$$

The function $(1 + \Delta_k)(u)$ is depicted (for $u \geq 0$) in Fig. 5.5.

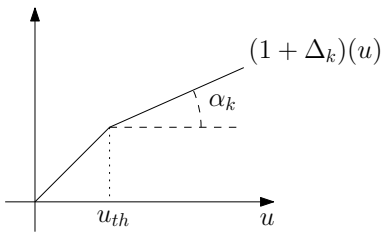

Figure 5.5: Clock synchronization with quasi–saturation. An instance of the memoryless perturbation considered.

To run a numerical simulation we consider a network of $N = 9$ agents interconnected through the matrix

$$\Gamma_0 = -I_N + 0.15(\mathcal{C}_N + \mathcal{C}_N^{-1}) + 0.30\mathcal{C}_N^5 + 0.40\mathcal{C}_N^{-5}$$

We assume for simplicity $T = 1$ and we set $f_1 = 1.7$, $f_2 = 1$, so that the transfer function of the clocks is

$$N_0(s) = \frac{f_1 s + f_2 q}{s^2} = \frac{1.7s + 1}{s^2},$$

One can check that feedback of any nonzero eigenvalues of Γ_0 with N_0 is stable. We take moreover $\alpha_k \in [0.2,\ 1]$, $\forall k = 1, \ldots, N$.

We check the synchronization criterion for this network using the multiplier π_Δ in Eq. 4.16 with $\lambda = 3$. In Fig. 5.7, also zoomed in the region of interest, are depicted the Popov plots of the feedbacks

$$\frac{\mu_i N_0}{1 - \mu_i N_0} = \frac{1.7s + 1}{s^2 - 1.7\mu_i s - \mu_i}$$

which, as one can see, all belong to the same half-plane described by the line with slope $\frac{1}{\lambda} = \frac{1}{3}$ and crossing $-\frac{1}{\alpha_{\min}} = -5$. Thus, Corollary 4.4.4 is satisfied and in fact, as we can see in Fig. 5.6, the clocks all converge to the same ramp.

Synchronization of clocks using randomized protocols

The synchronization protocol used so far requires perfect synchronicity among the agents, since they all periodically exchange their time readings and update their initial offsets and estimates of the inverses of the skews.

In this paragraph we drop this idealistic assumption and we consider randomized protocols, which has been widely studied in the classical consensus algorithm for asyn-

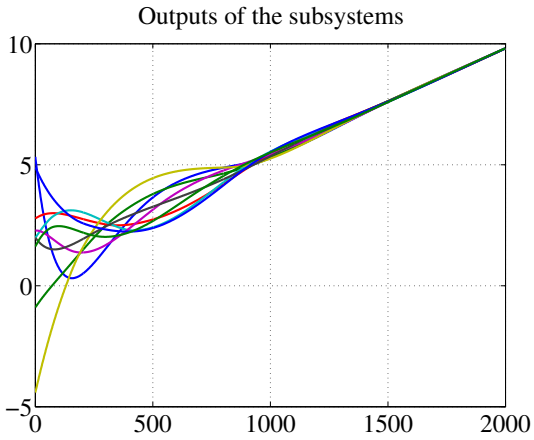

Figure 5.6: Clock synchronization with quasi–saturation. A typical trajectory of the outputs.

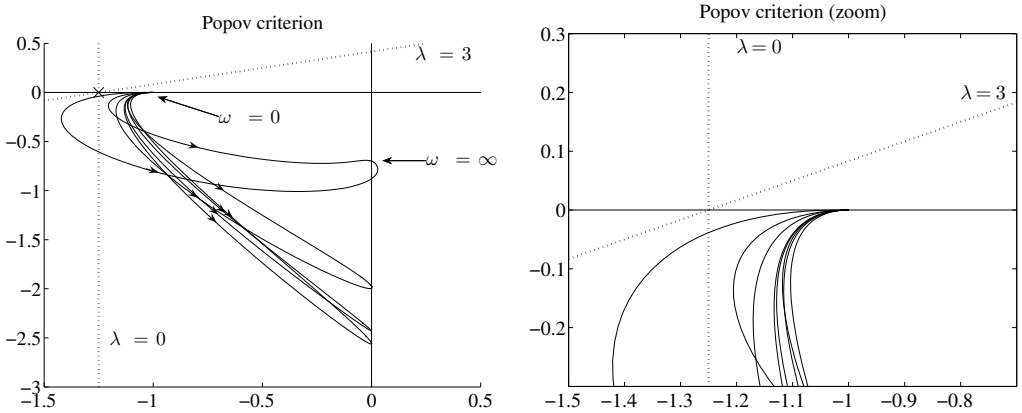

Figure 5.7: Left panel: the Popov plot in the case of quasi saturation. The big cross marks the point $-\frac{1}{\alpha_{\min}} + j0$. Right panel: particular showing that the Popov criterion is satisfied at low frequencies.

chronous scenarios. For a randomized consensus protocol, in fact, at each time instant there is some probability that a node, or a group of nodes, wakes up, calls its neighbors only, performs the update with them, and then returns to a rest state. The typical example is symmetric gossip, in which only one node wakes up, calls one of its neighbors, they exchange their values and update their state to the average of them. If we assume

that agent k wakes up and calls agent j, the update equations are

$$\begin{cases} x_k(t+1) = \frac{1}{2}(x_k(t) + x_j(t) \\ x_j(t+1) = \frac{1}{2}(x_k(t) + x_j(t) \\ x_i(t+1) = x_i(t), \forall, i \neq k, j \end{cases}$$

In matrix form this reads

$$\boldsymbol{x}(t+1) = P(t)\boldsymbol{x}(t)$$

in which $P(t)$ is a (randomly picked) matrix which expresses the gossip among the two nodes which perform the update. In case at time t it takes place a gossip among k and j, for example, we have

$$P(t) = I - \frac{1}{2}(\boldsymbol{e}_k\boldsymbol{e}_k^T + \boldsymbol{e}_j\boldsymbol{e}_j^T) + \frac{1}{2}(\boldsymbol{e}_k\boldsymbol{e}_j^T + \boldsymbol{e}_j\boldsymbol{e}_k^T) \tag{5.9}$$

where $\boldsymbol{e}_k$ is, as usual, the k-th vector of the canonical base of $\mathbb{R}^N$. Notice that $P(t)\mathbf{1} = \mathbf{1}$, but the associated graph is not strongly connected, so the single $P(t)$ cannot solve consensus.

To study randomized protocols, we define $\mathcal{F}$ to be the family of matrices associated with the instances of the protocol. For example, in the symmetric gossip, the elements of $\mathcal{F}$ are of the type in Eq. 5.9. We define moreover a probability distribution p_f on $\mathcal{F}$, which tell us which is the probability that the instance f is performed. We assume then $\{P(t)\}$ to be an i.i.d. matrix random process and we assume that each $P(t) \in \mathcal{F}$ is picked according to the distribution p_f.

The question is now whether there exists a suitable definition of consensus for the randomized protocols, and which are the conditions under which it is achieved. Following [139], we say that a randomized protocol achieves *probabilistic consensus* if

- if $\boldsymbol{x}(0) \in \operatorname{span}\{\mathbf{1}\} \subset \mathbb{R}^N$, then $\boldsymbol{x}(t+1) = \boldsymbol{x}(t), \forall t \geq 0$. Namely, if consensus is reached then no other iterations of the algorithm are needed;
- for any $\boldsymbol{x}(0) \in \mathbb{R}^N$, there exists a scalar random variable such that

$$\boldsymbol{x}(t) \overset{t\to\infty}{\longrightarrow} \alpha\mathbf{1}, \text{almost surely}$$

To give conditions for probabilistic consensus to be achieved, define the average graph $\mathcal{G}_{\bar{P}}$ to be the graph associated with $\bar{P} = \mathbb{E}P(t)$, namely the graph $\mathcal{G} = (\mathcal{V}, \mathcal{E})$ in which $\mathcal{V}$ is the set of agents and there exists an edge $(k, j) \in \mathcal{E}$ if there exists at least one element P of $\mathcal{F}$, which can be picked with non zero probability, such that $P_{kj} > 0$, or, in words,

if (k, j) "exists and can be chosen" by the algorithm. The following result, taken from [139], clarifies the situation.

Theorem 5.2.4 ([139])**.** *Assume that for any $k \in \mathcal{V}$ we have $P_{kk}(t) > 0$ almost surely. If $\mathcal{G}_{\bar{P}}$ is strongly connected then the algorithm achieves probabilistic consensus.*

This result is rather general an allows to check probabilistic consensus in many cases. However, our interest is on clock synchronization for which the analysis becomes more involving. For example, in randomized consensus protocols it is not problematic how much time elapses among two iterations of the algorithm. In clock synchronization, instead, the more time elapses, the more un–synchronized clocks tend to deviate one from each other. This must be taken into account.

Let thus $T(t)$ be the (random) time elapsed among the t-th and the $t+1$-th iterations of the algorithm. We consider the following model for the network of clocks

$$\begin{cases} \boldsymbol{x}(t+1) = \begin{bmatrix} I_N & T(t)D \\ 0 & I_N \end{bmatrix} \boldsymbol{x}(t) + \begin{bmatrix} f_1 \\ f_2 \end{bmatrix} \otimes I_N \boldsymbol{u}(t) \\ \boldsymbol{y}(t) = \begin{bmatrix} I_N & 0 \end{bmatrix} \boldsymbol{x}(t) \\ \boldsymbol{u}(t) = E(t)\boldsymbol{y}(t) \end{cases} \tag{5.10}$$

where I_N is the $N \times N$ identity matrix, D is a diagonal matrix whose (k, k)-th entry is the k-th skew δ_k, $\otimes$ is the Kronecker product, and $E(t) \in \mathbb{R}^{N \times N}$ takes the role which was of the constant matrix Γ_0. Analogously, a reasonable choice is $E(t) = -(I - P(t))$ where $\{P(t)\}$ is a family achieving probabilistic consensus. For example, if at time t we perform symmetric gossip among agents k and j we have

$$E(t) = -\frac{1}{2}(e_k e_k^T + e_j e_j^T) + \frac{1}{2}(e_k e_j^T + e_j e_k^T)$$

Notice that $E_{ij}\mathbf{1} = 0$, since if the clocks are synchronized the control must be zero, yet, again, the single $E(t)$ do not satisfy Assumption 4.3.2 since its kernel is not limited to $\operatorname{span}\{\mathbf{1}\}$.

A slight manipulation of the system Eq. 5.10 allows us to rewrite it as

$$\boldsymbol{x}(t+1) = \begin{bmatrix} I - f_1 E(t) & T(t)D \\ -f_2 E(t) & I \end{bmatrix} \boldsymbol{x}(t) \tag{5.11}$$

Let as usual $V \in \mathbb{C}^{N\times N-1}$ such that $V^*V = I_{N-1}$ and $V^*\mathbf{1} = 0$, and define

$$\begin{bmatrix}\bar{\boldsymbol{y}}(t)\\ \bar{\boldsymbol{z}}(t)\end{bmatrix} = \bar{\boldsymbol{x}}(t) = \begin{bmatrix}V^* & 0\\ 0 & V^*D\end{bmatrix}\boldsymbol{x}(t)$$

The goal of this section is to provide conditions on the gains f_1 and f_2 such that $\bar{\boldsymbol{x}}(t)$ converges to zero in mean–square. If this holds true, in fact, in particular $\bar{\boldsymbol{y}}(t)$ converges to zero in means–square and thus $\boldsymbol{y}(t)$ converges to the synchronization space span $\{\mathbf{1}\}$ in mean–square.

By simple computations (and using the fact that $E(t) = E(t)VV^*$) we obtain

$$\bar{\boldsymbol{x}}(t+1) = \begin{bmatrix}I - f_1\tilde{E}(t) & T(t)\\ -f_2\tilde{F}(t) & I\end{bmatrix}\bar{\boldsymbol{x}}(t), \tag{5.12}$$

where $\tilde{E}(t) = V^*E(t)V$ while $\tilde{F}(t) = V^*DE(t)V$. Notice that in case of symmetric protocols, in which each $E(t)$ is symmetric, it holds $\tilde{F}(t) = \tilde{D}\tilde{E}(t)$ where $\tilde{D} = V^*DV$.

Since our interest is on the second moment of $\bar{\boldsymbol{x}}(t)$, we define

$$\Sigma(t) = \mathbb{E}[\bar{\boldsymbol{x}}(t)\bar{\boldsymbol{x}}(t)^T] = \begin{bmatrix}\Sigma_{yy}(h) & \Sigma_{yz}(h)\\ \Sigma_{zy}(h) & \Sigma_{zz}(h)\end{bmatrix}$$

Assume now $T(t)$ to be an i.i.d. random process with $\mathbb{E}[T(t)] = \mu$ and $\mathbb{E}[(T(t)-\mu)^2] = \sigma^2$. Define

- $\bar{E} := \mathbb{E}[E(t)]$, $\tilde{E} := V^*\bar{E}V = \mathbb{E}\tilde{E}(t)$ and $\hat{E} = \mathbb{E}\tilde{E}(t) \otimes \tilde{E}(t)$

- $\tilde{F} := V^*D\bar{E}V = \mathbb{E}\tilde{F}(t)$ and $\hat{F} = \mathbb{E}\tilde{F}(t) \otimes \tilde{F}(t)$

and moreover $\hat{EF} = \mathbb{E}\tilde{E}(t) \otimes \tilde{F}(t)$ and $\hat{FE} = \mathbb{E}\tilde{F}(t) \otimes \tilde{E}(t)(t)$.

Using the fact that the matrix process $\{E(t)\}$ is i.i.d., it is easy to obtain the linear iteration

$$\Sigma(t+1) = \mathbb{E}Q(t)^T\Sigma(t)Q(t)$$

where $Q(t)$ are suitable matrices. In particular, we obtain the four linear iterations

$$\begin{aligned}
\Sigma_{yy}(t+1) &= \mathbb{E}(I - f_1\tilde{E}(t))\Sigma_{yy}(t)(I - f_1\tilde{E}(t)^+) + (I - f_1\tilde{E}(t))T(h)\Sigma_{yz}(t) \\
&\quad + T(h)\Sigma_{zy}(t)(I - f_1\tilde{E}(t)^T) + T(h)^2\Sigma_{zz}(t) \\
\Sigma_{yz}(t+1) &= \mathbb{E} - f_2(I - f_1\tilde{E}(t))\Sigma_{yy}(t)\tilde{F}(t)^T + (I - f_1\tilde{E}(t))\Sigma_{yz}(t) \\
&\quad - f_2T(h)\Sigma_{zy}(t)\tilde{F}(t)^T + T(h)\Sigma_{zz}(t) \\
\Sigma_{zy}(t+1) &= \mathbb{E} - f_2F(t)\Sigma_{yy}(t)(I - f_1\tilde{E}(t)^T) - f_2T(h)\tilde{F}(t)\Sigma_{yz}(t) \\
&\quad + \Sigma_{zy}(t)(I - f_1\tilde{E}(t)^T) + T(h)\Sigma_{zz}(t) \\
\Sigma_{zz}(t+1) &= \mathbb{E}f_2^2\tilde{F}(t)\Sigma_{yy}(t)\tilde{F}(t)^T - f_2\tilde{F}(t)\Sigma_{yz}(t) - f_2\Sigma_{zy}(t)\tilde{F}(t)^T + \Sigma_{zz}(t)
\end{aligned}$$

We study these iterations taking the vectorized version of the blocks of $\Sigma(t)$, namely defining

$$\begin{aligned}
Y(t) &= \operatorname{vect}\Sigma_{yy}(t) & Z(t) &= \operatorname{vect}\Sigma_{zz}(t) \\
W(t) &= \operatorname{vect}\Sigma_{yz}(t) & \bar{W}(t) &= \operatorname{vect}\Sigma_{zy}(t)
\end{aligned}$$

we also have

$$\begin{bmatrix} Y(t+1) \\ \bar{W}(t+1) \\ W(t+1) \\ Z(t+1) \end{bmatrix} = M(f_2) \begin{bmatrix} Y(t) \\ \bar{W}(t) \\ W(t) \\ Z(t) \end{bmatrix}$$

where

$$M(f_1, f_2) = M_0(f_1) + f_2M_1(f_1) + f_2^2M_2(f_1)$$

with

$$M_0(f_1) = \begin{bmatrix} I - f_1(I\otimes\tilde{E} + \tilde{E}\otimes I) + f_1^2\hat{E} & \mu(I - f_1(\tilde{E}\otimes I)) & \mu(I - f_1(I\otimes\tilde{E})) & \sigma^2 I \\ 0 & I - f_1(\tilde{E}\otimes I) & 0 & \mu I \\ 0 & 0 & I - f_1(I\otimes\tilde{E}) & \mu I \\ 0 & 0 & 0 & I \end{bmatrix}$$

$$M_1(f_1) = \begin{bmatrix} 0 & 0 & 0 & 0 \\ -(I\otimes\tilde{F} - f_1\hat{EF}) & 0 & -\mu(I\otimes\tilde{F}) & 0 \\ -(\tilde{F}\otimes I - f_1\hat{FE}) & -\mu(\tilde{F}\otimes I) & 0 & 0 \\ 0 & -(\tilde{F}\otimes I) & -(I\otimes\tilde{F}) & 0 \end{bmatrix}$$

and

$$M_2(f_1) = \begin{bmatrix} 0 & 0 & 0 & 0 \\ 0 & 0 & 0 & 0 \\ 0 & 0 & 0 & 0 \\ \hat{F} & 0 & 0 & 0 \end{bmatrix}.$$

Recall that our goal is to give conditions on f_1 and f_2 for the mean–square convergence of $\bar{\boldsymbol{x}}(t)$ to zero. The previous discussion shows that this is equivalent to check for conditions such that the matrix $M(f_2, f_1)$ is stable. In particular, we consider from now on f_1 fixed, so that the problem becomes to study the eigenvalues of a matrix of the type

$$M(f_2) = M_0 + f_2 M_1 + f_2^2 M_2$$

We use the following perturbation result taken from [140], in which we call an eigenvalue semi–simple it its algebraic multiplicity coincides with its geometric multiplicity.

Theorem 5.2.5. *Let be $M(alpha) \in \mathbb{R}^{N\times N}$ be a matrix dependent on the parameter α in a sufficiently smooth way so that the first derivative $\dot{M}(\alpha)|_{\alpha=0}$ exists. Let moreover $\mu_1, \ldots, \mu_m$ be semi–simple eigenvalues of $M(\alpha)$ with associated right eigenvectors $\boldsymbol{r}_1, \ldots, \boldsymbol{r}_m$ and left eigenvectors $\boldsymbol{l}_1^T, \ldots, \boldsymbol{l}_m^T$. Assume that these families of eigenvectors are chosen such that if*

$$\mathcal{R} = \begin{bmatrix} \boldsymbol{r}_1 & \ldots & \boldsymbol{r}_m \end{bmatrix} \qquad \mathcal{L} = \begin{bmatrix} \boldsymbol{l}_1^T \\ \vdots \\ \boldsymbol{l}_m^T \end{bmatrix}$$

then

$$\mathcal{L}\mathcal{R} = I_m$$

where I_m is the $m \times m$ identity. Then the derivative of μ_i with respect to α, in $\alpha = 0$, exists and it is the i-th eigenvalue of the matrix $\mathcal{L}M'\mathcal{R}$ where $M' = \dot{M}(\alpha)|_{\alpha=0}$.

Notice that in our case $\dot{M}(f_2)|_{f_2=0} = M_1$. Notice moreover that it is clear from the block–upper triangular structure of M_0 that this matrix has many eigenvalues in 1. The first step is to compute how much there are of them, and whether they are semi–simple. For simplicity, we define $\tilde{M}_0 = M_0 - I$ and we look for the kernel of $\tilde{M}_0$. Denoting by $\Lambda(\tilde{M}_0)$ the spectrum of $\tilde{M}_0$, we have

$$\Lambda(\tilde{M}_0) = \Lambda(f_1(I \otimes \tilde{E} + \tilde{E} \otimes I) + f_1^2 \hat{E}) \cup \Lambda(0_{(N-1)^2}) \cup \Lambda(f_1(I \otimes \tilde{E})) \cup \Lambda(f_1(\tilde{E} \otimes I)).$$

Due to the analogy with what is done in the proof of Theorem 5.2.4, we claim that

$\tilde{E}$ and $\hat{E}$ are both non singular matrices if the average graph $\mathcal{G}_{\bar{P}}$ is strongly connected. Moreover, we claim that $\tilde{E}$ is a negative definite matrix, so that if f_1 is sufficiently small all the eigenvalues of M_0 which are not in 1 are inside the unit circle.

This result immediately implies that the unique zero eigenvalues of $\tilde{M_0}$ are only due to the zero block $0_{(N-1)^2}$. Once we define

$$\mathcal{L} = \begin{bmatrix} 0 & 0 & 0 & \frac{\sigma^2}{f_1^2}\tilde{E}^{-1} \otimes \tilde{E}^{-1} \end{bmatrix}$$

$$\mathcal{R} = \begin{bmatrix} (f_1(I \otimes \tilde{E} + \tilde{E} \otimes I) - f_1^2\hat{E})^{-1}(f_1(I \otimes \tilde{E}\tilde{E} \otimes I) \\ \frac{f_1}{\mu} I \otimes \tilde{E} \\ \frac{f_1}{\mu} \tilde{E} \otimes I \\ \frac{f_1^2}{\sigma^2} \tilde{E} \otimes \tilde{E} \end{bmatrix}$$

it is just a matter of computation to show that

$$\mathcal{L}M_0 = \mathcal{L}, \qquad M_0\mathcal{R} = \mathcal{R}$$

Moreover, it is easy to check that the columns of $\mathcal{R}$ and the rows of $\mathcal{L}$ are linearly independent one each other, so we have a family of $N-1$ left and $N-1$ right eigenvectors, and the corresponding eigenvalues are semi–simple. To conclude, it is immediate to see that

$$\mathcal{L}\mathcal{R} = I_{(N-1)^2}.$$

We can now state and prove the following existence result.

Theorem 5.2.6. *Consider the randomized clock synchronization protocol for a network of clocks proposed in Eq. 5.11, where $\{E(t)\}$ is an i.i.d. matrix random process such that the corresponding $P(t) = -(I - E(t))$ achieves average consensus, and fix a positive, sufficiently small value for the parameter f_1 so that all the eigenvalues of M_0 are inside the unit circle, apart from those in 1. Assume the positive definiteness of the matrix*

$$Q = \tilde{E}^{-1}\tilde{F} \oplus \tilde{E}^{-1}\tilde{F}$$

where $\oplus$ is the Kronecker sum defined as $A \oplus B = A \otimes I_1 + B \otimes I_2$, I_1 and I_2 being identity matrices of suitable dimension. Then there exists a positive real scalar $\bar{f}_2$ such that if $f_2 \in (0, \bar{f}_2)$ such that the protocol achieves mean–square synchronization.

Proof. If $\mathcal{L}$ and $\mathcal{R}$ denote the matrices defined above, it is easy to obtain

$$\mathcal{L}M_1\mathcal{R} = -\frac{\sigma^2}{f_1\mu}\tilde{E}^{-1}\tilde{F} \oplus \tilde{E}^{-1}\tilde{F}$$

so by Theorem 5.2.5 and noticing that $\mu > 0$ it follows that

$$\frac{\mu_i(f_2)}{f_2}|_{f_2=0} < 0$$

for all the eigenvalues $\mu_i = 1$ of M_0. This implies that there exists a (possibly very small) interval $(0, \bar{f}_2)$ such that if f_2 belongs to it, all the eigenvalues of $M(f_2)$ are strictly inside the unit circle. □

The condition on the matrix Q in the previous theorem is simple to check in many cases of interest. For example, in case the protocol is symmetric, so that $\tilde{F} = \tilde{F}\tilde{E}$, and if $D = dI$, so that $\tilde{D} = dI_{N-1}$, we obtain

$$Q = d\tilde{E}^{-1}\tilde{E} \oplus d\tilde{E}^{-1}\tilde{E} = 2dI_{N_1}$$

which is always positive definite if $d > 0$.

More generically, under symmetric protocol and if $D = dI + \Delta$, we obtain

$$Q = 2dI_{(N-1)^2)} + T \oplus T$$

where $T = \tilde{E}^{-1}V^*\Delta V\tilde{E}$. It is easy to see that the eigenvalues of the Kronecker sum $A \oplus B$ are all the possible sums of one eigenvalue of A and one eigenvalue of B. Thus, the maximum absolute value of the eigenvalues of $T \oplus T$ is at most twice the absolute value of the eigenvalues of T. Since T and $V^*\Delta V$ share the same set of eigenvalues, one can study the spectrum of $V^*\Delta V$, which is hermitian, thus its eigenvalues are real. In particular, using the fact that $V^*V = I_{N-1}$ we have

$$|\frac{\boldsymbol{x}^*V^*\Delta V\boldsymbol{x}}{\boldsymbol{x}^*\boldsymbol{x}}| = |\frac{\boldsymbol{v}^*\Delta\boldsymbol{v}}{\boldsymbol{v}^*\boldsymbol{v}}| \leq \max_k |\Delta_{kk}|$$

so, making use of the variational characterization of the eigenvalues give by the Rayleigh–Ritz theorem, one concludes that the eigenvalues of T are in absolute value smaller than $\max_k |\Delta_{kk}|$.

By the previous reasoning, it is easy to see that Q is positive definite, and thus mean–square synchronization takes place, if $d > \max_k |\Delta_{kk}|$.

We want to remark that Theorem 5.2.6 is an existence–only result, namely we are unable, by now, to estimate the value $\bar{f}_2$, which heavily depends on the protocol, namely, on the family from which the matrices $E(t)$ are picked. Intuitively, this is due to the "quadratic term" $f_2^2 M_2$, which heavily depends on the randomized protocol which is used.

5.3 Distributed calibration algorithms for networks of cameras on a plane

In a network of cameras deployed in a plane one of the most important problems is calibration. Namely, each camera has to know how it is oriented, at any instant, with respect to a certain common reference frame. The importance of this is clear: assume that an external agent, which has to be tracked, is exiting from the range of the u-th camera and entering in that of the v-th one. In this case camera u has to communicate to camera v to move and follow the agent before camera u looses it. Clearly, both cameras must share the same reference frame.

Usually, this is set off-line by a human operator, or by a centralized unit. Instead, in this Section we present algorithms which aim to complete autonomy and avoid central control to carry on computations. This allows improved accuracy and possibility of periodical autonomous re–calibration.

The model for the network is, as usual, a graph $\mathcal{G} = (\mathcal{V}, \mathcal{E})$ in which $\mathcal{V}$ is the set of cameras, and $\mathcal{E}$ the set of edges, the couples of communicating cameras. The information which is used to calibrate the network, inspired by the works by Barooah and Hespanha [96, 141, 86] on localization, is the relative orientation among communicating cameras, which can be computed if their field of view overlaps.

Cameras calibration through relative orientations can be transformed into a consensus like problem over the manifold $\mathcal{S}_1$: this problem has already attracted much attention by research community. In [142, 13, 12] the authors propose a consensus algorithm on $\mathcal{S}_1$ based on the gradient flow of a potential defined using the chordal distance, namely, the Euclidean distance in the Euclidean space $\mathbb{R}^2$ in which $\mathcal{S}_1$ can be immersed. In [10] a similar approach based on the geodesic distance is proposed to study the more general calibration problem on $SE(3)$. The trouble with both these approaches is that the defined potentials are characterized by several nontrivial local minima in which, apart from particular initial conditions, it is easy to fall. Avoiding instead the problems of optimizing on manifold, the paper [143] proposes to constrain *a priori* the noisy measurements of relative orientations to sum to zero on cycles. Based on this construction, a least-square estimation algorithm, which is proved to be optimal on a ring graph, is presented. Our work tries somehow to exploit the best of these two approaches.

We choose to concentrate on the simple case of calibration in $SO(2) \sim \mathcal{S}_1$, and we use the geodesic distance. Our main idea is to break the estimation problem into two parts: first we estimate a sort of combinatorial object which is a vector in $\mathbb{Z}^M$ and takes care of the fact that noise around cycles in general does not sum up to 0. Once this is

done we estimate by solving a quadratic optimization problem like in the localization problem. Our method is consistent in the sense that in the noiseless case the algorithm converges to the optimal solution. We propose two different algorithms: one based on spanning trees, the other on minimal cycles.

Problem Formulation

We model a network of cameras as a connected undirected graph $\mathcal{G} = (\mathcal{V}, \mathcal{E})$, $\mathcal{V} = \{1, \dots, N\}$, equipped with an orientation (t, h).

Fix an external reference frame and let $(g_v, R_v) \in \mathbb{R}^2 \times SO(2)$ be the pose of camera v, for each $v \in \mathcal{V}$. The pose is made of two elements, namely the position of the camera in the plane, g_v, and its orientation with respect to the axis of the reference frame, R_v. The set of orientations is a manifold, and its elements can be thought as the set of 2×2 orthogonal matrices with determinant equal to $+1$, namely $R_v^T R_v = I_2$ and $|R_v| = +1$, for each v.

Here we are interested in calibration of orientations only, so we discard g_v. Moreover, we do not represent the orientations as matrices, but just as elements of $\mathbb{R}$ which give the measure of the orientation angle of the cameras. In other terms, the pose of camera v will be represented by a value $\bar{\theta}_v \in \mathbb{R}$, with the implicit convention that the orientation is given by

$$R_v := R_v(\bar{\theta}_v) = \begin{bmatrix} \cos\bar{\theta}_v & -\sin\bar{\theta}_v \\ \sin\bar{\theta}_v & \cos\bar{\theta}_v \end{bmatrix}$$

Notice that the map $\theta \to R(\theta)$ is surjective but clearly not injective. However, the parametrization using angles in $\mathbb{R}$ will turn out to be useful, so in the following we almost always treat orientations as real values.

Our aim is to solve the *calibration* problem, namely to obtain, for each node v, an estimate of its orientation, $\hat{\theta}_v$, as close as possible to the actual orientation. More formally, once we stack all the actual orientations in the vector $\bar{\boldsymbol{\theta}} \in \mathbb{R}^N$ and all the estimates in the vector $\hat{\boldsymbol{\theta}} \in \mathbb{R}^N$, we aim to minimize the following index

$$W(\hat{\boldsymbol{\theta}}) = \|(\hat{\boldsymbol{\theta}} - \bar{\boldsymbol{\theta}})_{2\pi}\|^2$$

where $(x)_{2\pi} = x - 2\pi q_{2\pi}(x)$ and $q_{2\pi}(x) = \lfloor \frac{x+\pi}{2\pi} \rfloor$. This is reasonable since the values $\bar{\theta}_v$'s and $\tilde{\theta}_v$'s are angles, so that if $\tilde{\theta}_v = \bar{\theta}_v + 2\pi h$, namely $(\hat{\theta}_v - \tilde{\theta}_v)_{2\pi} = 0$, they represent the same orientation, $R(\tilde{\theta}_v) = R(\bar{\theta}_v)$. For this reason, given $\bar{\boldsymbol{\theta}} \in \mathbb{R}^N$, we say that $\tilde{\boldsymbol{\theta}}$ is a *representative* of $\bar{\boldsymbol{\theta}}$ if $\tilde{\boldsymbol{\theta}} = \bar{\theta} + 2\pi \boldsymbol{l}, \boldsymbol{l} \in \mathbb{Z}$, i.e. if $(\bar{\boldsymbol{\theta}} - \hat{\boldsymbol{\theta}})_{2\pi} = 0$. It is manifest that to calibrate the network to $\bar{\boldsymbol{\theta}}$ is the same as to calibrate it to any representative of $\bar{\boldsymbol{\theta}}$.

In order to accomplish this task, cameras exchange information trough the communication graph $\mathcal{G}$ and update their estimate $\hat{\theta}_v$'s making use of a notion of relative distance among them. More precisely, we assume that for any edge $e \in \mathcal{E}$, the two communicating cameras $h(e)$ and $t(e)$ have their fields of view overlapping. By means of known algorithms, briefly recalled in the next paragraph, they can obtain a noisy measurement $\eta_{t(e),h(e)}$ of their relative orientation $\bar{\theta}_t(e) - \bar{\theta}_h(e)$. Without loss of generality, we assume that this measurement is an angle in $[-\pi, \pi)$, so that we have, for each $e \in \mathcal{E}$,

$$\eta_e = (\bar{\theta}_{t(e)} - \bar{\theta}_{h(e)} - \varepsilon_e)_{2\pi} = \bar{\theta}_{t(e)} - \bar{\theta}_{h(e)} - \varepsilon_e - 2\pi\bar{K}_e \tag{5.13}$$

where notice that $\bar{K}_{t(e),h(e)} = q_{2\pi}(\bar{\theta}_{t(e)} - \bar{\theta}_{h(e)} - \varepsilon_{t(e),h(e)})$. We assume that

$$\varepsilon_e \in (-\pi, \pi), \forall e \in \mathcal{E} \tag{5.14}$$

which is reasonable under very mild hypothesis on cameras.

Remark 5.3.1. In the manifold $SO(2)$, the relative difference among R_v and R_u is given by $R_{uv} = R_v^{-1} R_u \in SO(2)$, and it is known that if $R_v = R(\bar{\theta}_v)$ and $R_u = R(\bar{\theta}_u)$, then $R_{uv} = R(\bar{\theta}_u - \bar{\theta}_v)$, so $R_{uv} = R(\eta_{uv})$ in case of noiseless measurements.

Making use of the incidence matrix B of the graph $\mathcal{G}$, one can rewrite in a compact form the model for the measurements as

$$\boldsymbol{\eta} = B\bar{\boldsymbol{\theta}} - \boldsymbol{\varepsilon} - 2\pi\bar{\boldsymbol{K}}, \tag{5.15}$$

where $\bar{\boldsymbol{K}} \in \mathbb{Z}^M$.

Relative measurements reconstruction algorithm

For the purpose of recovering the relative measurements stacked in $\boldsymbol{\eta} \in \mathbb{R}^M$, on each edge, the corresponding cameras, labeled as $t(e)$ and $h(e)$, overlap their field of view, and are supposed to share a certain number of feature points. We assume the imaging model to be the so-called *ideal pin-hole*. Each camera is represented by a plane, called image plane, and a point, called optical center, that is the origin of the camera reference frame. Each camera knows the noisy projection of the shared points in $\mathbb{R}^3$ on its image plane, and has to reconstruct the relative pose. In the general 3D case at least 8 points in general position are necessary to the scope, see [144]. In our case, the network is assumed to be planar, in the sense that all the cameras lie on the same plane, for example because they are all positioned at the same height with respect to the soil. The only requirement for the reconstruction algorithm to properly work is that not all the feature points shared

by two communicating cameras lie on the same plane as the cameras, which is a mild assumption.

Cost function

The cameras, clearly, cannot directly measure their actual orientation, since otherwise the problem would be trivial. Our scope is to solve the calibration problem making use of the relative measurements of the orientations, and in this spirit we propose the following cost

$$V(\boldsymbol{\theta}) = \sum_{e \in \mathcal{E}} (\theta_{t(e)} - \theta_{h(e)} - \eta_e)_{2\pi}^2 = \|(B\boldsymbol{\theta} - \boldsymbol{\eta})_{2\pi}\|_2^2. \tag{5.16}$$

Remark 5.3.2. The cost is based on the geodesic distance among elements of $SO(2)$, which is the length of the minimum path connecting the elements of $SO(2)$. In our simple case, if $R_v = R(\theta_v)$ and $R_u = R(\theta_u)$, the geodesic distance is given by

$$d(R(\theta_1), R(\theta_2))^2 := d(\theta_1, \theta_2)^2 = (\theta_1 - \theta_2)_{2\pi}^2$$

In this light, the term $(\theta_{t(e)} - \theta_{h(e)} - \eta_e)_{2\pi}^2$ of the cost simply represents the geodesic distance among the angles η_e and $\theta_{t(e)} - \theta_{h(e)}$.

Some remarks must be done. First of all, in case of noiseless measurements, $V(\boldsymbol{\theta})$ attains the value zero, the global minimum, for any representative of $\bar{\boldsymbol{\theta}}$, and only for these points. However, even in this ideal idea case, it has multiple local minima, due to the geometry of the manifold $\mathcal{S}_1$. This has been shown in [142] for a slightly different cost based on the chordal distance, which shows nonetheless a similar behavior.

Such local minima do no correspond to good estimates of the actual orientations, so we need a procedure to avoid them. This procedure is based on the following way to tessellate $\mathbb{R}^N$. Define the regions

$$R_{\boldsymbol{K}}(\boldsymbol{\eta}) := \{\boldsymbol{\theta} \in \mathbb{R}^N : |B\boldsymbol{\theta} - \boldsymbol{\eta} - 2\pi\boldsymbol{K}| \leq \pi\mathbf{1}\}^2, \tag{5.17}$$

where $\boldsymbol{K} \in \mathbb{Z}^M$. These regions are convex and form a partition of $\mathbb{R}^N$. However, some of them can be empty, since they are defined by M constraints on N variables and in general $M > N$. It is trivial to see that if $\boldsymbol{\theta} \in R_{\boldsymbol{K}}(\boldsymbol{\eta})$, and only for these points, then

$$V(\boldsymbol{\theta}) = \|B\boldsymbol{\theta} - \boldsymbol{\eta} - 2\pi\boldsymbol{K}\|_2^2,$$

which is purely quadratic and convex in $R_{\boldsymbol{K}}(\boldsymbol{\eta})$. For this reason, in each $R_{\boldsymbol{K}}(\boldsymbol{\eta})$ there

[2] $|\boldsymbol{v}| \leq \boldsymbol{p}$, where both $\boldsymbol{v}, \boldsymbol{p} \in \mathbb{R}^n$, means $-p_i \leq v_i < p_i$ for all $i = 1, \ldots, n$.

can be at most one local minimum of $V(\boldsymbol{\theta})$. Notice that by the way $\boldsymbol{\eta}$ has been defined,

$$|B\bar{\boldsymbol{\theta}} - \boldsymbol{\eta} - 2\pi\bar{\boldsymbol{K}}| = |\boldsymbol{\varepsilon}| \leq \pi\mathbf{1} \tag{5.18}$$

so that $\bar{\boldsymbol{\theta}} \in R_{\bar{\boldsymbol{K}}}(\boldsymbol{\eta})$. If we have obtained an estimation $\hat{\boldsymbol{K}}$ such that $\hat{\boldsymbol{K}} = \bar{\boldsymbol{K}} + B\boldsymbol{l}$ for some $\boldsymbol{l} \in \mathbb{Z}^N$, then, clearly, $\bar{\boldsymbol{\theta}} + 2\pi\boldsymbol{l} \in R_{\hat{\boldsymbol{K}}}(\boldsymbol{\eta})$.

The main idea is thus the following: first of all, obtain a reasonable estimate $\hat{\boldsymbol{K}}$ of $\bar{\boldsymbol{K}}$. Then minimize the reshaped cost

$$V_{\hat{\boldsymbol{K}}}(\boldsymbol{\theta}) := \|B\boldsymbol{\theta} - \boldsymbol{\eta} - 2\pi\hat{\boldsymbol{K}}\|_2^2 \tag{5.19}$$

which is defined by first restricting $V(\boldsymbol{\theta})$ to the region $R_{\hat{\boldsymbol{K}}}(\boldsymbol{\eta})$ and then extending the quadratic form to $\mathbb{R}^N$.

A simple continuity argument then shows that, when the threshold $\bar{\varepsilon}$ tends to 0, the estimation $\hat{\boldsymbol{\theta}}$ converges to $\bar{\boldsymbol{\theta}} + 2\pi\boldsymbol{l}$. In other terms, with such a $\hat{\boldsymbol{K}}$, we have a guarantee that our solution is close to a feasible one, namely to a representative of the true $\bar{\boldsymbol{\theta}}$. In Section 5.4, we will analyze in deeper detail the performance of the algorithms.

Calibration as noisy consensus

The cost function

$$V(\boldsymbol{\theta}) = \|(B\boldsymbol{\theta} - \boldsymbol{\eta})_{2\pi}\|_2^2$$

has an interpretation in terms of consensus. In fact, once we perform the change of variables

$$\boldsymbol{x} = \boldsymbol{\theta} - \bar{\boldsymbol{\theta}}$$

it is easy to see that

$$V(\boldsymbol{x}) = \|(B\boldsymbol{x} - \boldsymbol{\varepsilon})_{2\pi}\|_2^2$$

In the Euclidean space, namely dropping the modulo 2π, a gradient descend for this cost is

$$\dot{\boldsymbol{x}}(t) = -\varepsilon B^T(B\boldsymbol{x} - \boldsymbol{\varepsilon})$$

which elementwise becomes

$$\dot{x}_k(t) = -\varepsilon \sum_{j \in \mathcal{N}_k} (x_k(t) - x_j(t) - \varepsilon_{kj})$$

This consensus protocol is the noisy version of the first discrete time algorithm proposed in Section 3.2. Notice that the effect of the noise is to make two agents appear more

distant (or closer) then what they are.

5.4 Some tools from graph theory

In this section we recall some known facts from algebraic graph theory not to included in Chapter 2 which will be instrumental in proving effectiveness of our algorithms.

Given a graph $\mathcal{G} = (\mathcal{V}, \mathcal{E})$, a spanning tree $\mathcal{T} = (\mathcal{V}, \mathcal{E}_\mathcal{T})$ of $\mathcal{G} = (\mathcal{V}, \mathcal{E})$ is simply a subgraph of $\mathcal{G}$ which is a tree. Notice that $|\mathcal{E}_\mathcal{T}| = N - 1$.

Changing slightly the definition, in this section a path h of length n is an ordered sequence of nodes $h = (v_1, v_2, \cdots, v_{n+1})$ such that $\{v_i, v_{i+1}\} \in \mathcal{E}$ for all $i = 1, \ldots, n$. A path $h = (v_1, v_2, \cdots, v_{n+1})$ is said to be closed if $v_1 = v_{n+1}$. A closed path $h = (v_1, v_2, \cdots, v_n, v_1)$ is said to be a cycle if $n \geq 3$ and $v_i \neq v_j$ for all $i, j \in \{1, \ldots, n\}$ with $i \neq j$. The support of a path is given by the set of its edges, namely, if $h = (v_1, v_2, \cdots, v_{n+1})$, then $\mathrm{supp}(h) := \{e \in \mathcal{E} \,|\, e = \{v_i, v_{i+1}\},\ \exists i = 1, \ldots, n\}$.

Consider now the $\mathbb{Z}$-module of $\mathbb{Z}^M$ of row vectors with elements in $\mathbb{Z}$. Given $\boldsymbol{r} \in \mathbb{Z}^M$, we define it support as

$$\mathrm{supp}(\boldsymbol{r}) := \{e \in \mathcal{E} \,|\, \boldsymbol{r}(e) \neq 0\}$$

We now associate to every path h, an element $r_h \in \mathbb{Z}^M$ as follows. First, if $h = (v_1, v_2)$, we put

$$r_h(e) = \begin{cases} B_{ev_1} & \text{if } e = \{v_1, v_2\} \\ 0 & \text{otherwise} \end{cases}$$

Then, for a generic path $h = (v_1, v_2, \cdots, v_{n+1})$ we put $r_h(e) = \sum_{i=1}^{n} r_{(v_i, v_{i+1})}(e)$.

Denote now by Γ the $\mathbb{Z}$-submodule of $\mathbb{Z}^M$ generated by all the vectors r_h as h varies in the set of closed paths. It holds true that Γ has dimension equal to $M - N + 1$. This fact is very well known in the slight different context where no orientation is considered and where vector spaces are used [14]; in our setting it will be a consequence of the considerations below which will also lead to the explicit construction of a $\mathbb{Z}$-basis for Γ.

Fix a spanning tree $\mathcal{T} = (\mathcal{V}, \mathcal{E}_\mathcal{T})$ of $\mathcal{G}$. Order arbitrarily the edges in $\mathcal{E} \setminus \mathcal{E}_\mathcal{T}$ as $e_1, \ldots, e_{M-N+1}$ and consider cycles $h_1, \ldots, h_{M-N+1}$ in $\mathcal{G}$ such that for each i we have that $\mathrm{supp}(h_i) \subseteq \mathcal{E}_\mathcal{T} \cup \{e_1, \ldots, e_i\}$ and $\boldsymbol{r}_{h_i}(e_i) = 1$. In words the cycle h_i is constructed with the edges in $\mathcal{E}_\mathcal{T} \cup \{e_1, \ldots, e_i\}$ containing e_i and oriented in such a way that $\boldsymbol{r}_{h_i}(e_i) = 1$.

We have the following result whose proof is given in the appendix.

Proposition 5.4.1. *We have that* $\Gamma = \{\boldsymbol{r} \in \mathbb{Z}^M \,|\, \boldsymbol{r}B = 0\}$ *and* $\{\boldsymbol{r}_{h_1}, \ldots \boldsymbol{r}_{h_{M-N+1}}\}$ *is a* $\mathbb{Z}$*-basis of it.*

We now propose two particular ways to select the family cycles $h_1, \ldots, h_{M-N+1}$

introduced above. The simplest way is to take h_i to be the only cycle in $\mathcal{G}$ with edges in $\mathcal{E}_\mathcal{T} \cup \{e_i\}$ and such that $\boldsymbol{r}_{h_i}(e_i) = 1$. Such cycles are called *($\mathcal{T}$-)fundamental cycles*.

Another possible construction is the following iterative one:

- Among all cycles whose edges are all in $\mathcal{E}_\mathcal{T}$ except one, choose one of minimal length. Call it h_1 and call e_1 the only edge in h_1 which is not in $\mathcal{E}_\mathcal{T}$.
- Suppose edges $e_1, \ldots, e_i$ and cycles $h_1, \ldots, h_i$ have been selected. Among all cycles whose edges are all in $\mathcal{E}_\mathcal{T} \cup \{e_1, \ldots e_i\}$ except one, choose one of minimal length. Call it h_{i+1} and call e_{i+1} the only edge in h_{i+1} which is not in $\mathcal{E}_\mathcal{T} \cup \{e_1, \ldots e_i\}$.

We will refer to this set of cycles as a set of *minimal cycles*.

From now on we will assume that a spanning tree $\mathcal{T}$ has been fixed. Once the spanning tree is fixed, we can construct a set of minimal cycles, denoted by $h_1^M, \ldots, h_{M-N+1}^M$, which will impose an order $e_1, \ldots, e_{M-N+1}$ on the edges in $\mathcal{E} \setminus \mathcal{E}_\mathcal{T}$. Finally from this order we can determine a set of fundamental cycles, denoted by $h_1^F, \ldots, h_{M-N+1}^F$. The corresponding row vectors associated with minimal and fundamental cycles will be denoted $\boldsymbol{r}_i^M$ and $\boldsymbol{r}_i^F$, respectively. A straightforward consequence of Proposition 5.4.1 is that there exist elements $t_{ij} \in \mathbb{Z}$ for $1 \leq i, j \leq M - N + 1$ such that

$$\boldsymbol{r}_i^F = \sum_{i,j} t_{ij} \boldsymbol{r}_j^M \tag{5.20}$$

for every $i = 1, \ldots, M - N + 1$. It can be shown that $t_{ii} = 1$ for all i and that $t_{ij} = 0$ if $j > i$.

Let R^F, $R^M \in \mathbb{Z}^{(M-N+1 \times \mathcal{E}}$ be the matrices having as rows the vectors $\boldsymbol{r}_i^F$ and $\boldsymbol{r}_i^M$ respectively. Clearly, (5.20) can be rewritten in matrix form as $R^F = TR^M$ where T is the square matrix having t_{ij} as entries.

Interpreting R^M and R^F as $\mathbb{Z}$-homomorphisms acting on $\mathbb{Z}^M$ and the incidence matrix B as a group homomorphism from $\mathbb{Z}^N$ to $\mathbb{Z}^M$, we have the following result.

Lemma 5.4.2. *It holds* $\ker R^M = \ker R^F = \mathrm{Im} B$.

Description of the algorithms

Both algorithms we now describe are based on the idea illustrated above of breaking the estimation problem into two steps: first give an estimate $\hat{\boldsymbol{K}}$ of $\bar{\boldsymbol{K}}$ and then minimize the quadratic function defined in Eq. 5.19. The two algorithms only differ in the first step, since the first one uses the fundamental cycles with respect to a chosen spanning tree, the second one instead the minimal cycles.

Regarding the first step, the main idea underlying both algorithms exploits the fact that the relative differences of the actual orientations $\bar{\theta}_v$ along a cycle must necessarily sum up to a multiple of 2π. More precisely, let h be an oriented cycle and let $\boldsymbol{r}_h$ be its representative vector. Then, from Eq. 5.15, using the fact that $\boldsymbol{r}_h B = 0$, we obtain that $\boldsymbol{r}_h \bar{\boldsymbol{K}} = -q_{2\pi}(\boldsymbol{r}_h \boldsymbol{\eta}) - q_{2\pi}(\boldsymbol{r}_h \boldsymbol{\varepsilon})$. Therefore, if it happens that the algebraic sum of the noise along the cycle h is below π in modulus, i.e. $|\boldsymbol{r}_h \boldsymbol{\varepsilon}| < \pi$, we obtain that

$$\boldsymbol{r}_h \bar{\boldsymbol{K}} = -q_{2\pi}(\boldsymbol{r}_h \boldsymbol{\eta}). \tag{5.21}$$

In other terms, in this case $\boldsymbol{r}_h \bar{\boldsymbol{K}}$ can be exactly computed on the basis of the measurements $\boldsymbol{\eta}$ along the cycle h. This would suggest to define $\hat{\boldsymbol{K}}$ in such a way that $\boldsymbol{r}_h \hat{\boldsymbol{K}} = -q_{2\pi}(\boldsymbol{r}_h \boldsymbol{\eta})$ for any cycle h, but this in general will not be possible since the various $\boldsymbol{r}_h$'s are linearly dependent. What must be done is to restrict the cycles to a subset for which the corresponding $\boldsymbol{r}_h$'s form a $\mathbb{Z}$-basis for the $\mathbb{Z}$-module Γ (generated, we recall, by the rows $\boldsymbol{r}_h$'s). The choice of this basis is the essential difference among the two algorithms.

The Tree-algorithm

Fix a spanning graph $\mathcal{T}$ and consider the $\mathbb{Z}$-basis relative to the fundamental cycles construction $\boldsymbol{r}_i^F$'s. Let us impose that $\boldsymbol{r}_i^F \hat{\boldsymbol{K}} = -q_{2\pi}(\boldsymbol{r}_i^F \boldsymbol{\eta})$ for any i. From Lemma 5.4.2 we know that this determines $\hat{\boldsymbol{K}}$ up to elements in the image of B as required. A concrete solution can be easily found by imposing $\hat{\boldsymbol{K}}_e = 0$ for every $e \in \mathcal{E}_{\mathcal{T}}$. Then, we easily obtain that, for any $i = 1, \ldots, M - N + 1$,

$$\hat{K}_{e_i} = -q(\boldsymbol{r}_i^F \boldsymbol{\eta})$$

This algorithm is very simple and easily implementable. As we will point out, however, its performances are for large graphs rather poor. A distributed way to compute $\hat{\boldsymbol{K}}$ is proposed below. Fix an anchor node, denoted by v^*, which will serve as a root in the tree $\mathcal{T}$. First of all, we propagate the measurements along the tree starting from the root, namely, given a node v and called $f(v)$ its father, we set

$$\hat{\theta}_{FE,\,v} = \hat{\theta}_{FE,\,f(v)} + \eta_{vf(v)}$$

initializing the value at the root as $\hat{\theta}_{FE,\,v^*} = \bar{\theta}_{v^*}$, if it is available, or simply $\hat{\theta}_{FE,\,v^*} = 0$. As a side effect, in this way, we also obtain a first estimate $\hat{\boldsymbol{\theta}}_{FE}$ of $\bar{\boldsymbol{\theta}}$.

Now we construct $\hat{\boldsymbol{K}}$. For each edge $e = \{t(e), h(e)\} \in \mathcal{E} \setminus \mathcal{E}_{\mathcal{T}}$, the nodes $t(e)$ and

$h(e)$ exchange their first estimates $\hat{\theta}_{FE,t(e)}$, $\hat{\theta}_{FE,h(e)}$ and compute $\hat{K}_e$ as

$$\hat{K}_e = \left\lfloor \frac{\hat{\theta}_{FE,t(e)} - \hat{\theta}_{FE,h(e)} - \eta_e}{2\pi} \right\rceil .$$

This is actually the only choice of $\hat{\boldsymbol{K}}$ for which $\hat{\boldsymbol{\theta}}_{FE} \in R_{\hat{\boldsymbol{K}}}(\boldsymbol{\eta})$.
Finally we obtain a final estimate of $\bar{\boldsymbol{\theta}}$, call it $\hat{\boldsymbol{\theta}}$, by minimizing the quadratic cost function in Eq. 5.19. This problem can be for example easily solved using a distributed Jacobi algorithm as shown in [141, 86].

Algorithm 1 Tree-Algorithm

(Input variables)
$\bar{\theta}_{v^*}$, value of the anchor
$\eta_e, e = 1, \dots, M$
$\mathcal{T}$ spanning tree

(Step A: first estimate $\hat{\boldsymbol{\theta}}_{FE}$)
$\hat{\theta}_{FE,v^*} = \bar{\theta}_{v^*}$;
for $i = 1, \dots, N$ **do**
  for $j = 2, \dots, N$ **do**
    if j is a son of i in $\mathcal{T}$ **then** $\hat{\theta}_{FE,j} = \hat{\theta}_{FE,i} + \eta_{j,i}$

(Step B: estimate $\hat{\boldsymbol{K}}$)
for $e \in \mathcal{E}$ **do**
  $\hat{K}_e = \left\lfloor \frac{\hat{\theta}_{FE,t(e)} - \hat{\theta}_{FE,h(e)} - \eta_e}{2\pi} \right\rceil$

(Step C: second estimate $\hat{\boldsymbol{\theta}}$)
Initial condition: $\hat{\boldsymbol{\theta}}(0) = \hat{\boldsymbol{\theta}}_{FE}$
compute $\hat{\boldsymbol{\theta}} = \operatorname{argmin} \left\| B\boldsymbol{\theta} - \boldsymbol{\eta} - 2\pi\hat{\boldsymbol{K}} \right\|_2^2$

Minimal cycles-algorithm

The second algorithm exploits instead the minimal cycles construction of a $\mathbb{Z}$-basis for Γ denoted, we recall, $\boldsymbol{r}_i^M$'s.
Let us impose that $\boldsymbol{r}_i^M \hat{\boldsymbol{K}} = -q_{2\pi}(\boldsymbol{r}_i^M \boldsymbol{\eta})$ for any i. From Lemma 5.4.2 we know that this determines $\hat{\boldsymbol{K}}$ up to elements in the image of B as required.
A concrete method for constructing such $\hat{\boldsymbol{K}}$ once the values $-q_{2\pi}(\boldsymbol{r}_i^M \boldsymbol{\eta})$ have been computed for every i, can be easily based on Proposition 5.4.1. We start, as in the

previous case, assigning $\hat{K}_e = 0$ on the edges in $\mathcal{E}_{\mathcal{T}}$. We then consider the remaining edges $e_1, e_2, \ldots, e_{M-N+1}$ and we define $\hat{\boldsymbol{K}}$ iteratively as

$$\hat{K}_{e_i} = -q(\boldsymbol{r}_i^M \boldsymbol{\eta}) - \sum_{e \neq e_i} \boldsymbol{r}_i^M(e) \hat{K}_e. \tag{5.22}$$

The last step of the *Minimal cycle-algorithm* is the same as that of the *Tree-algorithm*. The only difference being that, if we want to use iterative algorithms, the initial condition cannot be set to some particular value, so it is taken to be $(0, \ldots, 0)$ for simplicity.

Algorithm 2 Minimal cycles-algorithm

(Input variables)
1: $\eta_e, e = 1, \ldots, M$
2: $\mathcal{T}$ spanning tree
3: $\boldsymbol{r}_1, \ldots, \boldsymbol{r}_{M-N+1}$ minimal cycles set

(Step A: computation of $\boldsymbol{b} = -q_{2\pi}(R^M \boldsymbol{\eta})$)
4: **for** $i = 1, \ldots, M - N + 1$ **do** $b_{h_i} = -\left\lfloor \frac{\sum_{e \in h_i} \eta_e + \pi}{2\pi} \right\rfloor$

(Step B: estimate $\hat{\boldsymbol{K}}$)
5: **for** $e \in \mathcal{E}_{\mathcal{T}}$ **do** $\hat{K}_e = 0$
6: **for** $i = 1, \ldots, M - N + 1$ **do** $\hat{K}_{\bar{e}} = b_{h_i} - \sum_{e \in h_i, e \neq \bar{e}} \boldsymbol{r}_{h_e}(e) \hat{K}_e$

(Step C: second estimate $\hat{\boldsymbol{\theta}}$)
7: Initial condition: $\hat{\boldsymbol{\theta}}(0) = (0, \ldots, 0)$
8: compute $\hat{\boldsymbol{\theta}} = \operatorname{argmin} \left\| B\boldsymbol{\theta} - \boldsymbol{\eta} - 2\pi \hat{\boldsymbol{K}} \right\|_2^2$

This second algorithm allows much better performances than the *Tree-algorithm*, but it requires a greater order of communication and collaboration among nodes. In fact, we assume that, through some local collaboration among nodes, each minimal cycle corresponds to a "superagent", able to sense all the measurements along the edges of its cycle. Clearly, this is far more than just locally exchanging information.

Let us illustrate how the *Minimal cycles-algorithm* works with the following simple example.

Example 5.4.3. Consider the simple graph in Fig. 5.8. There $h_1, \ldots, h_5$ are minimal cycles and $1, \ldots, 13$ are edges. Assume that $b_1 = 1$, $b_2 = 2$, $b_3 = \cdots = b_5 = 0$, where $\boldsymbol{b} = -q_{2\pi}(R_0 \boldsymbol{\eta})$. The edges $1, \ldots, 8$ form a spanning tree $\mathcal{T}$ of the graph. First of all, thus, $\hat{K}_1 = \ldots \hat{K}_8 = 0$. Now, the cycles h_1 and h_2 are made of edges of the tree apart

from the edges 9 and 10 respectively. Thus h_1 sets $\hat{K}_9 = 1$ while h_2 sets $\hat{K}_{10} = -2$, since the direction of 10 is incoherent with the orientation of h_2. Once this is done, we know the value of $\hat{\boldsymbol{K}}$ of all the edges of h_3 and h_4, apart from 12 and 11 respectively. In order the sum over the cycles to be equal to b_3 and b_4, we obtain $\hat{K}_{12} = -1$ and $\hat{K}_{11} = 2$. At last, all the edges of h_5 have a value apart from 13, so it is set $\hat{K}_{13} = -1$. Now the sum of $\hat{\boldsymbol{K}}$ over the five minimal cycles correspond entry by entry to $\boldsymbol{b}$.

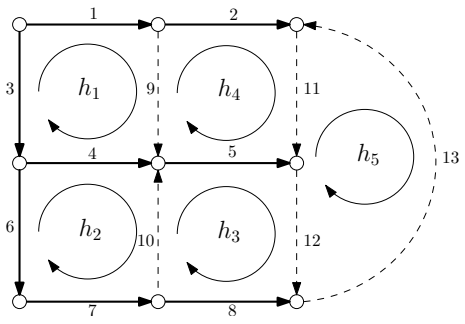

Figure 5.8: A simple graph to show how the second algorithm works.

Analysis and comparison of the algorithms

In this section we analyze the estimation $\hat{\boldsymbol{\theta}}$ for both algorithms and we make a comparison. Both algorithms propose a solution in two steps: first they construct the estimation $\hat{\boldsymbol{K}}$, then they derive the estimation $\hat{\boldsymbol{\theta}}$. We will first analyze the dependence of $\hat{\boldsymbol{\theta}}$ on $\hat{\boldsymbol{\theta}}$. Secondly, by means of closed formulae, a comparison between the estimates $\hat{\boldsymbol{K}}$ given by the two algorithms is provided. Finally we state a deterministic threshold for the noise in order to guarantee a correct estimate of $\bar{\boldsymbol{K}}$.

In both algorithms the estimate $\hat{\boldsymbol{\theta}}$ is defined to minimize the cost $V_{\hat{\boldsymbol{K}}}(\boldsymbol{\theta}) = \|B\boldsymbol{\theta} - \boldsymbol{\eta} - 2\pi\hat{\boldsymbol{K}}\|_2^2$. Since B has a kernel (which is spanned by $\mathbf{1}$[3]) of course $\hat{\boldsymbol{\theta}}$ is only determined up to multiples of $\mathbf{1}$. This non uniqueness can be avoided as follows. As already done in the previous Section, fix an anchor node $v^* \in \mathcal{V}$ that knows the true value of its orientation, and assume that it never changes its estimate. Then consider the vector $\boldsymbol{\xi} \in \mathbb{R}^N$ defined by $\xi(v^*) = 1$ and $\xi(v) = 0$ for any $v \neq v^*$. Now define the Green matrix associated to $\mathcal{G}$ and v^* as the solution of the following equations

$$\begin{cases} GB^TB = I - \mathbf{1}\boldsymbol{\xi}^T \\ G\boldsymbol{\xi} = 0. \end{cases} \tag{5.23}$$

[3] $\mathbf{1}$ represents a vector of suitable dimension whose entries are all equal to 1.

Writing down the stationary point equation for our quadratic problem and using the Green function we have just defined, it is straightforward to show that the following result holds true.

Proposition 5.4.4. *The minimum of $V_{\hat{\boldsymbol{K}}}(\boldsymbol{\theta})$ is attained at*

$$\hat{\boldsymbol{\theta}} = \bar{\boldsymbol{\theta}} - GB^T\boldsymbol{\varepsilon} - 2\pi GB^T(\bar{\boldsymbol{K}} - \hat{\boldsymbol{K}}). \tag{5.24}$$

Notice that, if $\hat{\boldsymbol{K}} = \bar{\boldsymbol{K}} + B\boldsymbol{l}$, with $\boldsymbol{l} \in \mathbb{Z}^N$, it is immediate to see that

$$\hat{\boldsymbol{\theta}} = \bar{\boldsymbol{\theta}} + 2\pi(I - \mathbf{1}\boldsymbol{\xi}^T)\boldsymbol{l} - GB^T\boldsymbol{\varepsilon} = \tilde{\boldsymbol{\theta}} - GB^T\boldsymbol{\varepsilon}$$

where $\tilde{\boldsymbol{\theta}} = \bar{\boldsymbol{\theta}} + 2\pi(I - \mathbf{1}\boldsymbol{\xi}^T)\boldsymbol{l}$ is a representative of $\bar{\boldsymbol{\theta}}$.

A natural choice for the performance index can be

$$\mathcal{E}(\hat{\boldsymbol{\theta}}) := \inf\{||\hat{\boldsymbol{\theta}} - \bar{\boldsymbol{\theta}} - 2\pi\boldsymbol{l}||_2 \mid \boldsymbol{l} \in \mathbb{Z}^N\}$$

and from (5.24) we can derive the estimation:

$$\mathcal{E}(\hat{\boldsymbol{\theta}}) \leq ||GB^T\boldsymbol{\varepsilon}||_2 + 2\pi \inf\{||GB^T(\hat{\boldsymbol{K}} - \bar{\boldsymbol{K}} - B\boldsymbol{l})||_2 \mid l \in \mathbb{Z}^N\}. \tag{5.25}$$

This illustrates how $\mathcal{E}(\hat{\boldsymbol{\theta}})$ is made of two terms. The first one, $||GB^T\boldsymbol{\varepsilon}||_2$, is unavoidable and only depends on the fact that the measurements are noisy. This term is the localization error in the works by Barooah and Hespanha on $\mathbb{R}^N$. The second term, instead, depends on the estimation $\hat{\boldsymbol{K}}$, and it is due to the geometry of $\mathcal{S}_1$.

To deepen the analysis of the second term, we need to work more on the graph theoretic side. We assume as before to have fixed an undirected graph $\mathcal{G} = (\mathcal{V}, \mathcal{E})$ equipped with an orientation $s : \mathcal{E} \to \mathcal{V}$ and $t : \mathcal{E} \to \mathcal{V}$ and a spanning sub-tree $\mathcal{T} = (\mathcal{V}, \mathcal{E}_\mathcal{T})$ with an anchor v^*. The incidence matrix $B \in \mathbb{Z}^{M\times N}$ of $\mathcal{G}$ can be partitioned by ordering edges in such a way that first to appear are those in $\mathcal{E}_\mathcal{T}$, and ordering vertices such that the anchor v^* is the first one. We obtain

$$B = \begin{bmatrix} B_\mathcal{T} \\ B_{\mathcal{T}^c} \end{bmatrix} = \begin{bmatrix} -\bar{B}_\mathcal{T}\mathbf{1} & \bar{B}_\mathcal{T} \\ -\bar{B}_{\mathcal{T}^c}\mathbf{1} & \bar{B}_{\mathcal{T}^c} \end{bmatrix}$$

where $\bar{B}_\mathcal{T} \in \mathbb{Z}^{|\mathcal{E}_\mathcal{T}|\times N-1}$, and $\bar{B}_{\mathcal{T}^c} \in \mathbb{Z}^{M-N+1\times N-1}$. It is a standard fact that $\bar{B}_\mathcal{T}$ is invertible and the following characterization of $\bar{B}_\mathcal{T}^{-1}$ holds true. For the sake of completeness a proof is reported in the appendix.

Lemma 5.4.5. *For any $k \neq v^*$ and $e \in E_{\mathcal{T}}$, we have*

$$[\bar{B}_{\mathcal{T}}^{-1}]_{ke} = \begin{cases} -1, & \text{if } e \text{ is in the path from } v^* \text{ to } k \text{ in } \mathcal{T} \\ 0, & \text{otherwise.} \end{cases} \tag{5.26}$$

We have the following result

Lemma 5.4.6. *It holds true that*

$$R^F = \begin{bmatrix} -\bar{B}_{\mathcal{T}^c}\bar{B}_{\mathcal{T}}^{-1} & I \end{bmatrix} \tag{5.27}$$

interpreting the identity matrix $I \in \mathbb{Z}^{M-N+1\times M-N+1}$.

Below, we will consider on the vector $\bar{\boldsymbol{K}}$ the relative splitting

$$\bar{\boldsymbol{K}} = (\bar{\boldsymbol{K}}_{\mathcal{T}}, \bar{\boldsymbol{K}}_{\mathcal{T}^c})$$

where $\bar{\boldsymbol{K}}_{\mathcal{T}} \in \mathbb{Z}^{N-1}$, $\bar{\boldsymbol{K}}_{\mathcal{T}^c} \in \mathbb{Z}^{M-N+1}$.

We now come to the main result in this section which give closed formulas for the estimations $\hat{\boldsymbol{K}}^F$ and $\hat{\boldsymbol{K}}^M$, obtained using, respectively, the fundamental and the minimal cycles algorithm based on the same spanning tree $\mathcal{T}$. Define

$$Q := \begin{bmatrix} 0 \\ T \end{bmatrix} \in \{\pm 1, 0\}^{M\times M-N+1}. \tag{5.28}$$

where, recall T is the matrix which transforms the base for Γ written in terms of the fundamental cycles, into the one written in terms of minimal cycles.

Proposition 5.4.7. *The following relations hold:*

$$\begin{aligned} \hat{\boldsymbol{K}}^F &= \bar{\boldsymbol{K}} + B\boldsymbol{l} + q_{2\pi}\left(QR^M\boldsymbol{\varepsilon}\right) \\ \hat{\boldsymbol{K}}^M &= \bar{\boldsymbol{K}} + B\boldsymbol{l} + Qq_{2\pi}\left(R^M\boldsymbol{\varepsilon}\right) \end{aligned} \tag{5.29}$$

where

$$\boldsymbol{l} := -\begin{bmatrix} 0 \\ \bar{B}_{\mathcal{T}}^{-1} \end{bmatrix} \bar{\boldsymbol{K}}_{\mathcal{T}}.$$

Proof. Let us focus on the first estimate, and recall that by construction $R^F\hat{\boldsymbol{K}}^F = -q_{2\pi}(R^F\eta)$ and $(\hat{\boldsymbol{K}}^F)_e = 0$ for every $e \in \mathcal{E}_{\mathcal{T}}$. From this we obtain

$$\hat{\boldsymbol{K}}^F = -\begin{bmatrix} 0 \\ I \end{bmatrix} q(R^F\eta) = q\left(\begin{bmatrix} 0 \\ R^F \end{bmatrix}\epsilon\right) + \begin{bmatrix} 0 \\ R^F\bar{\boldsymbol{K}} \end{bmatrix}. \tag{5.30}$$

Using now Lemma 5.27 we obtain

$$\begin{bmatrix} 0 \\ R^F \bar{\boldsymbol{K}} \end{bmatrix} = \begin{bmatrix} 0 \\ -\bar{B}_{\mathcal{T}^c} \bar{B}_{\mathcal{T}}^{-1} \bar{\boldsymbol{K}}_{\mathcal{T}} + \bar{\boldsymbol{K}}_{\mathcal{T}^c} \end{bmatrix} = -B \begin{bmatrix} 0 \\ \bar{B}_{\mathcal{T}}^{-1} \end{bmatrix} \bar{\boldsymbol{K}}_{\mathcal{T}} + \bar{\boldsymbol{K}}. \tag{5.31}$$

Substituting (5.31) in (5.30), and recalling that $R^F = TR^M$, we obtain the thesis.

Regarding the second estimate, notice that, from Eq. (5.22) we obtain that $\hat{\boldsymbol{K}}^M$ satisfies the relations $R^M \hat{\boldsymbol{K}}^M = -q(R^M \boldsymbol{\eta})$. Hence, pre-multiplying by T and using again the definition of R^F, we obtain $\hat{\boldsymbol{K}}^M = -\begin{bmatrix} 0 \\ T \end{bmatrix} q(R^M \boldsymbol{\eta})$. The result now follows, substituting Eq. 5.15 and using again (5.31). □

Proposition 5.4.7 shows how the difference of the two algorithms only consist in an inversion of the two operators $q_{2\pi}$ and Q. However, this turns out to have a big difference on the way performance depends on noise. Below we find conditions for both algorithms under which the noise term in the relation (5.29) vanishes.

Let L_0 be the maximum length of a minimal cycle and $L_{\mathcal{T}}$ the maximum length of a $\mathcal{T}$-fundamental cycle.
It is clear that $L_0 \leq L_{\mathcal{T}}$, and in general $L_{\mathcal{T}}$ depends on the number of nodes of the graph, as the examples in Section 5.5 will point out. We present now the main result of this section, which basically gives a noise threshold for both algorithms, under which it is guaranteed to have $\hat{\boldsymbol{K}} - \bar{\boldsymbol{K}} \in \mathrm{Im}_{\mathbb{Z}} B$.

Corollary 5.4.8. *If*

$$\textit{Tree-algorithm}: \bar{\varepsilon} < \frac{\pi}{L_{\mathcal{T}}}$$
$$\textit{Minimal Cycles-algorithm}: \bar{\varepsilon} < \frac{\pi}{L_0}$$

we have

$$\hat{\boldsymbol{K}} = \bar{\boldsymbol{K}} + B\boldsymbol{l}, \boldsymbol{l} \in \mathbb{Z}^N.$$

Proof. The statement can be easily derived from the closed formulas in Eq. (5.29). Otherwise a proof can be achieved with the following easy observations. The two cases can be analyzed in the same exact way. Below we give a proof for the *Minimal cycles-algorithm*. Notice that the assumption implies that $\bar{\boldsymbol{K}}$ satisfies Eq. (5.21) for any minimal cycle $h_1, \ldots, h_{M-N+1}$. Since, by definition, also $\hat{\boldsymbol{K}}$ satisfies the same equation, we obtain that $R^M(\hat{\boldsymbol{K}} - \bar{\boldsymbol{K}}) = 0$. By invoking Lemma 5.4.2, the thesis follows. □

If the assumptions of Corollary 5.4.8 hold, we have as a straightforward consequence

$\hat{\boldsymbol{\theta}} = \tilde{\boldsymbol{\theta}} + GB^T\boldsymbol{\varepsilon}$, where $\tilde{\boldsymbol{\theta}}$ is a representative of $\bar{\boldsymbol{\theta}}$.

In this case the error term is exactly the same appearing in the vector space case and can be analyzed exploiting the probabilistic assumptions made on the noise, namely that $\varepsilon_e \sim \mathcal{U}[-\bar{\varepsilon}, \bar{\varepsilon}]$, $\forall\, e \in \mathcal{E}$. In case this holds, from paper [96] we can obtain an estimate of the variance of the final estimate error in terms of the effective resistance of a suitable electrical network. Namely, take an electrical network whose nodes are the nodes of the graph $\mathcal{G}$ and where there is a resistance of 1 Ohm among all nodes for which an edge exists in $\mathcal{G}$. Denote by $\mathcal{R}_{uv}$ the effective resistance among any pair of nodes u, $v \in \mathcal{V} \times \mathcal{V}$. Then we have the following result.

Proposition 5.4.9 ([96])**.** *The estimate $\hat{\boldsymbol{\theta}} = \tilde{\boldsymbol{\theta}} + GB^T\varepsilon$ is unbiased, namely $\mathbb{E}\hat{\boldsymbol{\theta}} = \tilde{\boldsymbol{\theta}}$, and its v-th component has variance*

$$\mathbb{E}[(\hat{\theta}_v - \tilde{\theta}_v)^2] = \mathcal{R}_{vv^*} \tag{5.32}$$

where v^* is the anchor. As a consequence, the normalized scalar estimation variance is

$$\frac{1}{N}\mathrm{var}(\hat{\boldsymbol{\theta}} - \tilde{\boldsymbol{\theta}}) = \frac{1}{N}\sum_{v\in\mathcal{V}} \mathcal{R}_{vv^*} \tag{5.33}$$

which is the average effective resistance among the anchor and the other nodes of the network.

Remark 5.4.10. The previous Proposition gives mean and variance of the estimation error $\boldsymbol{\delta} = \hat{\boldsymbol{\theta}} - \tilde{\boldsymbol{\theta}}$. However, this is not entirely correct, since what we are really interested in is $\boldsymbol{\delta}_{2\pi} = (\hat{\boldsymbol{\theta}} - \tilde{\boldsymbol{\theta}})_{2\pi}$, which has still zero mean, and variance less then that in Eq. (5.33). Nonetheless, if the noise is big and $\hat{\boldsymbol{\theta}}$ is not near $\tilde{\boldsymbol{\theta}}$, the probability to end up in a point near another representative of $\bar{\boldsymbol{\theta}}$ is intuitively very small, so we preferred to give only the results in Proposition 5.4.9.

In principle, Proposition 5.4.7 can be of interest in more general situations even when the noise term does not vanishes. If for instance, the noise term in (5.29) is zero except in a bounded number of edges (due to the error of few malfunctioning cameras), it should be possible to prove, coupling (5.29) with (5.24), that the estimation error far from the malfunctioning cameras is little affected by their measurements. This type of analysis is left for further research.

5.5 Examples

In this section we compare the two algorithms we have proposed for several different graph topologies. We concentrate on grid-like topologies since they can be used to model real networks of cameras.

First of all, we give a simple example of how our algorithms can avoid the local minima in the original cost. Consider the simple ring graph with 3 agents in Fig. 5.9, and assume $\bar{\theta}_1 = \bar{\theta}_2 = \bar{\theta}_3 = 0$ for sake of simplicity (the problem becomes thus consensus on $\mathcal{S}_1$). Consider the ideal noiseless case, so that $\eta_{12} = \eta_{23} = \eta_{31} = 0$ and $\bar{K}_{12} = \bar{K}_{23} = \bar{K}_{31} = 0$. In the noiseless case we correctly estimate $\hat{\boldsymbol{K}} = \bar{\boldsymbol{K}}$.
Consider the case in which we have as initial conditions $\hat{\theta}_1(0) = 0$, $\hat{\theta}_2(0) = \frac{2}{3}\pi$ and $\hat{\theta}_3(0) = \frac{4}{3}\pi$.

If we use directly the original cost in Eq. (5.16), it is easy to see that the initial condition is a local maximum (in case of 5 or more agents the analogous configuration is a local minimum), so any gradient-descent like algorithm gets stuck. However, if we reshape the cost using our guess $\hat{\boldsymbol{K}}$, we have to minimize $V_{\hat{\boldsymbol{K}}}(\boldsymbol{\theta}) = \|B\boldsymbol{\theta} - 2\pi\hat{\boldsymbol{K}}\|_2^2 = \|B\boldsymbol{\theta}\|_2^2$, and we converge to the actual orientations fixing the anchor at $\hat{\theta}_1 = \bar{\theta}_1 = 0$.

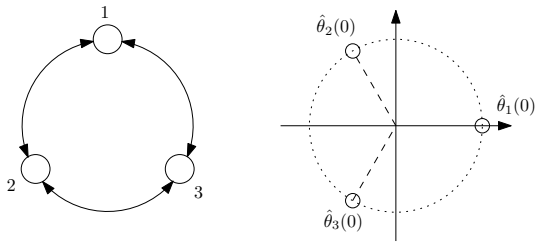

Figure 5.9: A simple ring with 3 agents. On the right the initial conditions.

In order to draw now a comparison among the two algorithms, consider the graphs shown in Fig.5.10. In both cases we have a line–like graph with many nodes deployed along one dimension, and the chosen spanning trees are shown in thick line. They are rooted on the anchor on the most left-top node. The set of the minimal cycles basis is simply the set of squares which form the graph.

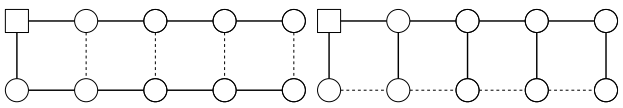

Figure 5.10: Two examples of spanning trees for a line–like graph. The proposed algorithms work in a similar manner for the one on the right, while the *Minimal cycles-algorithm* is far more effective for the one on the left.

For the graph on the left, if we take the tree and we add the last edge on the right we obtain a cycle with maximum length $L_{\mathcal{T}} = N$. On the contrary, the minimal cycles are of length $L_0 = 4$. As an immediate consequence, the *Minimal cycles-algorithm* has much better performances since the upper bound $\bar{\varepsilon} < \frac{\pi}{4}$ is independent on the number of nodes. On the contrary, in order the *Tree-algorithm* to produce a good estimate $\hat{\boldsymbol{K}}$, the magnitude of the noise should decrease with the dimension of the graph.

If we consider instead the spanning tree on the right, we can see that $L_{\mathcal{T}} = 4$ as well, since the spanning tree is chosen in a much better way. In this case, the two algorithms have comparable and good performance.

It is not always true, however, that the *Minimal cycles-algorithm* has good performances. For example, if we consider the ring graph in Fig. 5.11 we can easily see that there is only one minimal cycle. Here the two proposed algorithms basically coincide, comparing performances. In such a case, the *Tree-algorithm* is better, since it is easier to implement and completely distributed, it requires less information on the topology of the network, as well as less communications.
As a last example, consider the $2D$ grid on the right in Fig. 5.11. The comb-shaped spanning tree is the one in thick line. As before, here $L_{\mathcal{T}} \sim \sqrt{N}$ adding one of the edges on the bottom, while $L_0 = 4$. However, it can be shown that for the grid $L_{\mathcal{T}} \sim \sqrt{N}$ is actually the best one can do. So in this case the *Minimal cycles-algorithm* has always better performances than the *Tree-algorithm*. Notice that the choice of the spanning tree is fundamental to draw a comparison between the algorithms. Even if the tree is such that $L_{\mathcal{T}}$ is minimum, the choice of the better algorithm depends on the topology of the graph, since it could hold $L_{\mathcal{T}} > L_0$, as highlighted in the previous example. Furthermore the construction of such an optimal spanning tree is a NP-complete problem.

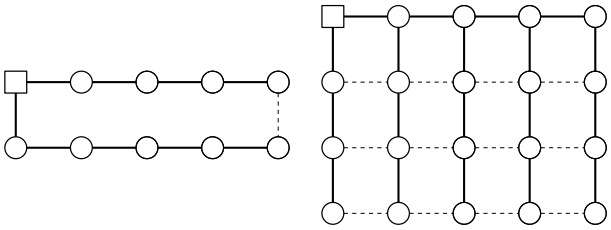

Figure 5.11: On the left a ring graph, for which the two algorithms have the same performance. On the right, a grid graph.

5.6 Numerical results

In this Section we provide a numerical comparison between the two approaches we propose in this paper. Specifically, in the experiments we simulate the *Tree-algorithm* and the *Minimal cycles-algorithm* on square grid graphs of size $N = n^2$ for n ranging from 3 up to 19. An example of square grid graph is depicted in Fig. 5.12 (left panel), where $n = 4$ and, in turn, $N = 16$.

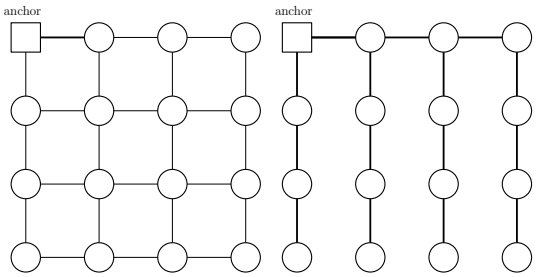

Figure 5.12: On the left a square grid graph for $n = 4$. On the right the correspondent spanning tree used in simulations.

In all our simulations we set $\bar{\theta}_1 = 0$, while, for $i \in \{2, \dots, N\}$, $\bar{\theta}_i$ is randomly sampled from a uniform distribution on $[-\pi, \pi]$. The values of the noises ε_e, $e \in \mathcal{E}$, are also randomly sampled, in this case from a uniform distribution on $[-\bar{\varepsilon}, \bar{\varepsilon}]$ where $\bar{\varepsilon} = \frac{\pi}{8}$.

The simulation results obtained are reported in Fig. 5.13. For each n the values we plot are averaged over 200 trials (a different $\bar{\boldsymbol{\theta}}$ and a different set of noises are generated for each trial).
The kind of spanning tree we use to run our algorithms is illustrated in Figure 5.13. Here we have $n = 4$, but for different values of n the spanning tree used is similarly built. Observe that, for the square grid graphs and the corresponding spanning tree we consider, we have $L_0 = 4$ independently from n, and $L_{\mathcal{T}} = 2n + 2$.

In Fig. 5.13, left panel, we show the value of the estimate error $e = \frac{1}{N}\|(\bar{\boldsymbol{\theta}} - \hat{\boldsymbol{\theta}})_{2\pi}\|^2$ for both the *Tree-algorithm* and the *Minimal cycles-algorithm*; in Fig. 5.13, right panel, we plot the value $e_K = \frac{1}{M}\|(\bar{\boldsymbol{K}} - \hat{\boldsymbol{K}})_{\mathrm{Im}_{\mathbb{Z}}B}\|^2$, where if $\boldsymbol{X} \in \mathbb{Z}^M$, $(\boldsymbol{X})_{\mathrm{Im}_{\mathbb{Z}}B}$ represents the projection out of the $\mathbb{Z}$-submodule spanned by the columns of B. This quantity is taken as a measure of the distance between the actual value $\bar{\boldsymbol{K}}$ and the estimates obtained through the algorithms. Notice that, since

$$\frac{\pi}{L_0} = \frac{\pi}{4} > \frac{\pi}{8} = \bar{\varepsilon}$$

it follows from Corollary 5.4.8 that the *Minimal cycles-algorithm* always correctly esti-

mates $\bar{\boldsymbol{K}}$, thus $e_K = 0$. On the contrary, observe that in the case of the *Tree-algorithm* e_K is increasing with the dimension of the graph. This is not surprising since $L_{\mathcal{T}}$ grows linearly with $\sqrt{N}$, and so intuitively the probability of the estimate to be bad becomes larger and larger.

As expected, one can check from Fig. 5.13 that the *Minimal cycles-algorithm* outperforms the *Tree-algorithm*. Also, it is not unexpected the log-shaped behavior of the norm of the error when the minimal cycles is used, as predicted by Proposition 5.4.9 and known behaviors of the variance for $2 - D$ graphs [96].

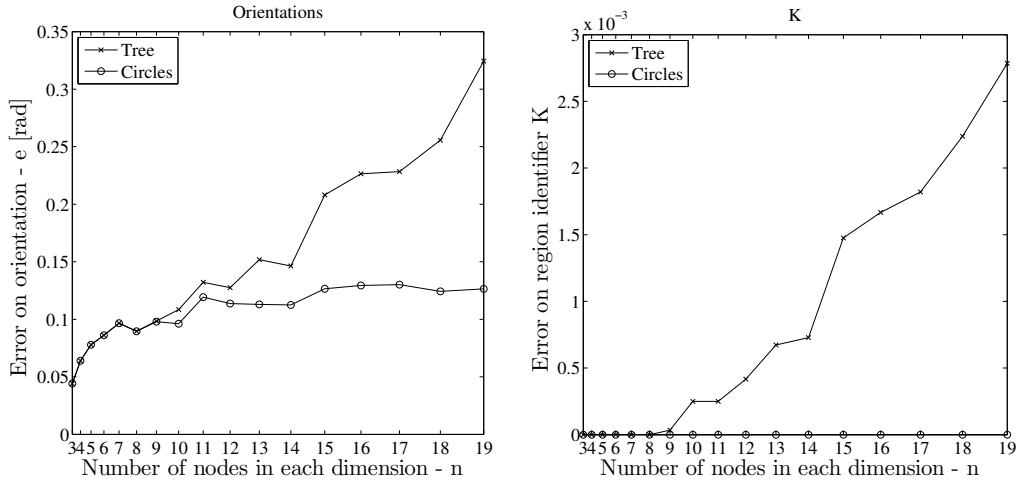

Figure 5.13: Left panel: Average error on the orientations (modulo 2π). Right panel: Average error on $\hat{\boldsymbol{K}}$.

Proofs of Lemmas

In this paragraph we give some algebraic properties of the row vectors $\boldsymbol{r}_h$ associated with the paths h. Start by observing that,

$$(\boldsymbol{r}_{(v_1,v_2)}B)_v = \sum_{e\in\mathcal{E}} \boldsymbol{r}_{(v_1,v_2)}(e)B_{ev} = B_{\{v_1,v_2\},v}B_{\{v_1,v_2\},v} = \begin{cases} 1, & \text{if } v = v_1 \\ -1, & \text{if } v = v_2 \\ 0, & \text{if } v \neq v_1, v_2. \end{cases}$$

In other words $\boldsymbol{r}_{(v_1,v_2)}B = \mathbf{1}_{v_1} - \mathbf{1}_{v_2}$, where the symbol $\mathbf{1}_v$ means the column vector in $\mathbb{R}^{\mathcal{V}}$ with the entry of position v equal to 1 and all the other entries equal to 0. Observe

moreover that, if $h = (v_1, v_2, \cdots v_n, v_{n+1})$, then

$$\boldsymbol{r}_h B = \sum_{i=1}^{n} \boldsymbol{r}_{(v_i, v_{i+1})} B = \sum_{i=1}^{n} \mathbf{1}_{v_i} - \mathbf{1}_{v_{i+1}} = \mathbf{1}_{v_1} - \mathbf{1}_{v_{n+1}}$$

which proves that, if h is a closed path, then $\boldsymbol{r}_h B = 0$.

Proof of Proposition 5.4.1. (a) The fact that $\Gamma \subseteq \{\boldsymbol{r} \in \mathbb{Z}^M \,|\, \boldsymbol{r}B = 0\}$ follows from the previous arguments.

(b) We now prove that the $\boldsymbol{r}_{h_i}$'s generate $\{\boldsymbol{r} \in \mathbb{Z}^M \,|\, \boldsymbol{r}B = 0\}$. Let $\boldsymbol{r} \in \mathbb{Z}^M$ such that $\boldsymbol{r}B = 0$. First notice that $\mathrm{supp}(\boldsymbol{r}) \subseteq \mathcal{E}_\mathcal{T}$ implies $\boldsymbol{r} = 0$. Indeed, if $\mathrm{supp}(\boldsymbol{r}) \subseteq \mathcal{E}_\mathcal{T}$ and $\mathrm{supp}(\boldsymbol{r}) \neq \emptyset$, then $\mathrm{supp}(\boldsymbol{r})$ would possess at least one leaf, namely a node v^* such that there exists only one edge $e^* \in \mathrm{supp}(\boldsymbol{r})$ containing v^*. In this case

$$0 = (\boldsymbol{r}B)_{v^*} = \sum_e \boldsymbol{r}(e) B_{ev^*} = \boldsymbol{r}(e^*) B_{e^* v^*}$$

which yields $\boldsymbol{r}(e^*) = 0$, a contradiction. Assume now that $\mathrm{supp}(\boldsymbol{r}) \not\subseteq \mathcal{E}_\mathcal{T}$. Recall that the edges in $\mathcal{E} \setminus \mathcal{E}_\mathcal{T}$ are ordered as $e_1, \ldots, e_{M-N+1}$. Then, we can define,

$$i(\boldsymbol{r}) := \min\{j \,|\, \mathrm{supp}(\boldsymbol{r}) \subseteq \mathcal{E}_\mathcal{T} \cup \{e_1, \ldots, e_j\}\}. \tag{5.34}$$

We now prove that $\boldsymbol{r}$ can be expressed as a $\mathbb{Z}$-combination of the $\boldsymbol{r}_{h_i}$'s by induction on $i(\boldsymbol{r})$. If $i(\boldsymbol{r}) = 1$, consider $\tilde{\boldsymbol{r}} = \boldsymbol{r} - \boldsymbol{r}(e_1)\boldsymbol{r}_{h_1}$. Clearly, by (a), $\tilde{\boldsymbol{r}}B = 0$ and $\mathrm{supp}(\tilde{\boldsymbol{r}}) \subseteq \mathcal{E}_\mathcal{T}$. Hence, by previous considerations, $\tilde{\boldsymbol{r}} = 0$, namely, $\boldsymbol{r} = \boldsymbol{r}(e_1)\boldsymbol{r}_{h_1}$. Suppose now that the claim holds true for $i(\boldsymbol{r}) \leq i - 1$ and let us prove it if $i(\boldsymbol{r}) = i$. Consider, as before, $\tilde{\boldsymbol{r}} = \boldsymbol{r} - \boldsymbol{r}(e_i)\boldsymbol{r}_{h_i}$. Clearly, by (a), $\tilde{\boldsymbol{r}}B = 0$ and $\mathrm{supp}(\tilde{\boldsymbol{r}}) \subseteq \mathcal{E}_\mathcal{T} \cup \{e_1, \ldots, e_{i-1}\}$. Then the induction proves the assertion.

(c) It remains to prove the $\mathbb{Z}$-independence of the row vectors $\boldsymbol{r}_{h_1}, \ldots \boldsymbol{r}_{h_{M_N+1}}$. Assume that $\alpha_i \in \mathbb{Z}$ are such that

$$\sum_i \alpha_i r_{h_i} = 0$$

We need to prove that $\alpha_i = 0$. If this were not the case, we could define $\ell := \max\{i \mid \alpha_i \neq 0\}$. Then $\sum_{i \leq \ell} \alpha_i r_{h_i} = 0$ and so

$$0 = \sum_{i \leq \ell} \alpha_i r_{h_i}(e_\ell) = \alpha_\ell r_{h_\ell}(e_\ell)$$

which would yield a contradiction, since by definition we have that $r_{h_\ell}(e_\ell) = 1$.

□

Proof of Lemma 5.4.2. The fact that $\mathrm{Im}B \subseteq \ker R^M$ follows from Proposition 5.4.1. The fact that $\ker R^M = \ker R^F$ follows from the fact that $R^F = TR^M$, where T is in invertible.

The only thing that remains to be shown is that $\ker R^F \subseteq \mathrm{Im}B$. Let $\boldsymbol{K} \in \ker R^F$. Since rows in R^F form a basis of Γ, we have that $r_h \boldsymbol{K} = 0$ for every h closed path. Let us fix a node $i_0 \in \mathcal{V}$. Then for any other node $i \in \mathcal{V}$ let γ_i be the path in the spanning tree connecting i_0 to i. Define now the column vector $\theta \in \mathbb{Z}^{\mathcal{V}}$ with components

$$\theta_i := r_{\gamma_i} \boldsymbol{K} = \sum_{e \in \mathcal{E}} r_{\gamma_i}(e) \boldsymbol{K}_e$$

We now show that $\boldsymbol{K}_e = \theta_{h(e)} - \theta_{t(e)}$, for any $e \in \mathcal{E}$ which would imply that $\boldsymbol{K} = B\theta$ and so $\boldsymbol{K} \in \mathrm{Im}B$. Consider the closed path h which is the concatenation of the paths $\gamma_{t(e)}$, $(t(e), h(e))$ and $-\gamma_{h(e)}$, where we recall that $-\gamma_{h(e)}$ denotes the path obtained reversing $\gamma_{h(e)}$. Observe that $\boldsymbol{r}_h = \boldsymbol{r}_{\gamma_{t(e)}} + \boldsymbol{r}_{(t(e),h(e))} - \boldsymbol{r}_{\gamma_{h(e)}}$. It follows that

$$0 = \boldsymbol{r}_h \boldsymbol{K} = \boldsymbol{r}_{\gamma_{t(e)}} \boldsymbol{K} + \boldsymbol{r}_{(t(e),h(e))} \boldsymbol{K} - \boldsymbol{r}_{\gamma_{h(e)}} \boldsymbol{K} = \theta_{t(e)} + K_e - \theta_{h(e)}$$

whence the thesis holds. □

Proof of Lemma 5.4.5. Denote $\mathcal{V}_1 = \mathcal{V} \setminus \{1\}$, where 1 is the anchor, and consider the matrix $\bar{B}_{\mathcal{T}} \bar{B}_{\mathcal{T}}^{-1} = I_{|\mathcal{V}_1|}$ to have rows and columns indexed by the edges of the tree. If e and e' are not directly connected to the anchor,

$$\sum_{k \in \mathcal{V}_1} [\bar{B}_{\mathcal{T}}]_{ek} [\bar{B}_{\mathcal{T}}^{-1}]_{ke'} = [\bar{B}_{\mathcal{T}}^{-1}]_{t(e)e'} - [\bar{B}_{\mathcal{T}}^{-1}]_{h(e)e'} = \delta_{ee'}.$$

By construction of $\bar{B}_{\mathcal{T}}^{-1}$, if $e = e'$ then $[\bar{B}_{\mathcal{T}}^{-1}]_{t(e)e'} = 0$ and $[\bar{B}_{\mathcal{T}}^{-1}]_{h(e)e'} = -1$ and the previous relation holds. If $e \neq e'$, then $[\bar{B}_{\mathcal{T}}^{-1}]_{t(e)e'}$ and $[\bar{B}_{\mathcal{T}}^{-1}]_{h(e)e'}$ are both -1 (if e' is on the path from the anchor to $t(e)$) or 0 (in any other case), so we obtain $\delta_{ee'} = 0$. If e or e' are directly connected to the anchor the proof follows in an analogous way. □

Proof of Lemma 5.4.6. Consider

$$C_{e,e'} = \sum_k [\bar{B}_{\mathcal{T}^c}]_{ek} [\bar{B}_{\mathcal{T}}^{-1}]_{ke'}$$

and by the previous interpretation of $\bar{B}_{\mathcal{T}}^{-1}$, we have $[\bar{B}_{\mathcal{T}^c}]_{ek} [\bar{B}_{\mathcal{T}}^{-1}]_{ke'} = 1$ if e' is on the path on $\mathcal{T}$ from the anchor to k and $k = h(e)$, we have $[\bar{B}_{\mathcal{T}^c}]_{ek} [\bar{B}_{\mathcal{T}}^{-1}]_{ke'} = -1$ if e' is on

the path on $\mathcal{T}$ from the anchor to k and $k = t(e)$ with incoherent orientation, and 0 in any other case. By inspection we obtain now the claim. □

6 Conclusions

In this dissertation we have studied one of the most simple and yet important problems in Network Controlled Systems, which is synchronization. By synchronization we mean a state of the network such that all the outputs of the agents are and remain equal in time.

The simplest synchronization problem we have studied is consensus, in which the agents have to agree on a constant value. We have considered in particular the linear consensus, in which the update of the local variable of an agent is a convex combination of the variables of its neighbors. It is known that there exist many performance metrics for the consensus algorithms, each suitable to measure a particular aspect of the procedure. It is also known that, for many realistically implementable network structures, the linear consensus algorithm performs worse and worse as the number of agents in the network increases. It is thus important to take into account this issue when designing a multi agent network.

We have decided to concentrate our attention on two particular metrics, which are the rate of convergence and an LQ cost. The rate of convergence is related on how fast consensus is achieved, and it is essentially a worst case metric. The LQ cost measures instead in a more uniform way the convergence to consensus, and is related to the norm of the difference among the trajectory of the states and the asymptotic consensus value.

The contributions of this dissertation to the Analysis of performance metrics for consensus algorithms are manifold. First of all, we have shown that the LQ cost can be

estimated using the average effective resistance of a resistive electrical network, whose edges are the edges of the communication graph, and in which each resistance is set to 1 Ohm. This result is important due to the appealing monotonicity properties of the average effective resistance. For example, it proves that, concerning the LQ cost, similarly weighted consensus protocols behave in a similar way.

Another contribution concerns the class of graphs we call geometric graphs, which resemble perturbed grids. We have shown that, under mild hypothesis, the rate of convergence of a geometric graph deployed in $\mathbb{R}^d$ and having N nodes can be estimated as $1 - \frac{C}{N^{2/d}}$, while the LQ cost behaves linearly in the number of nodes when $d = 1$, logarithmically when $d = 2$, and is bounded by a constant when $d \geq 3$. This unifies many results already known in literature both for regular d-dimensional tori and for random geometric graphs, and poses fundamental limits on the performances of graphs deployed for example on a plane, which is the most important and common case. Namely, any sensor network in $\mathbb{R}^2$ in which mild assumptions are satisfied (the nodes cannot be too dense or sparse, the communication range cannot be too wide, nodes which are near communicate via a limited number of hops) will behave qualitatively in the same manner.

These results unfortunately heavily lie on the assumption that the consensus protocol is reversible. Future research will concentrate on breaking this constraint, since there are many simple cases, not yet covered by the results here presented, in which the behaviors of the performance metrics are very well known. This is the case, for example, of a ring graph with directional communication, in which the single agent is allowed to send information to the node at its "right" and receive it from the node at its "left". The corresponding matrix is not reversible, thus we cannot use our result. This is clearly a weak point of our work which must be enforced.

The Synthesis Chapter moved from agreement on a constant value to agreement on time–varying trajectories, considering Higher Order Consensus Networks. The contribution of this dissertation to this research topic is mainly in presenting a framework which is able to cover many cases presented in the literature. The main theorem of this Chapter is a powerful tool which provides robust synchronization, in the sense that input/output characterizations for the perturbation operators and for the interconnection operator are presented. The importance of this result, and of the many corollaries proposed for particular cases of perturbations and interconnections, lies on the consolidate literature on Integral Quadratic Constraints, which provides multipliers able to characterize large families of possible operators. Also, the proposed criteria are often scalable, in the sense that they require to check a simple condition for each agent, instead of a unique one on the whole network, which would be computationally expensive. The required check is

often a graphic plot on the complex plane, a particularly simple and intuitive criterion. To conclude, the phenomenon of leader following, which is well–known in classic consensus, has been studied in the framework of Higher Order Consensus.

The weak point of the Chapter, which gives the main research direction for the future, is that the interconnection operator is required to be memoryless. Thus, it is not possible to consider as interconnections operator a generic matrix of transfer functions, for example representing delays. The main point here is the type of projection considered in this dissertation, which does not allow much flexibility. Another promising line of research is considering randomized protocols, instead of deterministic ones, motivated by the fact that simulation results show their effectiveness. The issue concerning randomized protocols is that they do not fit well with input/output techniques, which are related to the worst–case scenario. This research direction thus needs for more sophisticated theoretical tools.

The last Chapter of the dissertation is devoted to Application of the proposed algorithms to the problems of clock synchronization and cameras calibration.

The results previously proposed have been applied to a Higher Order Consensus network where clocks are modeled as double integrators. This yields bounds on the maximum differences allowed among the clocks in order to let synchronization happen. The results shown here are partial, in the sense that more realistic models of clocks exist. Since these models are characterized by nonlinear behaviors, it is expected that the analysis of robust synchronization will become more involved.

In clock synchronization, the increased complexity mainly depends on the type of agents in the network, which are no longer simple integrators but higher order systems. In cameras calibration, instead, the agents are still simple integrators, but the values they exchange and update are not elements of an Euclidean space anymore. In fact, cameras calibration can be seen as an optimization/consensus problem on the manifold $\mathcal{S}_1$. Unfortunately, the particular geometry of $\mathcal{S}_1$ makes the classical consensus algorithm useless. In the literature there is a huge effort to understand which is the largest set of initial conditions which allows convergence to a single point. Our contribution suggests how to avoid this problem. We propose a procedure based on an intuitive constraint, namely that the differences between the true relative orientations of the cameras along cycles must sum up to a multiple of 2π. This constraint allows to rewrite the optimization problem on $\mathcal{S}_1$ as an optimization problem on the Euclidean space, which can be easily solved. In the future, this procedure will be generalized to the much more difficult (and interesting) case of calibration on $SO(3)$.

Bibliography

[1] J. Tsitsiklis. *Problems in decentralized decision making and computation.* PhD thesis, Department of EECs, MIT, 1984.

[2] D. Acemoglu, M. A. Dahleh, I. Lobel, and A. Ozdaglar. Bayesian learning in social networks. Working paper, National Bureau of Economic Research, May 2008. Available Online.

[3] G. Como and F. Fagnani. Scaling limits for continuous opinion dynamics systems. *The Annals of Applied Probability*, 21(4):1537 – 1567, Aug. 2011.

[4] A. Okubo. Dynamical aspects of animal grouping: Swarms, schools, flocks and herds. *Advances in Biophysics*, 2:1 – 94, 1986.

[5] M. Talagrand. *Mean Field Models for Spin Glasses: Basic examples.* Springer, 2010.

[6] F. Pasqualetti, A. Bicchi, and F. Bullo. Consensus computation in unreliable networks: A system theoretic approach. *IEEE Transactions on Automatic Control*, 56(12), 2011.

[7] S. Sundaram and C. N. Hadjicostis. Distributed function calculation via linear iterations in the presence of malicious agents - part i: Attacking the network. In *Proceedings of the American Control Conference. ACC'08*, pages 1350–1355, 2008.

[8] S. Sundaram and C. N. Hadjicostis. Distributed function calculation via linear iterations in the presence of malicious agents - part ii: Overcoming malicious behavior. In *Proceedings of the American Control Conference. ACC'08*, pages 1356–1361, 2008.

[9] R. Carli, A. Chiuso, L. Schenato, and S. Zampieri. Distributed synchronization of noisy non-identical double integrators. *IEEE Transactions on Automatic Control*, 2011.

[10] Roberto Tron and René Vidal. Distributed image-based 3-d localization of camera sensor networks. In *CDC*, pages 901–908, 2009.

[11] R. Tron, B. Afsari, and R. Vidal. Average consensus on riemannian manifolds with bounded curvature. In *CDC*, 2011.

[12] L. Scardovi, A. Sarlette, and R. Sepulchre. Synchronization and balancing on the n-torus. *Systems & Control Letters*, 56(5), 2007.

[13] A. Sarlette and R. Sepulchre. Consensus optimization on manifolds. *SIAM Journal Control and Optimization*, 58(1):56–76, 2009.

[14] R. Diestel. *Graph Theory (Graduate Texts in Mathematics)*. Springer, 2005.

[15] F.R.K. Chung. *Spectral Graph Theory*, volume 92 of *Regional conference series in mathematics*. American Mathematical Society, 1997.

[16] C. Godsil and G. Royle. *Algebraic Graph Theory*. Graduate Texts in Mathematics. Springer, 2001.

[17] R. F. Curtain and H. Zwart. *An Introduction to Infinite Dimensional Linear Systems Theory*. Springer-Verlag, 1995.

[18] C. Desoer and M. Vidyasagar. *Feedback systems: input-output properties*. Academic Press, 1975.

[19] R. Olfati-Saber and R.M. Murray. Consensus protocols for networks of dynamic agents. In *American Control Conference, 2003. Proceedings of the 2003*, volume 2, pages 951 – 956, june 2003.

[20] A. Jadbabaie, Jie Lin, and A.S. Morse. Coordination of groups of mobile autonomous agents using nearest neighbor rules. *IEEE Transactions on Automatic Control*, 48(6):998 – 1001, june 2003.

[21] J. Cortes, S. Martinez, and F. Bullo. Robust rendezvous for mobile autonomous agents via proximity graphs in arbitrary dimensions. *Automatic Control, IEEE Transactions on*, 2006.

[22] J.A. Fax and R.M. Murray. Information flow and cooperative control of vehicle formations. *IEEE Transaction on Automatic Control*, 49(9):1465–1476, September 2004.

[23] R. Olfati-Saber. Distributed kalman filter with embedded consensus filters. In *Decision and Control, 2005 and 2005 European Control Conference. CDC-ECC '05. 44th IEEE Conference on*, 2005.

[24] R. Olfati-Saber. Distributed kalman filtering for sensor networks. In *Proc. of 46th Conference on Decision and control. CDC'07*, 2007.

[25] A. Speranzon, C. Fischione, and K. H. Johansson. Distributed and collaborative estimation over wireless sensor networks. In *Proc. of 45th Conference on Decision and control. CDC'06*, pages 1025–1030, 2006.

[26] L. Xiao, S. Boyd, and S. Lall. A scheme for robust distributed sensor fusion based on average consensus. In *Proc. of 4th International Symposium on Information Processing in Sensor Networks. IPSN '05*, pages 63–70, april 2005.

[27] D. P. Spanos, R. Olfati-Saber, and R. M. Murray. Approximate distributed kalman filtering in sensor networks with quantifiable performance. In *Proc. of 4th International Symposium on Information Processing in Sensor Networks. IPSN '05*, pages 133–139, april 2005.

[28] P. Alriksson and A. Rantzer. Distributed kalman filtering using weighted averaging. In *Prooceedings of the 17th International Symposium on Mathematical Theory of Networks and Systems*, 2006.

[29] R. Carli, A. Chiuso, L. Schenato, and S. Zampieri. Distributed kalman filtering based on consensus strategies. *Selected Areas in Communications, IEEE Journal on*, 26(4):622 –633, may 2008.

[30] G. Cybenko. Dynamic load balancing for distributed memory multiprocessors. *Journal of Parallel and Distributed Computing*, 7(2):279–301, 1989.

[31] J. E. Boillat. Load balancing and poisson equation in a graph. *Concurrency: Practice and Experience*, 7(4):289–313, may 1990.

[32] S. Ganeriwal, P. R. Kumar, and M. B. Srivastava. Timing-sync protocol for sensor networks. In *Proceedings of the 1st International Conference on Embedded Networked Sensor Systems. SenSys '03*, pages 138–149, 2003.

[33] S. Bolognani, S. Del Favero, and L. Schenato. Distributed sensor calibration and least-square parameter identification in wsns using consensus algorithms. In *Proc. of 46th Annual Allerton Conference on Communication, Control and Computing.*, pages 1191–1198, sept. 2009.

[34] L. Schenato and G. Gamba. A distributed consensus protocol for clock synchronization in wireless sensor network. In *Decision and Control, 2007 46th IEEE Conference on*, pages 2289 –2294, dec. 2007.

[35] G. Xiong and S. Kishore. Discrete-time second-order distributed consensus time syhchronization algorithm for wireless sensor networks. *J. Wirel. Commun. Netw. EURASIP*, 1(1):1–12, jan. 2009.

[36] A. Fagiolini, S. Martini, and A. Bicchi. Set-valued consensus for distributed clock synchronization. In *Proceedings of IEEE Conference on Automation Science and Engineering. CASE '09*, pages 116–121, august 2009.

[37] A. Nedic, A. Ozdaglar, and P.A. Parrilo. Constrained consensus and optimization in multi-agent networks. *Automatic Control, IEEE Transactions on*, 55(4):922 –938, april 2010.

[38] A. Nedic and A. Ozdaglar. Distibuted subgradient methods for multiagent optimization. *Automatic Control, IEEE Transactions on*, 54(1):48–61, jan. 2009.

[39] Z. Minghui and S. Martinez. On distributed optimization under inequality and equality constraints via penalty primal-dual methods. In *Prof of. American Control Conference. ACC'10*, pages 2434–2439, july 2010.

[40] B. Johansson, M. Rabi, and M. Johansson. A simple peer-to-peer algorithm for distribured optimization in sensor networks. In *Prof of. 46th IEEE Conference on Decision and Control. CDC'07*, pages 4705–4710, dec. 2007.

[41] S. Sundhar Ram, A. Nedic, and V. V. Veeravalli. Incremental stochastic subgradient algorithms for convex optimization. *SIAM Journal on Optimization*, 20(2):691–717, 2009.

[42] B. Johansson, C. M. Carretti, and M. Johansson. On distributed optimization using peer-to-peer communications in wireless sensor networks. In *Proc. of 5th Annual IEEE Communication Society Conference on Sensor, Mesh and Ad Hoc Communications and Networks. SECON '08*, pages 497–505, june 2008.

[43] B. Johansson, M. Rabi, and M. Johansson. A randomized incremental subgradient method for distributed optimization in networked systems. *SIAM Journal on Optimization*, 20(3):1157–1170, 2009.

[44] Hao Zhu, A. Cano, and G.B. Giannakis. Distributed demodulation using consensus averaging in wireless sensor networks. In *Signals, Systems and Computers, 2008 42nd Asilomar Conference on*, pages 1170 –1174, 26-29 2008.

[45] Hao Zhu, A. Cano, and G.B. Giannakis. Distributed consensus-based demodulation: algorithms and error analysis. *IEEE Transactions on Wireless Communications*, 9(6):2044–2054, june 2010.

[46] E. Lovisari and S. Zampieri. Performance metrics in the consensus problem: a survey. In *Proc. of 4th IFAC Symposium on System, Structure and Control. SSSC'10*, 2010.

[47] E. Lovisari and S. Zampieri. Performance metrics in the average consensus problem: a tutorial. *Annual Reviews in Control*, 2012.

[48] E. Lovisari, F. Garin, and S. Zampieri. A resistance-based approach to performance analysis of the consensus algorithm. In *Proceedings of the 44th Conference on Decision and Control CDC 2010*, pages 5714–5719, Dec. 2010.

[49] E. Lovisari, F. Garin, and S. Zampieri. A resistance-based approach to consensus algorithm performance analysis. In *Proc. of MTNS'10*, July 2010.

[50] E. Lovisari, F. Garin, and S. Zampieri. Resistance-based performance analysis of the consensus algoritm over geometric graphs. *SIAM Journal on Control and Optimization (submitted)*, .

[51] P.G. Doyle and J.L. Snell. *Random Walks and Electric Networks*. Carus Monographs. Mathematical Association of America, 1984.

[52] P. Gupta and P.R. Kumar. The capacity of wireless networks. *IEEE Transactions on Information Theory*, 46(2):388 –404, mar. 2000.

[53] S. Boyd, A. Ghosh, B. Prabhakar, and D. Shah. Randomized gossip algorithms. *IEEE Transactions on Information Theory*, 52(6):2508 – 2530, june 2006.

[54] D.A. Levin, Y. Peres, and E.L. Wilmer. *Markov Chains and Mixing Times*. American Mathematical Society, 2008.

[55] Wei Ren and R.W. Beard. Consensus seeking in multiagent systems under dynamically changing interaction topologies. *IEEE Transactions on Automatic Control*, 50(5), may 2005.

[56] R. Olfati-Saber, J.A. Fax, and R.M. Murray. Consensus problems in networks of agents with switching topology and time-delays. *IEEE Transactions on Automatic Control*, 49(9):1520 – 1533, sept. 2004.

[57] R. Olfati-Saber, J.A. Fax, and R.M. Murray. Consensus and cooperation in networked multi-agent systems. *Proceedings of the IEEE*, 95(1):215 – 233, jan. 2007.

[58] F. Fagnani and S. Zampieri. Average consensus with packet drop communication. *SIAM Journal on Control and Optimization*, 48:102–133, 2009.

[59] P.-A. Bliman and G. Ferrari-Trecate. Average consensus problems in networks of agentws with delayed communications. In *Proc. of 44th IEEE Conference on Decision and Control and European Control Conference. CDC-ECC '05*, pages 7066–7071, dec. 2005.

[60] S. Kar and J. M. F. Moura. Distributed consensus algorithms in sensor netowks with imperfect communcation: Link failures and channel noise. *IEEE Transactions on Signal Processing*, 57(1):355–369, jan. 2009.

[61] S. Kar and J. M. F. Moura. Distributed consensus algorithms in sensor networks: Quantized data and random link failures. *IEEE Transactions on Signal Processing*, 58(3):1383–1400, march 2010.

[62] Wei Ren and R.W. Beard. Consensus seeking in multiagent systems under dynamically changing interaction topologies. *IEEE Transactions on Automatic Control*, 50(5):655 – 661, may 2005.

[63] S. Boyd, A. Ghogh, B. Prabhakar, and D. Shah. Analysis and optimization of randomized gossip algorithms. In *Proc. of 43th IEEE Conference on Decision and Control. CDC'04*, volume 5, pages 5310–5315, dec. 2004.

[64] S. Patterson, B. Bamieh, and A. El Abbadi. Distributed average consensus with stochastic communication failures. In *Proc. of 46th IEEE Conference on Decision and Control. CDC'07*, pages 4215–4220, dec. 2007.

[65] Y. Hatano and M. Mesbahi. Agreement over random networks. *IEEE Transactions on Automatic Control*, 50(11):1867–1872, nov. 2005.

[66] R. Carli, F. Fagnani, A. Speranzon, and S. Zampieri. Communication constraints in the average consensus problem. *Automatica*, 44:671–684, 2008.

[67] J.C. Delvenne, R. Carli, and S. Zampieri. Optimal strategies in the average consensus problem. *Systems & Control Letters*, 58:759–765, 2009.

[68] A. Olshevsky and J. N. Tsitsiklis. Convergence rates in distributed consensus and averaging. In *Proc. of 45th IEEE Conference on Decision and Control. CDC'06*, pages 3387–3392, dec. 2006.

[69] V. D. Blondel, J.M. Hedrickx, A. Olshevsky, and J. N. Tsitsiklis. Convergence in multiagent coordination, consensus, and flocking. In *Proc. of 44th IEEE Conference on Decision and Control and European Control Conference. CDC-ECC '05*, pages 2996–3000, dec. 2005.

[70] R. Olfati-Saber. Algebraic connectivity ratio of ramanujan graphs. In *Proc. of American Control Conference. ACC'07*, pages 4619–4624, july 2007.

[71] A. Tahbaz-Saleh and A. Jadbabaie. Small world phenomenon, rapidly mixing markov chains, and averaging consensus algorithms. In *Proc. of 46th IEEE Conference on Decision and Control. CDC'07*, pages 276–281, dec. 2007.

[72] R. Olfati-Saber. Ultrafast consensus in small-world networks. In *Proc. of American Control Conference. ACC'05*, pages 2371–2378, june 2005.

[73] S. Boyd, P. Diaconis, P. Parrillo, and L. Xaio. Fastest mixing markov chain on graphs with symmetries. *SIAM Journal on Optimization*, 20(2):792–819, 2009.

[74] L. Xiao and S. Boyd. Fast linear iterations for distributed averaging. *Systems & Control Letters*, 52, 2004.

[75] S. Boyd, P. Diaconis, and L. Xiao. Fastest mixing markov chain on a graph. *SIAM Review*, 2004.

[76] L. Xiao, S. Boyd, and S.-J. Kim. Distributed average consensus with least-mean-square deviation. *Journal of Parallel and Distributed Computing*, 67(1):33–46, 2007.

[77] B. Johansson, A. Speranzon, M. Johansson, and K. Henrik. On decentralized negotiation of optimal consensus. *Automatica*, 44:1175–1179, april 2008.

[78] M. M. Zavlanos, D. E. Koditschek, and G. J. Pappas. A distributed dynamical scheme for fastest mixing markov chains. In *Proc. of American Control Conference. ACC'09*, pages 1436–1441, june 2009.

[79] K. Jung, D. Shah, and J. Shin. Distributed averaging via lifted markov chains. *IEEE Transactions on Information Theory*, 56(1):634–647, jan. 2010.

[80] P. Frasca, R. Carli, F. Fagnani, and S. Zampieri. Average consensus on networks with quantized communication. *International Journal of Robust and Nonlinear Control*, 19:1787 – 1816, 2008.

[81] R. Rajagopal and M. Wainwright. Network-based consensus averaging with general noisy channels. *IEEE Transactions on Signal Processing*, 2011.

[82] A. Kashyap, T. Basar, and R. Srikant. Quantized consensus. *Automatica*, 43:192–1203, 2007.

[83] J. Lavaei and R.M. Murray. On quantized consensus by means of gossip algorithm - part i: Convergence proof. In *American Control Conference, 2009. ACC '09.*, pages 394 –401, 2009.

[84] J. Lavaei and R.M. Murray. On quantized consensus by means of gossip algorithm - part ii: Convergence time. In *American Control Conference, 2009. ACC '09.*, pages 2958 –2965, 2009.

[85] M. Huang and J. H. Manton. Coordination and consensus of networked agents with noisy measurements: stochastic algorithms and asymptotic behavior. *SIAM Journal on Control and Optimization*, 48(1):134–161, 2009.

[86] P. Barooah and J. Hespanha. Estimation on graphs from relative measurements: Distributed algorithms and fundamental limits. *IEEE Control System Magazine*, 27(4):57–74, Aug. 2007.

[87] P. Diaconis and D. Stroock. Geometric bounds for eigenvalues of markov chains. *The Annals of Applied Probability*, 1(1):36–61, 1991.

[88] R. Carli. *Topics on the average consensus problem.* PhD thesis, PhD school in Information Engineering – University of Padua, 2008.

[89] M.R. Samatham and D.K. Pradhan. The de bruijn multiprocessor network: A versatile parallel processing and sorting network for vlsi. *IEEE Transactions on Computers*, 38(4):567–581, april 1984.

[90] M.R. Samatham. Augmented multiprocessor networks, July 1992. US Patent Number 5134690.

[91] N.G. de Bruijn. A combinatorial problem. *Koninklijke Nederlandse Akademie v. Wetenschappen*, 46, 1946.

[92] S. Hoory, N. Linail, and A. Wigderson. Expander graphs and their applications. *Bullettin of the American Mathematical Society*, 43(4):439 – 561, oct. 2006.

[93] J. Cortes, S. Martinez, and F. Bullo. Spatially-distributed coverage optimization and control with limited-range interactions. In *ESAIM. Control, Optimization & Calculus of Variations*, pages 691–719, 2004.

[94] J.W. Jaromczyk and G.T. Toussaint. Relative neighborhood graphs and their relatives. *Proceedings of the IEEE*, 80(9):1502 –1517, sep 1992.

[95] Godfried T. Toussaint. Some unsolved problems on proximity graphs, 1991.

[96] P. Barooah and J. Hespanha. Estimation from relative measurements: Error bounds from electrical analogy. In *Prooceedings of the 2nd International Conference on Intelligent Sensing and Information Processing, ICISIP '05*, 2005.

[97] P. Barooah and J. Hespanha. Estimation from relative measurements: Electrical analogy and large graphs. *IEEE Transactions on Signal Processing*, 56(6):2181–2193, june 2008.

[98] P. Barooah and J. Hespanha. Error scaling laws for linear optimal estimtation from relative measurements. *IEEE Transactions on Information Theory*, 55(12):5661–5673, dec. 2009.

[99] M. Fiedler. Algebraic connectivity of graphs. *Czechoslovak Mathematical Journal*, 23(2):298–305, 1973.

[100] Persi Diaconis and Laurent Saloff-Coste. Comparison techniques for random walk on finite groups. *The Annals of Probability*, 21(4):2131–2156, 1993.

[101] Persi Diaconis and Laurent Saloff-Coste. Comparison theorems for reversible markov chains. *The Annals of Probability*, 3(3):696–730, 1993.

[102] J. Fulman and E.L. Wilmer. Comparing eigenvalue bounds for markov chains: When does poincare beat cheeger? *The Annals of Applied Probability*, 9(1):1–13, 1999.

[103] M. Jerrum and A. Sinclair. Approximating the permanent. *SIAM Journal on Computing*, 18(6):1149–1178, 1989.

[104] R.A. Horn and C.R. Johnson. *Matrix Analysis*. Cambridge University Press, 1990.

[105] E. Behrends. *Introduction to Markov Chain (with special enphasys on rapid mixing)*. Vieweg Verlag, 1999.

[106] R. Carli, F. Garin, and S. Zampieri. Quadratic indices for the analysis of consensus algorithms. In *Proc. of ITA Workshop 2009*, 2009.

[107] B. Bamieh, M. Jovanovic, P. Mitra, and S. Patterson. Coherence in large-scale networks: Dimension dependent limitations of local feedback. *IEEE Transactions on Automatic Control*, 2009.

[108] F. Garin and L. Schenato. *Distributed estimation and control applications using linear consensus algorithms*, volume Networked control systems, A. Bemporad, M. Heemels, M. Johansson eds. of *Lecture Notes in Control and Information Sciences*, chapter 3. Springer, 2011.

[109] F. Garin and S. Zampieri. Mean square performance of consensus-based distributed estimation over regular geometric graphs. *SIAM Journal Control and Optimization*, 2011. to appear.

[110] D. Aldous and J. Fill. *Reversible Markov Chains and Random Walks on Graphs*. , . Draft available online at `http://www.stat.berkeley.edu/~aldous/RWG/book.html`.

[111] A. Giridhar. *In-Network Computation in Wireless Sensor Networks*. PhD thesis, University of Illinois, Urbana-Champaign, 2006.

[112] A. Giridhar and P.R. Kumar. Distributed clock synchronization over wireless networks: Algorithms and analysis. In *Proceedings of the 45th IEEE Conference on Decision and Control CDC'06*, pages 4915–4920, Dec. 2006.

[113] A. Ghosh, S. Boyd, and A. Saberi. Minimizing effective resistance of a graph. *SIAM review*, 50(1):37–66, 2008.

[114] D.J. Klein and M. Randić. Resistance distance. *Journal of Mathematical Chemistry*, 12:81–95, 1993.

[115] P. Barooah. *Estimation and Control with Relative Measurements: Algorithms and Scaling Laws*. PhD thesis, University of California, Santa Barbara, 2007.

[116] S.H. Low, F. Paganini, and J.C. Doyle. Internet congestion control. *Control Systems Magazine, IEEE*, 2002.

[117] F. Dörfler and F. Bullo. Synchronization and transient stability in power networks and non-uniform Kuramoto oscillators. *IEEE Transaction on Automatic Control*, . submitted.

[118] E. Lovisari and U.T. Jönsson. A nyquist criterion for synchronization in networks of heterogeneous linear systems. In *Proc. of 2th IFAC Workshop on Distributed Estimation and Control in Networked Systems. Necsys'10*, 2010.

[119] E. Lovisari and U.T. Jönsson. A framework for robust synchronization in heterogeneous multi–agent networks. In *Proc. of 50th IEEE Conference on Decision and Control. CDC'11*, 2011.

[120] S. Hara and H. Tanaka. $\mathcal{D}$-stability and robust stability conditions for lti systems with generalized frequency variables. In *Proceedings of 49th Conference on Decision and Control, CDC'10*, December 2010.

[121] U. Jönsson, C.-.Y Kao, and H. Fujioka. A popov criterion for networked systems. *Systems and Control Letters*, 56(9-10):603–610, 2007.

[122] U.T. Jönsson and C.-Y. Kao. A scalable robust stability criterion for systems with heterogeneous lti components. *IEEE Transaction on Automatic Control*, 2010.

[123] L. Scardovi and R. Sepulchre. Synchronization in networks of identical linear systems. *Automatica*, 45(11):2557 – 2562, 2009.

[124] I. Lestas and G. Vinnicombe. The s-hull approach to consensus. In *IEEE Conference on Decision and Control*, December 2007.

[125] I. Lestas and G. Vinnicombe. Scalable robustness for consensus protocols with heterogeneous dynamics. In *Proceedings of 16th IFAC World Congress*, September 2005.

[126] Ioannis Lestas and Glenn Vinnicombe. Heterogeneity and scalability in group agreement protocols: Beyond small gain and passivity approaches. *Automatica*, 46(7), 2010.

[127] U. Münz, A. Papachristodoulou, and F. Allgöwer. Delay robustness in consensus problems. *Automatica*, 2010 August.

[128] L. Scardovi, M. Arcak, and E.D. Sontag. Synchronization of interconnected systems with applications to biochemical networks: An input-output approach. *IEEE Transactions on Automatic Control*, june 2010.

[129] G.-P. Jiang, W. K.-S. Tang, and G. Chen. A state-observer-based approach for synchronization in complex dynamical networks. *IEEE Trans. on Circuits and Systems*, 2006.

[130] A. Megretski and A. Rantzer. System analysis via integral quadratic constraints. *IEEE Transactions on Automatic Control*, 42(6):819 –830, jun 1997.

[131] G. Zames and P. Falb. Stability conditions for systems with monotone and slope–restricted nonlinearities. *SIAM Journal of Control*, 6(1):89–108, 1968.

[132] K.J. Åström and B. Wittenmark. *Computer-Controlled Systems: Theory and Design (3rd edition)*. Prentice Hall, 1997.

[133] M. Maróti, B. Kusy, G. Simon, and Á. Ldeczi. The flooding time synchronization protocol. In *Proceedings of the 2nd International Conference on Embedded networked sensor systems. SenSys04*, November 2004.

[134] J. Elson, L. Girod, and D. Estrin. Fine-grained network time synchronization using reference broadcasts. In *Proceedings of the 5th symposium on Operating systems design and implementation. OSDI02*, December 2002.

[135] L. Schenato and F. Fiorentin. Average timesync: A consensus-based protocol for time synchronization in wireless sensor networks. In *Proceedings of 1st IFAC Workshop on Estimation and Control of Networked Systems. NecSys09*, September 2009.

[136] R. Solis, V. Borkar, and P.R. Kumar. A new distributed time synchronization protocol for multihop wireless networks. In *45th IEEE Conference on Decision and Control. CDC'06*, December 2006.

[137] R. Carli, A. Chiuso, L. Schenato, and S. Zampieri. A pi consensus controller for networked clocks synchronization. In *IFAC World Congress on Automatic Control (IFAC 08)*, 2008.

[138] R. Carli, E. D'Elia, and S. Zampieri. A pi controller based on asymmetric gossip communications for clocks synchronization in wireless sensors networks. In *Proceedings of the 50th IEEE Conference on Decision and Control. CDC'11*, 2011.

[139] F. Fagnani and Z. Zampieri. Randomized consensus algorithms over large scale networks. *IEEE Journal on Selected Areas of Communications*, 24(4):634–649, 2008.

[140] K. Cai and H. Ishii. Average consensus on general digraphs. Available Online, 1988.

[141] P. Barooah, N. M. da Silva, and J. Hespanha. Distributed optimal estimation from relative measurements for localization and time synchronization. In *Distributed Computing in Sensor Systems*, volume 4026 of *Lecture Notes in Computer Science*, pages 266–281. Springer, 2006.

[142] Alain Sarlette. *Geometry and Symmetries in Coordination Control*. PhD thesis, University of Liège, 2009.

[143] G. Piovan, I. Shames, B. Fidan, F. Bullo, and B. D. O. Anderson. On frame and orientation localization for relative sensing networks. *Automatica*, 2011.

[144] Y. Ma, S. Soatto, J. Kosecka, and S. Sastry. *An Invitation to 3D Vision: From Images to Geometric Models*. Springer Verlag, 2003.